PHYSIOLOGICAL FUNCTION OF THE PRION PROTEIN

IN PERIPHERAL NERVES

AND

IMPACT OF IMMUNIZATION ON PRION SUSCEPTIBILITY

DISSERTATION

zur

Erlangung der naturwissenschaftlichen Doktorwürde
(Dr. sc. nat.)

vorgelegt der

Mathematisch-naturwissenschaftlichen Fakultät

der

Universität Zürich

von

Juliane Elisabeth Irmgard Bremer

aus

Deutschland

Promotionskomitee

Prof. Dr. Adriano Aguzzi (Vorsitz und Leitung)

Prof. Dr. Martin Schwab

Prof. Dr. Ueli Suter

Zürich 2011

Die vorliegende Arbeit wurde von der Mathematisch-naturwissenschaftlichen Fakultät der Universität Zürich auf Antrag von Prof. Dr. Adriano Aguzzi angenommen.

TABLE OF CONTENTS

1 ABBREVIATIONS

AA	amino acid
ATP	adenosine-5'-triphosphate
APC	antigen presenting cell
Bax	Bcl-2–associated X protein
BDNF	brain-derived neurotrophic factor
BSA	bovine serum albumin
BSE	bovine spongiform encephalopathy
cAMP	cyclic adenosine monophosphate
CC_1	positively charged charge cluster of PrP^C (aa 23-27)
CC_2	positively charged charge cluster of PrP^C (aa 95-110)
CD	central domain (of PrP^C)
CDP	chronic demyelinating polyneuropathy
CFA	complete Freud's adjuvant
CJD	Creutzfeldt-Jakob disease
CMAP	compound muscle action potential
CMT	Charcot-Marie-Tooth disease
CNPase/ CNP	2',3'-cyclic nucleotide 3'-phosphodiesterase
CNS	central nervous system
CpG-ODN	cytidyl guanosyl (CpG) oligodeoxynucelotides (ODN)
CWD	chronic wasting disease
Dpl	protein doppel (doppelganger of the prion protein)
Dhh	desert hedgehog
DIGE	difference gel electrophoresis
DNA	deoxyribonucleic acid
DRG	dorsal root ganglion
DRM	detergent-resistant membrane
dpi	days post inoculation
EAE	experimental autoimmune encephalomyelitis
EGFP	enhanced green fluorescent protein
ELISA	enzyme-linked immunosorbent assay
EM	electron microscopy
Erk	extracellular-signal-regulated kinase
FDC	follicular dendritic cell
FFI	fatal familial insomnia
FSE	feline spongiform encephalopathy
Fyn	p59Fyn kinase (member of the Src kinase family)
GABA	gamma-aminobutyric acid

gCJD	genetic Creutzfeldt-Jakob disease
GDNF	glia cell line-derived neurotrophic factor
GFP	green fluorescent protein
GPI	glycosyl-phosphatidyl-inositol
GSS	Gerstmann-Sträussler-Scheinker syndrome
HC	hydrophobic core (of PrP^C)
HE	hematoxylin-eosin
i.c.	intracerebral
IEF	isoelectric focussing
i.p.	intraperitoneal
IPG	immobilized pH gradient
i.v.	intravenous
JNK	c-Jun N-terminal kinase
kDa	kilo Dalton
LPS	lipopolysaccharide
LRP1	low-density lipoprotein receptor-related protein 1
LT-α	lymphotoxin-alpha
LT-β	lymphotoxin-beta
MAG	myelin associated glycoprotein
MALDI-TOF/TOF	matrix-assisted laser desorption/ionization-tandem time-of-flight
MAP	mitogen-activated protein
MAPK	mitogen-activated protein kinase
MBP	myelin basic protein
MLN	mesenteric lymph node
MPZ	myelin protein zero (see also P0)
NaPTA	sodium phosphotungstic acid
N-CAM	neuronal cell adhesion molecule
NCV	nerve conduction velocity
Nfasc	neurofascin
NFH	neurofilament heavy chain
NGF	nerve growth factor
nNOS	neuronal nitric oxide synthase
NRG1	neuregulin 1
NSE	neuron specific enolase
NT3	neurotrophin-3
OR	octarepeat region (of PrP^C)
PBS	phosphate-buffered saline
PBST	phosphate-buffered saline (with) Tween-20
PCR	polymerase chain reaction

PK	proteinase K
PKA	protein kinase A
PKC	protein kinase C
P0	myelin protein zero (see also MPZ)
PLP/ PLP1	proteolipid protein
PMP22	peripheral myelin protein 22
PNS	peripheral nervous system
PRNP	gene encoding the human prion protein
Prnd	gene encoding the mouse doppel (doppelganger of the prion protein, Dpl)
Prnp	gene encoding the mouse prion protein
PrP^{C}	cellular isoform of the prion protein
PrP^{Sc}	pathological isoform of the prion protein
Rag1	recombination-activating gene 1
RIN	RNA integrity index
RML6 (or 5)	Rocky Mountain laboratory scrapie strain, passage 6 (or 5); originally derived from the Chandler sheep scrapie isolate
RNA	ribonucleic acid
RT	room temperature
sCJD	sporadic CJD
s.d.	standard deviation
SDS-PAGE	sodium dodecyl sulphate polyacrylamide gel electrophoresis
s.e.m	standard error of the mean
Shh	sonic hedgehog
STI1	stress-inducible protein I
SLIs	Schmidt-Lanterman incisures
SOD	superoxide dismutase
SSC	saline–sodium citrate
STAT	signal transducers and activator of transcription
STR	short tandem repeat
TBST	tris-buffered saline (with) Tween-20
TGF-β	transforming growth factor-beta
TME	transmissible mink encephalopathy
TNF-α	tumor necrosis factor-alpha
TSE	transmissible spongiform encephalopathy
vCJD	variant form of CJD
wks	weeks
wt	wildtype (mouse/ mice)

2 SUMMARY

Physiological Function of the Prion Protein in Peripheral Nerves

Peripheral neuropathies are frequent and often debilitating disorders in humans. Little is known about the molecular events maintaining structure and function of peripheral nerves and treatment options are often unsatisfactory. In a previous observation, Nishida et al. showed a peripheral neuropathy in aged mice lacking the cellular prion protein PrP^C (Ref.[1]), suggesting that it is a molecular player in peripheral nerve maintenance. The goal of this project was to revisit the status of peripheral nerve maintenance in mice in which the *Prnp* locus was inactivated.

I could show that ablation of PrP^C triggers a chronic demyelinating polyneuropathy (CDP) as identified by electron microscopy and electrophysiology. CDP was present in four independently targeted mouse strains. Ablation of the neighboring *Prnd* locus, or inbreeding to four distinct mouse strains, did not modulate the CDP. Furthermore, CDP in *Prnp* deficient mice was rescued by transgenic expression of PrP^C. Hence, presence or absence of *Prnp* itself - not of other genes - determined the presence of the CDP phenotype.

In order to identify on which cell type PrP^C would need to be expressed to maintain peripheral myelin, I generated transgenic mice expressing *Prnp* under transcriptional control of the proteolipid protein (PLP) promoter in myelinating cells only. I analyzed these mice along with other existing transgenic lines. CDP was triggered by neuron-specific, but not by Schwann cell-specific PrP^C depletion and was fully suppressed by neuronal, but not by Schwann cell-restricted, PrP^C expression. These results show that expression of PrP^C by neurons is essential for the long-term integrity of peripheral myelin sheaths, indicating that PrP^C acts in *trans* on the myelin sheath.

Previously, Baumann et al. had shown that transgenic expression of PrP lacking the central domain induced a young-onset peripheral neuropathy in the absence of wt *Prnp*[2]. In collaboration with my colleague, I generated and analyzed transgenic mice lacking either of two

parts of this central domain: the hydrophobic core or the charge cluster. In addition, I analyzed existing transgenic mice lacking various parts of the amino terminus of PrP^C. I identified an association between presence of CDP and those PrP^C variants nonpermissive for amino proximal cleavage. Complementary, transgenic mice expressing PrP^C variants undergoing proteolytic cleavage did not show CDP. By analyzing transgenic mice, expressing a secreted variant of PrP^C lacking its glycolipid membrane anchor, I could show that proper membrane anchorage is another prerequisite for proper PrP function. Not only was the trophic function of PrP^C exerted *in trans*, but it also correlated with the proteolytic processing of PrP^C in this large collection of transgenic mouse models. Hence, PrP^C is a critical messenger of transcellular axomyelinic communication and I hypothesize that regulated proteolysis of axonal PrP^C exposes domains that may interact with Schwann cell receptors.

Clarifying the molecular basis of these phenomena may lead to a better understanding of peripheral neuropathies. However, *Prnp*$^{-/-}$ nerve transcriptome and proteome as analyzed by microarray and 2D gel experiments turned out to be very stable. Therefore, the molecular pathogenesis of the *Prnp*$^{-/-}$ neuropathy remains to be determined.

Impact of Immunization on Prion Susceptibility

The susceptibility of humans and animals to prion infections is determined by the virulence of the infectious agent, by genetic modifiers, and by hitherto unknown host and environmental risk factors. Since the immune system has an essential role in peripheral prion pathogenesis, I hypothesized that stimulation of the immune system might increase the susceptibility to peripherally administered prions.

To test this, laboratory mice (C57BL/6) were confronted with a short-term challenge of CpG-ODN followed by repeated immunization with bovine serum albumin (BSA) and alum. This experimental protocol was devised with the goal of broadly stimulating, both the innate and the adaptive components of the immune system for a protracted period of time. Histological,

hematological analysis as well as serum markers identified changes indicative of moderate stimulation of the immune system.

I administered prions to these repeatedly immunized mice. Immunization greatly reduced the required dosage of peripherally administered prion inoculum necessary to induce scrapie in 50% of mice. No difference in susceptibility was observed following intracerebral prion challenge. Due to its profound impact onto scrapie susceptibility, the host immune status may determine disease penetrance after low-dose prion exposure, including those that may give rise to iatrogenic and variant Creutzfeldt-Jakob disease.

3 ZUSAMMENFASSUNG

Physiologische Funktion des Prion Proteins in Peripheren Nerven

Bei Menschen sind periphere Neuropathien häufige und oft stark behindernde Erkrankungen. Wenig ist über die molekularen Mechanismen bekannt, die für den Erhalt von Struktur und Funktion peripherer Nerven verantwortlich sind. Oft sind die therapeutischen Möglichkeiten eingeschränkt und daher unbefriedigend. Nishida et al. hat vor über 10 Jahren gezeigt, dass alte Mäuse, denen das zelluläre Prion Protein (PrP^C) fehlt, eine periphere Neuropathie aufweisen[1]. Dies weist darauf hin, dass PrP^C an den molekularen Mechanismen zum Nervenerhalt beteiligt ist. Ziel dieses Projekts war es, die periphere Neuropathie in PrP^C defizienten Mäusen erneut und eingehender zu untersuchen.

Ich konnte in elektronenmikroskopischen und elektrophysiologischen Studien zeigen, dass das Fehlen von PrP^C eine chronische demyelinisierende Polyneuropathie (CDP) induziert. Die CDP war in vier unabhängig voneinander erzeugten PrP^C defizienten Mausstämmen nachweisbar. Weder die Beseitigung des benachbarten Doppelgens (*Prnd*) noch die Rückkreuzung auf vier genetisch verschiedene Mausstämme hatte einen modulierenden Einfluss auf die CDP. Die CDP in PrP^C defizienten Mäusen konnte durch transgene Expression von PrP^C rückgängig gemacht werden. Das heisst, dass die An- oder Abwesenheit vom Prion Protein Gen (*Prnp*) alleine den CDP Phänotyp bestimmt und andere Gene offensichtlich keinen Einfluss haben.

Um den Zelltyp zu identifizieren, von dem PrP^C exprimiert sein muss, damit die Integrität peripherer Nerven erhalten bleibt, habe ich transgene Mäuse erzeugt, die *Prnp* myelinspezifisch unter transkriptioneller Kontrolle des Proteolipid Protein (PLP) Promotors exprimieren. Diese Mäuse habe ich zusammen mit bereits existierenden transgenen Mäusen untersucht. Die CDP wurde durch Neuron-spezifische, nicht aber durch Schwann Zell-spezifische PrP^C Depletion induziert. Andersherum konnte die CDP durch Neuron-spezifische, nicht aber durch Myelin-spezifische PrP-Expression vollständig unterdrückt werden.

Diese Ergebnisse zeigen, dass die PrP-Expression von Neuronen in *trans* essentiell ist für den Langzeit-Erhalt der peripheren Myelinscheiden.

Zuvor hatte Baumann et al. gezeigt, dass transgene Mäuse, die eine PrP Mutante ohne Zentrale Domäne exprimieren, in Abwesenheit von Wildtyp PrP^C eine bereits im Neugeborenenalter beginnende periphere Neuropathie aufweisen[2]. In Zusammenarbeit mit diesem Kollegen habe ich transgene Mäuse generiert und analysiert, denen eine der beiden Anteile der Zentralen Domäne fehlt: der hydrophobe Kern oder die Ladungsgruppe. Ausserdem analysierte ich bereits existierende transgene Mäuse, denen verschiedene Teile des PrP-Aminoterminus fehlen. Es zeigte sich eine Assoziation zwischen der Entstehung einer CDP und denjenigen PrP-Varianten, bei denen die aminoterminale Spaltung gestört war. Andersherum zeigten die transgenen Mäuse mit PrP-Varianten mit regelrechter aminoterminaler Prozessierung keine Neuropathie. Die Analyse transgener Mäuse mit sezerniertem PrP^C (ohne Glykolipid-Membrananker) ergab, dass eine regelrechte Membranverankerung ebenfalls essentiell ist für die regelrechte PrP^C Funktion.

Die myelinotrophische Funktion von PrP^C wurde also nicht nur in *trans* ausgeübt, sondern korrelierte auch mit der proteolytischen Prozessierung in einem grossen Kollektiv transgener Mäuse. Demnach ist PrP^C ein wichtiger Vermittler der transzellulären Axon-Glia-Kommunikation und ich vermute, dass die regulierte Proteolyse von axonalem PrP^C zur Freisetzung von Faktoren führt, die mit Schwann Zell-Rezeptoren interagieren können.

Die Aufklärung der molekularen Basis dieser Phänomene kann zu einem besseren Verständnis der Pathogenese peripherer Neuropathien beitragen. Sowohl Transkriptom als auch Proteom der *Prnp* defizienten Mäuse erwies sich in Microarray und 2D Gel Experimenten jedoch als sehr stabil, so dass die molekulare Pathogenese der $Prnp^{-/-}$ Neuropathie weiterhin offen bleibt.

Auswirkung von Immunisierung auf die Prionen-Suszeptibilität

Die Suszeptibilität, also die Empfänglichkeit von Menschen und Tieren für Prioneninfektionen wird durch die Virulenz des infektiösen Agenz, durch genetische Modifikatoren und durch bisher unbekannte Risikofaktoren des Wirts sowie durch Umweltfaktoren bestimmt. Da das Immunsystem eine essentielle Rolle in der peripheren Prionen-Pathogenese spielt, nahm ich

an, dass die Stimulation des Immunsystems die Suzeptibilität gegenüber peripher applizierten Prionen erhöhen kann.

Um diese Hypothese zu testen, wurden Labormäuse (C57BL/6) durch zwei CpG-ODN-Injektionen sowie wiederholte Injektionen von bovinem Serumalbumin und Alum immunisiert. Das Protokoll wurde derart gestaltet, dass sowohl das angeborene als auch das adaptive Immunsystem möglichst breit und langandauernd stimuliert werden. Histologische, hämatologische und laborchemische Untersuchungen wiesen auf eine moderate Stimulation des Immunsystems hin. Diesen wiederholt immunisierten Mäusen habe ich Prionen appliziert. Immunisierung führte zu einer Reduktion der peripher applizierten Prionendosis, die nötig ist, um in 50% der Mäuse Scrapie auszulösen und somit zu einer erhöhten Suszeptibilität. Hingegen wurde die Suszeptibilität bei Applikation von Prionen in das Zentrale Nervensystem durch Immunisierung nicht verändert. Der deutliche Einfluss auf die Scrapie-Suszeptibilität spricht dafür, dass der Immunstatus des Wirts die Erkrankungspenetranz bei Exposition gegenüber niedrigen Prionendosen wie bei iatrogener oder neuer Variante der Creutzfeldt-Jakob Erkrankung bestimmen kann.

4 DEFINITIONS

Immunization. Antigen specific immune response can be induced by active or passive specific immunization. In active immunization, antigens during natural infections or artificially administered antigens (vaccination) induce a protective immunity and generate an immunological memory. The adaptive immune system plays an active role - proliferation of antigen-reactive T and B cells results in the formation of effector and memory cells. Upon successful active immunization, a subsequent exposure to the pathogenic agent elicits a heightened immune response that eliminates the pathogen and prevents disease. In vaccinations, the boosting power of special non-specific stimulants or adjuvants like alum or CFA is sometimes used to enhance immunity. In passive immunization, preformed antibodies are injected to induce a rapid and specific but short-lived effect. It is usually applied in patients already exposed to disease, e.g. to tetanus[3].

LD50. The LD50 is a standardized measure for agents able to kill its host (poison, infectious agent etc.). LD50 (LD = “lethal dose”) is the dose that kills half (50%) of the exposed hosts and corresponds to the turning point of a cumulative dose-survival curve.

Prion. Prions are infectious agents, causing transmissible spongiform encephalopathies (TSEs). They have unconventional properties, like resistance to agents known to inactivate nucleic acids. The word prion is a portmanteau derived from “proteinaceous infectious” particle. The term prion does not have structural implications other than that a protein is an essential component of the transmissible agent[4-5].

'Protein-only' hypothesis. This hypothesis maintains that the prion, the transmissible agent, consists merely of protein and is capable of replicating and transmitting infections without the need for informational nucleic acids. Several lines of evidence suggest that this protein is an

abnormal form of PrP, perhaps identical with PrP^{Sc}. Yet, it could not be excluded that the prion needs to be associated with other non-informational molecules to be infectious[4-6].

PrP^{C}. The physiologically occurring form of the prion protein "PrP^{C}" with "C" referring to cellular. The cellular prion protein PrP^{C} is a GPI-linked extracellular membrane protein with two N-linked complex glycosylation sites. The mature PrP^{C} protein contains a well-defined carboxy-terminal globular domain, consisting of three alpha helices and two beta sheets and a structurally less-defined amino proximal region[6].

PrP^{Sc}. PrP^{Sc} is a conformational isoform of the normal cellular prion protein, which is almost invariably detected in TSE-infected tissues and cells and therefore serves as a surrogate marker for prions. "Sc" refers to scrapie, a prion disease occurring in sheep and goat or experimentally in mice. PrP^{Sc} is characterized by a beta-sheet-rich structure and is typically partially resistant to proteinase K (PK). It is widely accepted that prions mainly consist of PrP^{Sc}. However, it remains to be shown whether the infectious agent consists primarily or exclusively of a subspecies of PrP^{Sc}, or an intermediate form of PrP (termed PrP*), and which other non-protein compounds (e.g. lipid or polyanionic molecules) can contribute to infectivity[4, 6-8].

Susceptibility. Susceptibility is a measure of the likelihood to contract disease after exposure to a defined inoculum of a given pathogen.

Transmissible spongiform encephalopathy (TSE). A general term for diseases associated with the presence of prions in vacuolated central nervous system tissue, which can be transmitted from one affected host to another. It is a synonym for prion disease[4-5].

5 PHYSIOLOGICAL FUNCTION OF THE PRION PROTEIN IN PERIPHERAL NERVES

Parts of the 'Introduction', 'Material and Methods', 'Results' and 'Discussion' section are reproduced or adapted from the following publication:

"Axonal prion protein is required for peripheral myelin maintenance"

By Juliane Bremer, Frank Baumann, Cinzia Tiberi, Carsten Wessig, Heike Fischer, Petra Schwarz, Andrew D. Steele, Klaus V. Toyka, Klaus-Armin Nave, Joachim Weis, and Adriano Aguzzi

Published in Nature Neuroscience March 13th 2010, issue 13, volume 3, pages 310-318.

Parts of the 'Introduction' are adapted from the following publication:

"The Prion's Elusive Reason for Being"

By Adriano Aguzzi, Frank Baumann, and Juliane Bremer

Published in Annual Reviews Neuroscience 2008; issue 31: pages 439-477

5.1 Introduction

5.1.1 Architecture and function of peripheral nerves

In the mammalian nervous system, peripheral nerves contain a variable number of motor and sensory nerve fibers. Cell bodies of motor nerve fibers lie in the ventral horn of the spinal cord, while cell bodies of sensory neurons are localized in dorsal root ganglias (**Fig. 1**). Some nerves also contain autonomic nerve fibers.

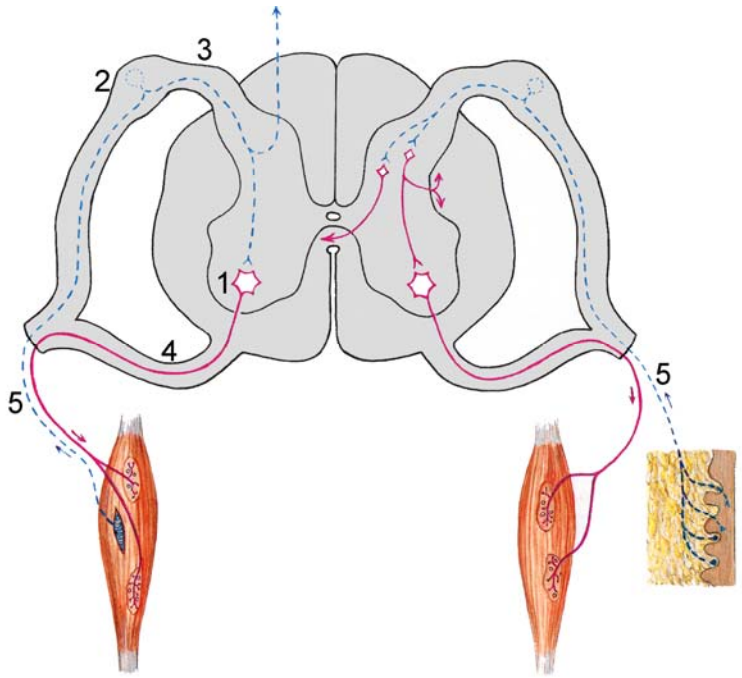

Figure 1. Organization of peripheral nerves. Cell bodies of motor nerves lie in the ventral horn of the spinal cord (1). Their axons leave the spinal cord through the anterior root (4) in order to innervate skeletal muscles. In the peripheral nerves, motor nerve axons are accompanied by sensory nerve processes (5) that conduct impulses from the skin (right side) or from muscle spindles (left side). Sensory nerve cell bodies lie in the dorsal root ganglias (2) and enter the spinal cord via the posterior root (3). They further conduct the sensory information to the brain and/or are connected via interneurons with the motor neurons (1). Adapted from[9], original source: Benninghoff / Drenckhahn: Anatomie, 16th edition © 2004 Elsevier GmbH, Urban & Fischer Verlag München.

Neurons coexist with glial cells. In the peripheral nervous system (PNS), there is one type of glial cell, the Schwann cell. Mature non-myelinating Schwann cells surround groups of small axons, forming Remak bundles. Larger axons > 1 μm are surrounded by myelinating Schwann cells. Each myelinating Schwann cell surrounds only one axonal section with specialized cell membrane extensions that spirally wrap around the axon. These wraps are condensed into a

multilamellar-compacted myelin sheath. Such an ensheathed section of up to 2 mm is called an internode as it reaches from one node of Ranvier to the next. The resulting myelin sheath insulates the ensheathed axon, serves to localize voltage-gated channels into distinct neuronal domains and and allows rapid saltatory conduction of action potentials[10-11]. Myelin can be subdivided into compacted myelin which serves as the insulator and the non-compacted myelin, which is a channel system continuous with the glial cytoplasm. This channel system allows cellular metabolites to come close to the periaxonal space. Schmidt–Lanterman incisures (SLIs) are local stacks of non-compacted myelin that spiral around the axon. At the nodes of Ranvier, voltage-dependent sodium channels are clustered in the axonal membrane. Nodes are flanked by a paranodal axo-glial junction forming strong diffusion barriers. Paranodes in turn are flanked by the juxtaparanodal region with clusters of potassium channels (**Fig. 2**)[12].

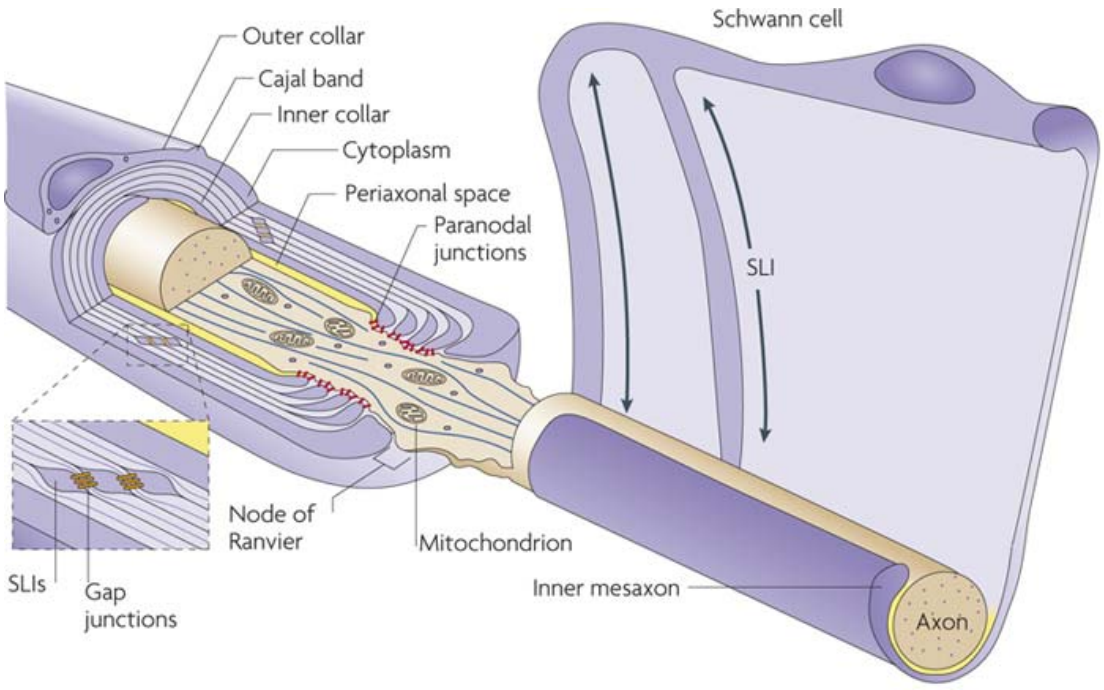

Figure 2. Scheme depicting a myelinated axon. On the right side, an unrolled sheath of a Schwann cell is shown. Compacted myelin (shown in pale blue) serves as an insulator of the axon (shown in brown), except for at widely spaced short gaps (nodes of Ranvier). Non-compacted myelin defines a channel system (shown in dark blue) that is continuous with the glial cytoplasm and brings cellular metabolites close to the periaxonal space (shown in yellow). Schmidt–Lanterman incisures (SLIs) are local stacks of non-compacted myelin that spiral around the axon, they are linked by gap junctions when stacked. Figure reprinted by permission from Macmillan Publishers Ltd: *Nature Reviews Neuroscience*[12], copyright 2010. www.nature.com/nrn. Licence number 2438450142816.

5.1.2 Axon-glia interactions

Neurons and glial cells interact extensively, both structurally and functionally, in the central and peripheral nervous systems. During development of peripheral nerves, axonal signals are known to recruit glial cells to promote their differentiation into myelinating glia and to regulate myelination. Axonal neuregulin 1 (NRG1) and Notch signalling control Schwann cell differentiation, proliferation and myelination[13-14]. The ratio between axonal diameter and myelinated fiber diameter (g-ratio) is known to be well-preserved. Axon-bound NRG1 type III interacting with Schwann cell ErbB2 and ErbB3 receptors is essential for differentiation of the myelinating Schwann cell phenotype and regulation of myelin sheath thickness[15-16]. Axonal electrical activity can control myelination by releasing axonal ATP and adenosine. Schwann cell differentiation and myelination are inhibited by axonal release of ATP, while oligodendrocyte myelination is indirectly stimulated by axonally released adenosine[11]. In turn, glial ensheathment and myelination induce reorganization of axon membrane structure[17]. Neurotrophins are a family of target-derived growth factors including nerve growth factor (NGF), brain-derived neurotrophic factor (BDNF), neurotrophin-3 (NT3), and glia cell line-derived neurotrophic factor (GDNF) which are involved in regulating myelination by either promoting Schwann cell myelination (NGF/ TrkA and BDNF/ $p75^{NTR}$) or promoting Schwann cell proliferation but inhibiting myelination (NT3/ TrkC receptor). Conversely, Schwann cell-derived GDNF can promote survival of axons[11]. Glial cells are also required for functional and structural axonal integrity and long-term survival. This fact is supported by knowledge from human diseases and findings in transgenic animals. In the demyelinating disorder Charcot-Marie-Tooth disease type I (CMT1), many disease-causing genes are exclusively expressed in Schwann cells, like peripheral myelin protein 22 (PMP22) and myelin protein zero (MPZ or P0). Besides developmental hypomyelination and segmental myelin brakedown, there is secondary, slowly progressive axonal degeneration which leads to denervation in CMT1. Denervation causes progressive muscle weakness and sensory deficits which are clinically more important than the reduction of nerve conduction velocities (NCV) caused by demyelination[18]. CMT2 is characterized by intact myelin (normal NCV), but reduced amplitudes, indicating axonal loss.

Typically, mutated genes encode proteins expressed specifically in the neuron. However, specific mutations affecting the extracellular domain of the myelin protein MPZ lead to CMT2[19-21]. Similarly, in central demyelinating diseases, like multiple sclerosis or leukodystrophies, progressive axonal degeneration is common[11].

Analyses of knockout mice lacking either the myelin component proteolipid protein (PLP or PLP1) or 2',3'-cyclic nucleotide 3' phoshodiesterase (CNPase) show that axonal integrity in the central nervous system (CNS) strongly depends on glial cell support. In the absence of either of these two proteins there is impairment of axonal transport followed by severe axonal degeneration[22-24]. Similarly, in the PNS, Schwann cells support axonal integrety independently of myelin itself. Knockout mice lacking the myelin associated glycoprotein (MAG) have normal myelination, but sciatic nerves show axonal degeneration and reduced axon calibers[11, 25-26]. In mice lacking myelin peroxisomes, progressive degeneration of axonal integrity was observed [27].

A summary of known axon-glia interactions is shown in **Fig. 3**. Recent findings and speculations hint to even more intense crosstalk between Schwann cells and axons. The finding that ribosomes can transfer from Schwann cells to axons indicates that Schwann cells even have the propensity to control axonal protein synthesis. In addition, trophic support of axons by glial cells has recently been hypothesized. Nave, for example, speculates that energy–rich metabolites like glycolysis products (pyruvate, lactate) could transfer from glia cells to axons and feed axonal mitochondria in long fiber tracts[12].

Figure 3. Axon-glia interaction during myelination and long-term myelin and axon maintenance

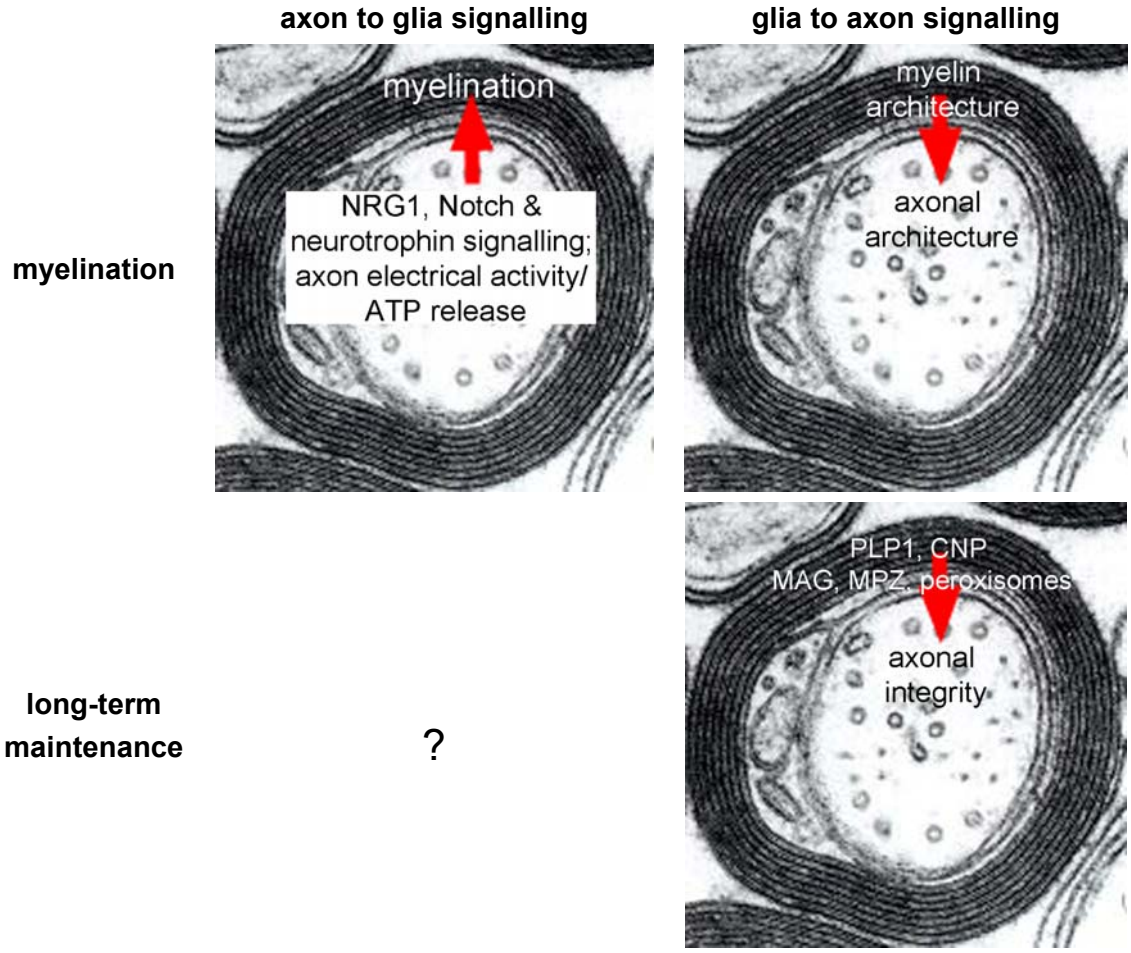

5.1.3 Peripheral neuropathies in humans

Peripheral neuropathies are common in humans and encompass several different disorders affecting the integrity of peripheral nerves. They can be caused by a pathologic process occurring in neurons or Schwann cells, altered signalling or adhesion between the two cell types or by a pathological process in the surrounding connective tissues or vessels. Often peripheral neuropathies occur as the manifestation of a disorder involving the whole body (a systemic disease), like Diabetes mellitus, infectious diseases, or autoimmune disorders. Peripheral neuropathies can occur in patients with cancer as a paraneoplastic syndrome which is by definition not due to local effects of the tumour cells, but caused by humoral effects of tumour cells or autoimmunity induced by an immune response against cancer cells.

Several toxic substances can cause peripheral neuropathies. The most common poison leading to peripheral neuropathies in the developed world is alcohol, but also medication (especially

chemotherapy) and several other intoxications can lead to degeneration of the peripheral nervous system (**Table 1**)[28].

Table 1. Cause of neuropathy in 1195 patients[28]	**frequency in %**
diabetes	34.8
unknown	22
alcohol	11.1
Guillain-Barre syndrome	6.3
infectious	5.4
vasculitis	4.1
chronic inflammatory demyelinating polyradiculoneuropathy (CIDP)	4.1
malabsorption	3.8
paraneoplastic	2.7
CMT	2.2
paraproteinemia	1.1
toxic	0.9
amyloidosis	0.5
hereditary neuropathy with liability to pressure palsy (HNPP)	0.2
others	0.9

Symptoms may be mild but can also cause complete paralysis. In some cases, if the causative agent is known, a specific therapy is possible, e.g. in infections. Though often, even if the cause is known, therapeutic options are poor and progression of the disease cannot be stopped. Hereditary peripheral neuropathies are less common, occuring in approximately one in 2500 people. They are named after three investigators who described them: Charcot-Marie-Tooth diseases (CMT). Autosomal dominant inheritance occurs in the majority of CMT cases. Spontanous mutations are the reason for sporadic occurance. Approximately two thirds of CMT neuropathies are demyelinating, one third is a primary axonal disorders. At least 30 genes are known to cause CMT neuropathies, and more than 45 distinct loci have been identified[29].

5.1.4 Physiological function of the cellular prion protein

The cellular prion protein PrP^C is a GPI-linked extracellular membrane protein with two N-linked complex glycosylation sites. PrP^C is highly abundant in the developing and mature nervous system, where it is expressed by neuronal and glial cells. This mature version originates from a precursor protein proteolytically processed in the endoplasmic reticulum and Golgi[30]. As

revealed by its atomic structure, the mature PrP^C protein contains a well-defined carboxy-terminal globular domain comprising residues 127-231 (murine numbering), consisting of three alpha helices and two beta sheets[31-32] and a structurally less-defined amino proximal region containing a stretch of several octapeptide repeats, termed the octarepeat region (OR), and framed by two positively charged charge clusters, CC_1 (aa 23-27) and CC_2 (aa 95-110). The amino proximal region and the carboxy-terminal domain are linked by a hydrophobic stretch of amino acids [aa 111-134, also termed hydrophobic core (HC)]. PrP^C, and particularly its central domain (CD), is well conserved between species, suggesting that it has an important function[6]. An astonishing number of independent lines of mice lacking PrP^C have been generated by homologous recombination in embryonic stem cells in many laboratories (henceforth collectively referred to as *Prnp*$^{-/-}$ mice). Mice with disruptive modifications restricted to the open reading frame are known as *Prnp*$^{o/o}$ [Zürich I][33] or *Prnp*$^{-/-}$ [Edinburgh][34]. They developed normally, and no severe pathologies were observed later in life. As predicted by the protein-only hypothesis, these mice were entirely resistant to prion infections[35]. In contrast with these earliest lines, three lines generated afterwards: *Prnp*$^{-/-}$ [Nagasaki, *Prnp*$^{Ngsk/Ngsk}$], Rcm0, and *Prnp*$^{-/-}$ [Zürich II, *Prnp*$^{ZrchII/ZrchII}$] developed ataxia and Purkinje cell loss later in life (**Fig. 4**). Because the phenotype was abolished by reintroduction of *Prnp* as a transgene, the originators of the Nagasaki mice concluded that it occurred because of the lack of PrP^C. This, however, would run counter to the lack of pathology in *Prnp*$^{o/o}$ Zurich-I mice. The discrepancy between the different lines of PrP knockout mice was not resolved until a novel gene (*Prnd*), encoding a protein called Doppel (Dpl), was discovered. *Prnd* is localized 16 kb downstream of *Prnp*. In all three lines of PrP^C-deficient mice developing ataxia and Purkinje cell loss, a splice acceptor site to the third exon of *Prnp* was deleted. This placed *Prnd* under transcriptional control of the *Prnp* promoter, resulting in the formation of chimeric transcripts and in overexpression of Dpl in the brain[36-38].

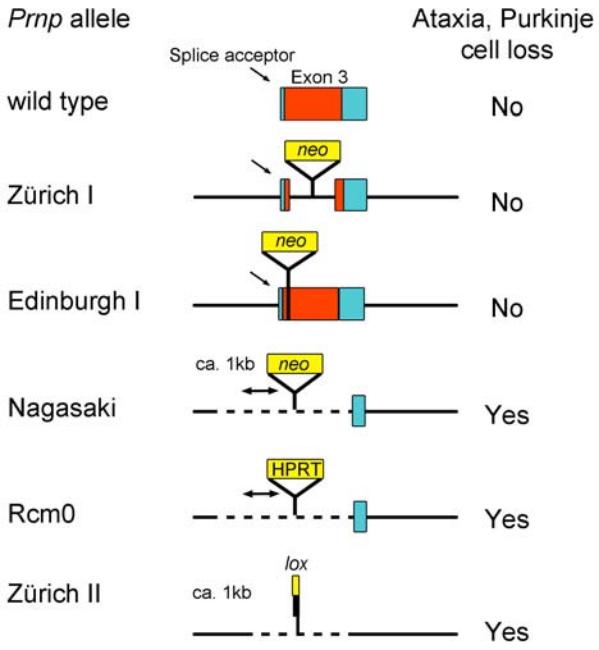

Figure 4. *Prnp* deficient mice. Different strategies used to disrupt the locus of the *Prnp* gene. The dotted line indicates the segment of *Prnp* DNA that has been deleted, and the yellow box indicates an inserted sequence. Red: open reading frame, turquoise: noncoding region; *neo:* neomycin phosphotransferase, HPRT: hypoxanthine phosphoribosyltransferase; *lox:* a 34-bp recombination site from phage P1. Adapted from "Weissmann, C. & Aguzzi, A. Perspectives: neurobiology. PrP's double causes trouble. *Science* 286, 914-915 (1999), figure: Knock knock. Which phenotype is there?" [39]. Reprinted with permission from AAAS, reference # 10-29817. www.sciencemag.org

Several cellular processes in the nervous system have been reported to be influenced by the *Prnp*-genotype including neuronal survival, neurite outgrowth, synapse formation, maintenance and function and maintenance of myelinated fibers (**Fig. 5**). In addition, Nishida et al. identified late-onset peripheral neuropathy in $Prnp^{Ngsk/Ngsk}$ and $Prnp^{o/o}$ mice[1, 33].

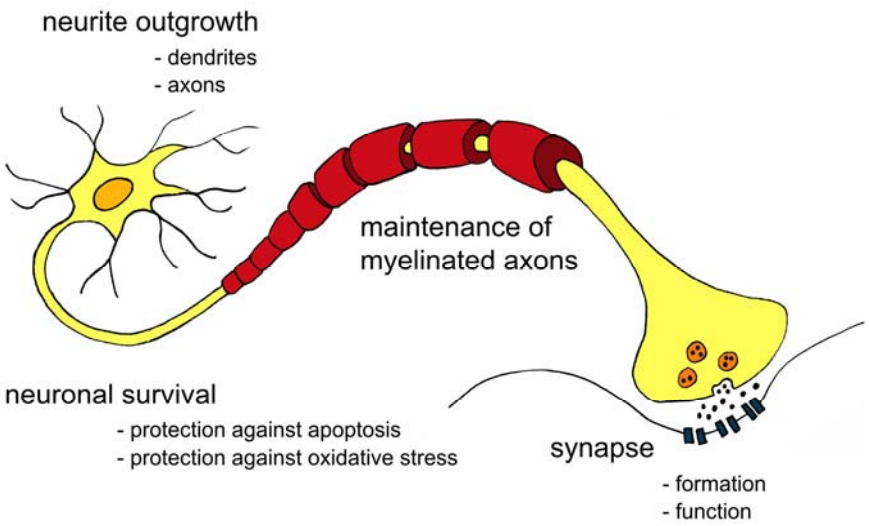

Figure 5. Physiological processes involving PrP^C. Several processes in the nervous system are influenced by PrP^C: Neurite outgrowth, including growth of axons and dendrites, was observed to be reduced in neurons lacking PrP^C. PrP^C has often been reported to promote neuronal survival, in particular following apoptotic or oxidative stress. Cerebellar granule cell apoptosis was observed in mice expressing toxic N-terminal deletion mutants of PrP. In addition, the latter transgenic mice show an impaired maintenance of myelinated axons in the white matter. Another site of PrP^C action might be the synapse, which is often affected in the first stage of prion diseases and whose formation was found to be reduced in neuronal cultures devoid of PrP^C. Furthermore, electrophysiological studies indicate a role of PrP^C in synapse function, especially in neurotransmitter release. Adapted and reprinted, with permission, from the *Annual Review of Neuroscience*, Volume 31 ©2008 by Annual Reviews. www.annualreviews.org.

One of the most frequently suggested functions of PrP^C is a survival-promoting effect on neuronal and nonneuronal cells, which has been observed *in vitro* as well as in *in vivo* studies. This neuroprotective function, or cytoprotective function in general [reviewed in [40]], has been mediated by antiapoptotic or antioxidative mechanisms.

Antiapoptotic function. Neurons derived from *Prnp*$^{-/-}$ mice were originally reported to be more susceptible to the induction of apoptosis by serum-deprivation than cells expressing PrP^C (Ref. [41]), but this effect may have been brought about by Dpl overexpression rather than by PrP^C ablation. However, several studies indicate that PrP^C has a cytoprotective function by decreasing the rate of apoptosis after particular apoptotic stimuli such as Bax overexpression or TNF-α. Bax overexpression induces apoptosis in human neuronal cells. Coexpression of wt PrP^C, but not of PrP lacking the octarepeats, reversed the Bax-mediated induction of apoptosis[42].

The presence of PrP in the cytosol, be it due to reverse translocation from the endoplasmic reticulum or through direct cytosolic expression, was virulently neurotoxic[43]. However, other studies failed to confirm the toxicity of cytosolic PrP and claimed that it can instead protect against Bax-mediated apoptosis in human primary neurons[44]. In this context, PrP^C inhibited the proapoptotic conformational change of Bax and cytochrome c release from mitochondria[45].

In a screening approach for proteins protecting cancer cells from apoptosis, researchers investigated the gene-expression profile in an established cell clone of MCF-7 breast cancer cell line resistant to TNFα-induced apoptosis: PrP^C was overexpressed 17-fold. In line with this finding, overexpression of PrP^C converted MCF-7 cells sensitive to TNFα-induced apoptosis into resistant cells[46].

The neuroprotective function of PrP^C in the postischemic rodent brain has been intensively studied. Levels of PrP^C after ischemia were increased compared with controls[47-48]. Moreover, adenovirus-mediated overexpression of PrP^C reduced infarct size in rat brain and improved neurological behavior after cerebral ischemia[47]. Conversely, in a mouse model of ischemic brain injury *Prnp*$^{o/o}$ mice displayed significantly increased infarct volumes after ischemic brain injury when compared with wt mice[49-50]. Two groups of researchers showed that mice lacking PrP^C

had enhanced postischemic caspase-3 activation[50-51]. An increase in Erk-1/-2, STAT-1, and JNK-1/-2 phosphorylation and activation was identified, suggesting PrP^C's possible involvement in cellular signaling[51]. Also, a reduced amount of phospho-Akt in the gray matter suggested that PrP^C deficiency brings about an impairment of the antiapoptotic phosphatidylinositol 3-kinase/Akt pathway[50]. Finally, Mitteregger et al. claimed that the OR is required within PrP^C for the neuroprotection in the ischemic mouse brain[52], although the genetic homogeneity of the mice tested in the latter experiment was not controlled for.

Protection against oxidative stress. Besides its possible antiapoptotic function, there are many reports about an antioxidative effect of PrP^C. These two effects are not necessarily mutually exclusive. Oxidative stress may be involved in TSE pathogenesis. However, one must remember that oxidative stress is very unspecific and is seen in different kinds of damage to the nervous system with impaired mitochondrial function like defects in the ubiquitin-proteasome system, protein aggregation and inflammation.

Many investigators believe that the main function of PrP^C consists of protecting against oxidative stress (see[53] for a review). First hints came from in vitro studies of rat pheochromocytoma cells. Those selected for resistance to copper toxicity or oxidative stress showed higher levels of PrP^C (Ref [54]). Primary neuronal cells lacking PrP^C were more susceptible to hydrogen peroxide (H_2O_2) than wt cells. The increased peroxide toxicity went along with a significant decrease in glutathione reductase activity measured in PrP^C-deficient neurons[55]. Also, PrP^C-deficient primary neurons were more susceptible to treatment with agents inducing oxidative stress compared with wt cells, a phenomenon that was explained by a reduced Cu/Zn superoxide dismutase (SOD) activity observed in vivo[56-57]. Higher levels of oxidative damage to proteins and lipids were identified in the brain lysates derived from *Prnp*$^{-/-}$ compared with wt mice[58-59].

PrP^C itself could have SOD activity and thereby mediate the antioxidative function[60]. However, there is significant controversy about this alleged SOD activity. Others failed to confirm this proposed SOD activity in vitro[61] and in vivo[62]. Furthermore, PrP^C expression level did not significantly influence SOD activity in vivo[62-63].

Mitochondria play an important role not only in oxidative stress but also in the induction of apoptosis. Morphological alterations in mitochondria have been described in scrapie-infected hamsters[64] and mice[65] as well as in mice lacking PrP, in which the number of mitochondria was reduced[66].

Role of PrP^C in synapses. Synapses have developed into a sort of hot spot in prion research. Several immuno-electron microscopy studies could show that PrP^C is localized in synaptic boutons, where it is mainly presynaptic[67-70]. However, others described a much broader distribution of neuronal PrP^C (Ref [71-72]). Because PrP^C is processed and broken down into various fragments, not all of which are recognized by the antibodies used in these studies, one might speculate that some PrP^C degradation products acquire distinct subcellular topologies.

Early pathologic changes occurring in prion diseases involve synapse loss and PrP^{Sc} deposition in synaptic terminals[73-77]. Synaptic vesicle proteins associated with exosomes and neurotransmission are reduced in brains of patients with spongiform encephalopathy[78]. Synaptic disorganization and loss are fundamental and constant features of prion disease, irrespective of the presence or absence of spongiform change, neuronal loss, and severe gliosis[79]. Abnormal electrophysiological recordings in scrapie-infected mouse and hamster hippocampal and cortical slices further support the synaptic dysfunction during the course of prion disease[80-81]. In a terminal disease state, PrP^{Sc} accumulation in synaptosomes correlated with alterations in the GABAergic system[82]. Despite the above evidence, it should be noted that synaptic changes can represent nonspecific phenomena that are seen in essentially all brain diseases at one stage or another.

The generally held view that PrP^C is an important protein in synapses is supported by electrophysiological studies of CA1 hippocampal neurons derived from PrP^C-deficient mice. Excitatory glutamatergic synaptic transmission, $GABA_A$ receptor--mediated fast inhibition, long-term potentiation, and late afterhyperpolarization were reduced or absent in mice lacking PrP^C [83-86]. Some of the findings could be explained by alterations in Ca-activated K+ currents[84, 87]. However, these alterations in synaptic transmission were not confirmed by others[88], and glutamatergic synaptic transmission was even observed to be increased in PrP^C-deficient mice

by yet another laboratory[89-90]. Another report underscores the impact of aging on these alterations, describing a reduction in the level of posttetanic potentiation and long-term potentiation only in old PrP^C-deficient mice[91]. In summary, the impact of the loss of PrP^C on hippocampal electrophysiological parameters is still being hotly debated despite a full decade of research efforts. Some of the discrepancies may depend on additional genetic modifiers for which investigators have not rigorously controlled.

Other alterations in PrP^C-deficient mice might be related to synaptic dysfunction such as altered circadian rhythms and sleep[92] and impaired hippocampal-dependent spatial learning[93]. The neuromuscular junction is another site where PrP^C is concentrated, primarily enriched in subsynaptic endosomes[94]. A potentiation of acetylcholine release from presynaptic axon terminals was observed after administration of recombinant PrP at nanomolar concentrations to mouse phrenic-diaphragm preparations[95]. The suggestion of an involvement of PrP^C in synapse formation originated from in vitro observations in hippocampal neurons, in which synapse-like contacts were increased after addition of recombinant PrP[96].

It is unknown whether the role of PrP^C in synapses is related to its previously mentioned antiapoptotic or antioxidative effects or whether it is mainly due to the involvement of PrP^C in neurotransmitter release (e.g., via direct interaction with synapsin1 and synaptophysin). However, it is also possible that a yet unidentified process could be responsible or several of these processes could be interrelated.

Neurite outgrowth. Several lines of evidence indicate PrP^C's involvement in neuronal development, differentiation, and neurite outgrowth. Axon or dendrite outgrowth was associated with PrP^C-dependent activation of signal transduction pathways including p59Fyn kinase (Fyn), cAMP/protein kinase A (PKA), protein kinase C (PKC), and MAP kinase (MAPK) activation [96-99]. Fyn activation in this context was dependent on the recruitment of neural cell adhesion molecule (N-CAM) to lipid rafts[99]. Recent studies show that PrP^C positively regulates neural precursor proliferation during development and adult mammalian neurogenesis[100].

Maintenance of white matter. Central nervous system white matter, composed mainly of myelinated axons, might be disrupted in prion diseases and prionopathies. In some cases of

GSS, cerebellar and frontal white matter are affected[101]. In an experimental model of human TSEs in rodents, vacuolation in myelinated fibers with splitting of myelin lamellae was observed [102-103]. PrP^C is present in purified myelin fractions derived from brain homogenates[104]. Several transgenic mice expressing deletion mutants of PrP^C (Refs [2, 105-106]) as well as *Prnp*$^{-/-}$ mice accidentally overexpressing Dpl[1] show vacuolation and degeneration of myelinated fibers in the central nervous system.

Molecular mechanisms mediating the function of PrP^C. Despite the overwhelming number of reports about alterations in mice and cells lacking PrP^C summarized above, little is known about the molecular mechanisms involved in these cellular processes.

One explanation for the diversity of the suggested physiological functions of this PrP^C is that it may exert pleiotropic effects, thereby modulating the function of several cellular pathways. Examples for such a general cellular process would be stabilization of protein complexes and the targeting of cell components to certain cellular sites, such as rafts or endosomes.

Signaling. The attachment of PrP^C to the membrane by a GPI anchor, its localization in detergent-resistant membranes, also known as lipid rafts, in many cell types may suggest an involvement in cellular signaling[106] as is the case for other raft-associated proteins. Moreover, as I describe below, PrP^C could also influence cellular signaling events by its involvement in endocytic pathways.

Several signaling pathways or signaling components, such as Akt, Fyn, cAMP, and Erk1/2, are modulated by PrP^C expression, its cross-linking, or its interaction with another protein. Antibody-mediated cross-linking of PrP^C induced activation of the Fyn, a family member of nonreceptor Src-related kinases, in neuronal differentiated cells in a caveolin-1-dependent manner[107]. As a downstream event, the same group claims to have identified Erk1/2 phosphorylation[108]. PrP^C cross-linking additionally modulates serotonergic receptor activity in differentiated neuronal cells[109]. The finding that PrP^C cross-linking modulates activity of serotonergic receptors in differentiated neuronal cells awaits replication and *in vivo* confirmation. However, Fyn activation and downstream activation of Erk1/2 were also seen in a hypothalamic cell line[110].

Several studies indicated PrP^C involvement in neurite outgrowth and neuronal survival. Chen et al. reported increased neuronal survival and neurite outgrowth from neurons when cultured on Chinese hamster ovary (CHO) cells transfected to express mouse PrP^C. Although Fyn activity in this context was involved mainly in neurite outgrowth, the PI3 kinase/Akt pathway as well as regulation of Bcl-2 and Bax expression contributed to the survival effect elicited by PrP^C. Cyclic AMP/ PKA and Erk signaling pathways contributed to both neurite outgrowth and neuronal survival[97, 99].

Some investigators suggested that engagement of PrP^C with stress-inducible protein I (STI1) induces neuroprotective signals that rescue cells from apoptosis via cAMP/protein kinase A and the Erk signaling pathways[111-112]. Interaction with STI1 induced different signaling pathways, promoting neuroprotection by PKA activation and neuritogenesis by activation of the MAPK pathway[98].

Endocytosis and Internalization of PrP^C. PrP^C is rapidly internalized from the cell membrane. This internalization of PrP^C could be crucial for its function, e.g., by influencing signal transduction pathways. Endocytosis of membrane receptors does not necessarily downregulate receptor activity. While being internalized, both tyrosine kinase and G protein-coupled receptors may remain activated and produce intracellular responses along the endosome-lysosome pathway[113]. Internalization of tyrosine kinase receptors was functionally important in studies: TrkA receptors, for example, mediate NGF-dependent cell survival while they are located at the cell membrane, whereas internalization is required for induction of neurite outgrowth[114-115].

The mechanism of PrP^C internalization is still controversial because both raft/caveolae and caveolae-like[116-119] as well as clathrin-dependent endocytosis may be operative[120-121]. These mechanisms may be equally important. In addition, internalization of the same ligand/receptor complex by distinct endocytotic pathways can result in different signaling outcomes. TGF-β receptor, for example, is degraded after endocytosis via caveolae, but internalization via clathrin-coated pits promotes its signaling[122]. However, in lymphocytes and neuronal cells that do not express caveolin, internalization can occur in a lipid raft-associated noncaveolar, clathrin-

independent process[123-124]. Therefore additional, less well-characterized endocytosis pathways including caveolae-like endocytosis might be involved in internalization of PrP^C.

For endocytosis by clathrin-coated pits, PrP^C would need to leave the lipid rafts prior to internalization because the rigid structure of raft lipids is unlikely to accommodate the tight curvature of coated pits. This phenomenon occurred after binding of copper to the OR[121, 125], but its physiological significance is unknown. Low-density lipoprotein receptor-related protein 1 (LRP1) was later described to mediate PrP^C endocytosis[126], and CC1 region was essential for its internalization in neuroblastoma cells[121, 125]. Sunyach et al. suggested that heparin sulfate proteoglycans are part of the endocytotic complex involving PrP^C (Ref [125]). Glypican-1, a GPI-anchored heparan sulfate-containing cell-associated proteoglycan, interacts and cointernalizes with PrP^C in N2a after induction with copper ions. In cells expressing PrP, which lacks the OR, internalization of glypican-1 is reduced, suggesting a possible role for PrP^C in the cointernalization of other cellular components[127].

PrP^C might participate in the correct localization of some other proteins in lipid rafts. Neuronal nitric oxide synthase (nNOS), for example, involved in various nervous system processes such as development, synaptic plasticity, regeneration, and regulation of transmitter release was associated with lipid rafts in wt mice. In contrast, in brains of PrP^C-deficient as well as scrapie-infected mice, nNOS was not associated with rafts, and activity of nNOS was reduced. Therefore PrP^C could be important for the proper cellular localization of other proteins[128]. Similarly N-CAM was recruited to lipid rafts by PrP^C (Ref [99]).

However, PrP^C is involved in a number of cellular functions and how endocytosis influences them in vivo remains widely unknown; internalization of PrP^C could contribute to downregulation of a signaling event but could also be necessary for signaling. However, a general involvement of PrP^C in vesicle formation could be a possible explanation for most of the suggested molecular functions of PrP^C because it could regulate signaling and influence synaptic transmission.

PrP and cell adhesion. Several reports are consistent with a possible function of PrP^C as a cell adhesion or recognition molecule. Some interaction partners of PrP^C identified so far have a role in adhesion, including laminin[129-130], a structural component of basement membrane, laminin-

receptor precursor[131-132], and N-CAM[133]. These three molecules are involved in adhesion in a diversity of signal transduction pathways, in differentiation, and in neurite outgrowth[134-135]. Interaction of laminin or N-CAM with PrP^C has been associated mainly with its suggested role in neuritogenesis and neurite outgrowth[99, 129-130]. Sales et al. also proposed that PrP^C in its synaptic location might stabilize opposing synaptic membranes through adhesive mechanisms[69].

The evidence reported so far could indicate that PrP^C is involved in adhesive mechanisms, but this is likely not its sole function. Adhesion molecules that interact biochemically with PrP^C could additionally transduce a PrP^C-dependent signal. The neurite-outgrowth-promoting interaction between PrP^C and N-CAM, for example, was associated with activation of Fyn[99].

5.2 Scientific aims

The peripheral neuropathy observed by Nishida et al. suggests that PrP^C plays a role in peripheral neuropathies.

The goal of this project was to revisit the status of peripheral nerves in mice from which the *Prnp* locus was inactivated.

I aimed to identify the cell type, neuron or Schwann cell, which is structurally or functionally affected by the lack of PrP^C and at which age this occurs.

Since PrP^C was reported to be expressed by neurons and Schwann cells, I sought to identify the cell type on which PrP^C would need to be expressed to maintain peripheral nerves.

By transcriptomics and proteomics approaches, I intended to unravel a molecular signature of the $Prnp^{-/-}$ neuropathy.

Furthermore, I sought to pinpoint PrP's function in peripheral nerves to certain protein domains.

5.3 Mice, material and methods

5.3.1 Mice

I housed mice and performed animal experiments in accordance with the Swiss Animal Protection Law and in compliance with the regulations of the veterinary office (canton Zurich). *Prnp*$^{o/o}$ mice[33] were kept on a mixed background (C57Bl/6;129Sv), or backcrossed to Balb/c for >17 generations. *Prnp*$^{Edbg/Edbg}$ and wt mice (both 129/Ola) were kindly provided by Jean Manson. Sciatic nerves of *Prnp*$^{Edbg/Edbg}$ mice[136] backcrossed for >8 generations to C57Bl/6 mouse strain were provided by Andrew Steele and *Prnp*$^{GFP/GFP}$ mice[137] by Walker Jackson. *Tg*GPI^{-}PrP mice (line 44)[138] were kindly provided by Bruce Chesebro and Michael Oldstone. *Tga20* mice[139], *tg*NSE-PrP and *tg*MBP-PrP mice[104], *tg*C4, *tg*E11, *tg*F35 (ref. [106]), *Prn*$^{o/o}$[140], and *Prnd*$^{-/-}$ mice[141], were kept on a mixed genetic background (C57Bl/6;129Sv). Apart from the *tg*GPI^{-}PrP, *tg*E11, and *tg*F35 lines, mice were maintained homozygous for the transgene. *Rag1*$^{-/-}$ mice [142] were intercrossed twice with *Prnp*$^{o/o}$ mice to obtain *Rag1*$^{-/-}$ *Prnp*$^{o/o}$ mice. *Tg*Dhh-Cre mice were provided by Dies Meijer, *tg*NFH-Cre and *tg*Prnp^{flox} by Giovanna Mallucci. *Tg*Dhh-Cre mice were first bred to *Prnp*$^{o/o}$ mice on an FVB background, provided by John Collinge and subsequently crossed to *tg*Prnp^{flox}. *Tg*Prnp^{flox} were either kept in homozygous breedings or crossed to *Prnp*$^{o/o}$ mice (FVB). *Tg*NFH-Cre were bred to *tg*Prnp^{flox} mice. For generation of *tg*PLP-PrP, the *Prnp* open reading frame was amplified by PCR using the following primers (forward [fw]: *Asc*I-PrP GGG GGC GCG CCa att tag gag agc caa gca ga; reverse [rev]: *Pme*I-PrP: CAG GTT TAA ACc acg aga atg cga agg aac a) and cloned (using restriction enzymes *Asc*I and *Pme*I) into a PLP promoter cassette kindly provided by Wendy B. Macklin. The transgenic construct was linearized by *Apa*I and *Sac*II. Transgenic constructs for generation of *tg*PrP$_{\Delta HC}$ and *tg*PrP$_{\Delta CC}$ are based on pPrPHG[139]. A *Pme*I/*Nhe*I fragment of pPrPHG was subcloned in pMECA backbone. To create *Prnp*$_{\Delta HC}$ and *Prnp*$_{\Delta CC}$ cDNA, this plasmid was used as template to obtain two PCR fragments for each construct. For *Prnp*$_{\Delta HC}$ primer sets RAMP fw (CTA TCA GTC ATC ATG GCG AAC C)/ RAMP 111 ex-rc (CCA AAA TGG ATC ATG GGC CTC ACA TGC TTG AGG TTG GTT T) and RAMP 111–134 fw (AAA CCA ACC TCA AGC ATG

TGA GGC CCA TGA TCC ATT TTG G)/ RAMP rc (CAT CAT CTT CAC ATC GGT CTC G) and for $Prnp_{\Delta CC}$ the sets RAMP fw/ RAMP 111-93 ex-rc (GCT GCC GCA GCC CCT GCC ACA CCC CCT CCT TGG CCC CAT C) and RAMP 93-111 fw (GAT GGG GCC AAG GAG GGG GTG TGG CAG GGG CTG CGG CAG C)/ RAMP rc were used. The resulting PCR product pairs either for $Prnp_{\Delta HC}$ or $Prnp_{\Delta CC}$ were purified, mixed in stoichiometric amounts, and annealed. The flanking primers RAMP fw and RAMP rc were then added and the fusion products were amplified. These products were purified, cloned into pMECA pPrPHG subcloning vector (using *Xma*I/*Bst*EII), and subsequently *Pme*I/*Nhe*I were used to clone the constructs into the pPrPHG plasmid. All linearized transgenic constructs were injected into fertilized $Prnp^{+/+}$ or $Prnp^{+/-}$ oocytes (C57Bl/6;DBA/2) and bred to $Prnp^{o/o}$ (B6/129Sv) and maintained as heterozygous lines. Transgene positive mice were identified by PCR using the following primer pairs: *tg*PLP-PrP (fw: TCA TTT TTA AGA ATG GGA CAG CTG G; rev: TTT GCT GGG CTT GTT CCA CT); *tg*$PrP_{\Delta CC}$ and *tg*$PrP_{\Delta HC}$ (exon 2 primer pE2 fw CAA CCG AGC TGA AGC ATT CTG CCT; exon 3 primer Mut217 rev: CCT GGG ACT CCT TCT GGT ACC GGG TGA CGC).

5.3.2 Short tandem repeat (STR) analysis

Genome-wide STR analysis of 206 distinct STRs was performed using fluorescently labeled primers (**Supplementary Table 1**). Genomic DNA was purified from tail biopsies and amplified by PCR using 1-5 ng of DNA, 7.5 ml of 2x PCR colorless Taq-mastermix (Promega), 1.5 µl fluorescently labeled primer mix (FAM, VIC, NED, all from Applied Biosystems). Cycling conditions were: 95°C 5 min, 30 repetitions of 95°C for 30 s, 60°C for 30 s and 72°C for 30 s, followed by 72°C for 7 min. PCR reactions were diluted 1:100 in deionized water. Subsequently, 2 µl of the diluted reactions were added to 10 µl of Hi-Di Formamide (Applied Biosystems) containing 0.04 µl GeneScan 600LIZ size standard (Applied Biosystems) per well. Samples were denatured at 94°C for 2 min and subjected to electrophoresis on a 16-capillary sequencer 3130xl (Applied Biosystems). Analysis, allele-calling, binning and calibration of various mouse

strains was done manually and in combination with an in-house developed software (Applied Biosystems).

5.3.3 Ultrastructural investigations

Mice were anesthetized and transcardially perfused with PBS followed by fixative (3.9% glutaraldehyde in 0.1 M phosphate buffer, pH 7.4). Tissues were embedded in Epon using standard procedures. Semithin sections (500 nm) were stained with 1% toluidine blue. Ultrathin sections (70-90 nm) were mounted on copper grids coated with Formvar membrane and contrasted with uranyl acetate and lead citrate. The specimens were examined using a Philips CM12 electron microscope (FEI, Eindhoven, The Netherlands) operating at 80 kV and pictures were taken with a Gatan Bioscan 1k x 1k digital camera (Gatan GmbH, Munich, Germany). For morphometrical analysis of axon size-density distribution, semithin sections of at least three different mice per genotype were photographed and analyzed by a semi-automatized software developed in-house. Axonal density or cumulative axonal density was plotted against axonal size (area in μm^2). Mean and standard error of the mean (s.e.m.) are displayed. S.e.m. did not always result in visible error bars. G-ratio and onion bulb formation were assessed on electron microscopy images and quantified using Analysis software (Olympus) and homebred scripts.

5.3.4 Immunohistochemistry

Sciatic nerves were dissected and either fixed in 4% formalin and embedded in paraffin, or snap frozen in OCT medium. Longitudinal paraffin sections (2 µm) and frozen sections (10 µm) of sciatic nerves were incubated with the following antibodies: rat anti-CD68 for macrophages (Serotec MCA 1957; 1:100), rabbit anti-CD3 for T-cells (clone SP7, NeoMarkers; 1:300) or rat anti-B220/CD45R for B-cells (Pharmingen; 1:400). Secondary antibodies were: goat anti-rat IgG (Caltag lab R40000; 1:150) followed by donkey anti-goat, conjugated with alkaline phosphatase (Jackson lab 705-055-147; 1:80) or followed by donkey anti-goat conjugated with peroxidase (Jackson lab 705-035-147; 1: 200) or goat anti-rabbit conjugated with peroxidase (Jackson lab

111-035-144; 1:200). Slides were mounted in DAKO aqueous mounting medium and analyzed on an Axiophot microscope (Zeiss), equipped with a JVC digital camera (KY-F70; 3CCD).

5.3.5 Electrophysiological investigations

Motor nerve conduction of sciatic nerves in 12, 28, 35, or 53-week old anesthetized mice was investigated as described[143]. Upon supramaximal stimulation of the tibial nerve at the ankle ("distal") and stimulation of the sciatic nerve at the sciatic notch ("proximal"), the compound muscle action potentials (CMAP) were recorded with needle electrodes in the foot muscles. Nerve conduction velocities in meter per second were calculated from distal and proximal latencies. F-wave latencies were recorded and the shortest latencies were taken upon repeated stimulation at the ankle.

5.3.6 Western Blots and ELISA

Sciatic nerves were homogenized in buffer (1% Triton X 100, 137 mM NaCl, 2 mM EDTA, 20 mM Tris HCl pH 8) using a polytron PT 3100 (kinematica). Protein concentration was measured using BCA protein assay (Pierce). 20 µg of total protein were boiled in LDS (Invitrogen) containing 5% β-mercaptoethananol and electrophoresed through a NuPAGE® Novex 12% Bis-Tris Gel (Invitrogen). For PNGase F treatment, 20ug of protein were incubated in denaturation buffer and subjected to a 2 hours PNGase f (NEB) digest at 37°C. All gels were transferred to nitrocellulose (Schleicher & Schuell) using XCell II Blot Module (Invitrogen). Membranes were blocked with TBST containing 5% Top-Block (Sigma), decorated with monoclonal antibody POM1 or POM3[144], antibodies against CNPase (Abcam), MPZ (P0), MAG (Zymed), PMP22 (Abcam), NRG-1 (C20 and H210, Santa Cruz), Erk, p-Erk, Akt, p-Akt (Cell Signaling Technology), flotillin (BD Bioscience) followed by incubation with the secondary anti-mouse IgG_1 (Zymed) or anti-rabbit IgG (Calbiochem) and visualized using SuperSignal West Pico Chemiluminescent Substrate System (Pierce) and Amersham Hyperfilm ECL films (GE

Healthcare). In addition, PrP^C concentration was determined by sandwich ELISA with biotinylated mAbs as previously described[144]. 96-well plates were coated with 400 ng/ml of POM1 antibody overnight at 4°C. Plates were washed with PBS containing 0.1 % (v/v) Tween 20 (PBST) and blocked with 5% TopBlock in PBST for 2 h at room temperature. After washing, wells were incubated with nerve homogenates 150 µg/ml in 1% TopBlock/ PBST for 2 h at room temperature or with serially diluted recombinant PrP as standard. After washing, plates were incubated with biotinylated POM2 antibody for detection (1:10,000), followed by incubation with avidin-HRP (Pharmingen No. 554058; 1:10,000), both in 1% TopBlock/ PBST. Plates were developed with 2.2-azino-diethy-benzothiazolinsulfonate (Boehringer), and optical density was measured at 405 nm. Homogenates from *Prnp*$^{o/o}$ sciatic nerves served as control.

5.3.7 Extraction of detergent-resistant membranes and step density gradient centrifugation

Experimental procedure was performed as previously described[2] with slight modifications. Sciatic nerves were homogenized in PBS with 9% sucrose including protease inhibitors (complete, Roche) to produce a 10 % (w/v) homogenate. After centrifugation (5 min, 2,500 rcf, 4°C), protein concentration was measured with BCA (Pierce). Triton X-100 extraction was performed with 100 µg of total protein for 1 h on a rotation wheel at 4°C in a final volume of 100 µl lysis buffer (PBS with 9% sucrose and final concentration of 1% Triton X-100). Extracts were mixed with two volumes (200 µl) of 60% Optiprep (Axonlab) to reach a final concentration of 40%. All lysates were loaded at the bottom of Beckman ultracentrifuge tubes. The lysate was then overlaid with an Optiprep step gradient in MES Buffer (10mM MES, 2mM EDTA, 1mM DTT, protease inhibitors): 1.6 ml of 30% Optiprep and 300 µl of 5%. Total volume of the gradient was 2.2 ml, gradients were centrifuged for 2 h at 55,000 rpm at 4°C in a TLS55 Beckman rotor. Fractions of 200 µl were collected and analyzed by Western blot.

5.3.8 RNA isolation and quantitative PCR

Sciatic nerves were homogenized in trizol (Invitrogen) by using polytron PT 3100 (kinematica). RNA was extracted and subsequently purified on RNeasy columns (Qiagen) as described by the manufacturers. Synthesis of cDNA was performed with QuantiTect, Reverse Transcription kit (Qiagen). Samples were analyzed by real-time PCR using QuantiFast SYBR Green PCR kit (Qiagen) and 7900HT (Fast Real-Time PCR systems; Applied Biosystems). The following primer combinations were used: *Prnp* fw: TGGCTACATGCTGGGGAGC, *Prnp* rev: TTCTCCCGTCGTAATAGGC; *Prnd* fw: CTA CGC GGC TAA CTA TTG, *Prnd* rev: CGC CGG TTG GTC CAC; GAPDH fw: CCA CCC CAG CAA GGA GAC T; GAPDH rev: GAA ATT GTG AGG GAG ATG CT.

5.3.9 Immunofluorescence

Freshly cut frozen sections (10 µm, air-dried) and dissociated mouse DRG cultures on cover slips were fixed/ permeabilized using ice-cold ethanol or methanol (-20°C). Sections were blocked in either 5% BSA and 0.3% Triton X-100 (Sigma) in PBS, 3% BSA and 3% donkey serum (Jackson ImmunoResearch Laboratories), 3% BSA and MOM Blocking reagent (Vector lab), or 2% FCS. Antibodies were diluted in blocking buffer or in antibody diluent (Ventana). Antibodies against the following antigens were used: sodium channel (Sigma), PrP^C (POM1)[144], Neurofascin (Abcam), paranodine/Caspr (provided by J.A. Girault), Versican (V1, provided by M.T. Dours-Zimmermann), JamC (Santa Cruz), Neurofilament NF-H (Calbiochem), MBP (Serotec). POM1 antibody was directly labelled with Alexa Fluor dye 488 (Invitrogen) as previously described for Cy5-labelling of POM2[137]. For detection of the remaining primary antibodies, the following secondary antibodies were used: biotinylated anti-mouse IgG (Vector laboratories)/ streptavidin Alexa 488 (Invitrogen), anti-rabbit Alexa 594 and anti-rat Alexa 488 (Invitrogen). Slides were mounted in DAKO aqueous mounting medium. Images were acquired on an Olympus BX61TRF fluorescent microscope equipped with an F-View camera. JamC positive area was quantified with Analysis software (Olympus). Each data point represents the

mean value of one mouse, which is derived from three independent visual fields per mouse. At least n=3 mice were analyzed.

5.3.10 *In situ* hybridization

Sense and antisense probes for *Prnp* were derived from a pBluescript KS plasmid containing a 290bp *Asp*718/ *Bst*EII fragment of mouse *Prnp*. Probes were digoxygenin (DIG) labelled as described by the manufacturer with a DIG-labeling kit (Roche). *In situ* hybridization was performed on freshly cut frozen sections (10µm, air-dried) post fixed in 4% PFA in PBS. Following treatment with 0.1M HCl and acetylation, sections were prehybridized for 2 h in hybridization buffer without probe (50% formamide, 5x SSC, 5x Denhardt's solution, 250µg/ml E. coli t-RNA (Roche)). Hybridization was performed with hybridization buffer containing 50ng x $50\mu l^{-1}$ DIG-labelled RNA sense or antisense probe which was previously denatured at 85°C for 5 min. Sections were incubated first for 30 min. at 85°C, and then over night at 58°C. Washing was performed in pre-warmed SSC of different concentrations. Sections were incubated with AP conjugated anti-DIG antibody (Roche) diluted 1:3,000 in buffer 1 (100mM Tris-HCl pH 7.5; 150mM NaCl) containing 1% blocking reagent (Roche). Detection was performed in buffer 3 (100mM Tris-HCl pH 9.5; 150mMNaCl; 50mM MgCl2) containing 1mM Levamisol; NBT and BCIP (Sigma). Slides were mounted in DAKO aqueous mounting medium and analyzed by microscopy as described above.

5.3.11 In vitro myelination

Cultures and analyses of dissociated mouse DRG cultures were performed as described[145] with slight modifications. Prior to culturing, round coverslips (18mm, Menzel-Gläser, Merck AG, CB00180RA1) were placed in 12 well plates (Nunc) and coated with Poly-D-Lysine (PDL, Sigma P6407-5MG) and collagen (BD Bioscience, #354236). For PDL coating, PDL was dissolved in sterile water at 1 mg/ml. Aliquots were stored at –20 ºC as 100x stock solution or diluted in tissue culture grade sterile water. 400 µl of the final solution were placed on each

cover slip and left in the tissue culture hood for at least 1 h. After removing the PDL solution, coverslips were washed twice with sterile tissue culture grade water. After removing the last wash, they were left to dry in the tissue culture hood. Prior to collagen coating, the collagen solution was diluted 2:1 (20 ml collagen solution plus 10 ml 0,02% acetic acid in water) to a concentration of 2.2 mg/ml. 400 µl were put onto each coverslip. 300 µl of the collagen solution were sucked back into the pipette. When all the coverslips were covered, the collagen is gelled by exposure to ammonia fume. The 12-well plates were placed without the lid in a styrofoam box with a Whatman paper on the bottom. Several drops of ammonia solution (28%) were spotted on the Whatman paper, the lid of the styrofoam box was closed and left for 15 minutes in the hood. After removing them from the styrofoam box, 12-well plates were left in the hood to dry completely (usually overnight). Embryos (embryonal day 13) were dissected under the binocular in ice-cold L-15 Medium (Leibovitz's L-15 Medium, Invitrogen, 31415-029). DRGs were separated and collected on the bottom of a 15 ml tube by centrifugation (700 rpm, 3 min). DRGs were washed with 1 ml Trypsin 0.25% w/o EDTA in PBS and centrifuged again (700 rpm, 1 min). 1.5 ml Trypsin 0.25% w/o EDTA in PBS were added and DRGs were incubated for 45 min at 37°C. DRGs were again collected by centrifugation (700 rpm, 5 min). DRG cells were separated and resuspeded in 1 ml of M1-medium: MEM (#41090, Invitrogen), containing Glutamax (Invitrogen), 10% FCS (Perbio Science), Penicillin/ Streptomycin (Invitrogen), and nerve growth factor (mouse NGF 2.5S grade II, N-100, alomone labs) at a concentration of 50 ng/ml. Cells were counted and 30.000 dissociated living cells were seeded in the middle of the PDL/collagen coated coverslip in a drop of 80 µl M1-medium. After overnight incubation in the tissue culture incubator, 1 ml of M1-medium is added. Medium needs to be replaced every other day. At day 6-7 in culture, myelination was initiated by supplementing the medium with 50 µg/ml Ascorbic acid (Sigma A4544). Again, the medium needs to be replaced every other day.

5.3.12 Behavioral tests

Hot plate test: To measure pain threshold, mice were placed on a hot plate (constant temperature: 52 ± 0.5°C). The parameter recorded was the latencies to lick a hind-paw, or jump. If no licking or jumping responses occurred, mice where removed after 60 seconds. Each animal is tested only once and mice are not habituated to the apparatus prior to testing. *Grip strength test:* To test grip strength, mice were carefully picked up by the base of the tail and lowered towards a horizontal wooden bar (diameter 3 mm). After grasping the bar they were gently pulled back until they let go of the bar. The bar was attached to a spring balance (maximum 300 g) that allowed determining the force at which the mice released their grip. Grip strength was tested five times in a row with an interval of two minutes between trials. *Accelerating rotarod test:* Mice were placed on a rotating rod with a speed slowly accelerating from 4 to 40 rpm (Ugo Basile, model 47600, Comerio, Italy). Maximum speed was reached after 245 s. The latencies at which the animal fell off the rod were recorded. Animals not falling off were removed after 300 s. Mice were tested five times in a row with an interval of 30 minutes between trials. The median is recorded (untrained mice). Fourty-eight hours later, the same mice are tested again five times, again the median latency to fall is recorded (trained mice).

5.3.13 2D Difference gel electrophoresis (2D DIGE) of peripheral myelin

An overview over the experimental setup is shown (**Fig. 6**). Myelin was extracted from sciatic nerves of 7 mice per genotype in the age of 28 days. Nerves were homogenized in 0.29 M sucrose including protease inhibitors (complete, Roche). Sucrose gradient was set up by filling 17 ml 0.85 M sucrose in a centrifugation tube, and adding homogenate in 17 ml 0.29 M sucrose on top. Samples were separated by centrifugation at 75,000 g for 45 min. Interphases were collected and transferred into a new centrifugation tube which was filled with distilled water and centrifuged (15 min, 75,000 g). Supernatant was removed, again. For osmotic shock, water was added to the myelin pellet and the sample is incubated for 10 min. The sample was centrifuged 15 min, 12,000 g. The pellet was dissolved in the appropriate buffer: TBS (137 mM NaCl, 20

mM Tris/HCl, pH 7.4) for DIGE or nerve lysis buffer (137 mM NaCl, 20 mM Tris/HCl, pH 8, 2mM EDTA, 1% Triton X100), including complete protease inhibitors (Roche) for confimatory Western blots. For DIGE experiments, myelin (containing 480 μg proteins in 300 μl) was delipidated by adding 600 μl of methanol and vortexing, followed by addition of 300 μl chloroform and vortexing, and addition of 450 μl of water and centrifugation (1 min., 9,000 g). Upper phase was discarded. Again, 450 μl of methanol were added, sample was vortexed and centrifuged (5 min., 16,100 g). Supernatant was discarded. The pellet was dried and dissolved in lysis buffer (7M Urea, 2M Thiourea, 2% ASB-14, 20mM Tris pH 9.0), protein concentration was determined using 2D Quant Kit (GE Healthcare). 80 μg of each sample (2x wt, 2x *Prnp*$^{-/-}$) was used for each gel. A pool of all the samples served as control and was labelled with Cy2. The four samples were once labelled with Cy3 and once with Cy5 (for dye switch), resulting in 8 aliquots for 4 gels (on each gel a pair of wt and *Prnp*$^{-/-}$ beside the standard was loaded). CyDyes (GE Healthcare) was dissolved in DMF (Dye working solution: 400 pmol/μl). For labelling, 1 μl of Dye working solution was added to each sample, or 4μl Cy2 to the standard, mixed by vortexing, briefly centrifuged, incubated at 4°C for 30 min. Then, 1 μl of lysine solution was added to each sample, vortexed, briefly centrifuged, 10 min. incubated at 4°C. The same volume of sample buffer (7 M Urea, 2 M Thiourea, 2 % ASB-14, 1.5 % DTT, 1% Ampholytes 10μl/ml) was added (total volume 153 μl) and sonication was performed. Rehydration buffer (7 M Urea, 2 M Thiourea, 2% ASB-14, 0,5% Immobiline/Ampholytes 5μl/ml) was added to a total volume of 360 μl, sample was centrifuged. For isoelectric focussing (IEF) an IPGphor (GE Healthcare) was used, 340 ml of sample were loaded onto an IPG (immobilized pH gradient)-strip (GE Healthcare, 18 cm, pH 3-11), covered with mineral oil and exposed to an electric field: 50V, 12h, 12 μA (8-9 μA at the beginning); 300V, 1h, 13 μA; 1000V, 1h, 14 μA; 1000-3000V, 0.5h, 14.5 μA; 3000V, 3h, 17,5 μA (12 μA at the end of this step); 3000-8000V, 0,5h, 18 μA; 8000V, 4h, 22 μA (31 μA at the beginning, and 26-27 μA at the end). IGP-strips were equilibrated in SDS-Equilibration buffer (50 mM Tris/HCl pH 8.8, 6 M Urea, 30 % Glycerol, 2 % SDS, 0.002 % bromphenol blue), including 1 % DTT (equilibration 2 x 5 min.) or 4% Iodacetamid (equilibration 1 x 10 min.). IGP-strip was loaded on top of a 8-16 % gradient gel and run at 6 mA per gel (200

V) over night. SeeBlue® Plus2 Pre-Stained Standard (Invitrogen) was used as a molecular weight standard. Gels were scanned using a Typhoon-Scanner (GE Healthcare), data was analyzed using proteomweaver 3.1 software (Definiens, Munich, Germany).

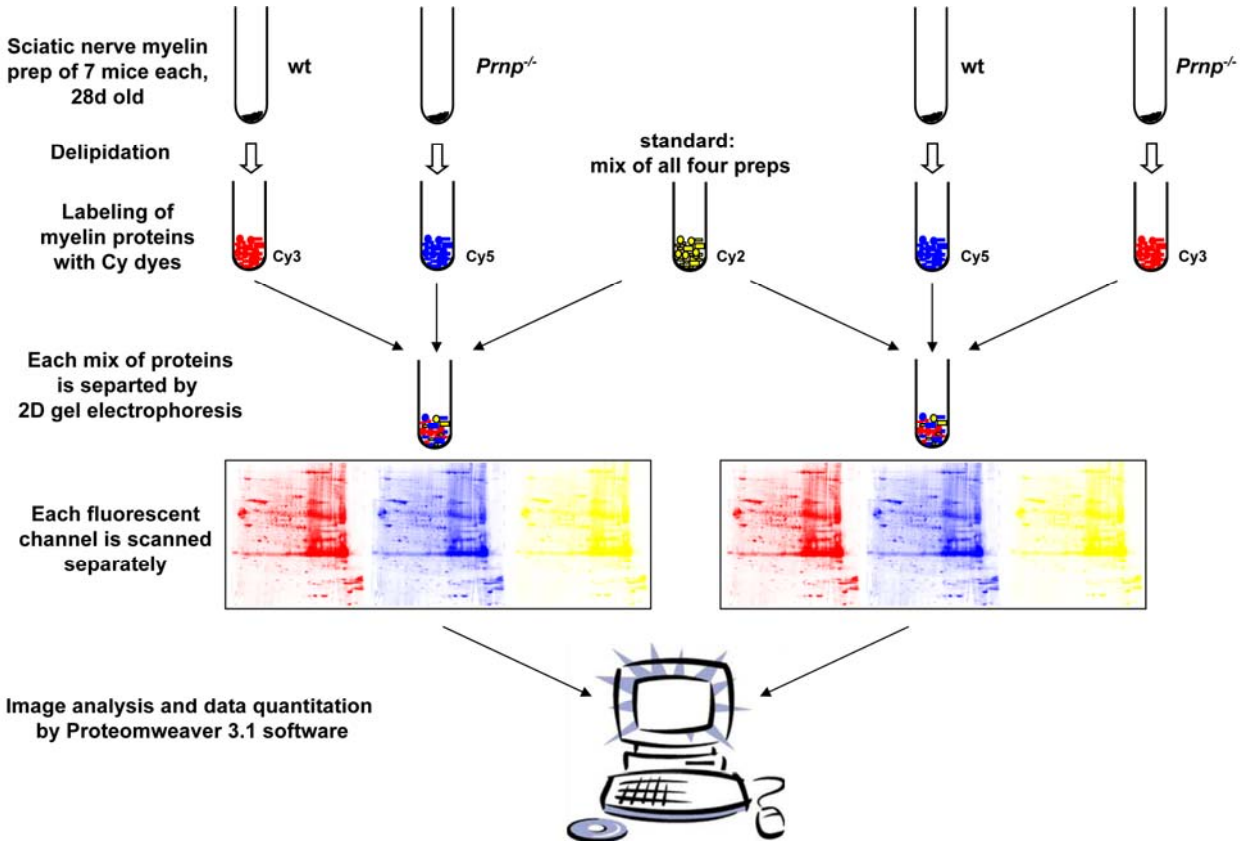

Figure 6. Experimental setup of the DIGE experiment. Setup is shown for one pair of wt and *Prnp*$^{-/-}$ samples, the schema shows the principle of dye switch and use of the standard sample in each of the two gels.

5.3.14 mRNA microarray experiment of peripheral nerves

RNA was extracted from sciatic nerves by homogenizing them in Trizol (Invitrogen), extracting RNA with chloroform, and further purification using RNeasy (Qiagen) as described by the manufacturer. RNA quality was tested by Bioanalyser (Agilent), only samples with RNA integrity index (RIN) of at least 7.45 were used for further analysis. For microarray, 600 ng of RNA were used. RNA was first reversely transcribed into cDNA which was then transcribed into fluorescent cRNA using Cyanine 3-CTP and the Low RNA Input Linear Amplification Kit (Agilent) as

described by the manufacturer. RNA Spike-In Kit, one color, was added to each RNA sample for control. Fluorescent cRNA was purified using RNeasy (Qiagen). Quality of labelled cRNA was tested using Nanodrop (Thermo Scientific). For further analysis only those samples with a yield of at least 2 μg were accepted. Dye incorporation rate – calculated as 1000 x (pmol/ μl divided by ng/ μl) – was between 9.0 and 14.3 pmol/ ng. Hybridization was performed using whole mouse genome 4x44K microarrays (Agilent) and the gene expression hybridization kit (Agilent) as described by the manufacturer. Assembled chambers of sandwiched slides were placed in the hybridization oven for 17 hours at 65°C at 10 rpm. After hybridization, chambers were disassembled in wash buffer 1 (Agilent), washed in buffer 1 followed by buffer 2 (Agilent) and placed into the scanner (Agilent).

5.3.15 Statistical analysis

For comparison of normally distributed data, including density of digestion chambers, and electrophysiological measurements of *Prnp*$^{o/o}$ compared to wt mice, I performed unpaired, two-tailed student's t-tests after equality of variances was tested by the F-test. In the case of unequal variances (density of digestion chambers in 30-week old mice), unpaired t-test with Welch's correction was used. For comparison of JamC positive area of *tg*NSE-PrP, *tg*PLP-PrP, wt and *Prnp*$^{o/o}$, I performed first one-way ANOVA followed by Bonferroni's post-test for multiple comparisons. For statistics on behavioral test results, and on STR analysis, I performed Mann-Whitney tests. For statistical analysis of fibers with g-ratio > 0.81, I performed square root transformation, followed by two-tailed student's t-test. For statistics on onion bulb formation, two-tailed Fisher's exact test was used. P-values were as indicated in the figures. SPSS (SPSS Inc.) and Prism software (GraphPad Software) were used for statistical tests. Error bars in the graphs and numbers following the ± sign represent standard deviation (s.d.) unless otherwise indicated.

5.4 Results

5.4.1 Peripheral polyneuropathy in *Prnp*$^{-/-}$ mice

At 60 weeks of age, all investigated PrP^{C}-deficient mice (*Prnp*$^{o/o}$; n=52) showed extensive chronic demyelinating polyneuropathy (CDP) (**Fig. 7**). CDP was 100% penetrant and was evident in all investigated peripheral nerves including sciatic and trigeminal nerves as well as dorsal and ventral spinal roots. Identical pathologies were detected in sciatic nerves of *Prnp*$^{o/o}$ mice on a C57Bl/6;129Sv (B6/129Sv) hybrid background (data not shown), *Prnp*$^{o/o}$ mice backcrossed to Balb/c mice for >17 generations (**Fig. 7**), *Prnp*$^{Edbg/Edbg}$ mice (inbred 129/Ola; n=6, **Fig. 7**), *Prnp*$^{Edbg/Edbg}$ backcrossed to C57Bl/6 mice for >8 generations (n=2, data not shown), and *Prnp*$^{GFP/GFP}$ mice carrying a targeted substitution of *Prnp* with EGFP[137] (n=3; **Fig. 7**). No signs of neuropathy were detected in age- and strain-matched wt mice (C57Bl/6, B6/129Sv, Balb/c, 129/Ola; **Fig. 7** and data not shown). Axon morphometry showed that large fibers (**Fig. 8**) were predominantly affected. Genetic reintroduction of PrP^{C} via crosses to *tga20* mice[139] (n=3), or introduction of one hemizygous *Prnp* allele (n=4), fully prevented the polyneuropathy (**Fig. 7-8**). The *Prnd* gene encodes the PrP^{C} analogue, Dpl, whose overexpression can induce neurodegeneration in certain *Prnp*$^{-/-}$ strains[36]. However, it was also suggested that Dpl might partly compensate for loss of function in *Prnp*$^{-/-}$ mice[36]. In order to uncover any potential contribution of Dpl to the CDP, I investigated *Prn*$^{o/o}$ mice lacking both *Prnd* and *Prnp*[140]. Morphology, extent of degeneration (or demyelination), and ultrastructural features of the CDP in 60-week old *Prn*$^{o/o}$ mice were similar to those of *Prnp*$^{o/o}$ mice, whereas mice selectively lacking *Prnd* but retaining *Prnp*[141] showed normal sciatic nerve morphology (**Fig. 9**). In contrast to *Prnp*$^{Ngsk/Ngsk}$ mice, I did not detect any *Prnd* mRNA in sciatic nerves of *Prnp*$^{o/o}$ mice (**Fig. 9**).

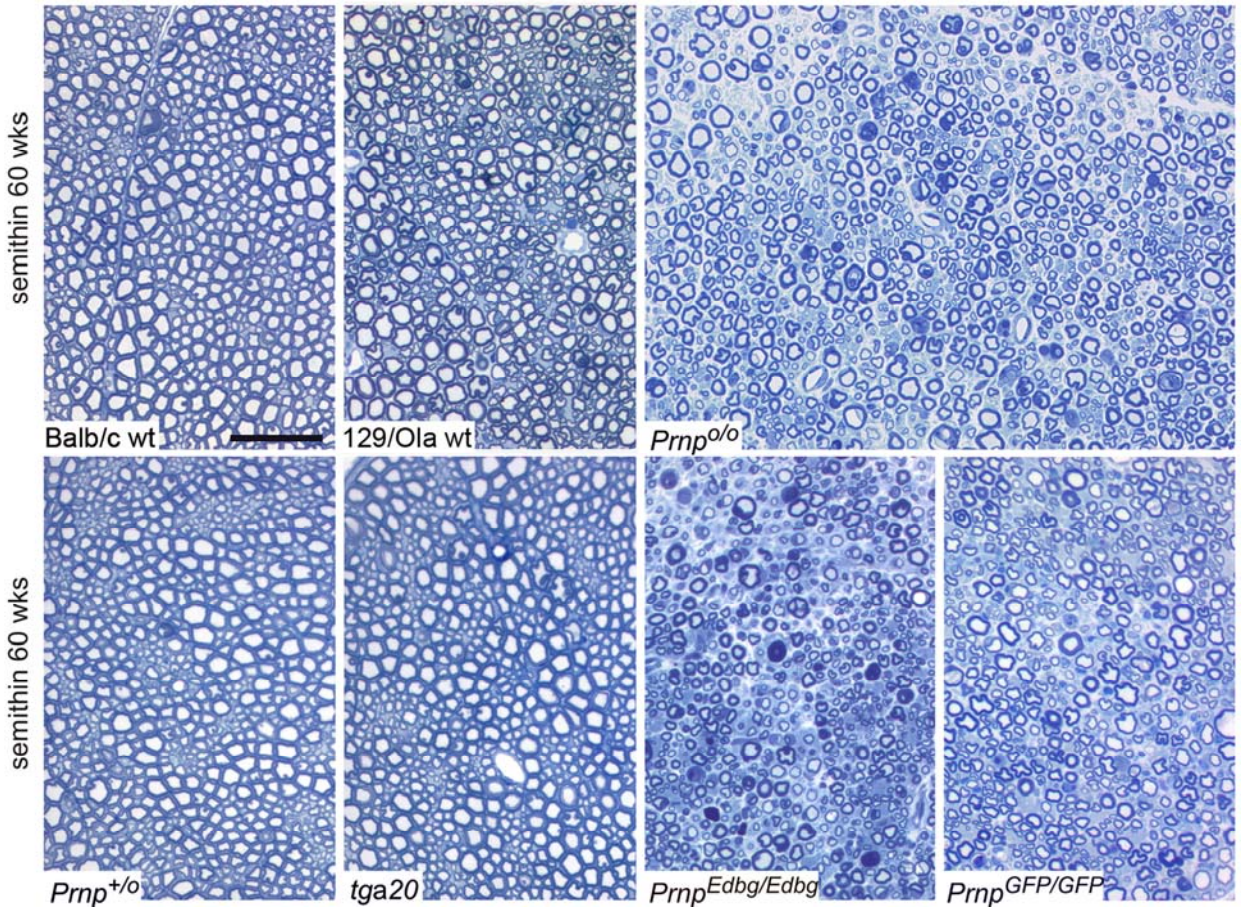

Figure 7. Peripheral polyneuropathy in *Prnp*$^{o/o}$ mice. Toluidine blue-stained semithin cross sections of sciatic nerves of wt (Balb/c and 129/Ola), *Prnp*$^{o/o}$ (Balb/c), *Prnp*$^{+/-}$(Balb/c), and *tga20* (B6/129Sv), *Prnp*$^{Edbg/Edbg}$ (129/Ola), *Prnp*$^{GFP/GFP}$ (C57Bl/6) mice, all at 60 to 70 weeks of age (wks).

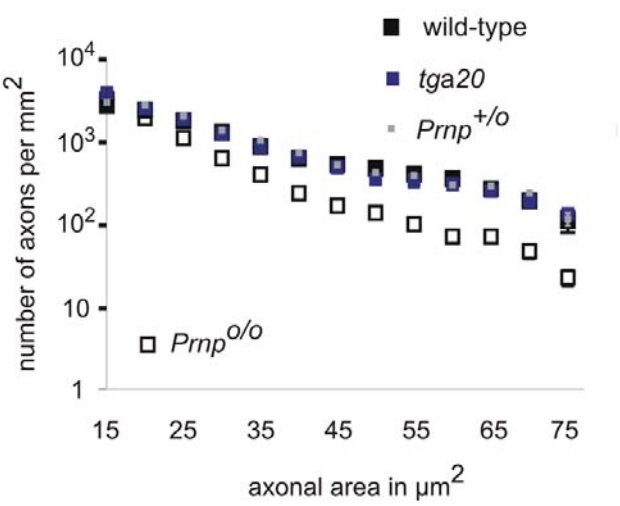

Figure 8. Axonal density-size distribution. Axonal density within nerves (number of axons/mm^2) was quantified morphometrically and plotted against the cross-sectional areas (µm^2) of axons.

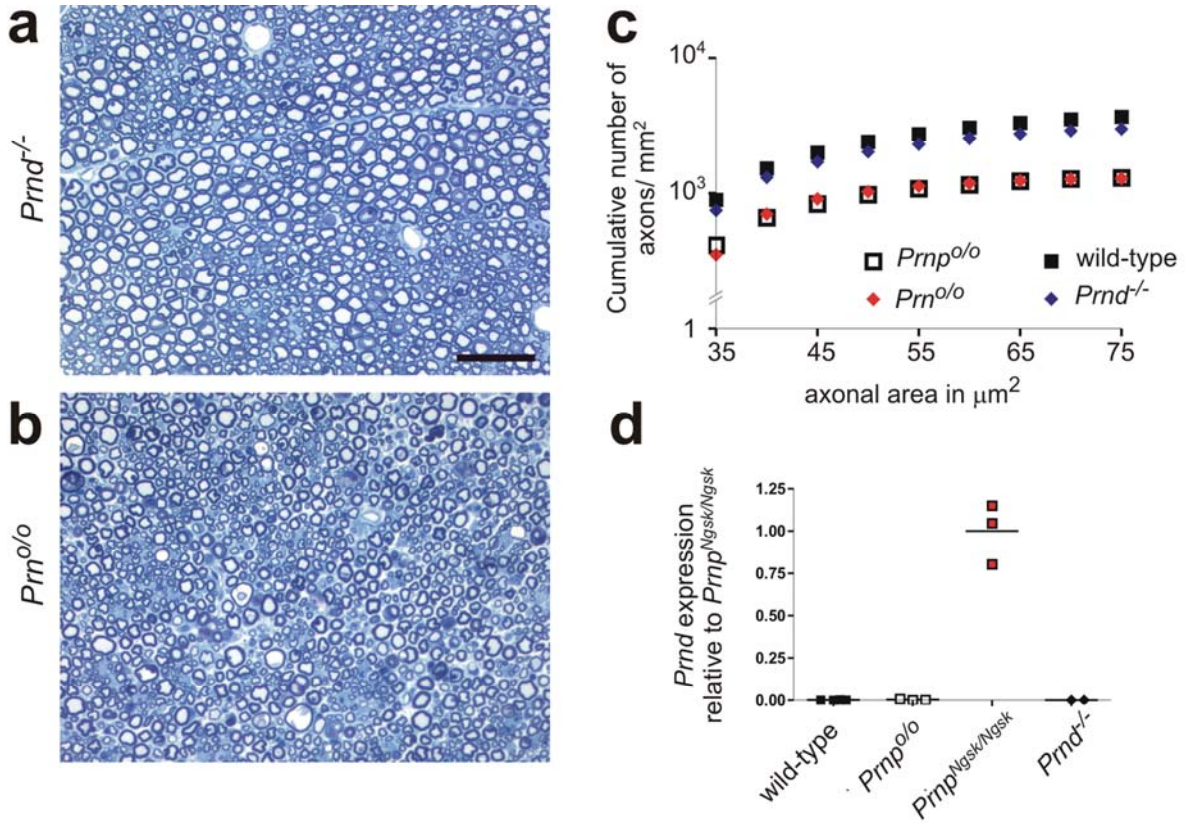

Figure 9. No role for Doppel in *Prnp$^{o/o}$* polyneuropathy. Semithin cross sections of sciatic nerves of mice lacking Doppel gene (*Prnd$^{-/-}$* mice), and mice lacking both, *Prnp* and *Prnd* (*Prn$^{o/o}$* mice) at 60 weeks of age, both on a mixed B6/129Sv background (**a** and **b**). Quantitation of cumulative axonal density-size distribution is shown compared to wt, and *Prnp$^{o/o}$* mice (**c**). *Prnd* mRNA expression in wt, *Prnp$^{o/o}$*, *Prnd$^{-/-}$* compared to *Prnp$^{Ngsk/Ngsk}$* mice. Scale bar = 50 μm.

CD68 immunostaining detects macrophages ingesting myelin debris of degenerating nerve fibers ("digestion chambers"), and proved to be a sensitive marker of early pathology in PrP^{C}-deficient nerves. CD68^{+} digestion chambers were significantly more prevalent in sciatic nerves of 10-, 30- and 60-week old *Prnp$^{o/o}$* mice than in age-matched wt mice (**Fig. 10**), indicating that the onset of polyneuropathy was much earlier than previously appreciated.

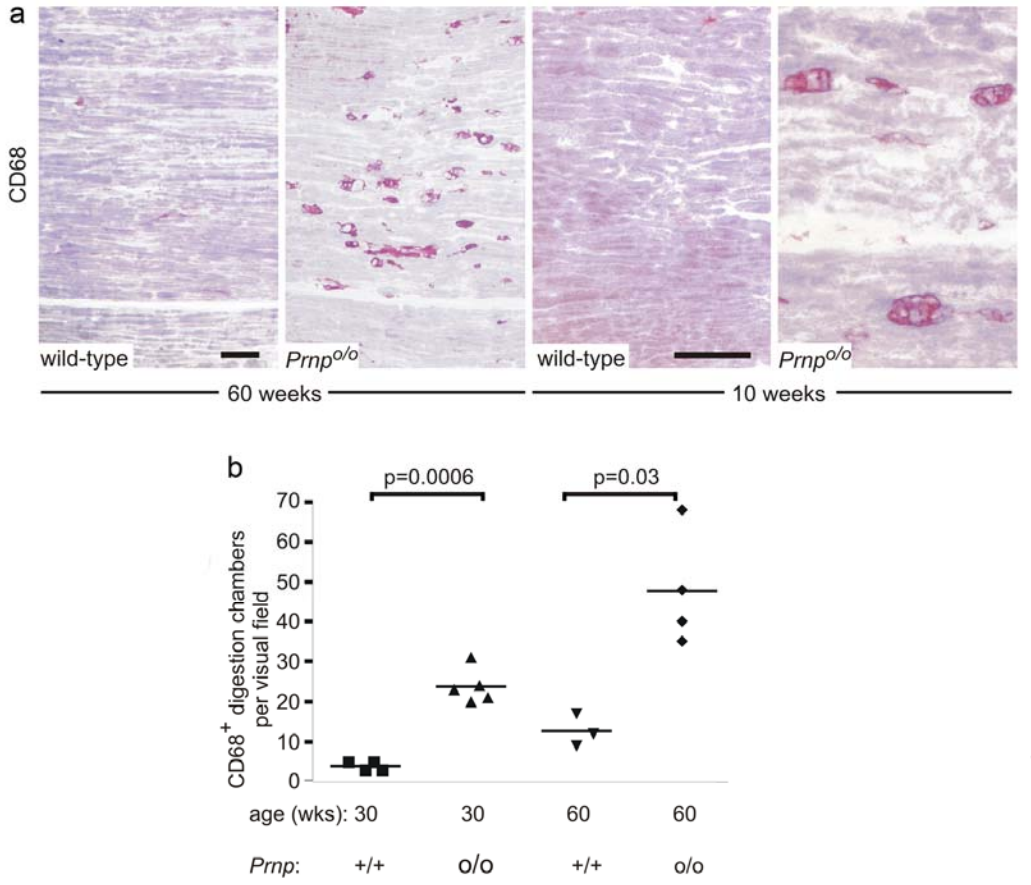

Figure 10. CD68^{+} gigestion chambers. CD68-immunostained longitudinal sections of sciatic nerves. More digestion chambers with macrophages and myelin debris are visible in *Prnp*$^{o/o}$ (Balb/c) than in wt (Balb/c) nerves at 60 and 10 weeks of age, respectively (**a**). Quantification shows significantly more digestion chambers in sciatic nerves of 30- and 60-week old *Prnp*$^{o/o}$ mice (**b**). All scale bars = 50μm.

5.4.2 The polyneuropathy of *Prnp*$^{o/o}$ mice is demyelinating

Peripheral neuropathies can target either axons, myelin sheaths, or both. Disruption of each of these structures gives rise to stereotypical, ultrastructurally and electrophysiologically recognizable phenotypes. I therefore analyzed nerves by electron microscopy (EM) and electrophysiology. Sciatic nerves of 60-week old *Prnp*$^{o/o}$ mice showed characteristic ultrastructural signs of demyelination. Whereas the ratio between myelin thickness and axonal diameter was constant in sciatic nerves of wt mice (**Fig. 11**), *Prnp*$^{o/o}$ nerve fibers displayed thinned myelin sheaths despite normal axonal morphology (**Fig. 11**). Quantification of the g-ratio (axonal diameter/fiber diameter) revealed a higher percentage of fibers with thinned myelin (g-ratio > 0.81) in *Prnp*$^{o/o}$ than in wt mice (**Fig. 12**). Several axons were covered only by a single

layer of myelin, suggesting incipient remyelination. “Onion bulbs”, resulting from repeated cycles of de- and remyelination and eventual Schwann cell degeneration, encircled 2.1 ± 0.54% of fibers in 4 of 4 *Prnp*$^{o/o}$ nerve but no fibers of wt nerves (**Fig. 11b-c,** p=0.029). Demyelinated axons were occasionally surrounded by remyelinating Schwann cells with prominent rough endoplasmic reticulum (**Fig. 11d**). Some *Prnp*$^{o/o}$ nerve fibers were covered by abnormally thick myelin sheaths resulting from focal myelin folding, often associated with nodes of Ranvier (**Fig. 11e**). Macrophages occasionally invaded the space between myelin sheaths and axons (**Fig. 11f**). In wt Remak bundles, several unmyelinated nerve fibers were ensheathed by single Schwann cells (**Fig. 11g**). In contrast, *Prnp*$^{o/o}$ Remak bundles often displayed reduced numbers of unmyelinated fibers combined with abnormal branching of Schwann cell processes (**Fig. 11h**). Collagen pockets, possibly indicating axon loss, were present in *Prnp*$^{o/o}$ nerves but absent from wt nerves (data not shown).

I then determined the onset of CDP by investigating younger mice. Electron microscopy of 30-week old *Prnp*$^{o/o}$ mice revealed morphological alterations and g-ratio deviations that were less pronounced, yet qualitatively similar, to those of 60-week old *Prnp*$^{o/o}$ mice (**Fig. 12** and data not shown). In contrast, morphological alterations were absent from 10-week old mice with the exception of a small number of digestion chambers (**Fig. 10**), suggesting disrupted myelin maintenance rather than impaired myelination. Accordingly, expression and phosphorylation of the Akt and Erk kinases, which are crucially involved in myelination[146], were unaffected in 10- and 30-day old *Prnp*$^{o/o}$ nerves (**Fig. 13**), and there was no difference in the expression of the major peripheral nerve myelin proteins CNPase, MPZ/P0, MAG, and PMP22 (**Fig. 13**).

In order to assess myelin biogenesis and homeostasis using an additional independent method, I cultured dissociated mouse dorsal root ganglia (DRG) and induced myelination. Morphologically normal myelin was formed in both wt and *Prnp*$^{o/o}$ cultures. There was no difference in the density of MBP-positive segments (data not shown). However, the length of the latter was slightly reduced in *Prnp*$^{o/o}$ compared to wt in two independent experiments (**Fig. 14**). I did not observe reduced cell survival in *Prnp*$^{o/o}$ cultures as determined by propidium iodide (PI) incorporation (data not shown).

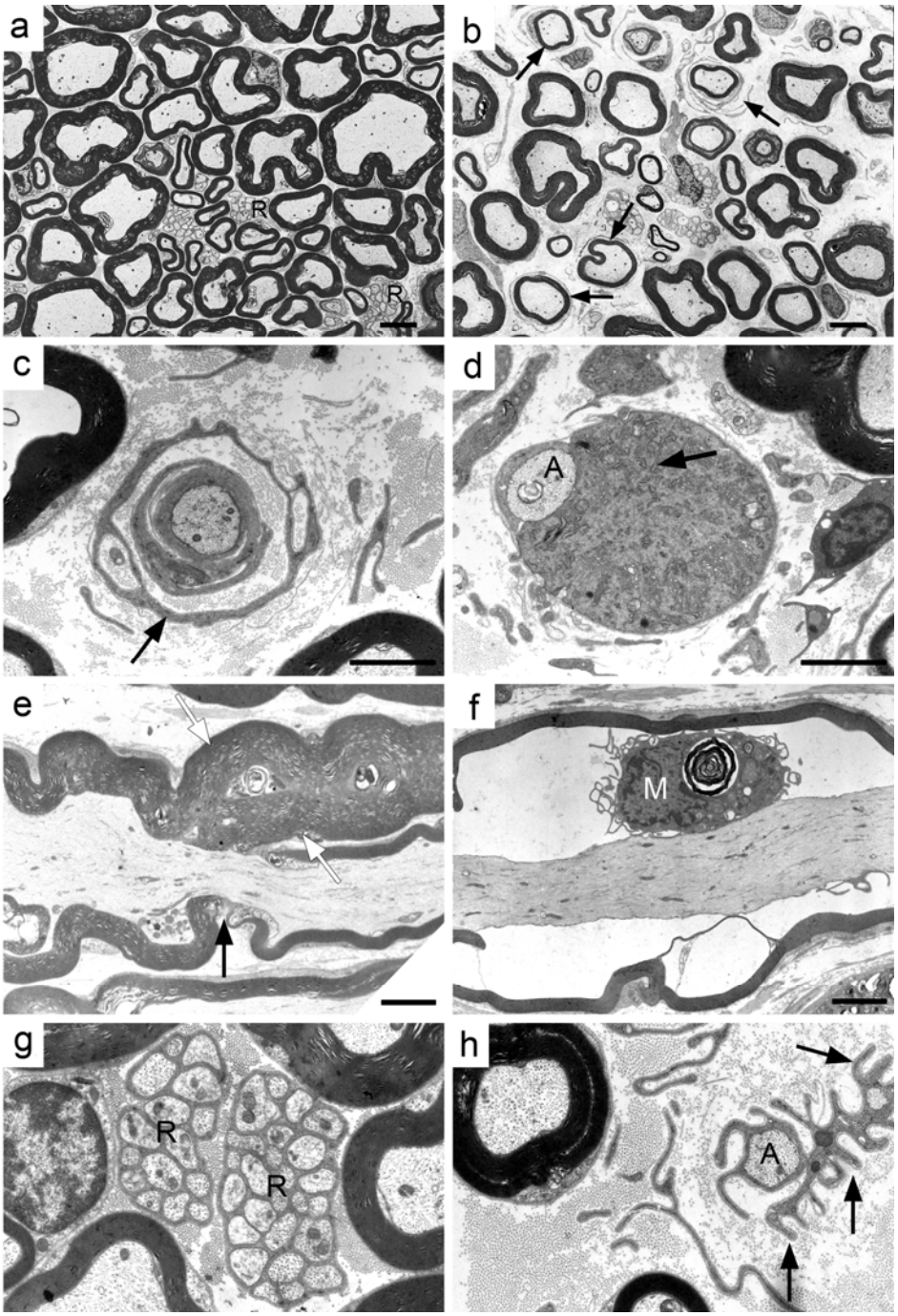

Figure 11. Ultrastructural alterations in *Prnp*$^{o/o}$ sciatic nerves. Electron microscopy of sciatic nerves of 60-week old *Prnp*$^{o/o}$ (**b-f** and **h**) and wt (**a** and **g**) mice (both on Balb/c). Cross sections of wt mice show normally myelinated nerve fibers (**a**) and regular unmyelinated axons in Remak bundles (R) (**a** and **g**). Cross sections of *Prnp*$^{o/o}$ nerves show thinly myelinated axons, surrounded by onion bulb formations (arrows) (**b-c**), axons (A) surrounded by Schwann cells with prominent rough endoplasmic reticulum (arrow) and increased density of other organelles (**d**), as well as loss of unmyelinated axons in Remak bundles (**h**). Schwann cells ensheathing unmyelinated axons (A) frequently show abnormal branching of cytoplasmic processes (arrows). Longitudinal sections of *Prnp*$^{o/o}$ nerves reveal macrophages (M) within the axon-glia interface (**f**) and focally folded myelin (white arrows) in the vicinity of a node of Ranvier (black arrow) (**e**). The right internode displays thinner myelin than the left one, indicating de- and remyelination. Scale bars: a-b = 8 μm, c-h = 5 μm.

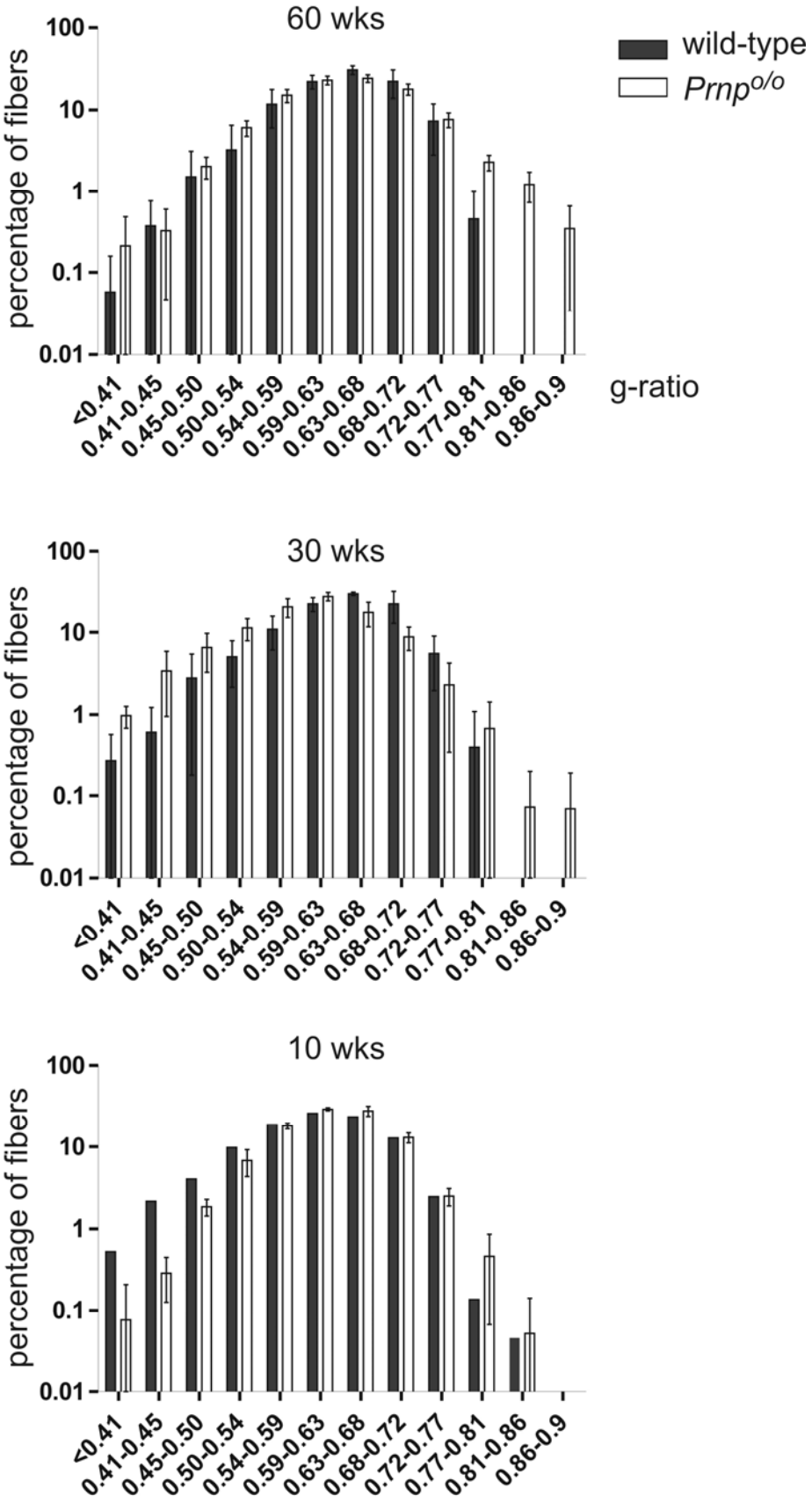

Figure 12. Time course analysis of g-ratio distribution in *Prnp*$^{o/o}$ mice. G-ratio was quantified on EM images of 10-, 30-, and 60-week old *Prnp*$^{o/o}$ compared to wt mice, both on a Balb/c background. Percentages of fibers in each g-ratio class are shown.

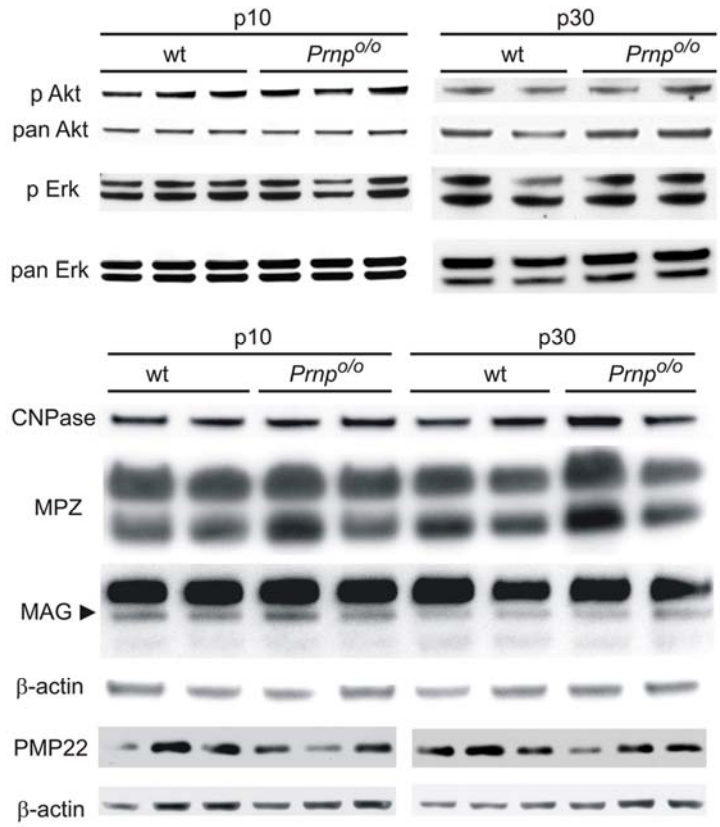

Figure 13. Akt/Erk phosphorylation, and myelin protein expression in *Prnp$^{o/o}$* nerves. No difference in expression and phosphorylation of the kinases Akt and Erk by Western blot in 10- and 30-day old *Prnp$^{o/o}$* compared to wt mice. Similarly, no difference in expression of myelin proteins CNPase, myelin protein zero (P0; MPZ), peripheral myelin protein 22 (PMP22), and myelin associated glycoprotein (MAG) is found by Western blot in 10- and 30-day old *Prnp$^{o/o}$* compared to wt mice.

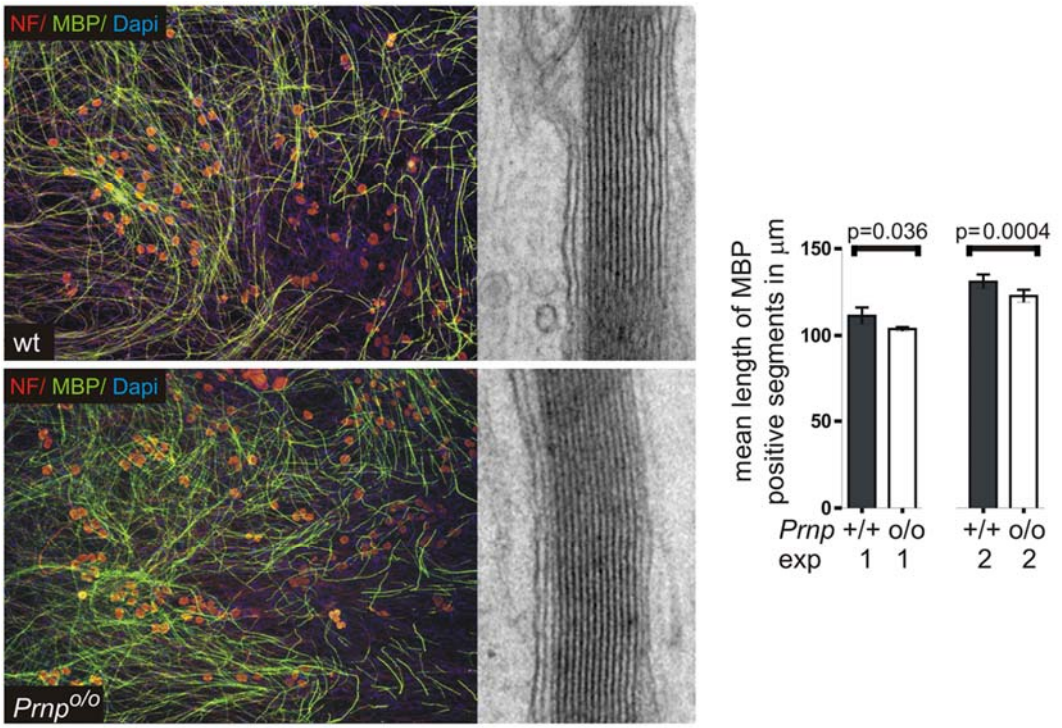

Figure 14. In vitro myelination. Myelination was induced in dissociated mouse DRG cultures. Forty days following induction of myelination, cultures derived from wt and *Prnp$^{o/o}$* mice expressed myelin basic protein (MBP) and formed ultrastructurally normal myelin, as shown by immunofluorescence co-staining for neurofilament (NF) and MBP, as well as electron microscopy (EM). Length of MBP positive segments in two independent experiments was measured and mean values for each cover slip are plotted and compared.

Electrophysiological investigations were performed on sciatic nerves of 11, 28, and 53-week old *Prnp*$^{o/o}$ and wt mice. Nerve conduction velocities were significantly reduced in *Prnp*$^{o/o}$ mice at 11, 28, and 53 weeks of age (**Fig. 15**). F-wave latencies, a further indicator of nerve conduction velocity, were marginally increased in 11 and 28-week old *Prnp*$^{o/o}$ mice and significantly prolonged in 53-week old mice (**Fig. 15**). There were no significant reduction in compound muscle action potential (CMAP) amplitudes in *Prnp*$^{o/o}$ mice (28 wks: *Prnp*$^{o/o}$: 10.5 ± 2.6 mV vs. wt: 10.8 ± 3.1 mV; 53 wks: *Prnp*$^{o/o}$: 10.6 ± 2.1 mV vs. wt: 11.5 ± 3.7 mV, following distal stimulation). Reduced nerve conduction velocities with unaltered or only slightly altered CMAP amplitudes are typically observed in demyelinating neuropathies. These combined electrophysiological and ultrastructural findings strongly support the conclusion that myelin sheaths, rather than axons, were primarily affected in *Prnp*$^{o/o}$ mice.

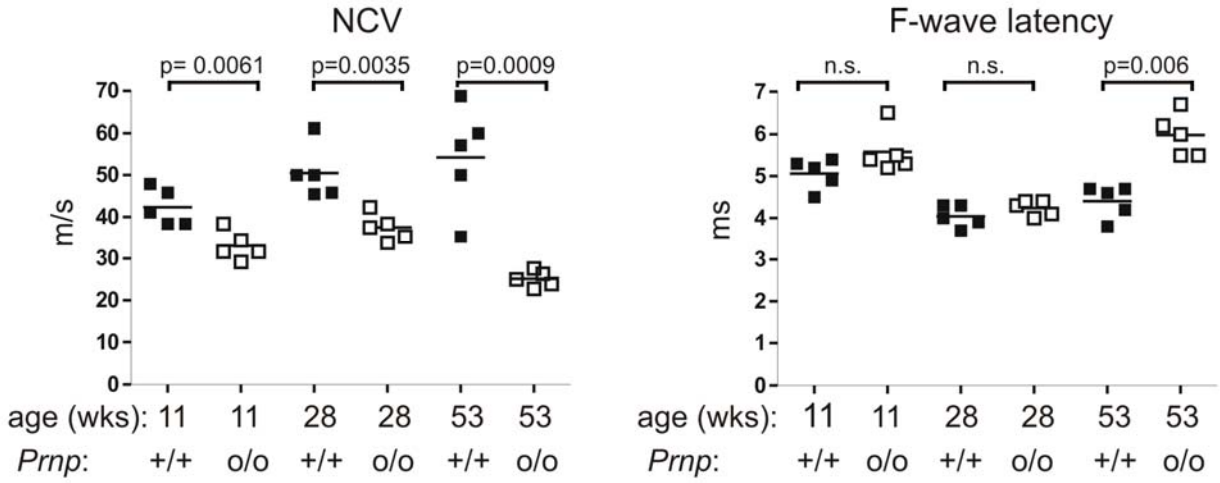

Figure 15. Electrophysiology of *Prnp*$^{o/o}$ mice. Motor nerve conduction velocities (NCV) were significantly reduced in *Prnp*$^{o/o}$ at 11 wks (33.0 ± 3.5 m/s [*Prnp*$^{o/o}$] vs. 42.3 ± 4.4 m/s [wt]), at 28 wks (37.5 ± 1.5 m/s [*Prnp*$^{o/o}$] vs. 50.5 ± 2.8 m/s [wt]), and at 53 wks (25.1 ± 0.87 m/s [*Prnp*$^{o/o}$] vs. 54.2 ± 5.6 m/s [wt]) (**a**). F-wave latencies were only marginally increased in *Prnp*$^{o/o}$ mice at 11 wks (5.6 ± 0.5 ms [*Prnp*$^{o/o}$] vs. 5.1 ± 0.4 ms [wt]) and 28 wks (4.2 ± 0.2 ms [*Prnp*$^{o/o}$] vs. 4.0 ± 0.3 ms [wt]), but were significantly prolonged at 53 wks (6.0 ± 0.5 ms [*Prnp*$^{o/o}$] vs. 4.4 ± 0.4 ms [wt]).

In a further set of experiments, I found that the altered NCV and F-wave latencies of one-year old *Prnp*$^{o/o}$ mice were restored to normal by transgenic expression of *Prnp* in *tga20* mice[139] (**Fig. 16**).

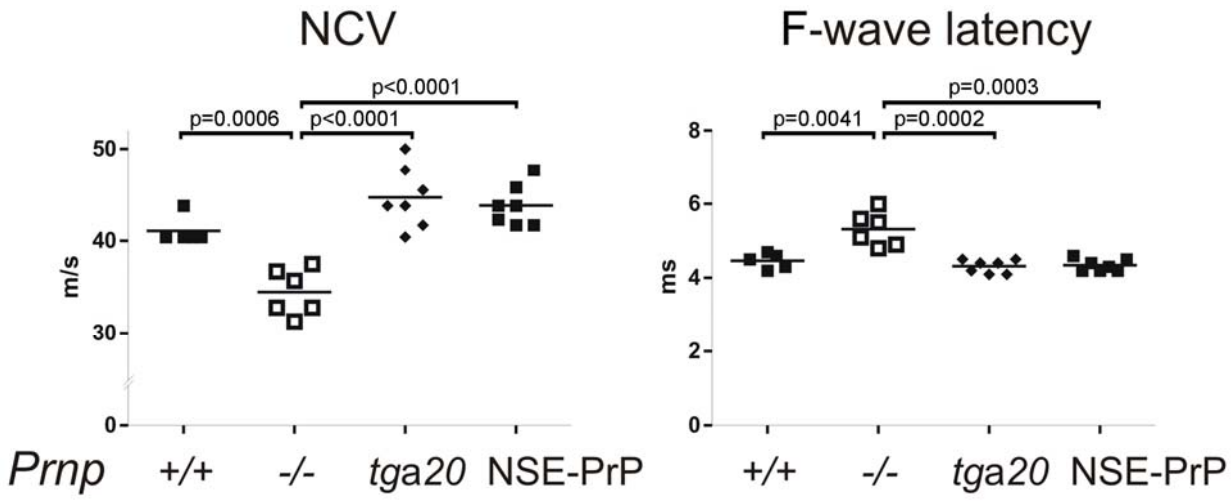

Figure 16. Electrophysiology of *tga20* and *tg*NSE-PrP mice. Motor nerve conduction velocities (NCV) and F-wave latencies of one-year old *tga20*, and *tg*NSE-PrP in comparison to wild type and *Prnp*$^{o/o}$. All mice in this experiment were on a mixed B6/129Sv background.

I then assessed the clinical consequences of CDP with a battery of behavioral assays. On accelerating rotarods, the latency to fall of female 12, 30 and 60-week old *Prnp*$^{o/o}$ mice backcrossed >17 times to Balb/c mice (n=8 to 11) was similar to that of female wt Balb/c mice (n=8 to 10; **Fig. 17**). In the hot plate test, time was measured until mice started to lick their hind paw. After 60 s (endpoint of the test) 8 of 9 wt mice, but only 2 of 11 *Prnp*$^{o/o}$ mice (all 60-week old), had licked their feet. The time lag of licking was significantly longer in *Prnp*$^{o/o}$ mice with median value, first and third quartile at 60 s (**Fig. 17**). Heat response was marginally delayed also in 12 and 30-week old *Prnp*$^{o/o}$ mice. However, these relatively subtle results of the hot-plate findings were not confirmed in 60-week old C57Bl/6 *Prnp*$^{Edbg/Edbg}$ mice which fared similarly to C57Bl/6 wt mice in both hot-plate and rotarod tests (data not shown). The grip strength test revealed a highly significant difference between 60-week old wt and *Prnp*$^{o/o}$ mice. Younger *Prnp*$^{o/o}$ mice (12-and 30-week old) also showed somewhat reduced grip strength (**Fig. 17**). Assuming that these abnormalities were primarily caused by the CDP, this finding suggests that both afferent and efferent fibers were functionally affected in *Prnp*$^{o/o}$ mice.

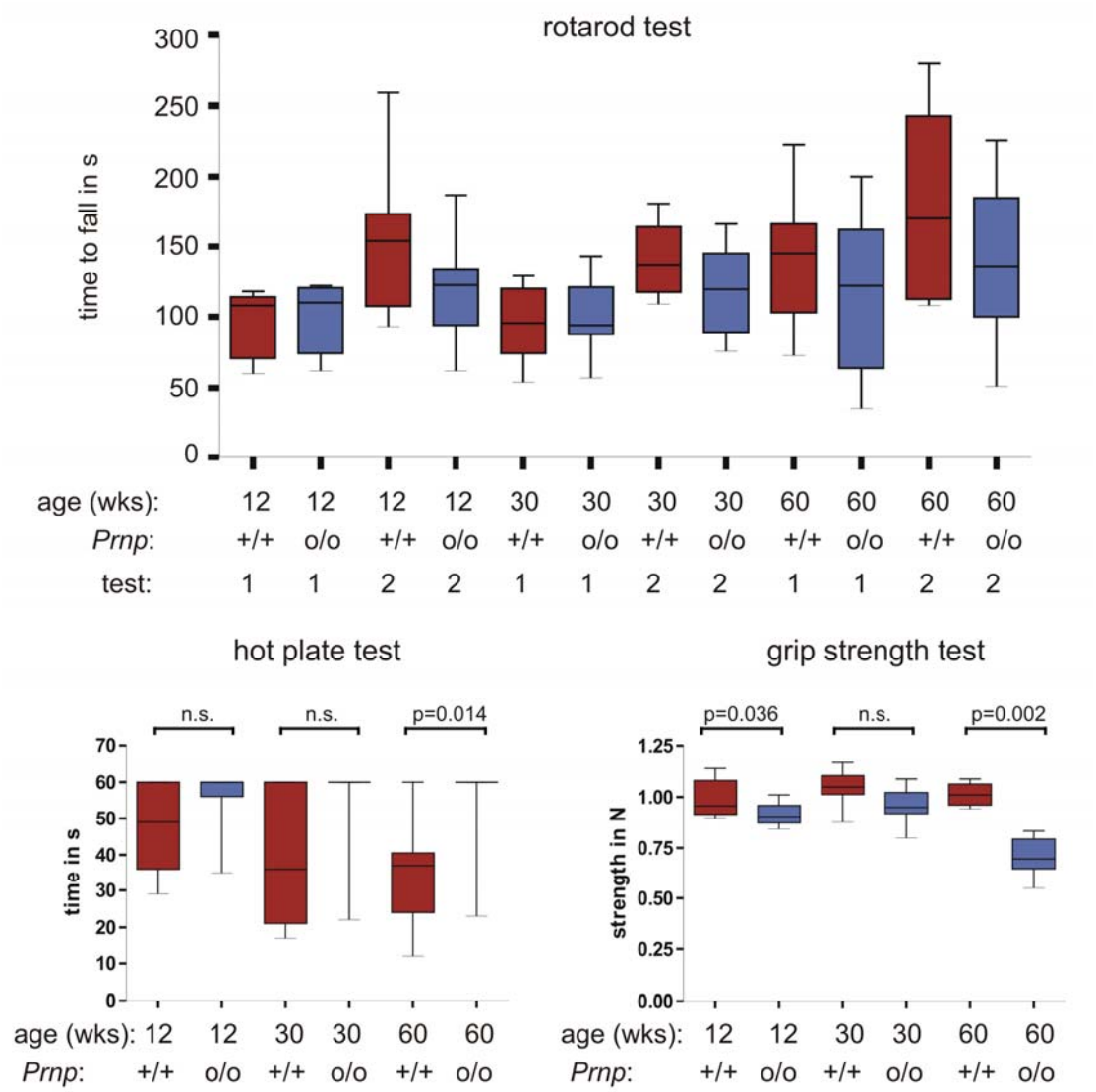

Figure 17. Behavioral tests of *Prnp*$^{o/o}$ mice. Behavioral tests of 12, 30, and 60-week old *Prnp*$^{o/o}$ mice: No difference in the performance on the rotarod test when compared to wt mice. There was some training effect, as both mouse groups displayed slightly longer latencies to fall two days after the first test. At the age of 60 weeks, significantly worse performance in the hot plate and at the age of 12 and 60 weeks significantly lower grip strength. All mice were kept in the Balb/c background.

5.4.3 Neuronal expression of PrP^{C} is required for myelin sheath maintenance

I then sought to define the cell types in which PrP^{C} expression is required to prevent demyelination. I first investigated sciatic nerves of *Prnp*$^{o/o}$ mice expressing the *tg*NSE-PrP transgene[104] which drives PrP^{C} expression from the neuron-specific enolase promoter. *Prnp* mRNA in *tg*NSE-PrP nerves was 1.9 ± 0.2% of wt (**Fig. 18b**, p<0.0001), indicating little or no *Prnp* transcription by Schwann cells. Nevertheless, ELISA measurements and immunoblots

(**Fig. 18a**) indicated PrP^C protein concentration in *tg*NSE-PrP sciatic nerves (113 ± 5.98 ng/mg total protein) approached that of wt nerves (132 ± 1.22 ng/mg). I conclude that essentially all PrP^C in *tg*NSE-PrP mice was of axonal origin. Accordingly, PrP^C immunoreactivity of *tg*NSE-PrP nerves was exclusively found along axons, whereas in wt mice it was also detectable in non-compact myelin (**Fig. 18e**). Semithin cross sections of sciatic nerves of 60-week old *tg*NSE-PrP mice showed no pathology (**Fig. 18f**), and axon size morphometry, quantification of thinly myelinated nerve fibers (g-ratio > 0.81) and onion bulb formation confirmed complete rescue of CDP (**Fig. 19**). Therefore, neuronal expression of PrP^C suffices to prevent $Prnp^{o/o}$ polyneuropathy.

To study the effects of myelin-restricted PrP^C expression, I created transgenic mice expressing PrP^C under the control of the proteolipid protein (PLP) promoter, which is active in myelinating Schwann cells and oligodendrocytes. Seven *tg*PLP-PrP lines were derived. Line 159, henceforth shorthanded as *tg*PLP-PrP, displayed similar levels of total PrP^C as wt mice in sciatic nerves (126 ± 1.54 ng/mg total protein) and by Western blot (**Fig. 18a**) despite 12-fold higher *Prnp* mRNA levels (Fig. 11b, p=0.0007), and was used for further analysis. Immunofluorescence confirmed myelin-specific expression of PrP^C in *tg*PLP-PrP mice (**Fig. 18e**). I also investigated *tg*MBP-PrP mice that express PrP^C under control of the myelin basic protein promoter[147]. *Tg*MBP-PrP mice expressed approximately 5% of wt PrP^C protein in sciatic nerves (data not shown). At 60 weeks of age, both *tg*PLP-PrP $Prnp^{o/o}$ (**Fig. 19**) and *tg*MBP-PrP $Prnp^{o/o}$ mice (data not shown) showed CDP qualitatively similar to that of $Prnp^{o/o}$ mice. Again, CDP of *tg*PLP-PrP mice was fully suppressed by introducing a hemizygous wt *Prnp* allele (*tg*PLP-PrP $Prnp^{+/o}$; data not shown). *Tg*PLP-PrP $Prnp^{o/o}$ mice had significantly more thinly myelinated fibers (g-ratio > 0.81) and onion bulbs than *tg*NSE-PrP and wt mice, but somewhat less than $Prnp^{o/o}$ mice (**Fig. 19**), indicating a weak anti-CDP effect of the *tg*PLP-PrP transgene. At the age of 35 weeks, $Prnp^{o/o}$ mice displayed significantly prolonged F-wave latencies which were completely normalized by introduction of the *tg*NSE-PrP transgene (**Fig. 18c**). Similarly, in one-year old mice the NSE-PrP transgene normalized the electrophysiological alterations of $Prnp^{-/-}$ mice (**Fig. 16**). F-wave latencies of *tg*PLP-PrP mice were not significantly different from

those of *Prnp*$^{o/o}$ mice (**Fig. 18c**). These data support the surprising notion that the demyelinating polyneuropathy of *Prnp*$^{o/o}$ mice is rescued by neuron-restricted expression of PrP^{C}.

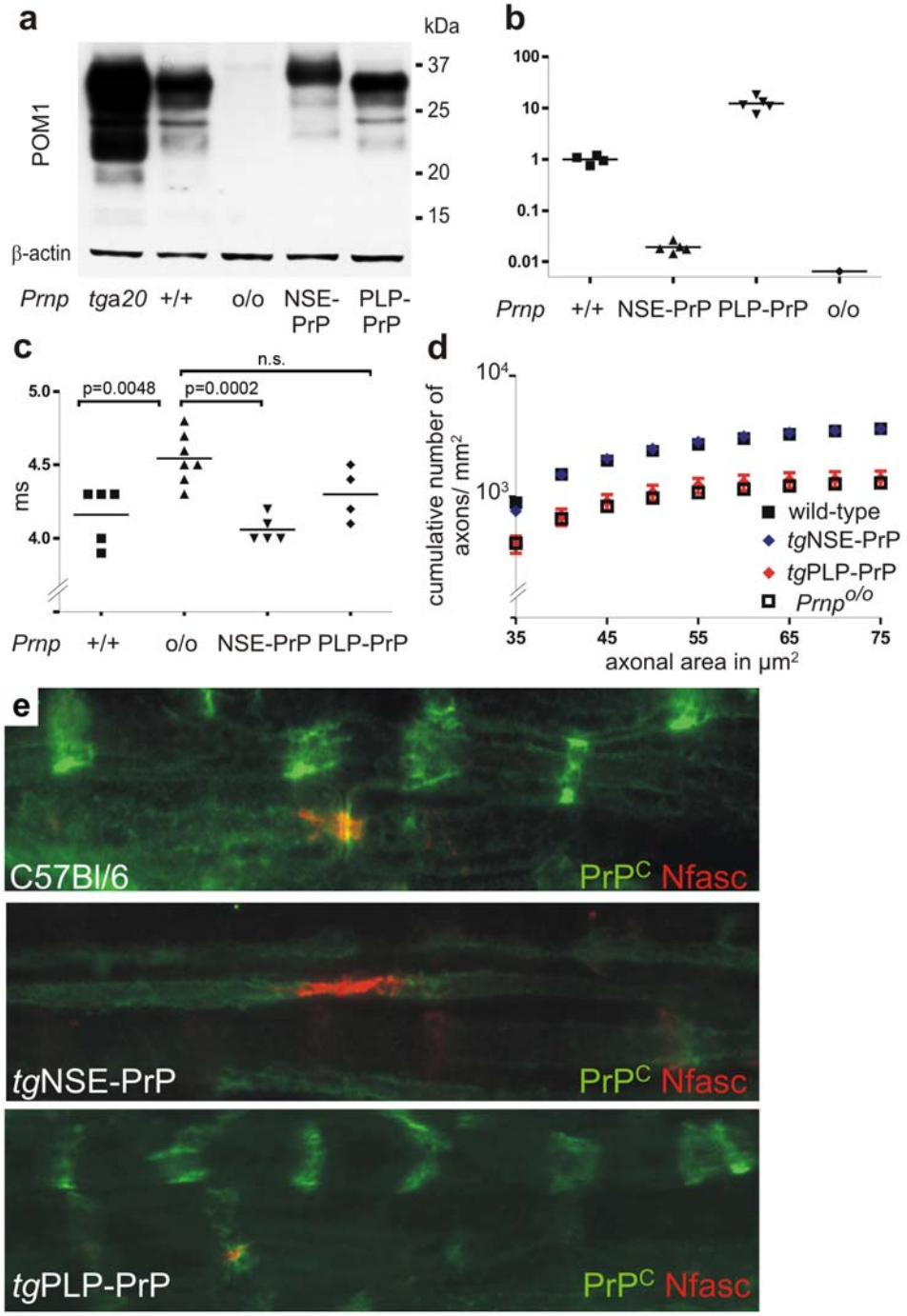

Figure 18. Mice with cell-type specific expression of PrP^{C}. a-b, e: *Prnp* mRNA and PrP^{C} protein content of *tg*NSE-PrP and *tg*PLP-PrP sciatic nerves investigated by Western blot (**a**) and real-time PCR (**b**; values on ordinate are normalized against wt mRNA). PrP^{C} localization was studied by immunofluorescence (**e**). Normal F-wave latencies in 35-week old *tg*NSE-PrP (4.1 ± 0.09 ms [*tg*NSE-PrP] and 4.2 ± 0.2 ms [wt]), prolonged latencies in age-matched B6/129Sv *Prnp*$^{o/o}$ (4.5 ± 0.2 ms) and *tg*PLP-PrP mice (4.3 ± 0.2 ms) (**c**). Quantitation of cumulative axonal density-size distribution indicates nearly normal distribution in *tg*NSE-PrP and reduced large size axon density in *Prnp*$^{o/o}$ and *tg*PLP-PrP (**d**).

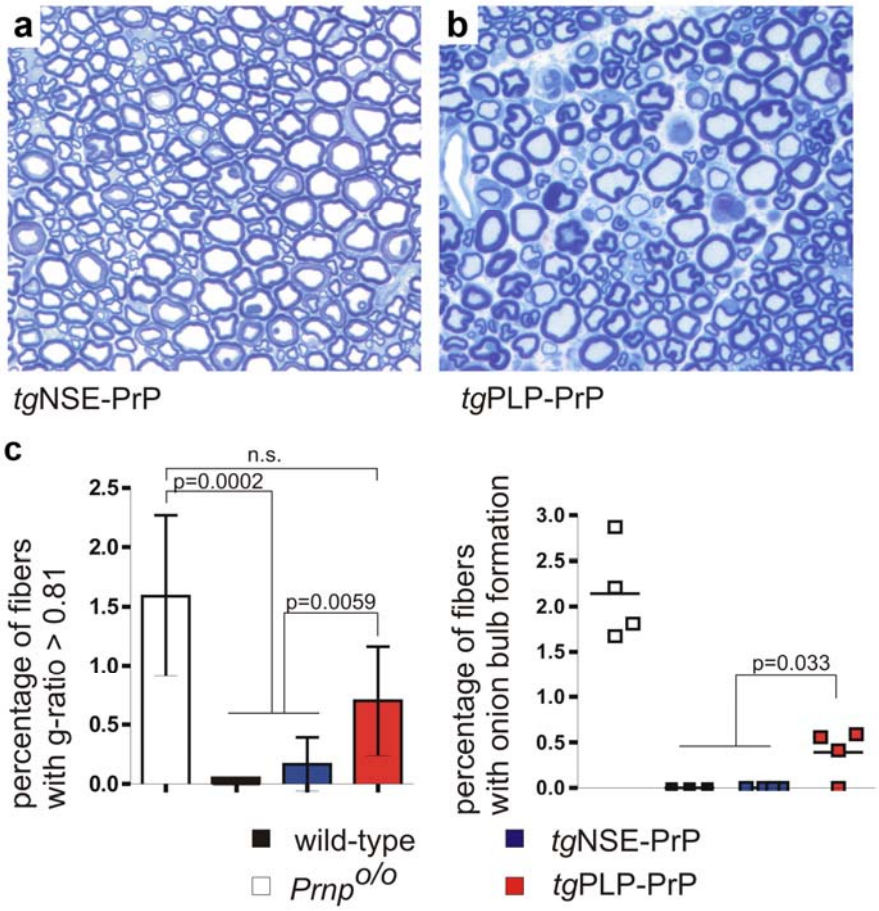

Figure 19. Expression of PrP^{C} by neurons is essential for myelin sheath maintenance. a-b: Semithin sections of 60-week old *tg*NSE-PrP, and *tg*PLP-PrP stained with toluidine blue. **c:** Percentage of fibers with g-ratio > 0.81 and onion bulb formation in wt, *Prnp*$^{o/o}$, *tg*NSE-PrP, and *tg*PLP-PrP mice.

I then investigated the effects of neuron-specific PrP^{C} depletion on peripheral myelin homeostasis. Transgenic mice carrying a floxed *Prnp* minigene on a *Prnp*$^{o/o}$ background (line *tg*37), henceforth termed *tgPrnp*^{flox}, were crossed to mice expressing Cre under control of the neuron-specific neurofilament heavy chain promoter, termed *tg*NFH-Cre[86]. Recombination efficiency was tested in DRG and spinal cord by *in situ* hybridization: whereas *tgPrnp*^{flox} mice displayed robust *Prnp* transcription in spinal cords and in DRG neurons, the signal was completely abrogated from all spinal cord neurons and ≈70% DRG neurons of *tgPrnp*^{flox} x *tg*NFH-Cre mice (**Fig. 20**). Accordingly, total PrP^{C} protein expression in sciatic nerves was markedly reduced following neuronal depletion of *Prnp* (**Fig. 21**).

TgPrnp^{flox} and *tgPrnp*^{flox} x *tg*NFH-Cre sciatic nerves displayed similar *Prnp* mRNA expression (data not shown), excluding that Cre genotoxicity had affected endogenous *Prnp* transcription

by Schwann cells. *TgPrnp*^{flox} x *tg*NFH-Cre mice developed a CDP similar to that of *Prnp*$^{o/o}$ mice, featuring frequent thinly myelinated fibers and prominent onion bulb formation (**Fig. 22**).

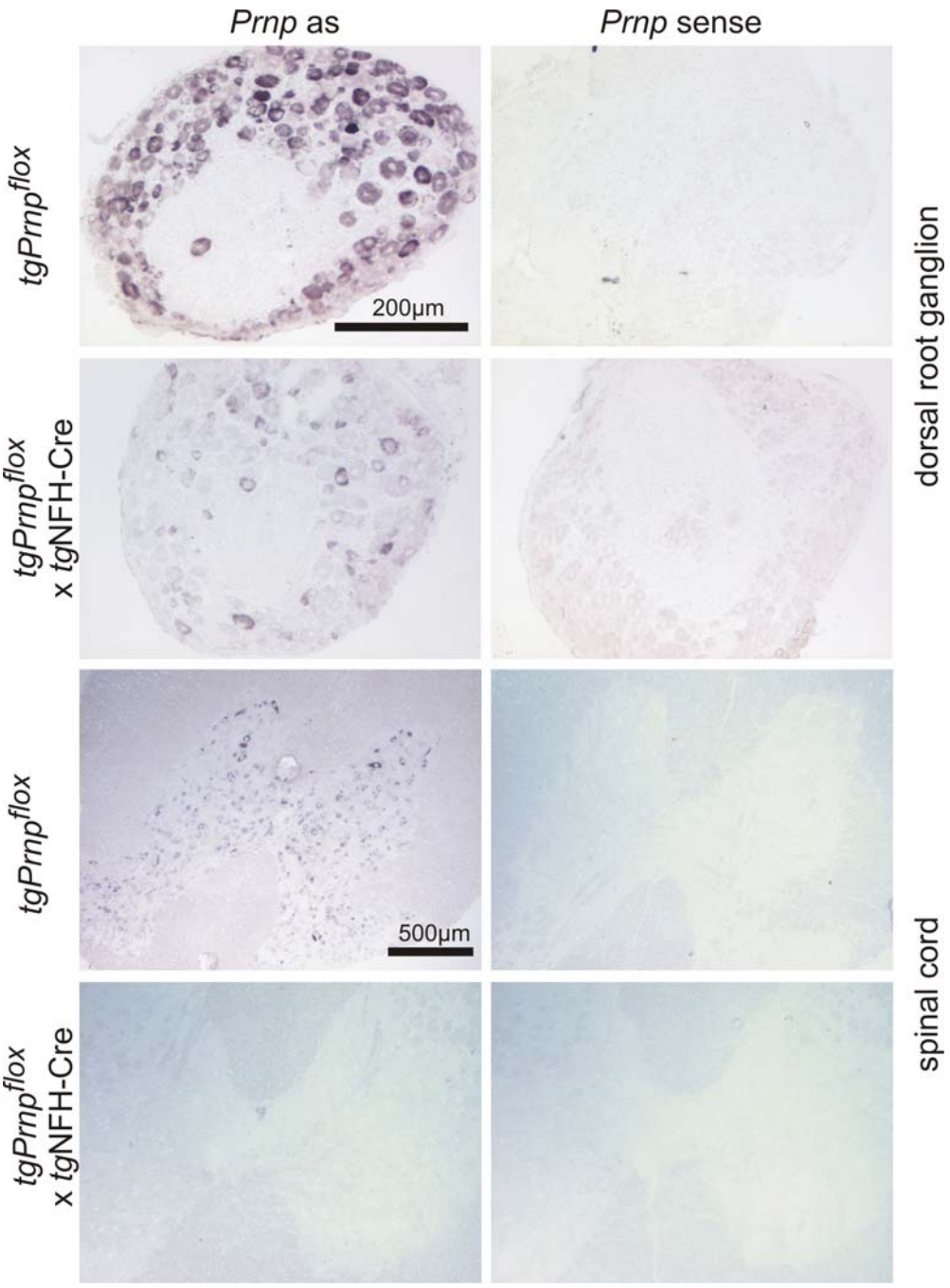

Figure 20. *Prnp in situ* hybridization of mice with neuron-specific depletion of PrP^{C}. Expression of *Prnp* mRNA was analyzed by *in situ* hybridization in 60-week old *tg*NFH-Cre and *tgPrnp*^{flox} x *tg*NFH-Cre mice. *Prnp* antisense probe and *Prnp* sense probe are shown as indicated. *TgPrnp*^{flox} mice display expression of *Prnp* in dorsal root ganglia (DRG) neurons and in spinal cord neurons. After recombination, *Prnp* was undetectable in ~70% of DRG neurons and in all spinal cord neurons.

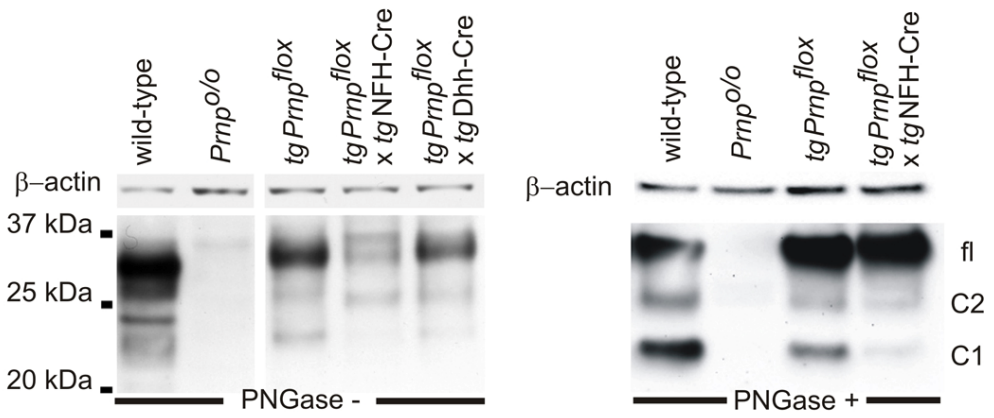

Figure 21. Western blot of PrP^{C} expression in *tgPrnp^{flox}* and following conditional depletion of *Prnp.* Samples were treated with PNGase or left untreated; antibody: POM1.

I then removed PrP^{C} from Schwann cells by breeding *tgPrnp*^{flox} mice with the pan-Schwann cell deletor *tg*Dhh-Cre (backcrossed to *Prnp*$^{o/o}$). I detected a profound depletion of PrP^{C} from Schwann cells in 6-week old *tg*Dhh-Cre x *tgPrnp*^{flox}. In contrast to age-matched *tgPrnp*^{flox} mice on the *Prnp$^{o/o}$* background, which showed PrP^{C} in both Schwann cells and axons, *tg*Dhh-Cre x *tgPrnp*^{flox} showed PrP^{C} only along axons (**Fig. 23**). In addition, *Prnp* mRNA expression was significantly reduced in *tg*Dhh-Cre x *tgPrnp*^{flox} in sciatic nerves (19 ± 11% of wt expression in *tgPrnp*^{flox} and 6 ± 1% in *tg*Dhh-Cre x *tgPrnp*^{flox} mice; p=0.016). Quantification of g-ratio and onion bulb formation in the resulting mice revealed no difference against *tgPrnp*^{flox} mice (**Fig. 22**). Hence, Schwann cell PrP^{C} is dispensable for peripheral myelin maintenance.

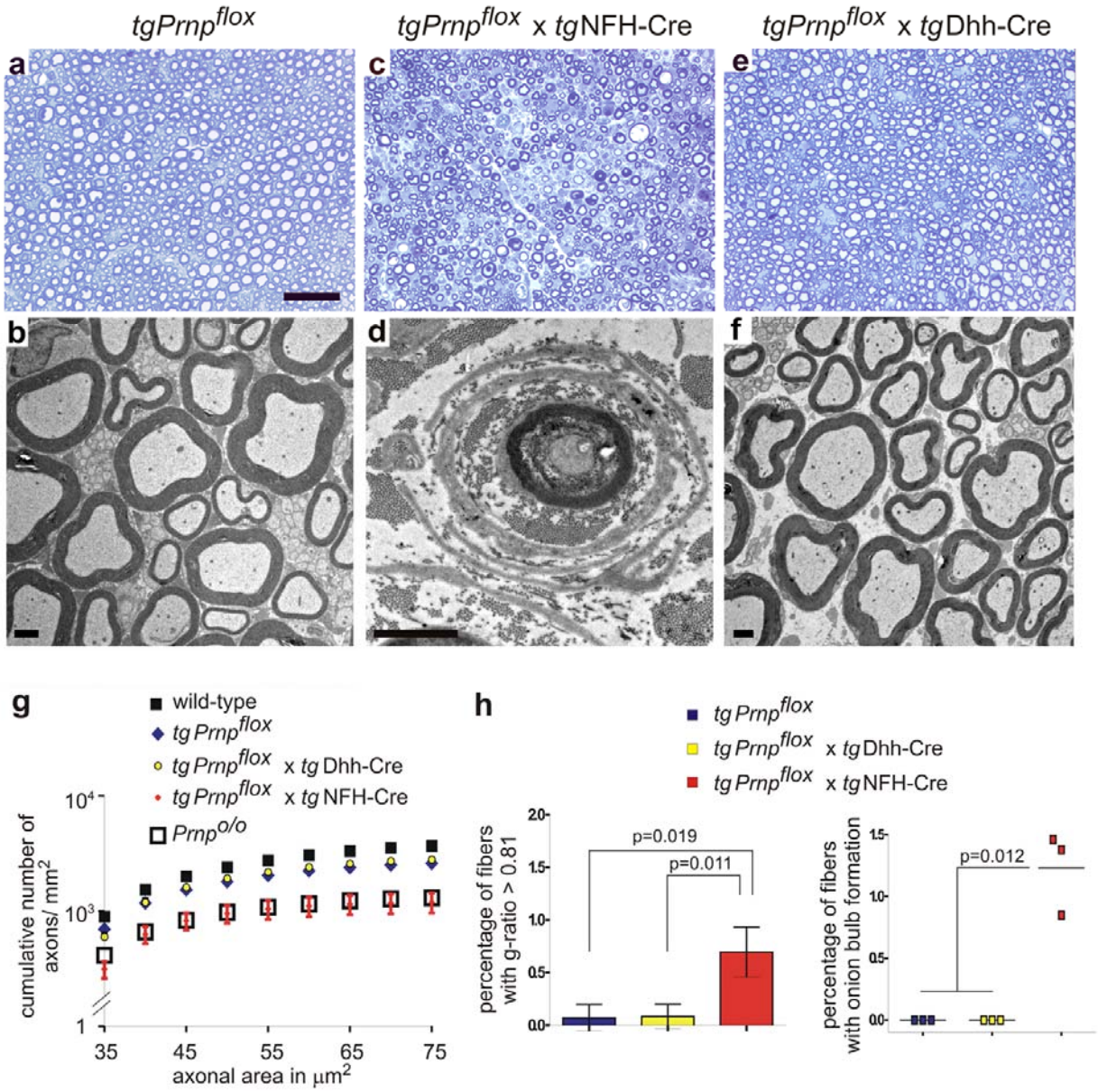

Figure 22. Neuron-specific but not Schwann cell-specific depletion of PrP^C induces CDP. *Prnp*$^{o/o}$ mice carrying a floxed *Prnp* transgene, termed *tgPrnp*^{flox}, were crossed to *tg*NFH-Cre expressing Cre in neurons or to *tg*Dhh-Cre expressing Cre in Schwann cells. **a-f:** Morphological analysis of sciatic nerves at 60 weeks of age. Toluidine blue-stained semithin sections showing demyelinating polyneuropathy in sciatic nerves of *tgPrnp*^{flox} x *tg*NFH-Cre mice with neuronal PrP^C depletion (**c**). Electron microscopy (EM) showing onion bulb formation in a *tgPrnp*^{flox} x *tg*NFH-Cre mouse (**d**). In contrast, *tgPrnp*^{flox} x *tg*Dhh-Cre and *tgPrnp*^{flox} on a *Prnp*$^{o/o}$ background showed normal morphology of sciatic nerves in semithin sections (**a** and **e**) and EM (**b** and **f**). Scale bar in a = 50 µm; scale bar in b, d, and f = 2 µm. Quantification of cumulative axonal density-size distribution indicating severe reduction of large axons in *tgPrnp*^{flox} x *tg*NFH-Cre as seen in *Prnp*$^{o/o}$ nerves (**g**). Percentage of fibers with g-ratio > 0.81 and onion bulb formation in *tgPrnp*^{flox} x *tg*NFH-Cre was significantly increased compared to *tgPrnp*^{flox} x *tg*Dhh-Cre and *tgPrnp*^{flox} mice (**h**).

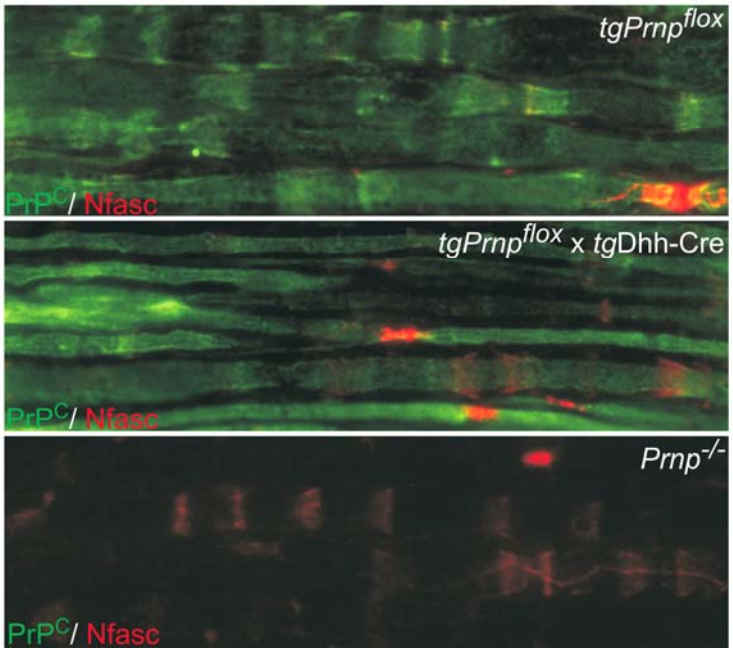

Figure 23. Depletion of Schwann cell PrP^C in *tg*Dhh-Cre x *tgPrnp^{flox}* mice. Immunofluorescence staining of sciatic nerve sections for PrP^C, using POM1 (anti-PrP^C-antibody) labelled with Alexa488 (green). Neurofascin (Nfasc) staining for control (red). While PrP^C was localized in Schwann cells and along axons in *tgPrnp^{flox}*, in *tgPrnp^{flox}* x *tg*Dhh-Cre it was detectable only along axons. *Prnp$^{o/o}$* served as control.

5.4.4 PrP^C biogenesis in peripheral nerves

Monoclonal antibodies POM1 and POM3, which recognize epitopes in the C-terminus of PrP^C (around aa 140-152) and within the charge cluster (aa 95-100), respectively[144], were used to investigate the relative prevalence of full-length PrP^C and of its C-terminal fragments C1 and C2 by immunoblotting. In contrast to brain, sciatic nerve contained more C1 fragment than full-length PrP^C (**Fig. 24**). C1 is generated by α-cleavage at aa 110/111/112, whereas C2 is derived by β-cleavage in the octarepeat region or at position 96 (ref. [148, 149]). Neuronal depletion of *Prnp* in *tgPrnp^{flox}* x *tg*NFH-Cre mice reduced the amount of C1 fragment (**Fig. 21**). The POM1 antibody, which recognizes all three forms of PrP^C, revealed their presence in non-compact myelin, Schmidt-Lanterman incisures (SLIs), paranodes, and along axonal surfaces (**Fig. 18**). Therefore, PrP^C immunoreactivity was associated with both neurons and Schwann cells.

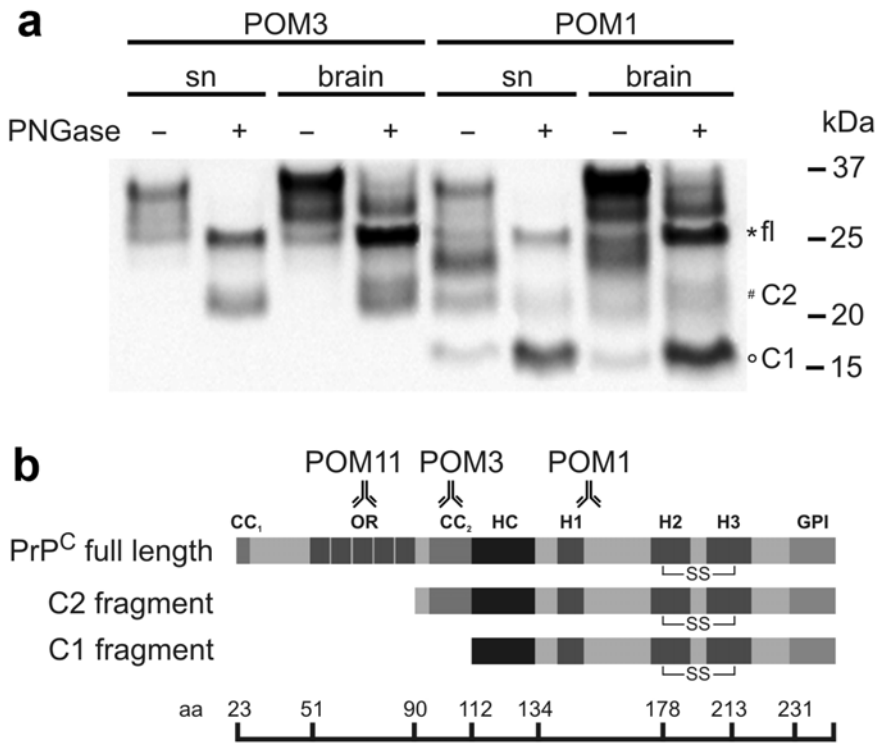

Figure 24. PrP^C expression and proteolytic processing in sciatic nerves. Western blot analysis comparing PrP^C protein expression in the sciatic nerve with that in brain of wt mice, using two different monoclonal antibodies, POM1 and POM3, for detection. Following PNGase treatment of protein lysates, two bands were recognized by POM3 antibody, while POM1 detected three bands (**a**). This band pattern is explained by the localization of antibody epitopes and by the existence of three PrP isoforms, each containing an intact carboxy terminus: full length PrP, C2, and C1 fragment (**b**).

5.4.5 Domains of PrP^C required for myelin maintenance

Might a secreted, soluble PrP^C variant rescue the CDP? I addressed this question in *tg*GPI$^-$PrP mice (line #44) lacking the GPI anchor[138].The concentration of GPI$^-$PrP in sciatic nerves was determined by Western blot (POM11) to be ca. 20-25% of wt full-length PrP^C (**Fig. 25a**). *Tg*GPI$^-$PrP mice lacked any detectable C-terminal fragments C1 and C2 (**Fig. 25b**), suggesting that membrane anchorage is essential for regulated PrP^C proteolysis in peripheral nerves. Sciatic nerves of 68-week old *tg*GPI$^-$PrP (n=3) displayed CDP similarly to *Prnp*$^{o/o}$ nerves (**Fig. 26**).

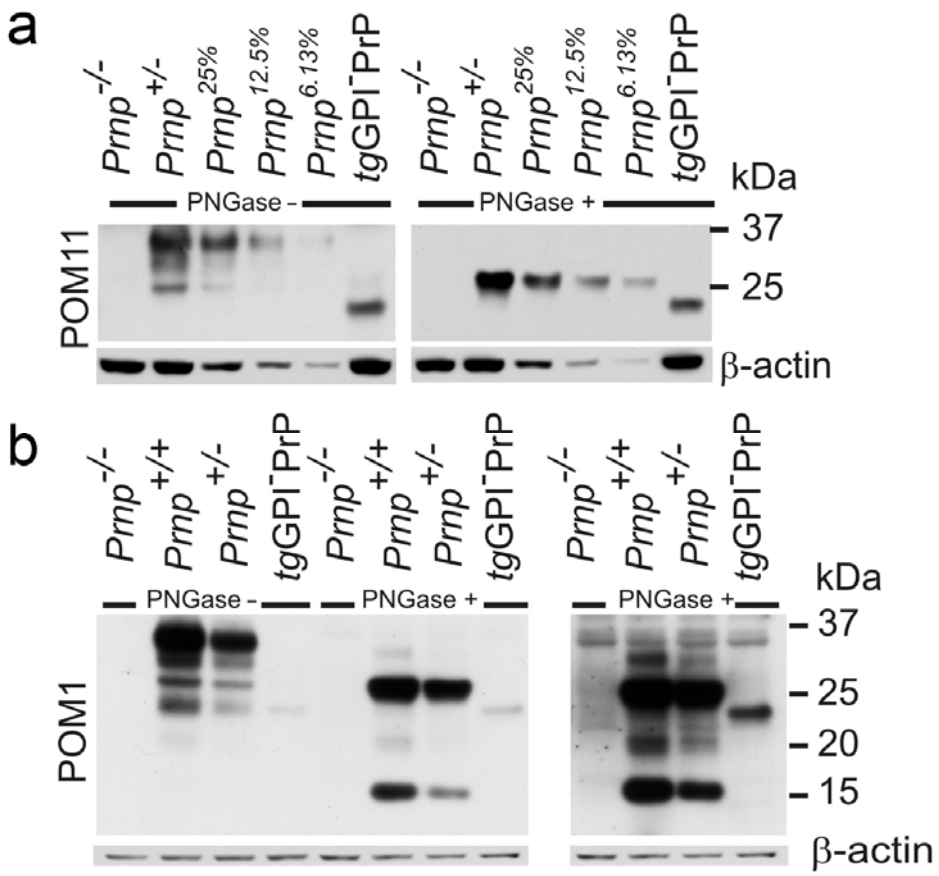

Figure 25. PrP^{C} expression and proteolytic processing in sciatic nerves of *tg*GPI^{-}PrP mice. *Tg*GPI^{-}PrP mice were analyzed for PrP^{C} expression with POM11 antibody, before and after PNGase treatment in comparison to serially diluted *Prnp*$^{+/-}$ sciatic nerve lysates (**a**). For analysis of PrP processing, I used antibody POM1 which detects all holo-PrP^{C} and all C-terminal fragments (**b**). POM1 detected GPI^{-}PrP to a lesser extent than POM11. However, no formation of C-terminal fragments was observed, even after very long exposures (right side).

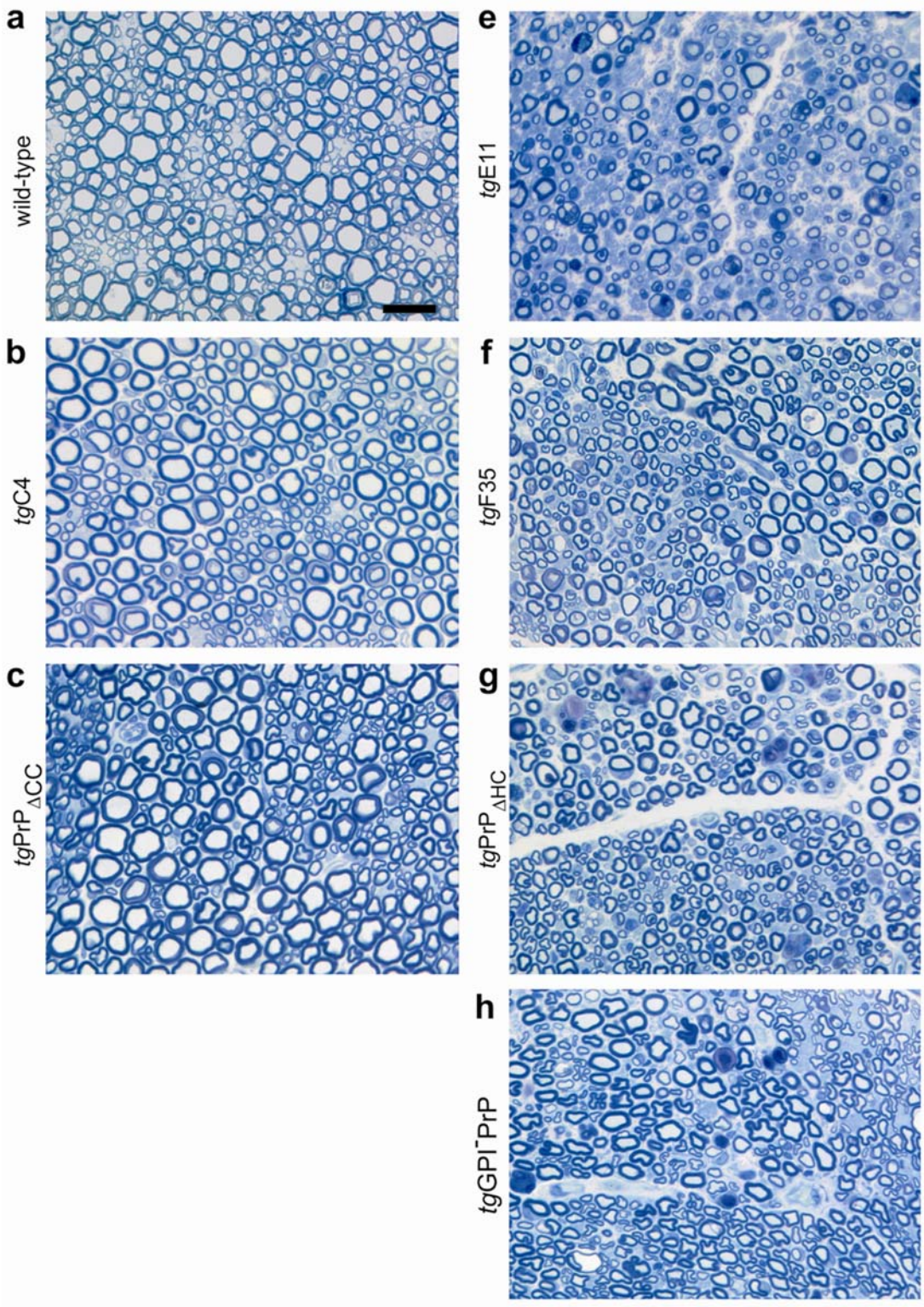

Figure 26. Peripheral neuropathy in transgenic mice expressing PrP deletion mutants. Toluidine blue-stained semithin cross sections of sciatic nerves of transgenic mice are shown. 60-week old wt (**a**), *tg*C4 x *Prnp*$^{o/o}$ (**b**), *tg*$_{\Delta CC}$ x *Prnp*$^{o/o}$ (**c**) all showed a normal morphology of the sciatic nerve fibers. In contrast, terminally sick *tg*E11 x *Prnp*$^{o/o}$ (30-week old; **e**), *tg*F35 x *Prnp*$^{o/o}$ (90-day old; **f**), *tg*PrP$_{\Delta HC}$ x *Prnp*$^{o/o}$ (109-day old; **g**), as well as 60-week old *tg*GPI^{-}PrP x *Prnp*$^{Edbg/Edbg}$ (i) showed peripheral neuropathy. Scale bar = 20 μm.

The flexible amino proximal domain of PrP comprises a charge cluster (CC_1), the octarepeat region (OR) and a central domain with a second charge cluster (CC_2) and a hydrophobic core (HC) (**Fig. 24b and 27a**). I found that PrP^C lacking the octarepeats ($PrP_{\Delta C}$, line *tg*C4)[106] fully rescued the CDP (**Fig. 26**), indicating that the octarepeat region is unnecessary for myelin maintenance. In addition to full-length $PrP_{\Delta C}$, *tg*C4 sciatic nerve lysates contained the two proteolytic fragments C1 and C2 (**Fig. 27**).

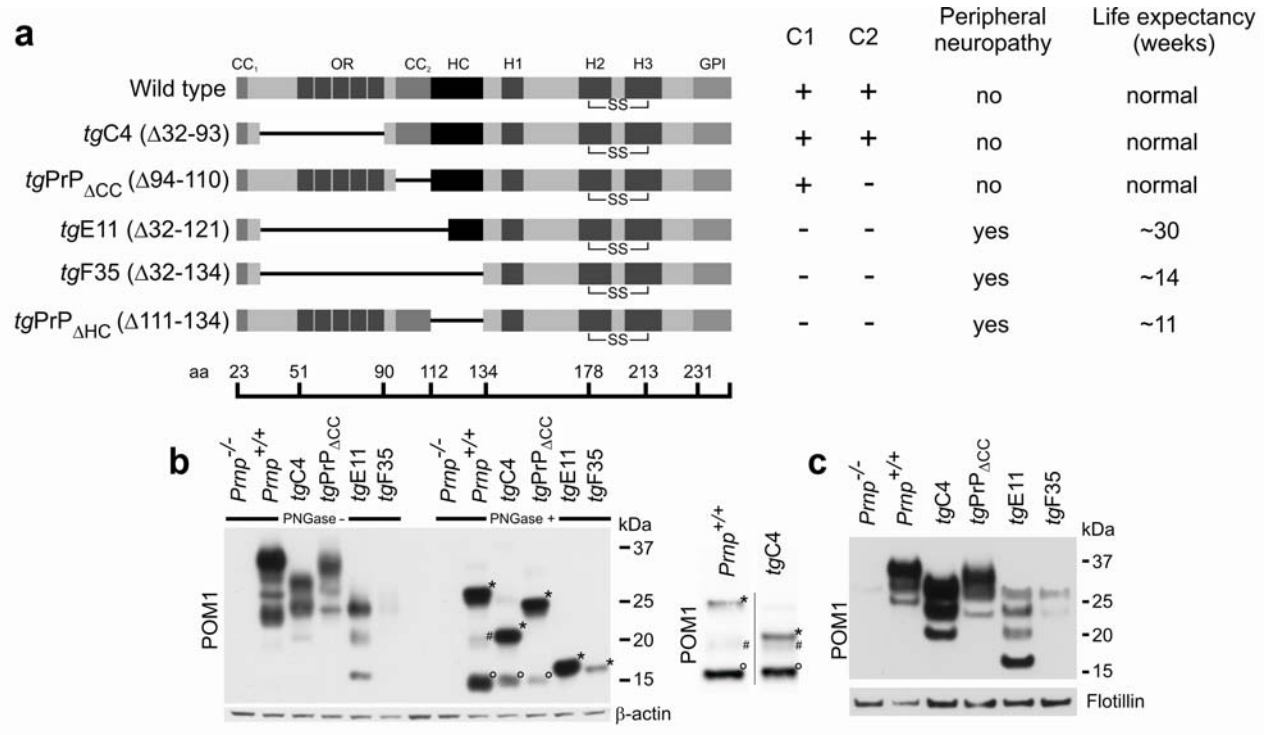

Figure 27. Role of amino-terminal domains in the pathogenesis of *Prnp*$^{o/o}$ polyneuropathy. Transgenic constructs, presence of PrP C-terminal fragments in the respective transgenic mice, presence of peripheral neuropathy, and life expectancy (**a**). Mice expressing deletion mutants of PrP were analyzed for PrP expression and processing in sciatic nerves. Western blots before and after PNGase treatment of lysates are shown. Full-length PrP is marked by *****, C2 fragment by #, and C1 fragment by **°**. A Western blot with better separation of full-length and C2 fragment for *tg*C4 mice is shown (all lanes are from the same blot, but intervening lanes were deleted for clarity) (**b**). Detergent-resistant membranes (DRM) were prepared from sciatic nerves of different transgenic and wt mice and subjected to step density gradient centrifugation. Fractions containing DRM were analyzed by Western blot for presence of PrP^C and flotillin as control (**c**). Western blots of the various fractions from this experiment are shown in **Fig. 28**.

I then used the "half-genomic" pPrPHG backbone[139] to derive a PrP^C variant lacking the CC_2 domain (aa 94-110) termed *tg*$PrP_{\Delta CC}$. Transgenic mice were generated by microinjection of the *tg*$PrP_{\Delta CC}$ construct; offspring of founder #46 were used for analysis. Sciatic nerves of *tg*$PrP_{\Delta CC}$

mice contained C1 fragment, albeit less than wt nerves, and were devoid of C2 fragment (**Fig. 27**). Upon crossing to *Prnp*$^{o/o}$ mice, *tg*PrP$_{\Delta CC}$ mice did not develop CDP at 60 weeks of age (**Fig. 26**). In contrast, *Prnp*$^{o/o}$ mice expressing PrP^{C} variants devoid of aa 32-134 and aa 32-121 (termed *tg*F35 and *tg*E11, respectively)[106] completely lacked C1 and displayed a CDP qualitatively similar to that of *Prnp*$^{o/o}$ mice (**Fig. 26-27**). I prepared detergent-resistant membranes (DRMs) from sciatic nerves of wt, *Prnp*$^{o/o}$ and the various PrP deletion-mutant transgenic mice by detergent extraction followed by step density-gradient centrifugation. The buoyancy of the PrP deletion-mutants was similar to that of PrP^{C}, indicating that they reside in similar membrane microdomains (**Fig. 27c and 28**).

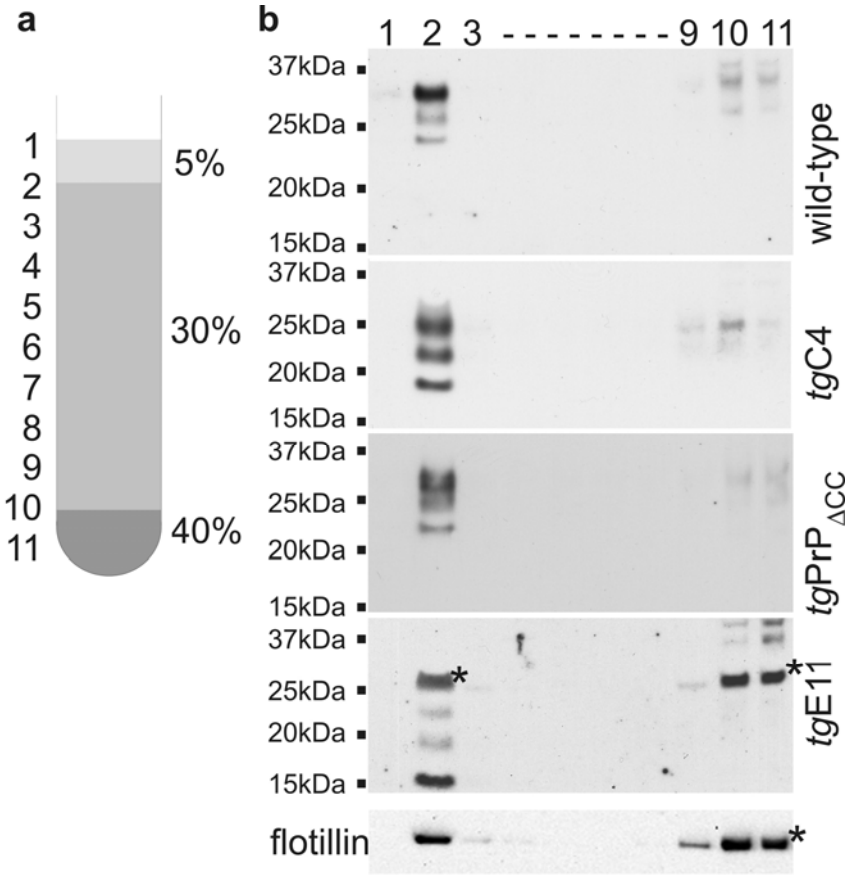

Figure 28. PrP^{C} and PrP deletion mutants co-localize with flotillin in detergent-resistant membranes (DRM) in sciatic nerves. DRM were extracted using 1% Triton X100. Homogenates were subjected to step density gradient ultracentrifugation. Set up of the Optiprep gradient is shown (**a**). After the separation, 11 fractions of 200 μl each were recovered and analyzed by Western blot with anti-PrP antibody POM1 or anti-flotillin antibody. Non-specific bands, detected also by the secondary antibody only, are marked with a star (**b**).

Finally, I generated transgenic mice expressing a PrP variant lacking the hydrophobic core HC (aa 111-134). The transgenic construct was again based on pPrPHG, and transgenic mice were termed *tg*PrP$_{\Delta HC}$ (line 1146). *Tg*PrP$_{\Delta HC}$ x *Prnp*$^{o/o}$ mice showed a reduced life expectancy (survival 80 ± 3.5 days; data not shown) and displayed severe CDP (**Fig. 26**). In addition, terminally sick *tg*PrP$_{\Delta HC}$ mice developed central nervous white-matter vacuolation and intensive astrogliosis in cerebellum, brain stem and corpus callosum (**Fig. 29**). The brain of *tg*PrP$_{\Delta HC}$ mice lacked all C-terminal fragments (data not shown).

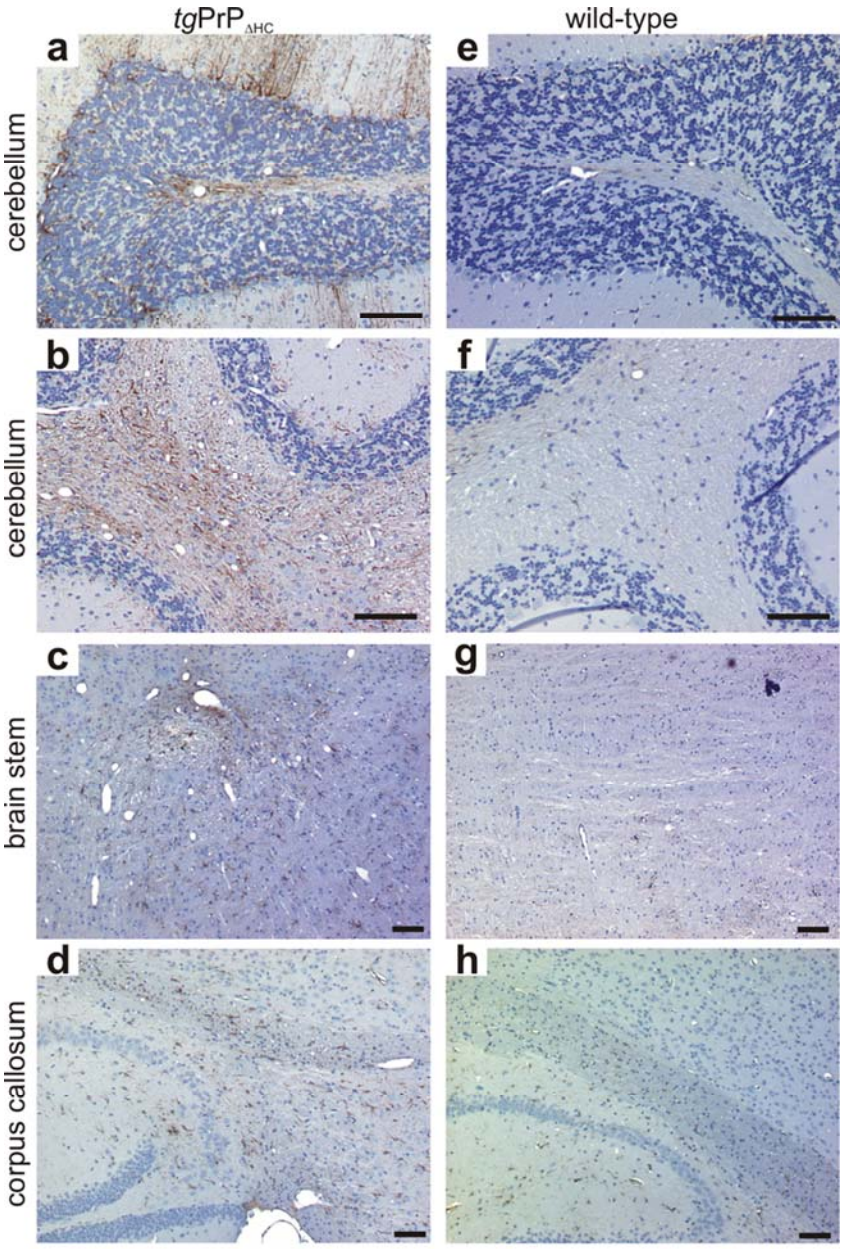

Figure 29. Vacuolation and astrogliosis in terminally sick *tg*PrP$_{\Delta HC}$ mice. GFAP immunohistochemistry of cerebellum, brain stem, and corpus callosum sections of *tg*PrP$_{\Delta HC}$ mice and age-matched wt mice.

5.4.6 No involvement of lymphocytes in *Prnp*$^{-/-}$ polyneuropathy

In order to determine whether an altered lymphocyte function could play a role in the *Prnp*$^{o/o}$ neuropathy, I crossed *Prnp*$^{o/o}$ mice to *Rag1*$^{-/-}$ mice that lacked the *Rag1* gene and therefore all B- and T-cells. At the age of 60 weeks, double knockout mice (*Prnp*$^{o/o}$ *Rag1*$^{-/-}$) displayed a peripheral polyneuropathy identical to the one found in *Prnp*$^{o/o}$ mice (**Fig. 30**). For control, I analyzed *Rag1*$^{-/-}$ mice with wt *Prnp* expression and observed no signs of polyneuropathy (**Fig. 30**). This indicates that functional B- and T-cells are not a prerequisite for the pathogenesis of the *Prnp*$^{o/o}$ polyneuropathy. Accordingly, immunohistochemical stains failed to reveal increased CD3^{+} or B220^{+} lymphocytes in sciatic nerves of 60-week old *Prnp*$^{o/o}$ mice (data not shown).

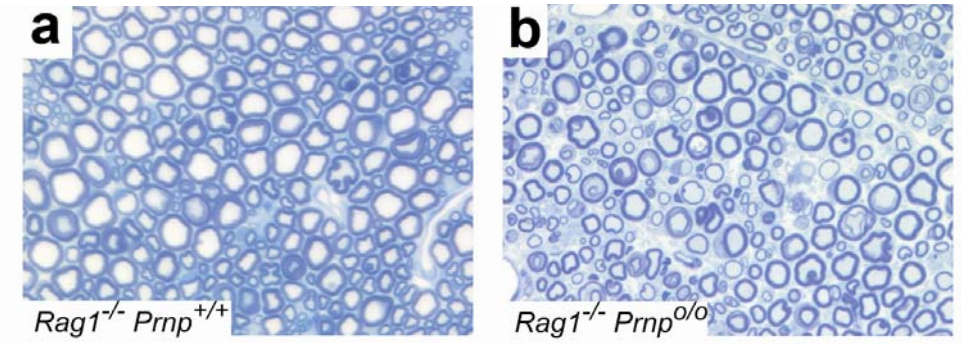

Figure 30. Role of lymphocytes in the pathogenesis of *Prnp*$^{o/o}$ polyneuropathy. Toluidine blue-stained semithin cross sections of sciatic nerves of 60-week old *Rag1*$^{-/-}$ *x Prnp*$^{+/+}$ showed a normal morphology of the sciatic nerve (**a**) and peripheral neuropathy in *Rag1*$^{-/-}$ *x Prnp*$^{o/o}$ (**b**).

5.4.7 Increased number of SLIs in *Prnp*$^{o/o}$ mice

The structure and saltatory conduction of peripheral nerve fibers depend on the proper arrangement of nodes of Ranvier and paranodes. I therefore assessed expression and localization of nodal and paranodal proteins by immunofluorescence. Sodium channels, neurofascin, the paranodal proteins Caspr and JamC, and the extracellular versican were normally distributed in *Prnp*$^{o/o}$ mice (**Fig. 31**), and JamC showed the normal pattern of association with paranodal myelin and SLIs. However, I observed an increased density of SLIs along internodes of 8-month old *Prnp*$^{o/o}$ mice. In 8-month old *tg*NSE-PrP, SLI density was similar to wt mice, whereas SLI density in *tg*PLP-PrP x *Prnp*$^{o/o}$ mice, which expressed PrP^{C} exclusively in Schwann cells, was similar to that of *Prnp*$^{o/o}$ nerves (**Fig. 32**).

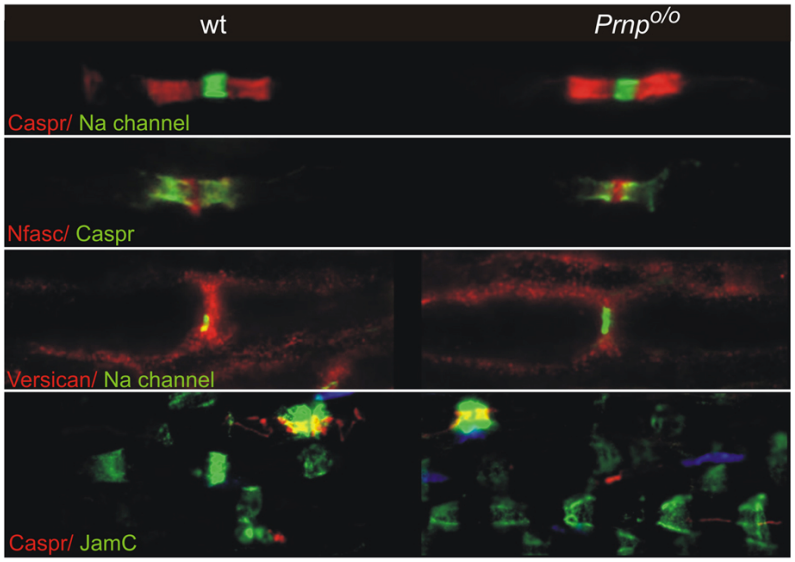

Figure 31. Architecture of *Prnp*$^{o/o}$ nerves. Immunofluorescence of 10-week old *Prnp*$^{o/o}$ compared to wt mice show normal localization of nodal proteins [sodium (Na) channels, neurofascin 186 (Nfasc)], of paranodal Caspr, and of versican as a component of the extracellular matrix. JamC, present in non-compact myelin of both *Prnp*$^{o/o}$ and wt, shows higher density of SLIs in *Prnp*$^{o/o}$ compared to wt.

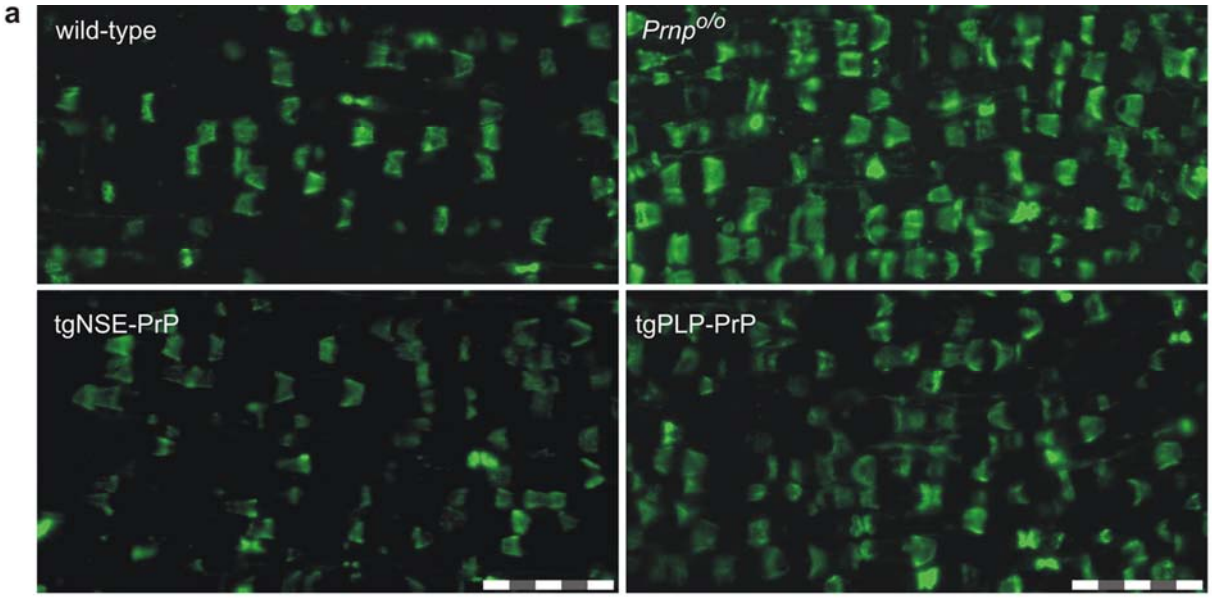

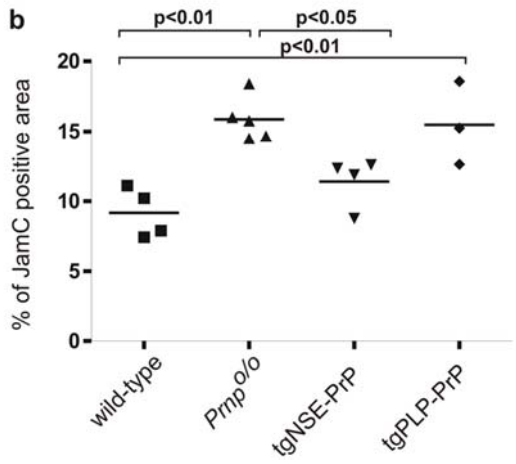

Figure 32. Increased density of SLIs in *Prnp*$^{o/o}$ mice. JamC immunofluorescence of longitudinal sciatic nerve sections of 35-week old C57Bl/6, *Prnp*$^{o/o}$ (B6/129Sv) *tg*NSE-PrP, and *tg*PLP-PrP. JamC positive areas include SLIs and paranodes of non-compact myelin (**a**). Percentage of JamC positive area (**b**). In contrast to wt and *tg*NSE-PrP, *Prnp*$^{o/o}$ sciatic nerves show an increase in JamC positive area. Similarly, in *tg*PLP-PrP, percentage of JamC positive area was increased. Scale bar = 50 μm.

5.4.8 Normal Neuregulin-1 expression in developing *Prnp*$^{o/o}$ nerves

Neuregulin-1 (NRG1) type III regulates Schwann cell development and myelination. By western blot analysis, I did not observe any difference in NRG1 expression or processing in developing peripheral nerves (**Fig. 33**).

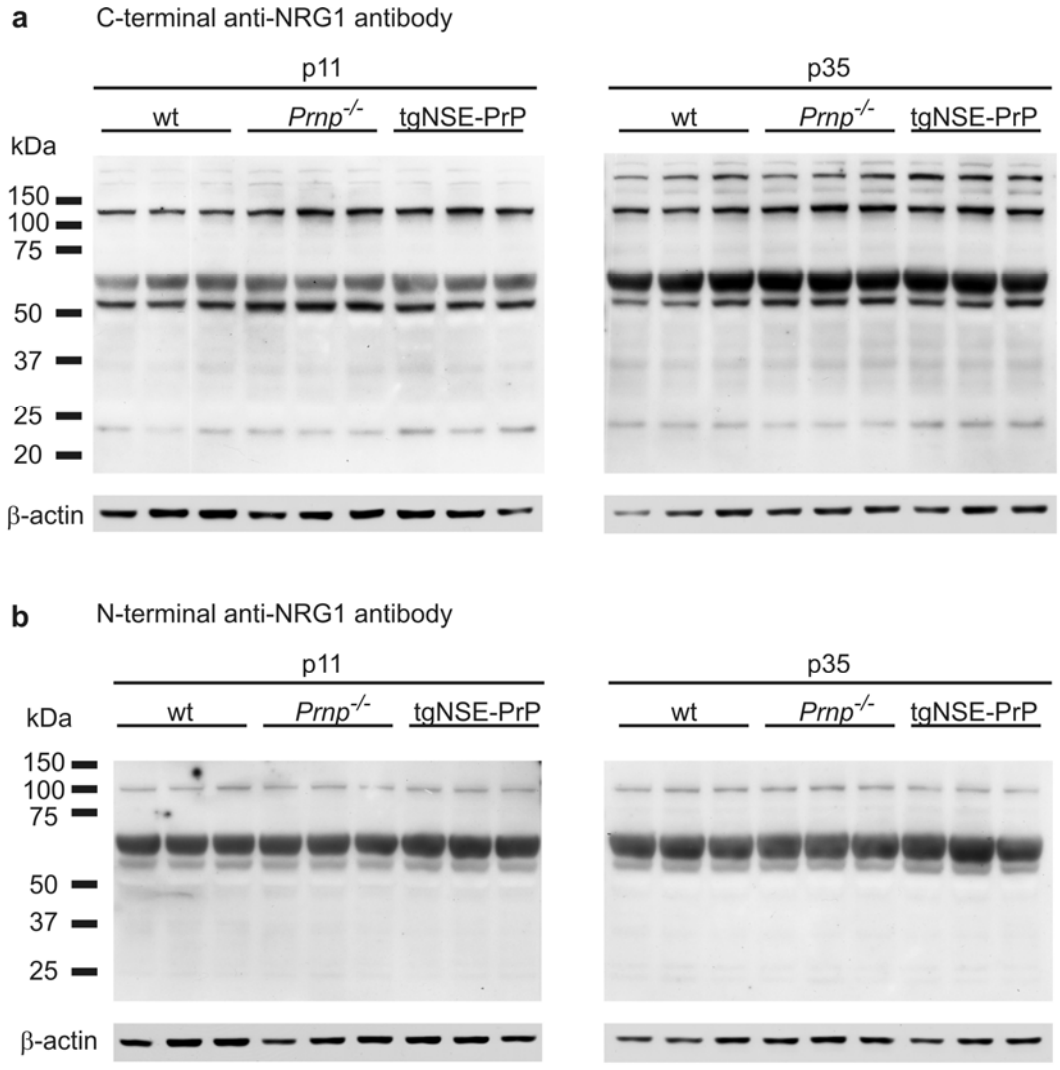

Figure 33. Normal neuregulin-1 expression and processing in *Prnp*$^{o/o}$ sciatic nerves. Western blot using anti-NRG1 against the carboxy- (**a**) or against the amino-terminus (**b**) showed no difference in expression and processing in wt, *Prnp*$^{o/o}$, and tgNSE-PrP at 11 (p11) and 35 (p35) days of age.

5.4.9 No morphological alterations in central *Prnp*$^{o/o}$ myelin

Since prion diseases mainly affect the CNS, I analyzed whether myelinopathy in *Prnp*$^{o/o}$ extends to the central nervouse system. In white matter of spinal cord, corpus callosum and optic nerve, I failed to detect myelin degeneration in 60-week old *Prnp*$^{o/o}$ mice (**Fig. 34**).

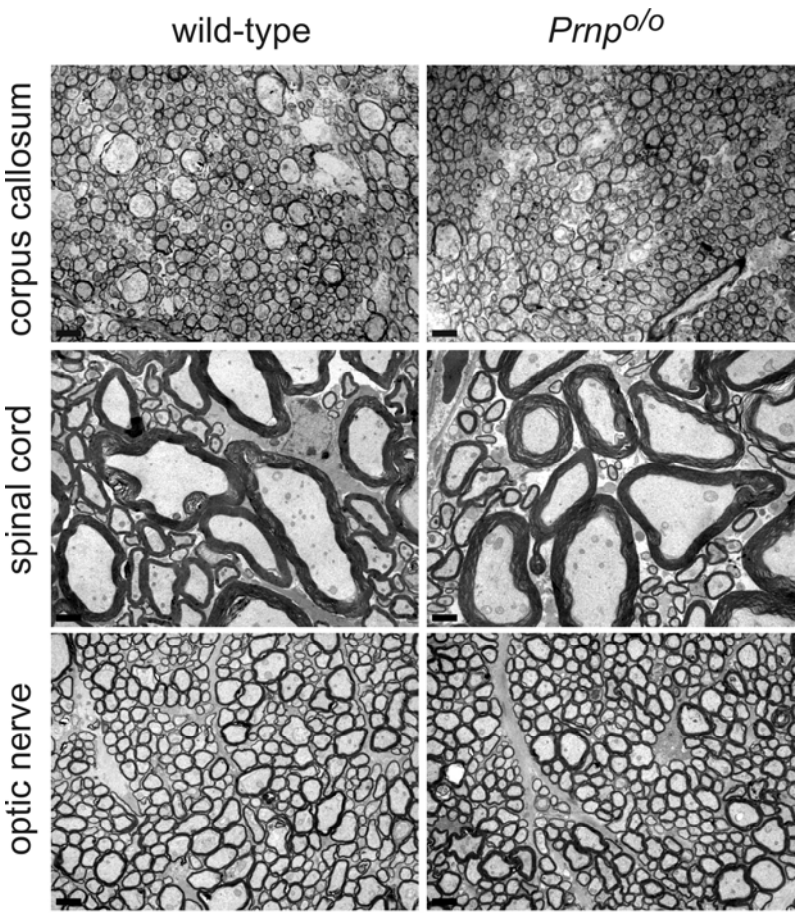

Figure 34. Normal ultrastructure of *Prnp*$^{o/o}$ central nervous system white matter at 60 weeks of age. Sixty-week old *Prnp*$^{o/o}$ compared to wt mice were analyzed by electron microscopy. No morphological abnormalities were observed in corpus callosum, spinal cord white matter and optic nerve. Scale bar = 2 μm. Corpora callosa were analyzed in mixed B6/129Sv mice whereas spinal cords and optic nerves belonged to Balb/c mice.

5.4.10 Genomic analyses

I analyzed DNA short tandem repeats (STR) in 37 mice for the presence of mouse strain-specific polymorphisms that may contribute to the observed phenotypes. Twenty-two STRs covered chromosome 2 (on which *Prnp* resides) and 184 STRs covered the rest of the genome. I was unable to identify any genetic association other than *Prnp* that would explain the CDP phenotype. The genetic markers not flanking the *Prnp* locus were similar in mice with and without neuropathy. This was true for mice on the mixed background B6/129Sv (*tg*NSE-PrP, *Prnp*$^{o/o}$, *tg*PLP-PrP, *tg*DelC4, *tg*PrP$_{\Delta CC}$, *tg*F35) and for mice on FVB (*tgPrnp*^{flox}, *tgPrnp*^{flox} x

*tg*NHF-Cre, *tgPrnp*^{flox} x *tg*Dhh-Cre; **Fig. 35**). When comparing wt and *Prnp*$^{o/o}$ mice on the Balb/c background, STR polymorphisms delineated a genomic region of ca. 14 cM segregating with the *Prnp*^{o} allele and CDP. Since this region was preserved in *Prnp*$^{o/o}$ mice whose neuropathy was suppressed by an unlinked *Prnp* transgene (e.g. *tg*NSE-PrP), it is unlikely that it determined the CDP phenotype (**Fig. 36-38**).

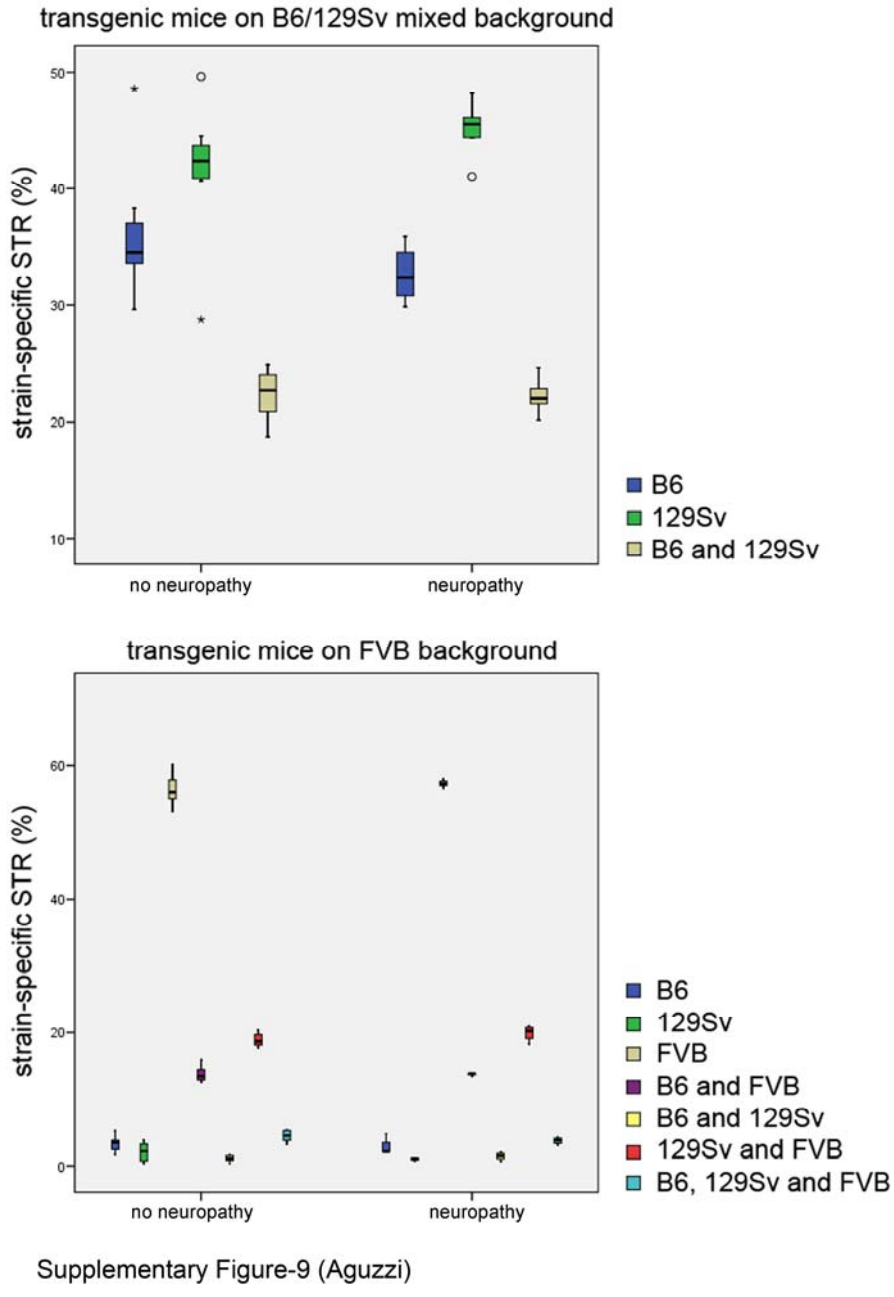

Figure 35. Analysis of polymorphic STR in the entire genome in transgenic mice. Percentage of strain-specific STR in the entire genome (without chromosome 2) are shown by box plots in transgenic mice with or without neuropathy, on B6/129Sv mixed background (upper plot) or those mice backcrossed to FVB (lower plot). Mann-Whitney U-test (2-tailed) did not reveal any significant difference in the composition of genetic background in mice with and without neuropathy.

name of marker:			D2Mit1	D2Mit61	D2Mit327	D2Mit100	D2Mit308	D2Mit395	D2Mit405	D2Mit396	D2Mit493	*Prnp locus*	D2Mit107	D2Mit279	D2Mit70	D2Mit208	D2Mit411	D2Mit209	D2Mit422	D2Mit21	D2Mit513	D2Mit285	D2Mit113	D2Mit148	neuropathy
position in cM:			1	34	40.4	47.5	65.6	66.9	68.9	69	72.1	75	75.6	76.1	76.1	76.7	77.6	78.9	79.7	80	81	86	103	105	
Prnp$^{o/o}$	allele	1	nodiff	129Sv	B6 and 129Sv	129Sv	129Sv	129Sv	B6 and 129Sv	129Sv	129Sv		129Sv		129Sv	129Sv	129Sv	B6 and 129Sv		B6 and 129Sv	129Sv		129Sv	nodiff	yes
	allele	2	129Sv	129Sv	B6 and 129Sv	129Sv	129Sv	129Sv	B6 and 129Sv	129Sv	129Sv		129Sv	129Sv	129Sv	129Sv	nodiff	B6 and 129Sv			129Sv	129Sv	B6	129Sv	
Prnp$^{o/o}$	allele	1	B6	129Sv	B6 and 129Sv	129Sv	129Sv	129Sv		129Sv	129Sv		129Sv	129Sv	129Sv	129Sv	129Sv	B6 and 129Sv	129Sv		129Sv		129Sv	nodiff	yes
	allele	2	129Sv	129Sv		129Sv	129Sv	129Sv		129Sv	129Sv		129Sv	129Sv	129Sv	129Sv	nodiff	B6 and 129Sv	129Sv		129Sv	129Sv	B6	129Sv	
Prnp$^{o/o}$	allele	1		129Sv	B6 and 129Sv	129Sv		129Sv		129Sv			129Sv			129Sv	129Sv	B6 and 129Sv				129Sv	129Sv		yes
	allele	2	129Sv	129Sv	B6 and 129Sv	129Sv	129Sv	129Sv					129Sv			129Sv		B6 and 129Sv	129Sv		129Sv	129Sv			
*tg*C4	allele	1		B6	B6 and 129Sv	B6	129Sv	129Sv	B6 and 129Sv	129Sv	129Sv			129Sv		129Sv	129Sv	B6 and 129Sv	129Sv	B6 and 129Sv	129Sv	129Sv	129Sv	129Sv	no
	allele	2	129Sv	B6	B6 and 129Sv	B6	129Sv	129Sv	B6 and 129Sv	129Sv	129Sv			129Sv		129Sv	129Sv	B6 and 129Sv	129Sv	B6 and 129Sv	129Sv	129Sv	129Sv	129Sv	
*tg*PrP$_{ACC}$	allele	1		129Sv	B6 and 129Sv	129Sv	129Sv	129Sv	B6 and 129Sv	129Sv	129Sv			129Sv		129Sv	129Sv	B6 and 129Sv	129Sv	B6 and 129Sv	129Sv	129Sv	129Sv	129Sv	no
	allele	2				129Sv	129Sv	129Sv	B6 and 129Sv	129Sv	129Sv		129Sv	129Sv		129Sv	129Sv	B6 and 129Sv	129Sv	B6 and 129Sv	129Sv	129Sv	129Sv	129Sv	
*tg*PrP$_{ACC}$	allele	1	129Sv	129Sv	B6 and 129Sv	129Sv	129Sv	129Sv	B6 and 129Sv	129Sv	129Sv			129Sv		129Sv	129Sv	B6 and 129Sv	129Sv	B6 and 129Sv	129Sv	129Sv	129Sv	129Sv	no
	allele	2	129Sv	129Sv	B6 and 129Sv	129Sv	129Sv	129Sv	B6 and 129Sv	129Sv	129Sv		129Sv	129Sv		129Sv	129Sv	B6 and 129Sv	129Sv	B6 and 129Sv	129Sv	129Sv	129Sv	129Sv	
*tg*PrP$_{ACC}$	allele	1	129Sv	129Sv	B6 and 129Sv	129Sv	129Sv	129Sv	B6 and 129Sv	129Sv			129Sv	129Sv	129Sv	129Sv	129Sv	B6 and 129Sv	129Sv	B6 and 129Sv	129Sv	129Sv	129Sv	nodiff	no
	allele	2	B6	B6	B6 and 129Sv	129Sv	129Sv	129Sv		129Sv			129Sv	129Sv	129Sv	129Sv	B6	B6 and 129Sv	129Sv	B6 and 129Sv	129Sv	129Sv	B6	129Sv	
*tg*F35	allele	1	129Sv	129Sv	B6 and 129Sv	129Sv	129Sv	129Sv	B6 and 129Sv	129Sv	129Sv			129Sv		129Sv	129Sv	B6 and 129Sv	129Sv	B6 and 129Sv	129Sv	129Sv		129Sv	yes
	allele	2	129Sv	129Sv	B6 and 129Sv	129Sv	129Sv	129Sv	B6 and 129Sv	129Sv	129Sv		129Sv	129Sv		129Sv	129Sv	B6 and 129Sv	129Sv	B6 and 129Sv	129Sv	129Sv		129Sv	
*tg*F35	allele	1	129Sv	129Sv	B6 and 129Sv	129Sv	129Sv	129Sv	B6 and 129Sv	129Sv	129Sv			129Sv		B6	129Sv	B6 and 129Sv	129Sv	B6 and 129Sv	129Sv	129Sv	129Sv	129Sv	yes
	allele	2	129Sv	129Sv	B6 and 129Sv	129Sv	129Sv	129Sv	B6 and 129Sv	129Sv	129Sv			129Sv		129Sv	129Sv	B6 and 129Sv	129Sv	B6 and 129Sv	129Sv	129Sv	129Sv	129Sv	
*tg*NSE-PrP	allele	1		129Sv	B6 and 129Sv	129Sv	129Sv	129Sv		129Sv	129Sv		129Sv	129Sv	129Sv	129Sv	129Sv	B6 and 129Sv	129Sv	B6 and 129Sv	129Sv	129Sv			nodiff	no
	allele	2		129Sv	B6 and 129Sv	129Sv	129Sv	129Sv		129Sv	129Sv		129Sv	129Sv	129Sv			B6 and 129Sv	129Sv		129Sv	129Sv				
*tg*NSE-PrP	allele	1		129Sv	B6 and 129Sv	B6	129Sv	129Sv	B6 and 129Sv	129Sv	129Sv		129Sv	129Sv	129Sv	129Sv	129Sv	B6 and 129Sv	129Sv	B6 and 129Sv	129Sv			nodiff	no
	allele	2	129Sv	129Sv	B6 and 129Sv	129Sv	129Sv	129Sv	B6 and 129Sv	129Sv	129Sv		129Sv	129Sv	129Sv	129Sv	129Sv	B6 and 129Sv	129Sv	B6 and 129Sv	129Sv	129Sv		nodiff	
*tg*NSE-PrP	allele	1	B6	129Sv	B6 and 129Sv	B6	129Sv	129Sv	B6 and 129Sv	129Sv	129Sv			129Sv	129Sv	129Sv	129Sv	B6 and 129Sv	129Sv	B6 and 129Sv	129Sv	129Sv	B6	nodiff	no
	allele	2	B6	129Sv	B6 and 129Sv		129Sv	129Sv	B6 and 129Sv	129Sv	129Sv		129Sv	129Sv	129Sv		129Sv	B6 and 129Sv	129Sv	B6 and 129Sv	129Sv	129Sv	B6		
*tg*PLP-PrP	allele	1	B6	129Sv	B6 and 129Sv	129Sv	129Sv	129Sv		129Sv	129Sv		129Sv	129Sv		129Sv	129Sv	B6 and 129Sv	129Sv	B6 and 129Sv	129Sv	129Sv	129Sv	129Sv	yes
	allele	2	129Sv	129Sv	B6 and 129Sv	129Sv	129Sv	129Sv		129Sv	129Sv		129Sv	129Sv		129Sv	129Sv	B6 and 129Sv	129Sv	B6 and 129Sv	129Sv	129Sv	129Sv	129Sv	
*tg*PLP-PrP	allele	1	B6	129Sv	B6 and 129Sv	129Sv	129Sv	129Sv		129Sv					129Sv		129Sv	B6 and 129Sv		B6 and 129Sv		129Sv	129Sv		yes
	allele	2	129Sv	129Sv	B6 and 129Sv	129Sv	129Sv	129Sv		129Sv				129Sv	129Sv		129Sv	B6 and 129Sv	129Sv	B6 and 129Sv		129Sv	129Sv	129Sv	

Figure 36. Analysis of polymorphic STR on chromosome 2 in transgenic mice on B6/129Sv genetic background. Name of marker, position on chromosome 2 in cM, strain origin for each polymorphic marker is indicated for the two alleles of each mouse by a colored box labeled with the respective strain (129Sv, B6), or where the marker corresponds to two strains, with "*129Sv and B6*". Empty boxes indicate that the analysis could not be ascribed to a certain genetic background. "*No diff*" means this polymorphic marker showed the same result for all strains analyzed (Balb/c, FVB, B6, 129Sv). In the right red column, presence or absence of neuropathy are indicated for each individual mouse.

name of marker			D2Mit327	D2Mit100	D2Mit308	D2Mit395	D2Mit405	D2Mit396	D2Mit493	*Prnp* locus	D2Mit279	D2Mit208	D2Mit411	D2Mit136	D2Mit209	D2Mit422	D2Mit21	D2Mit513	D2Mit285	D2Mit113	D2Mit148
position in cM			40.4	47.5	65.6	66.9	68.9	69	72.1	75	76.1	76.7	77.6	78	78.9	79.7	80	81	86	103	104
Balb/c	allele	1	Balbc	B6 and Balbc	Balbc	Balbc	Balbc	Balbc	Balbc		Balbc	Balbc	Balbc	Balbc	Balbc		Balbc	Balbc	Balbc	Balbc	
	allele	2	Balbc	B6 and Balbc	Balbc	Balbc		Balbc	Balbc		Balbc	Balbc		Balbc	Balbc			Balbc	Balbc	Balbc	Balbc and 129Sv
Balb/c	allele	1	Balbc	B6 and Balbc	Balbc	Balbc	Balbc	Balbc	Balbc		Balbc	Balbc	Balbc		Balbc	Balbc and 129Sv	Balbc	Balbc	Balbc	Balbc	nodiff
	allele	2	Balbc	B6 and Balbc	Balbc	Balbc		Balbc	Balbc		Balbc	Balbc	nodiff		Balbc	Balbc and 129Sv		Balbc	Balbc	Balbc	Balbc and 129Sv
Balb/c	allele	1	Balbc	B6 and Balbc	Balbc	Balbc	Balbc	Balbc	Balbc		Balbc	Balbc	Balbc		Balbc		Balbc	Balbc	Balbc		
	allele	2	Balbc	B6 and Balbc	Balbc	Balbc		Balbc	Balbc		Balbc	Balbc	nodiff		Balbc			Balbc	Balbc		Balbc and 129Sv
Balb/c	allele	1	Balbc	B6 and Balbc	Balbc	Balbc		Balbc	Balbc			Balbc	Balbc	Balbc	Balbc	Balbc and 129Sv	Balbc	Balbc	Balbc		
	allele	2	Balbc		Balbc	Balbc	Balbc	Balbc	Balbc			Balbc	nodiff	Balbc	Balbc	Balbc and 129Sv		Balbc	Balbc	Balbc	
Balb/c *Prnp*$^{o/o}$	allele	1	Balbc	B6 and Balbc		129Sv		129Sv	Balbc			129Sv	Balbc		B6 and 129Sv	Balbc and 129Sv		Balbc	Balbc	Balbc	
	allele	2	Balbc	B6 and Balbc	129Sv	129Sv			Balbc		129Sv	129Sv	nodiff		B6 and 129Sv	Balbc and 129Sv		Balbc	Balbc	Balbc	Balbc and 129Sv
Balb/c *Prnp*$^{o/o}$	allele	1	Balbc	B6 and Balbc	129Sv	Balbc			Balbc		129Sv	129Sv	Balbc		B6 and 129Sv	Balbc and 129Sv		Balbc		Balbc	
	allele	2	Balbc	B6 and Balbc	129Sv	129Sv			Balbc		129Sv	129Sv	Balbc		B6 and 129Sv	Balbc and 129Sv		Balbc		Balbc	Balbc and 129Sv
Balb/c *Prnp*$^{o/o}$	allele	1	Balbc	B6 and Balbc	129Sv	129Sv		129Sv	Balbc		129Sv	129Sv	Balbc	129Sv	B6 and 129Sv	Balbc and 129Sv		Balbc	Balbc	Balbc	nodiff
	allele	2	Balbc	B6 and Balbc	129Sv	129Sv			Balbc		129Sv	129Sv	nodiff	129Sv	B6 and 129Sv	nodiff	Balbc	Balbc	Balbc		Balbc and 129Sv
Balb/c *Prnp*$^{o/o}$	allele	1	Balbc		129Sv	129Sv		129Sv	Balbc			129Sv	Balbc		B6 and 129Sv	Balbc and 129Sv	Balbc	Balbc	Balbc		
	allele	2	Balbc		129Sv	129Sv			Balbc		129Sv	129Sv	nodiff		B6 and 129Sv	Balbc and 129Sv		Balbc	Balbc		Balbc and 129Sv
Balb/c *Prnp*$^{o/o}$	allele	1	Balbc	B6 and Balbc	129Sv	129Sv		129Sv	Balbc			129Sv	Balbc	129Sv	B6 and 129Sv		Balbc	Balbc	Balbc	Balbc	
	allele	2	Balbc	B6 and Balbc	129Sv	129Sv	Balbc		Balbc		129Sv	129Sv	nodiff	129Sv	B6 and 129Sv			Balbc	Balbc	Balbc	Balbc and 129Sv
Balb/c *Prnp*$^{o/o}$	allele	1	Balbc	B6 and Balbc	129Sv	Balbc	Balbc	Balbc	Balbc		Balbc	Balbc	Balbc		B6 and 129Sv		Balbc	Balbc	Balbc	Balbc	
	allele	2	Balbc	B6 and Balbc	129Sv	129Sv			Balbc		129Sv	129Sv	nodiff	Balbc	B6 and 129Sv		Balbc	Balbc	Balbc		Balbc and 129Sv
Balb/c *Prnp*$^{o/o}$	allele	1	Balbc	B6 and Balbc		129Sv		129Sv	Balbc		129Sv	129Sv	Balbc		B6 and 129Sv	Balbc and 129Sv		Balbc	Balbc	Balbc	nodiff
	allele	2	Balbc	B6 and Balbc	129Sv	129Sv			Balbc		129Sv	129Sv	nodiff		B6 and 129Sv	Balbc and 129Sv		Balbc	Balbc	Balbc	Balbc and 129Sv
Balb/c *Prnp*$^{o/o}$	allele	1	Balbc	B6 and Balbc		129Sv		129Sv	Balbc		129Sv	129Sv	Balbc		B6 and 129Sv	Balbc and 129Sv		Balbc	Balbc	Balbc	
	allele	2	Balbc	B6 and Balbc	129Sv	129Sv			Balbc		129Sv	129Sv	nodiff		B6 and 129Sv	Balbc and 129Sv		Balbc	Balbc	Balbc	
Balb/c *Prnp*$^{o/o}$	allele	1	Balbc		129Sv	129Sv		129Sv	Balbc			129Sv	Balbc		B6 and 129Sv	Balbc and 129Sv	Balbc	Balbc	Balbc	Balbc	
	allele	2	Balbc		129Sv	129Sv	Balbc		Balbc			129Sv	nodiff		B6 and 129Sv	Balbc and 129Sv	Balbc	Balbc	Balbc	Balbc	

Figure 37. Analysis of polymorphic STR on chromosome 2 in *Prnp*P$^{o/o}$P mice backcrossed to Balb/c compared to wt Balb/c mice. Name of marker, position on chromosome 2 in cM, strain origin for each polymorphic marker is indicated for the two alleles of each mouse by a colored box labeled with the respective strain (Balb/c, 129Sv, B6), or where the marker corresponds to two strains, with "*B6 and Balb/c*", "*129Sv and Balb/c*", or "*129Sv and B6*". Empty boxes indicate that the result could not be ascribed to a certain genetic background. "*No diff*" means this polymorphic marker showed the same result for all strains analyzed (Balb/c, FVB, B6, 129Sv).

name of marker			D2Mit1	D2Mit327	D2Mit100	D2Mit395	D2Mit396	D2Mit493	*Prnp* locus	D2Mit279	D2Mit411	D2Mit422	D2Mit21	D2Mit513	D2Mit404	D2Mit285	D2Mit113	D2Mit148	neuropathy
position in cM:			1	40.4	47.5	66.9	69	72.1	75	76.1	77.6	79.7	80	81	81.7	86	103	105	
tgPrnp^{flox}	allele	1		B6 and 129Sv	129Sv	129Sv	129Sv	B6			FVB	129Sv and FVB		B6	FVB	B6	FVB	FVB	no
	allele	2	FVB	FVB	129Sv	129Sv	129Sv	129Sv and FVB		129Sv	FVB	129Sv and FVB		129Sv and FVB	FVB	FVB	FVB	FVB	
tgPrnp^{flox}	allele	1		B6 and 129Sv	129Sv	129Sv	129Sv	B6			FVB	129Sv and FVB		B6	FVB	B6	FVB	FVB	no
	allele	2	FVB	FVB	129Sv	129Sv	129Sv	129Sv and FVB		129Sv	FVB	129Sv and FVB		129Sv and FVB	FVB	FVB	FVB	FVB	
tgPrnp^{flox}	allele	1		B6 and 129Sv	129Sv	129Sv	129Sv	B6		129Sv	FVB	129Sv and FVB		B6	FVB	B6	FVB	FVB	no
	allele	2	FVB	FVB	129Sv	129Sv	129Sv	129Sv and FVB		129Sv		129Sv and FVB		129Sv and FVB		FVB			
tgPrnp^{flox}	allele	1		B6 and 129Sv		129Sv	129Sv	B6				129Sv	B6 and 129Sv	B6	FVB	B6	FVB		no
	allele	2		B6 and 129Sv		129Sv	129Sv	129Sv and FVB		129Sv			B6 and 129Sv	129Sv and FVB		FVB	FVB		
tgPrnp^{flox}	allele	1		B6 and 129Sv	129Sv	129Sv	129Sv	B6			FVB	129Sv and FVB	B6 and 129Sv	B6		B6			no
	allele	2		B6 and 129Sv	129Sv	129Sv	129Sv	B6		129Sv	FVB	129Sv and FVB		B6	FVB	B6			
tgPrnp^{flox}	allele	1	FVB	B6 and 129Sv	129Sv	129Sv	129Sv	B6			FVB	129Sv and FVB	B6 and 129Sv	B6		B6		FVB	no
	allele	2	FVB	B6 and 129Sv	129Sv	129Sv	129Sv	B6		129Sv	FVB	129Sv and FVB		B6	FVB	B6		FVB	
*tg*Dhh-Cre x *tgPrnp*^{flox}	allele	1		B6 and 129Sv	129Sv	129Sv	129Sv	B6			FVB	129Sv		B6		B6	FVB	FVB	no
	allele	2	FVB	FVB	129Sv	129Sv	129Sv	129Sv and FVB			FVB		B6 and 129Sv	129Sv and FVB		FVB	FVB		
*tg*Dhh-Cre x *tgPrnp*^{flox}	allele	1	FVB	B6 and 129Sv	129Sv	129Sv	FVB				FVB	129Sv		B6	FVB	B6	FVB	FVB	no
	allele	2	FVB	FVB	129Sv	129Sv	FVB			129Sv				129Sv	FVB	FVB	FVB		
*tg*Dhh-Cre x *tgPrnp*^{flox}	allele	1		B6 and 129Sv	129Sv	129Sv	129Sv	B6			FVB	129Sv		B6	FVB	B6	FVB	FVB	no
	allele	2	FVB	FVB	129Sv	129Sv	129Sv	129Sv and FVB		129Sv	FVB		B6 and 129Sv	129Sv and FVB		FVB	FVB		
*tg*Dhh-Cre x *tgPrnp*^{flox}	allele	1		B6 and 129Sv	129Sv	129Sv	129Sv	B6			FVB	129Sv		B6		B6		FVB	no
	allele	2	FVB	FVB	129Sv	129Sv	129Sv	129Sv and FVB		129Sv	FVB	129Sv	B6 and 129Sv	129Sv and FVB		FVB			
*tg*NFH-Cre x *tgPrnp*^{flox}	allele	1	FVB	B6 and 129Sv	129Sv	129Sv	129Sv			129Sv	FVB	129Sv and FVB	B6 and 129Sv	B6	FVB	B6	FVB	nodiff	yes
	allele	2	FVB	B6 and 129Sv	129Sv	129Sv	129Sv			129Sv	FVB	129Sv and FVB		129Sv and FVB	FVB	FVB	B6	nodiff	
*tg*NFH-Cre x *tgPrnp*^{flox}	allele	1	FVB	B6 and 129Sv	129Sv	129Sv	129Sv	B6		129Sv	FVB	129Sv and FVB	B6 and 129Sv	B6	FVB	B6	FVB	FVB	yes
	allele	2	FVB	B6 and 129Sv	129Sv	129Sv	129Sv	129Sv and FVB		129Sv	FVB	129Sv and FVB	B6 and 129Sv	129Sv and FVB	FVB	FVB	B6	FVB	
*tg*NFH-Cre x *tgPrnp*^{flox}	allele	1	FVB	B6 and 129Sv	129Sv	129Sv	129Sv			129Sv	FVB	129Sv and FVB		B6		B6	FVB	nodiff	yes
	allele	2	FVB	B6 and 129Sv	129Sv	129Sv	129Sv			129Sv	FVB	129Sv and FVB		129Sv and FVB		FVB	FVB	nodiff	
*tg*NFH-Cre x *tgPrnp*^{flox}	allele	1	FVB	B6 and 129Sv	129Sv	129Sv	129Sv	129Sv and FVB		129Sv	FVB	129Sv and FVB		129Sv and FVB		FVB	B6	nodiff	yes
	allele	2	FVB	B6 and 129Sv	129Sv	129Sv	129Sv	129Sv and FVB		129Sv	FVB	129Sv and FVB		129Sv and FVB		FVB	B6	nodiff	

Figure 38. Analysis of polymorphic STR on chromosome 2 in transgenic mice backcrossed to FVB genetic background. Name of marker, position on chromosome 2 in cM, strain origin for each polymorphic marker is indicated for the two alleles of each mouse by a colored box labeled with the respective strain (FVB, 129Sv, B6), or where the marker corresponds to two strains, with "*129Sv and FVB*", "*129Sv and B6*". Empty boxes indicate that the result could not be ascribed to a certain genetic background. "*No diff*" means this polymorphic marker showed the same result for all strains analyzed (Balb/c, FVB, B6, 129Sv). In the right red column, presence or absence of neuropathy are indicated for each individual mouse.

5.4.11 Stability of early *Prnp*$^{o/o}$ myelin proteome

Myelin extracts from *Prnp*$^{O/O}$ compared to wt mice did not show any gross alteration in myelin protein composition in 1D gels (SDS-PAGE) stained with Coomassie blue (**Fig. 39**). To analyze more subtle differences in the myelin proteome, I performed DIGE experiments and identified eight proteins which were differentially expressed in myelin of 4-week old *Prnp*$^{O/O}$ compared to wt mice (proteins with fold change ≥ 1.3, $p<0.05$). Spots of differentially expressed proteins were excised from the gel and analyzed by MALDI-TOF/TOF. A representative gel is shown in **Fig. 40**. The eight proteins and the ratio of protein amount in *Prnp*$^{O/O}$ compared to wt myelin are listed in **Tab. 2**.

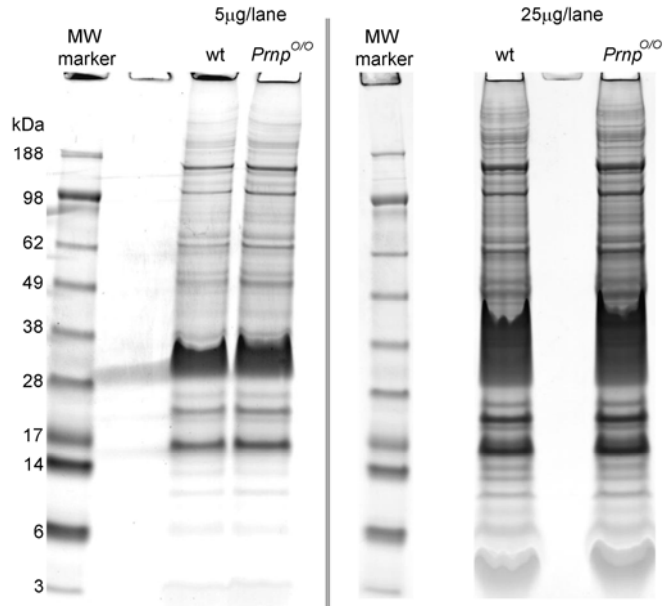

Figure 39. Myelin extracts of *Prnp*$^{o/o}$ compared to wt mice. Different amounts of myelin extracted from 4-week old *Prnp*$^{o/o}$ compared to wt mice were analyzed by SDS-PAGE. Gels were stained with Coomassie blue. No gross alteration in the protein composition was visible.

Figure 40. Myelin extracts of *Prnp*$^{o/o}$ compared to wt mice. Myelin proteins were extracted from 4-week old *Prnp*$^{o/o}$ and wt mice, dye-labelled and analyzed by DIGE. Eight protein spots were differentially expressed, excised and analyzed by MALDI-TOF/TOF.

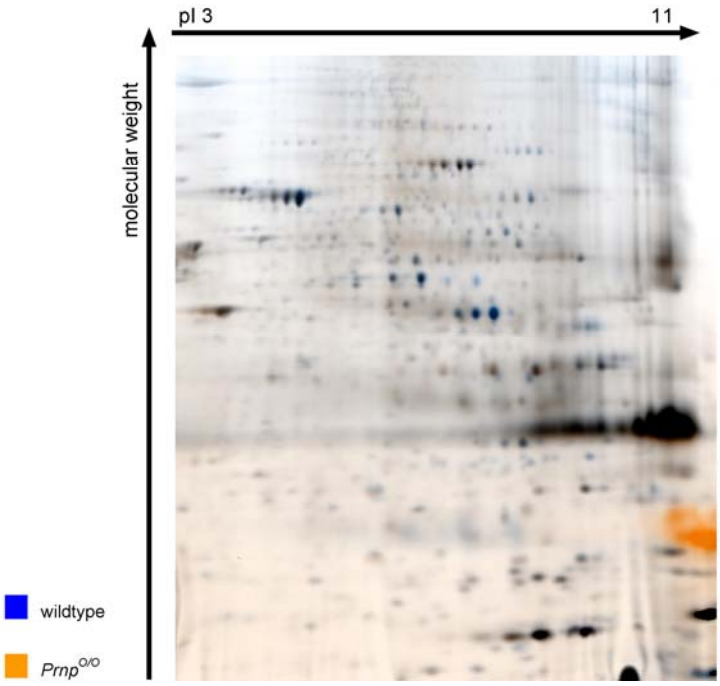

Table 2. Differentially expressed proteins identified by DIGE/ MALDI-TOF/TOF

Proteins with fold change ≥ 1.3, p<0.05	***Prnp*$^{O/O}$/ wt**
enolase B	0.6
creatine kinase M (CKM)	0.6
septin 9	1.4
tubulin alpha 1A	1.5
actin related protein 2/3 (ARPC2)	1.3
PIP transfer protein alpha	1.5
dynein light chain 1/2/ DLC8	1.5
alpha Crystallin B	1.7

For confirmation of the DIGE results, I performed regular Western blots with independent myelin protein extracts of 4-week old mice. The only protein whose differential expression could be verified by Western blot was septin 9 (**Fig. 41, Tab. 3**). On mRNA level, there was no significant difference in septin 9 expression (data not shown). Interestingly, the differential protein expression level of septin 9 was associated with a differential localization of septin 9 in *Prnp*$^{O/O}$ compared to wt myelin. Immunofluorescence showed septin 9 in SLIs of *Prnp*$^{O/O}$ mice, in contrast, septin 9 was absent from wt SLIs. However, septin 9 was also present in SLIs of *tgNSE-PrP* mice (**Fig. 42**). Therefore, absence of PrP^{C} from the myelin sheath correlates with the presence of septin 9 in SLIs. Since *tgNSE-PrP* mice lack signs of neuropathy, the differential localization of septin 9 in SLIs did not correlate with neuropathy and is therefore unlikely to be pathogenetically relevant for the *Prnp*$^{O/O}$ neuropathy. In addition, septin 7, a known binding partner of septin 9 was expressed at wt levels in sciatic nerves of *Prnp*$^{O/O}$ mice (**Fig. 41**).

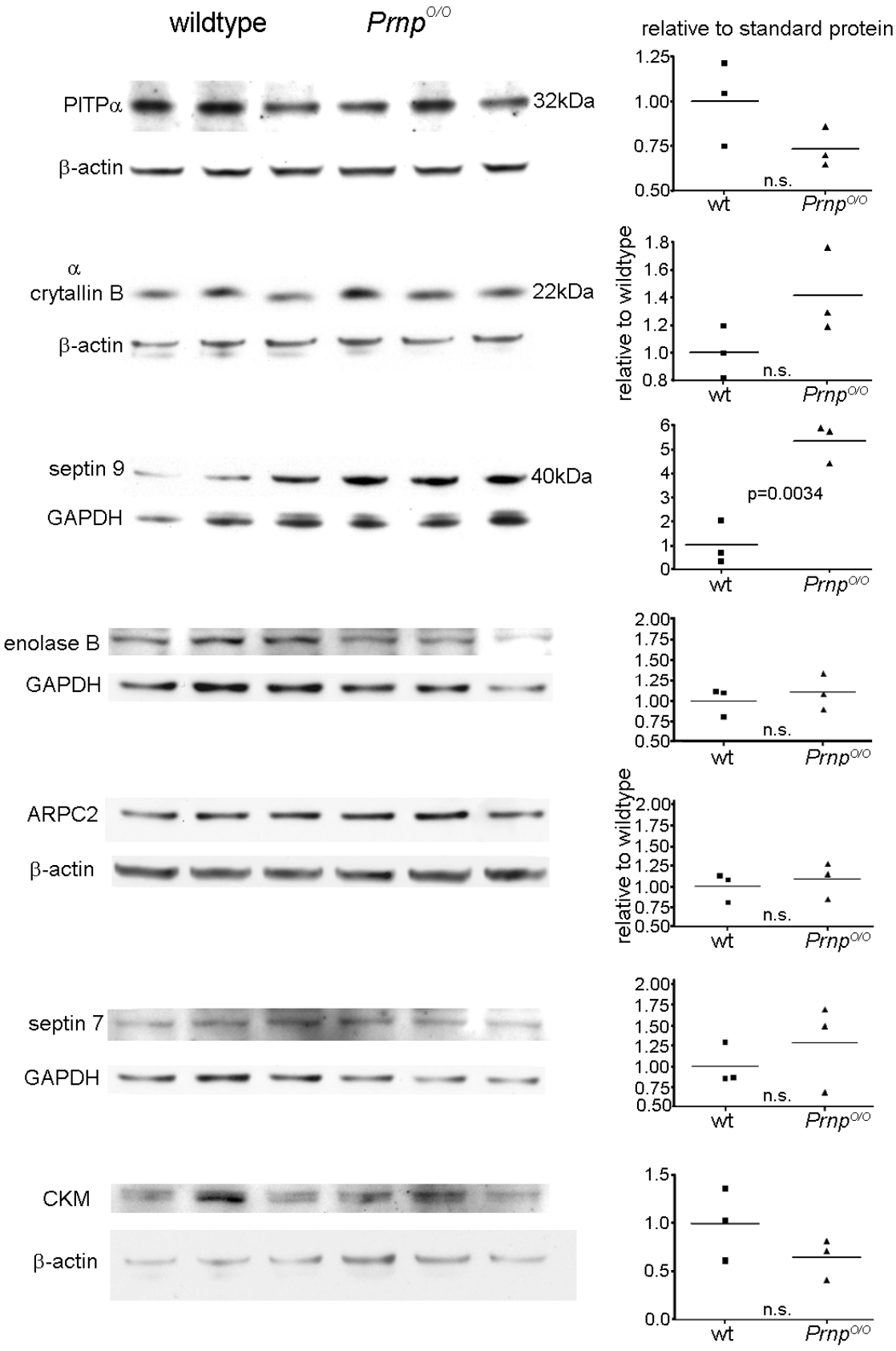

Figure 41. Myelin extracts of *Prnp*$^{o/o}$ compared to wt mice. Myelin proteins were extracted from seven-week old *Prnp*$^{o/o}$ and wt mice, and analyzed by Western blots. Those proteins identified by DIGE to be differentially expressed in *Prnp*$^{O/O}$ compared to wt were analyzed. In addition, septin 7 expression was analyzed. Only septin 9 was confirmed to be differentially expressed.

Table 3. Western blot results of myelin proteins identified by DIGE

	***Prnp*$^{o/o}$/ wt (p value)**	**DIGE: *Prnp*$^{o/o}$/ wt**
enolase B	1.10 (p=0.56)	0.6
creatine kinase M (CKM)	0.65 (p=0.23)	0.6
septin 9	**5.35 (p=0.0034)**	1.4
tubulin alpha 1A	*no difference*	1.5
actin related protein 2/3 (ARPC2)	1.09 (p=0.62)	1.3
PIP transfer protein alpha	0.73 (p=0.15)	1.5
dynein light chain 1/2/ DLC8	*not determined*	1.5
alpha Crystallin B	1.41 (p=0.12)	1.7

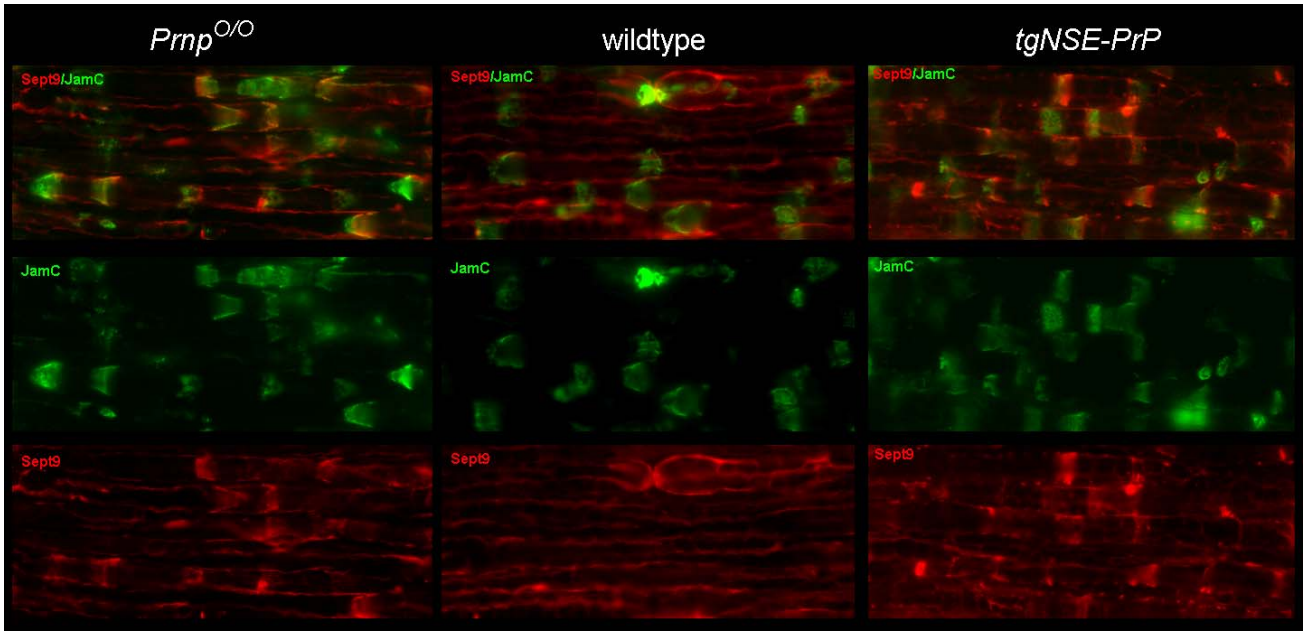

Figure 42. Localization of septin 9 in *Prnp*$^{o/o}$, wt, and *tgNSE-PrP* nerves. Immunofluorescence images of longitudinal sections of *Prnp*$^{O/O}$, wt, and *tgNSE-PrP* nerves. Co-staining for JamC and septin 9 is performed, showing that septin 9 is present in *Prnp*$^{O/O}$ and *tgNSE-PrP* SLIs, but absent from SLIs of wt mice.

5.4.12 Stability of early *Prnp*$^{o/o}$ nerve transcriptome

Since there was no relevant difference in the early *Prnp*$^{O/O}$ myelin proteome, I investigated the early myelin transcriptome – in 5-week old mice. To exclude that genes unlinked to the *Prnp* locus ("genetic background genes") cause transcriptome alterations, I analyzed *Prnp*$^{O/O}$ sciatic nerve transcriptome compared to wt in two different genetic backgrounds (five *Prnp*$^{O/O}$ backcrossed to C57Bl/6 compared to five C57Bl/6 and five *Prnp*$^{O/O}$ backcrossed to Balb/c

compared to five Balb/c). Only nine mRNAs were identified to be differentially expressed (>1.5 fold change, $p < 0.01$) in *Prnp*$^{O/O}$ compared to wt on both genetic backgrounds, C57Bl/6 and Balb/c (**Fig. 43**). Of these nine mRNAs, one was *Prnp*, four genes were localized around the *Prnp* gene. These genes originate most likely from the ES cell genome, which is derived from a 129Sv substrain and cannot be compared to Balb/c and C57Bl/6 wt genes. One mRNA is currently unidentified. One mRNA was upregulated on one background and downregulated in the other. The remaining two mRNAs (neuregulin 1 and adiponutrin) were further analyzed by real time PCR. Differential expression could not be verified by real time PCR (data not shown). Therefore, I analyzed the original data again with less stringent criteria (genes identified in one background > 2 fold change, $p < 0.01$ and in the other background > 2 fold change, $0.05 > p > 0.01$ as well as genes identified in one background > 2 fold change, $p < 0.01$ and undetected in other background; **Fig. 44**).

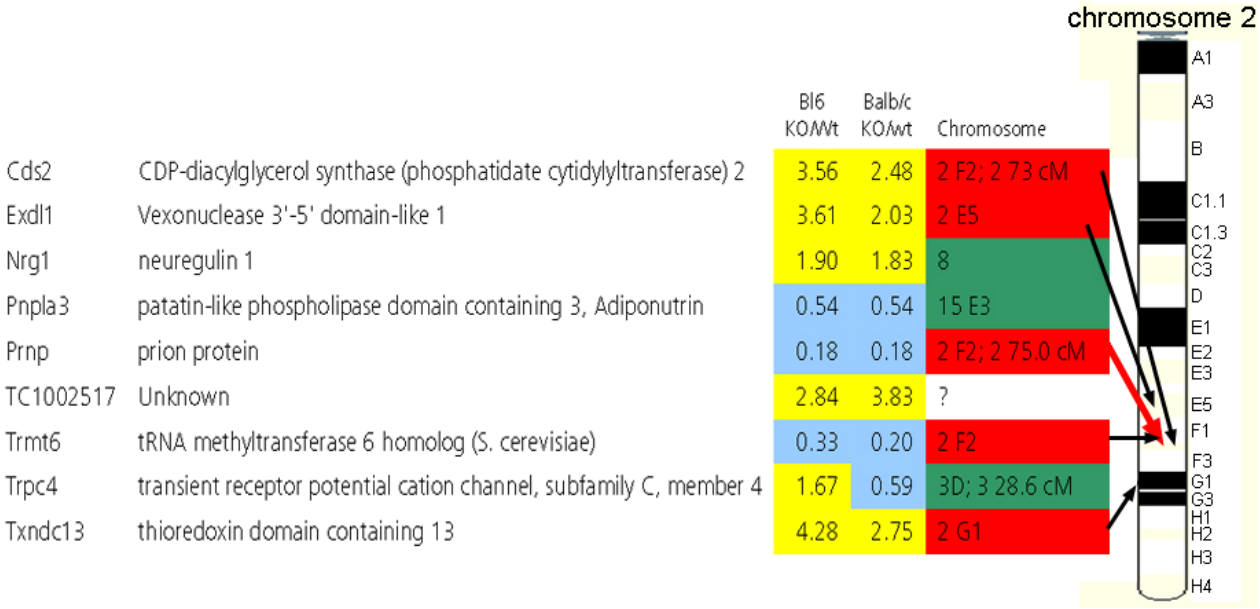

Figure 43. Genes identified by microarray to be differentially expressed in *Prnp*$^{o/o}$ (KO) compared to wt nerves. Sciatic nerves of 5-week old *Prnp*$^{O/O}$ mice were analyzed by microarray for alterations in their transcriptome when compared to wt mice. Mice on two different genetic backgrounds (Balb/c and C57Bl/6 = Bl6) were analyzed and only those genes with alterations > 1.5 fold and p values < 0.01 in both genetic backgrounds are listed. On the right side the chromosomal localization is indicated. For genes on chromosome 2, the localization is indicated by a black arrow, localization of *Prnp* is shown by a red arrow.

		Bl6 KO/wt	p value	Balb/c KO/wt	p value
Shh	Sonic hedgehog	3.001	0.0015	2.66	0.012
Crlf1	cytokine receptor-like factor 1	2.42	0.0004	1.68	0.031
Dazl	deleted in azoospermia-like	n.d.	n.d.	3.86	0.00015
Inmt	indolethylamine N-methyltransferase	n.d.	n.d.	0.45	0.0064
Daf2	decay accelerating factor 2	n.d.	n.d.	2.22	0.00029
Loxl2	16 days neonate thymus cDNA, RIKEN, clone:A130090I05	10.73	0.002	n.d.	n.d.
Anks1b	ankyrin repeat and sterile alpha motif domain containing 1B	2.18	0.0004	n.d.	n.d.
Apoc3	apolipoprotein C-III	0.43	0.0071	n.d.	n.d.
Apoc3	apolipoprotein C-III	0.47	0.0023	n.d.	n.d.

Figure 44. Genes identified by microarray to be differentially expressed in *Prnp*$^{o/o}$ (KO) compared to wt nerves. Mice on two different genetic backgrounds (Balb/c and C57Bl/6 = Bl6) were analyzed and those genes identified in one background > 2 fold change, $p < 0.01$ and in the other background > 2 fold change, $0.05 > p > 0.01$ as well as genes identified in one background > 2 fold change, $p < 0.01$ and undetected in the other background are listed.

The only gene whose differential expression could be verified on both genetic backgrounds by real time PCR was sonic hedgehog (Shh; **Fig. 45**). However, in older mice (35 weeks, mixed background) this difference was reversed – there was a lower Shh expression in *Prnp*$^{O/O}$: ~30% of wt expression, p=0.06; ~25% of *tgNSE-PrP* p=0.01 (data not shown).

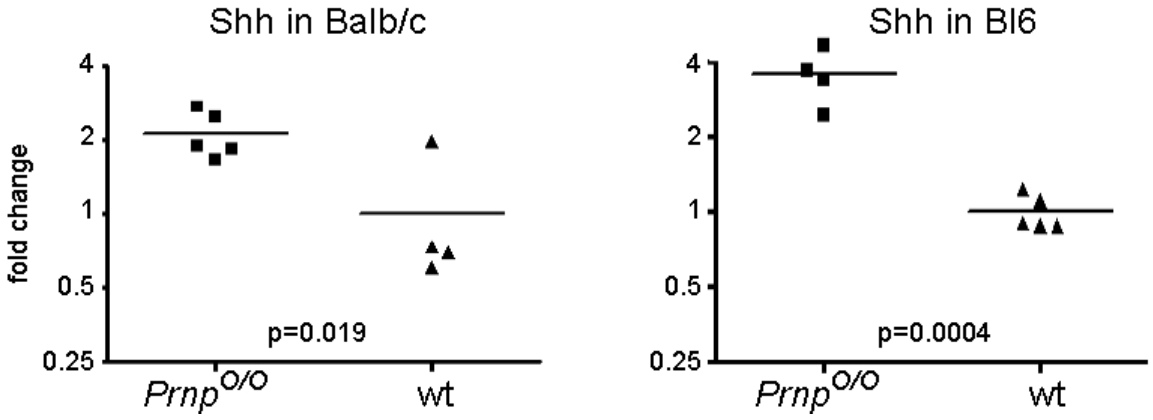

Figure 45. Sonic hedgehog was differentially expressed in *Prnp*$^{O/O}$ mice compared to wt. Differential expression of sonic hedgehog (Shh) was verified in independently extracted sciatic nerve mRNA on two different genetic backgrounds (Balb/c and C57Bl/6 = Bl6; 5-week old).

5.4.13 Increased amounts of IgG_1 in *Prnp*$^{o/o}$ nerves

In Western blot studies, I detected a higher amount of IgG_1 in peripheral nerves of young (10- and 35-day old) *Prnp*$^{O/O}$ compared to wt and *tgNSE-PrP* nerves. Absence of the signal in Rag1$^{-/-}$ nerves indicates that the signal was indeed an immunoglobulin (**Fig. 46**). In *tgNSE-PrP* nerves lacking signs of neuropathy, the increase of IgG_1 was reversed to wt levels (**Fig.47**). However, as indicated by the presence of neuropathy in *Prnp*$^{O/O}$ Rag1$^{-/-}$ mice (**Fig. 30**) which lack immunoglobulins, the presence of IgG_1 alone does not explain development of neuropathy. A similar amount of other serum proteins, like albumin and IgG_{2a}, in *Prnp*$^{O/O}$ and wt nerves indicates that the blood-nerve barrier is intact in *Prnp*$^{O/O}$ mice (**Fig. 48**).

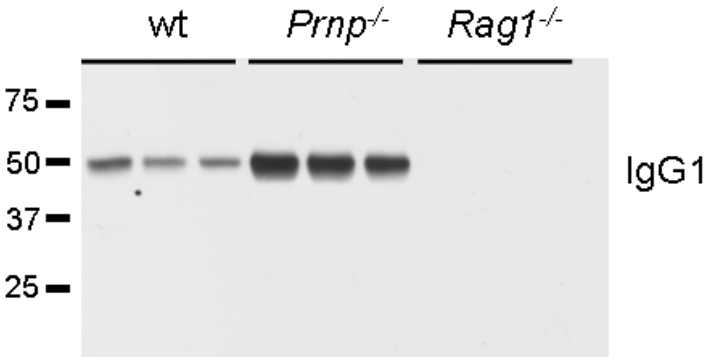

Figure 46. IgG_1 in sciatic nerves of 10-day old *Prnp*$^{O/O}$ and wt mice. Higher amount of IgG_1 in sciatic nerves of 10-day old *Prnp*$^{O/O}$ compared to wt mice. Signal was absent in Rag1$^{-/-}$nerves. Molecular weight is shown on the left side (in kDa).

Figure 47. IgG_1 in sciatic nerves of 10-day old *tgNSE-PrP*, *Prnp*$^{O/O}$ and wt mice. The NSE-PrP transgene reversed the higher amount of IgG_1 in sciatic nerves of 10-day old *Prnp*$^{O/O}$ mice. Amount of IgG_1 relative to control protein Nfasc is shown.

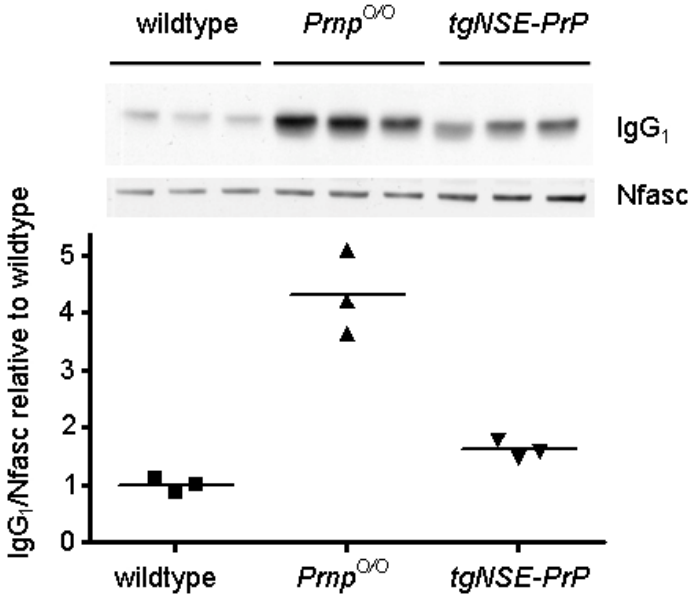

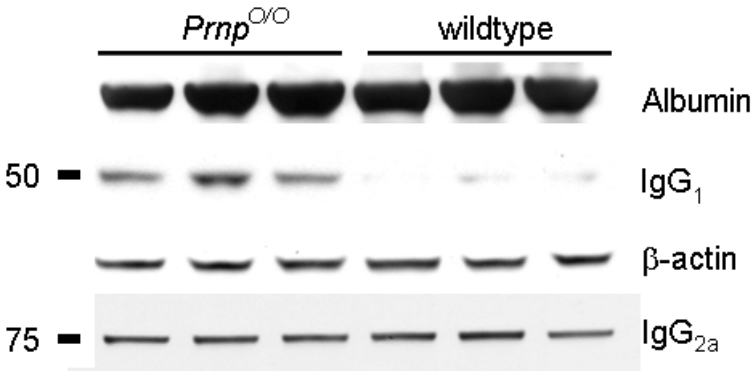

Figure 48. IgG_1, IgG_{2a} and albumin in sciatic nerve myelin of *Prnp*$^{O/O}$ and wt mice. Higher amount of IgG_1 myelin extracted from sciatic nerves of 35-day old *Prnp*$^{O/O}$ compared to wt mice. In contrast, amount of albumin and IgG_{2a} was similar. Molecular weight is shown on the left side (in kDa).

5.5 Discussion

5.5.1 Absence of genetic confounders in *Prnp*$^{-/-}$ CDP

CDP was associated with four independently targeted *Prnp* knockout lines, including pure 129/Ola *Prnp*$^{Edbg/Edbg}$ mice. *Prnp*-flanking genes in *Prnp*$^{Edbg/Edbg}$ and *Prnp*$^{GFP/GFP}$ mice did not cause CDP, as both strains were made in 129/Ola-derived ES cells, and 129/Ola wt mice did not develop any neuropathy. Breeding to various strains and genome-wide STR analyses failed to identify any role for genes outside of the *Prnp* locus in the pathogenesis of CDP. *Prnp*$^{o/o}$ and *Prnp*$^{Edbg/Edbg}$ mice suffered from CDP despite normal expression of Dpl, indicating that Dpl upregulation did not cause the polyneuropathy. CDP was present in mice lacking both *Prnp* and *Prnd*[140] but absent from mice selectively lacking *Prnd*[141]. Therefore Dpl, unlike PrP^{C}, is dispensable for the maintenance of peripheral nerves.

5.5.2 Time course of *Prnp*$^{-/-}$ CDP

The first signs of CDP (mild electrophysiological alterations, reduced grip strength, and CD68^{+} digestion chambers) became detectable around 10 weeks of age, i.e. immediately after completion of peripheral myelination. Accordingly, ultrastructural examinations confirmed the initial formation of morphologically normal myelin in the absence of PrP^{C}. I conclude that demyelination is early but not congenital. Akt and Erk phosphorylation, which is regulated during myelination[146], was indistinguishable between *Prnp*$^{o/o}$ and wt myelinating nerves. Assuming that any differences have not been obfuscated by neuronal Akt/Erk, these results suggest that PrP^{C}, even if it modulates Akt, Fyn, cAMP, and Erk1/2 (ref. [97, 99, 107, 108, 110]), exerts its effects on myelin through different pathways.

5.5.3 Bahavioral tests of *Prnp*$^{-/-}$ mice

The clinical manifestations of the polyneuropathy were limited to reduced grip strength and nociception. These phenotypes are consistent with incomplete demyelination and may explain

some of the reported behavioral abnormalities of *Prnp*$^{o/o}$ mice[150-151]. Nazor et al. reported vacuolation and astrogliosis in *Prnp*$^{-/-}$ mice[152]. Interestingly, they also observed a decreased latency-to-fall in accelerating rota-rod tests of *Prnp*$^{-/-}$ mice. This is in contrast to my observation of an unaltered performance in rotarod test. No difference in non-accelerating rota-rod was also described by others[153]. A possible explanation is the difference in the genetic background, as Nazor et al. investigated mice on FVB background while I and others used mice on a C57/Bl6, Balb/c or a mixed genetic background (C57Bl/6;129Sv). In contrast, I observed a difference in the response to thermal stimulus in the hot plate test. In another study, Meotti et al. proposed an involvement of PrP^{C} in nociceptive transmission, based on the finding that *Prnp* $^{-/-}$ mice were more resistant than wt mice to thermal nociception in the tail-flick test[150]. However, in contrast to my results, no significant difference was found on the hot plate test in the latter study. This again may indicate background-dependent differences in the clinical manifestation of the neuropathy. It should be noted that the hot plate test measures the response to a thermal stimulus which requires both nociception and motor response. I hypothesize that worse performance of *Prnp*$^{-/-}$ in the hot plate test in my study is the consequence of impaired motor function, since the effort of mice to lick paws was visible and the mice showed signs of pain in their paws (slight elevation of feet to avoid contact to hot plate, crying noise when mice were touched afterwards). This might be more pronounced on Balb/c background than on other backgrounds. Consistent with the apparent motor impairment in the hot plate test, in the grip strength test I observed reduced muscle strength in *Prnp*$^{-/-}$ mice. In summary, behavioral tests in my study together with the findings of others suggest that *Prnp*$^{-/-}$ mice may have altered nociception and strength, but to which extent these behavioral alterations manifest strongly depends on the genetic background and/or the environmental conditions. *Prnp*$^{-/-}$ neuropathy is a likely explanation for the observed behavioral phenotype. In general, performance in behavioral tests is known to depend strongly on the genetic background of mice, for nociception[154], motor function[155] and cognition[156]. Nico et al. reported that some behavioral abnormalities in *Prnp*$^{-/-}$ mice compared to wt are observed only in situations of acute stress, indicating that environmental conditions might also influence behavior[151].

5.5.4 Rescue of *Prnp*$^{o/o}$ neuropathy in *trans*

Since PrP^C-deficient sciatic nerves showed classic ultrastructural and electrophysiological features of demyelinating neuropathies, I was surprised to discover that CDP rescue required expression of PrP^C by neurons, but not by Schwann cells. This unexpected result was confirmed in five genetic paradigms: tissue-restricted *Prnp* expression in neurons or Schwann cells, and tissue-specific ablation of *Prnp* by neuron- or Schwann-cell-restricted Cre transgenes. Therefore, peripheral myelin requires neuronal PrP^C in *trans*, suggesting that PrP^C is involved in directional communication from axons to Schwann cells (**Fig. 49**).

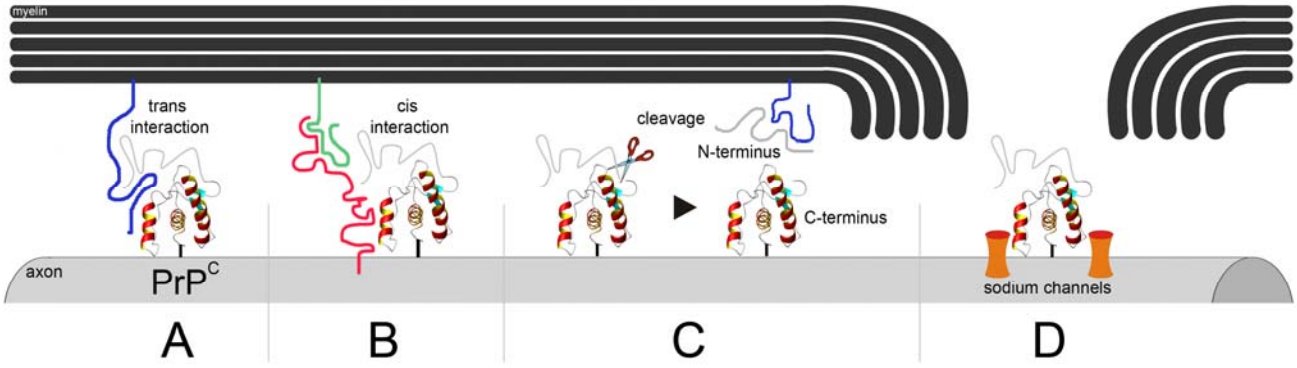

Figure 49. Hypothetical mechanisms of myelin maintenance by neuronal PrP^C. A-B: Neuronal PrP^C may interact in *trans* with Schwann cells. This interaction could be mediated by direct binding of full length PrP^C to an adaxonal myelin surface component (A) or by a neuronal protein complex containing PrP^C which in turn interacts with myelin (B). C: Regulated proteolysis may liberate a bioactive, myelinotrophic amino-terminal PrP^C fragment that travels to, and interacts directly with, the myelin sheath. This model may account for the observed correlation of PrP^C cleavage with myelin homeostasis. D: Alternatively, PrP^C may exert indirect effects on Schwann cells, e.g. by modulating the activity of sodium channels, without causing visible and electrophysiologically measurable alterations of the axon.

Although the *tg*PLP-PrP transgene produced a partial rescue of CDP, the lack of pathology after Schwann-cell specific depletion argues against an essential role of PrP^C in Schwann cells. The partial rescue may be explained by the excessive myelin-specific expression of PrP^C in *tg*PLP-PrP mice. Some of this surplus PrP^C may be transferred to neurons by “GPI painting”[157], or may release myelinotrophic fragments from adaxonal myelin into the axon-glia interspace.

Alternatively, PrP^C might have an additional, cell-autonomous role in Schwann cells which may be related to the localisation of SLIs.

Tissue-specific expression patterns of transgenes do not always accurately reflect those of the parental genes. I therefore investigated whether PrP^C expression in the above mice was as intended. Since peripheral nerves consist mostly of Schwann cell bodies and neuronal processes, their extracts contain predominantly Schwann cell mRNA, whereas neuronal mRNA is localized mainly in DRGs and spinal cord neurons. Indeed, quantitative RT-PCR analyses revealed abundant *Prnp* transcripts in *tg*PLP-PrP nerves, but only little in *tg*NSE-PrP sciatic nerves. In contrast, PrP protein levels in *tg*PLP-PrP and *tg*NSE-PrP nerves were similar to wt nerves. Hence, transgenic expression in *tg*NSE-PrP is largely restricted to the neurons, and suppression of polyneuropathy is not due to illegitimate PrP^C expression in Schwann cells. Furthermore, *in situ* hybridization confirmed that the floxed *Prnp* transgene was excised in most *tgPrnp*^{flox} x *tg*NFH-Cre neurons, whereas the similar levels of *Prnp* mRNA in *tgPrnp*^{flox} x *tg*NFH-Cre and *tgPrnp*^{flox} in sciatic nerves excludes ectopic recombination events.

Signaling from neuron to ensheathing glial cells (axon-to-glia signal) during myelination has been studied extensively, namely the initial formation of myelin sheaths involving the principle known mediator, Neuregulin. In contrast, signalling in the opposite direction, from myelin to the axon (glia-to-axon signal) has been shown to be essential for long-term maintenance of axonal functional integrity[11]. One example of the latter is CNPase; despite its localization in non-compact myelin, CNPase deficient mice develop axonal rather than myelin degeneration[22]. Other myelin components essential for long-term functional integrity of axons are intact myelin peroxisomes, and PLP in the CNS, as well as MAG and ciliary neurotrophic factor (CNTF) in the PNS[25, 27, 158-160]. In addition, the anterograde myelin sheath degradation occurring after axonal cuts indicates that myelin health depends on axonal signals whose molecular nature is largely unknown. Importantly, the evidence reported here identifies PrP^C as a previously unknown crucial neuronal mediator of peripheral myelin maintenance.

Whereas neuronal NRG1 type III regulates Schwann cell development and myelination via ErbB receptors on myelinating cells[161], PrP^C appears to fulfill a different role: rather than disrupting primary myelination, its absence impairs long-term myelin maintenance. Therefore, these two proteins are unlikely to utilize identical transduction pathways. However, PrP^C modulates the activity of BACE[162] which cleaves NRG1 type III and regulates myelination[163-164], begetting the question whether PrP^C may influence myelin maintenance via BACE and NRG1 type III. However, I failed to detect any difference in NRG1 expression in *Prnp*$^{o/o}$ nerves and in PrP^C catabolism in BACE1$^{-/-}$ nerves (data not shown). PrP^C might interact with myelin components directly or through other axonal proteins (**Fig. 35**). Some of the reported PrP^C interacting protein have a role in myelin homeostasis[165] and represent candidate mediators of its myelinotrophic effects. Laminin, laminin receptor, and components of the dystroglycan complex, which is also a laminin receptor, have been reported to interact with PrP^C [129-130, 166-167]. Signals emanating from laminins have a profound impact on Schwann cells (reviewed by [168]), including myelin maintenance[169]. Mutations in α2-laminin cause demyelinating neuropathies in mice and humans. However, there are some morphological differences between mice with altered laminin/ laminin receptor function and *Prnp*$^{-/-}$ mice. Nodal abnormalities and inability of Schwann cells to radially sort axons are typical for alterations in laminin function that are not observed in *Prnp*$^{-/-}$ mice. However, neuronal PrP^C could directly or indirectly interact with or modulate Schwann cell laminin receptors to maintain the myelin sheath. Due to its localization in the adaxonal myelin, MAG is also a very interesting canditate protein reported to interact biochemically with PrP^C in the CNS[165]. However, its role in the molecular function of PrP^C in peripheral nerves remains to be determined.

5.5.5 Structural motifs and cleavage of PrP^C in myelin maintenance

The octarepeat region has often been reported to be required for the function of the PrP^C, for example in the neuroprotective effect of PrP^C in brain ischemia[52] and for the internalization of PrP^C (Ref [121]). Mechanistically, copper binding and/or protection against oxidative stress has been ascribed to this region. However, the octarepeat repeat region was dispensable for the maintenance of the myelin sheath in the peripheral nerves, whereas mice expressing PrP lacking the central domain (aa 94–134) developed CDP[2]. The hydrophobic core (HC), but not the charge cluster (CC_2), of this central PrP^C domain was essential for peripheral myelin maintenance. Consistent with this finding, transgenic mice expressing toxic mutant PrP lacking amino acids 94-121 were shown to display a peripheral neuropathy[2]. The earlier onset and the stronger phenotype in these transgenic mice imply a gain-of-function rather than a loss-of-function as this seen in *Prnp*$^{-/-}$ mice. This shows that distinct domains within PrP^C can exhibit distinct functions.

PrP^C undergoes regulated proteolysis in late secretory compartments[148, 170-172]. I observed an association between presence of CDP and lack of C1-fragment in sciatic nerves. All transgenic mice showing CDP (*tg*E11, *tg*F35, *tg*GPI$^-$PrP, *tg*$PrP_{\Delta HC}$) lacked C1, whereas all PrP mutants rescuing the CDP (*tg*C4 and *tg*$PrP_{\Delta CC}$) produced abundant C1. Cleavage of PrP^C appears therefore to be linked to its myelinotrophic function. This conjecture may also explain the requirement for membrane anchorage of PrP^C for myelin maintenance revealed using *tg*GPI$^-$PrP mice, since anchorless PrP^C did not undergo regulated proteolysis.

Analogous to NRG1, cleavage of axonal PrP^C may produce bioactive fragments which in turn may transmit signals to Schwann cells (**Fig. 35**). Alternatively, cleavage might suppress a PrP^C-mediated signal, whose abrogation may result in uncontrolled signaling and toxicity.

Theoretically, axonal PrP^C may exert indirect actions on myelin. However, this would require the unlikely assumption that lack of PrP^C damages axons to an extent that it affects myelin maintenance, while being morphologically and electrophysiologically undetectable.

Several studies have suggested an involvement of PrP^C in synaptic function (reviewed in [173]). However, the amplitudes of foot muscle CMAPs following distal stimulation were not

significantly altered in 53-week old *Prnp*$^{o/o}$, arguing against a major presynaptic defect in neuromuscular synaptic transmission. This of course does not exclude a synaptic function of PrP^C in the central nervous system. Furthermore, since it is well established that neuronal electrical activity has an impact on Schwann cells and the myelin sheath [174], it is possible that synaptic dysfunction in the spinal cord or modulation of axonal ion channel or pump activities along the nerve fibers contributes to the observed myelin damage in *Prnp* $^{-/-}$ mice. In this context it is of interest that PrP^C has been shown to interact at least biochemically with the catalytic subunit of P-type ATPase[175].

5.5.6 Increased density of SLIs in *Prnp*$^{-/-}$ nerves

As an early alteration in *Prnp*$^{0/0}$ nerves, I indentified an increased density of SLIs. Like the neuropathy, the latter was dependent on the neuronal PrP^C. Increased density of SLIs was previously reported in different myelin mutant mice: Shiverer[176], cerebroside sulfotransferase knockout mice[177], desert hedgehog-null mice[178], Caspr-null mice[179]. However, the molecular mechanism behind the increased density of SLIs in the absence of neuronal PrP^C in peripheral nerves remains to be determined.

5.5.7 No role of lymphocytes in pathogenesis of *Prnp*$^{-/-}$ neuropathy

It has often been suggested that PrP^C has a physiological function in the immune system[180]. Some neuropathies in humans are mediated by auto-antibodies or auto-reactive T-cells. Lymphocytes have been reported to aggravate the neuropathy in mice overexpressing proteolipid protein (PLP) in oligodendrocytes[181]. However, as indicated by the presence of peripheral neuropathy in *Prnp*$^{0/0}$ *Rag1*$^{-/-}$ mice, the presence of functional T- and B-lymphocytes is not required for *Prnp*$^{-/-}$ neuropathy.

5.5.8 CNS in *Prnp*$^{-/-}$ mice

I did not observe any morphological alterations in central *Prnp*$^{-/-}$ myelin. Nevertheless, subliminal myelin pathologies may extend to central myelin in *Prnp*$^{-/-}$ mice[152], and transgenic mice expressing toxic PrP^{C} mutants show both peripheral and central myelinopathy[2, 104]. PrP^{C} deficiency was reported to affect synaptic function[85-86]. However, the amplitudes of foot muscle CMAPs following distal stimulation were not significantly altered in 53-week old *Prnp*$^{o/o}$, arguing against a major presynaptic defect in neuromuscular synaptic transmission. Recently, an involvement of neuronal PrP^{C} in olfactory function was reported[182]. Non-myelinating Schwann cells and olfactory ensheathing cells are morphologically similar and both cell types are intensively studied for their potential to promote axonal regeneration following spinal cord injury [183]. Therefore, the underlying mechanism of peripheral neuropathy and olfactory dysfunction might be similar. Potentially, as in the PNS, communication between axon and olfactory ensheathing cells is disrupted in the absence of PrP^{C}. However, until now, a morphological analysis of the olfactory bulb has not been performed. This could help to identify which cell type is primarily affected in this system.

5.5.9 PrP^{C} in peripheral nerves of humans and livestock

PrP^{C} has been linked previously to peripheral neuropathies in humans. Preclinical peripheral neuropathy often occurs in patients suffering from sporadic CJD[184]. A genetic form of CJD (E200K) is associated with a demyelinating neuropathy[185]. However, with regard to isolated peripheral neuropathies, in one study, scientists failed to identify any mutations in the *PRNP* gene in humans[186]. *PRNP* mutations could be rare and therefore not present in the investigated cohort. More likely is that *PRNP* mutations cause a CNS abnormality with peripheral involvement merely being an accompanying symptom (as in CJD E200K).

Recently, scientists have succeeded in generating *Prnp* deficient farm animals, such as cattle[187] and goats[188-190]. It has been reported that these animals are phenotypically and histopathologically normal. However, to my knowledge, investigation of peripheral nerves in

these animals, electrophysiologically or ultrastructurally, has not been reported. This would certainly be interesting, as it might have important implications on the use of these animals for agriculture.

5.5.10 Stability of *Prnp*$^{o/o}$ nerve transcriptome and myelin proteome

The sciatic nerve transcriptome and proteome of *Prnp*$^{O/O}$ mice, as analyzed by microarray and DIGE did not appear to harbour any obvious abnormalities. The only protein found to be differentially expressed in myelin of wt and *Prnp*$^{o/o}$ nerves was Septin 9. Higher amounts of septin 9 protein were associated with SLIs in *Prnp*$^{o/o}$ nerves. However, this abnormal localization correlated with absence of PrP^{C} from myelin (in *Prnp*$^{o/o}$ nerves and *tgNSE-PrP*), but not with presence of neuropathy (neuropathy in *Prnp*$^{o/o}$ mice, but not in *tgNSE-PrP* mice). Therefore, the significance of this finding remains unknown. Interestingly, septin 9 is associated with hereditary neuralgic amyotrophy, a recurrent, painful brachial plexus neuropathy with axonal degeneration[191]. Several isoforms of septin 9 are known to be generated by alternative splicing, and septin 9 is believed to promote tumorigenesis. Septins are members of a conserved family of cytoskeletal GTPases. Different members of the septin family, e.g. septin 7, 9 and 11, form complexes[192-193]. Although the function of septin 9 in myelinated nerves fibers is unknown, the expression of septins in myelin and myelinating cells was recently reported[192].

By microarray, only sonic hedgehog (Shh) expression was found to be higher in young *Prnp*$^{O/O}$ compared to wt nerves in a background-independent manner. However, in nerves of 35-week old *Prnp*$^{O/O}$ mice, Shh expression was lower than in in wt, and it is therefore unclear what the significance of Shh signaling is in the *Prnp*$^{O/O}$ neuropathy. Shh was previously found to be upregulated following sciatic nerve injury and to induce BDNF expression, which in turn improved survival of motor neurons[194]. In *Prnp*$^{O/O}$ mice it could simply represent an early marker of nerve damage. If and how Shh contributes to *Prnp*$^{O/O}$ neuropathy could be tested by pharmacological inhibition of Shh signalling with cyclopamine in mice, by local administration of the drug with pumps as described previously in rats[194]. First the impact of this drug on *Prnp*$^{O/O}$

nerve structure and electrophysiological properties could be tested. If nerves showed a more or a less severe neuropathy compared to nerves of untreated *Prnp*$^{0/0}$, one could further investigate which factors are involved.

I observed several differences between the *Prnp*$^{o/o}$ and wt transcriptomes on a single genetic background (C57Bl/6 or Balb/c) only. This exemplifies the importance of correct genetic controls, when performing microarray analyses. In addition, of the genes found to be altered in *Prnp*$^{o/o}$ compared to wt on both genetic backgrounds, many were localized around *Prnp* on chromosome 2, suggesting that embryonic stem cell-derived genes not eliminated by genetic backcrossing caused artifical transcriptional changes.

Incidentally, I detected a higher amount of IgG_1 in *Prnp*$^{O/O}$ nerves compared to wt. Since albumin and IgG_{2a} did not show a similar difference, this finding was most likely not caused by an increased permeability of the blood-nerve barrier. Elevated IgG_1 was not caused by local expression of IgG_1 because (1) the difference was observed before newborn mice produce their own IgG_1 – all the IgG is derived from the mother at this age, and (2) by real time PCR, I failed to detect IgG_1 mRNA (data not shown). Since serum levels in wt and *Prnp*$^{O/O}$ newborn mice were similar (data not shown), it is unlikely that elevated IgG_1 levels were due to increased amounts of circulating immunoglobulins. In any case, the presence of IgG_1 was not a prerequisite for developing neuropathy, as indicated by the presence of neuropathy in *Prnp*$^{O/O}$ Rag1$^{-/-}$ mice. A current hypothesis is that macrophages infiltrating *Prnp*$^{O/O}$ nerves import IgG_1 (but not IgG_{2a}) bound to their Fc receptors. Alternatively, clearance of immunoglobulins from peripheral nerves may be altered in *Prnp*$^{O/O}$ mice.

There are several possible explanations for why I was unable to detect early alterations in *Prnp*$^{0/0}$ myelin proteome or nerve transcriptome. First, the chosen time points for the analyses may have been too early. However, the first histological, behavioral and electrophysiological signs of neuropathy were observed only shortly thereafter at the age of 10 weeks, marked by an increased number of digestion chambers, reduced grip strength, and reduced NCV. By analyzing mice younger than 10 weeks, I intended to prevent secondary changes due to activation and/or increased density of macrophages in 10-week old P*rnp*$^{O/O}$ nerves. Other

possible explanations for the inability to detect any difference are (1) alterations affected mainly cellular molecules that were not analyzed, e.g. lipid components, (2) alterations involved signaling molecules that are too short-lived to be detected, or (3) that the methods used were not adequate for the detection of all existing transcriptomic or proteomic alterations. Concerning the latter, the incidental finding of higher amount of IgG_1 in *Prnp*$^{O/O}$ mice compared to wt showed that DIGE was not sufficient to detect all the proteome differences in *Prnp*$^{O/O}$ nerves. In the future, additional methods will be used, including ICAT (isotope-coded affinity tag), LC-MS/MS (lipid chromatography-tandem mass spectrometry), and 2D-16-BAC (2D-16-benzyldimethyl-n-hexadecylammonium chloride)/ SDS-PAGE to detect early alterations. It has previously been shown that one method alone does not suffice to detect all myelin proteins being present[195].

6 IMPACT OF IMMUNIZATION ON PRION SUSCEPTIBILITY

'Introduction' (in parts), 'Material and Methods', 'Results' and parts of the 'Discussion' are taken from the following publication:

"Repetitive Immunization Enhances the Susceptibility of Mice to Peripherally Administered Prions"

By Juliane Bremer, Mathias Heikenwalder, Johannes Haybaeck, Cinzia Tiberi, Nike Julia Krautler, Michael O. Kurrer, Adriano Aguzzi

Published in PLoS one 2009 Sep 25; issue 4 (9); e7160

Parts of the 'Introduction' are adapted from the following publication:

"The Prion's Elusive Reason for Being"

By Adriano Aguzzi, Frank Baumann, and Juliane Bremer

Published in Annu Rev Neurosci. 2008; issue 31: pages 439-477

6.1 Introduction

6.1.1 Prion diseases

Prion diseases, or transmissible spongiform encephalopathies (TSE), are infectious neurodegenerative conditions that typically lead to cognitive and motor dysfunction [196-197]. With the exception of rare, chronically presymptomatic carriers[198], prion diseases are progressive, fatal, and presently incurable. Prions propagate during the course of the disease and form aggregates containing PrP^{Sc}, a misfolded, beta-sheet-rich isoform of the cellular prion protein PrP^{C}, which is encoded by the *PRNP* gene[6, 199]. Although the normal cellular prion protein PrP^{C} can easily be digested with proteinase K (PK), the beta-sheet-rich, misfolded form PrP^{Sc} is partially proteinase K (PK) resistant. Typical neuropathological features include neuronal loss, astrogliosis and spongiform changes[196-197].

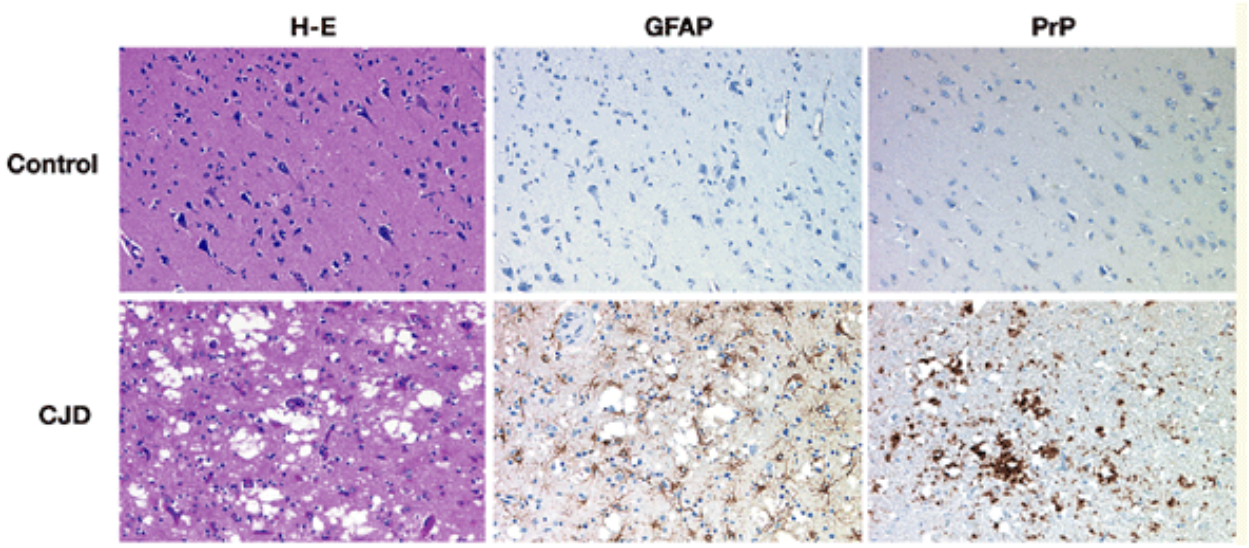

Figure 50. Histopathology of Creutzfeldt Jakob Disease. Frontal cortex sections of the brain of a patient who died of non-cerebral cause (upper row) and of a patient suffering from Creutzfeldt–Jakob disease (CJD; lower row). Sections are stained with haematoxylin-eosin (H-E, left panels), with antibodies against glial fibrillary acidic protein (GFAP, middle panels) and with antibodies against the prion protein (PrP, right panels). Neuronal loss and prominent spongiosis are visible in the H-E stain. Strong proliferation of reactive astrocytes (gliosis) and perivacuolar prion protein deposits are detectable in the GFAP and PrP immunostains of the CJD brain samples. Figure reprinted by permission from Macmillan Publishers Ltd: *Nature Reviews Molecular Cell Biology*[200], copyright 2001. http://www.nature.com/nrm. Licence number 2438450274580.

The word “prion” is a portmanteau derived from “proteinaceous infectious” particle. Naturally, the latter is by no means a qualifying attribute, because all conventional infectious agents - including all viruses and bacteria - are proteinaceous to some degree. What sets prions apart, as proposed by Prusiner, is that the actual infectious particle consists merely of protein and is capable of replicating and transmitting infections without the need for informational nucleic acids. This postulate counters the established molecular biological central dogma, which predicates that nucleic acids are the basis for self-replicating biological information in all living beings, including even the most elementary infectious particles.

Prion diseases have occurred in humans and animals for many years. A disease similar to scrapie was recorded in the mid-eighteenth century, and scholars heavily debated its origin. A crucial experiment showing incontrovertible transmissibility of scrapie to goats was performed by Cuille & Chellè in the 1930s[201]. The first cases of human prion disease, Creutzfeldt-Jakob disease (CJD), were reported in the 1920s[202-203]. The number of human and animal diseases recognized as TSEs has increased steadily and now includes Gerstmann-Sträussler-Scheinker syndrome (GSS), fatal familial insomnia (FFI), and Kuru in humans; bovine spongiform encephalopathy (BSE) in cattle; chronic wasting disease (CWD) in deer and elk; and transmissible mink encephalopathy. BSE has been inadvertently transmitted to a variety of captive animals, causing feline spongiform encephalopathy (FSE) and a plethora of diseases in zoo animals including kudus, nyalas, and greater cats, for example.

Creutzfeldt-Jakob disease CJD was initially described as a sporadic disease with no known cause (sCJD). The incidence of CJD is low in all ethnicities and typically affects ~1 person in one million each year. Very rapid cognitive decline, causing dementia, is the main symptom. Cerebellar symptoms, including ataxia and myoclonus, are also frequent presenting symptoms. Death often occurs within few weeks of the first signs of disease, and a fulminant, “apoplectiform” course of disease has been documented in the past. Somatic mutations in the *PRNP* gene analogous to those in the germline of genetic CJD patients (see below) have been hypothesized to underlie cases of sporadic CJD. Alternatively, Aguzzi & Glatzel[204] suggested that some cases of alleged sCJD derive from heretofore unrecognized prion infections. Finally,

PrP^{C} may possess a finite, albeit extremely low, propensity to self-assemble into ordered aggregates of PrP^{Sc}, thereby stochastically initiating prion replication and, ultimately, a sporadic form of disease. The latter scenario could be regarded as the bad-luck hypothesis. However, none of this has been proven, and therefore the cause of sCJD is still unknown.

Variant Creutzfeldt-Jakob disease and Bovine Spongiform Encephalopathy. Public understanding of prion disease remained limited for a long time. However, this mindset changed completely when BSE was first reported in the early 1980s[205]. In the following years until mid 2009, BSE affected ~190,500 cows (http://www.oie.int/). Some investigators suggested that BSE could cause a new variant form of CJD (vCJD) in humans. A direct experimental proof that vCJD represents transmission of BSE prions to humans cannot be produced. However, epidemiological, biochemical, neuropathological evidence and transmission studies strongly suggest that BSE has transmitted to humans in the form of vCJD[206-209]. The incidence of vCJD rose between 1994, when the first patients suffering from vCJD presented with their initial symptoms, and 2001, raising fears that a very large epidemic may be looming. Currently, vCJD has affected 225 individual victims worldwide (http://www.cjd.ed.ac.uk/). Most of the affected individuals lived in United Kingdom and France. Fortunately, in the United Kingdom, the incidence appears be decreasing since the year 2001 to one diagnosed case yearly in 2007 and 2008. In France, the number of probable and definite cases of vCJD increased from 0-3 diagnosed cases per year in 1996-2004 to 6 per year in 2005 as well as in 2006. In 2007-2009, the number of cases was back to 0-3 again, totaling 25 cases (http://www.invs.sante.fr/publications/mcj/donnees_mcj.html). Almost all vCJD patients to date have been found to be homozygous for methionine (Met) at codon 129 of the *PRNP* gene. Some scientists have predicted a multiphasic human BSE endemic with a second increase in the incidence of vCJD affecting people heterozygous at codon 129 of the *PRNP* gene assuming a 30-year mean incubation time[210]. Others believe the incidence of vCJD is subsiding[211] (**Fig. 51**).

a

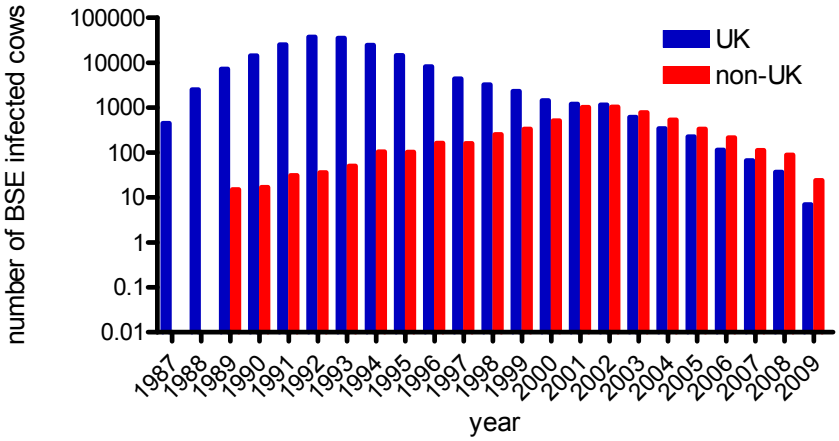

b

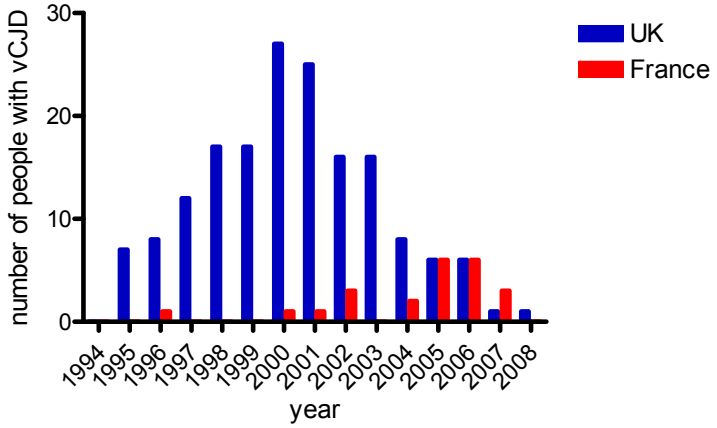

Figure 51. BSE and vCJD cases reported worldwide. (a) Reported cases of bovine spongiform encephalopathy (BSE) in the United Kingdom (UK) (*blue*), and in countries excluding the UK (*red*). Non-UK BSE cases include cases from countries both within and outside of the European Union (EU). Data are as of mid 2009. (b) Reported cases of variant Creutzfeldt-Jakob disease (vCJD) in the UK (*blue*) and in countries outside the UK (*red*). Non-UK vCJD cases include those reported in France, Republic of Ireland, Italy, United States, Canada, Saudi Arabia, Japan, the Netherlands, Portugal, and Spain. Data are as of December 2009 and include cases of vCJD in patients who resided in the UK in the 1980s or 1990s (see the National Creutzfeldt-Jakob Disease Surveillance Unit Web site for vCJD data (http://www.cjd.ed.ac.uk/). Adapted and reprinted, with permission, from the *Annual Review of Neuroscience*, Volume 31 ©2008 by Annual Reviews. www.annualreviews.org.

It is important to note, however, that the above considerations apply primarily to the epidemiology of primary transmission from cows to humans. By now, a pool of preclinically infected humans may have been built. Human-to-human transmission may present with characteristics very different from those of primary cow-to-human transmission, including

enhanced virulence, shortened incubation times, disregard allelic prion gene barriers, and unconventional modes of infection, including blood-borne transmission. Considering the time it will take to eradicate these secondary transmissions in the population, vCJD is not likely to disappear entirely in the coming four decades.

Iatrogenic CJD is inadvertently transmitted during the course of medical or surgical procedures. The first documented case of iatrogenic prion transmission occurred in 1974 and was caused by corneal transplantation of a graft derived from a patient suffering from sCJD[212]. Iatrogenic CJD is also rare, most often observed in individuals that have received cadaveric dura mater implants and human growth hormone. Some of these individuals received gonadotrophin extracted from human pituitary glands or had stereotactically placed electrodes in their brains[213]. Four cases of vCJD transmission by blood transfusions have been reported recently in the United Kingdom[214-216] (see also http://www.cjd.ed.ac.uk/TMER/TMER.htm) The fact that preclinically infected individuals can transmit vCJD underscores the important medical need for sensitive diagnostic tools, which could be used for screening blood units prior to transfusion, for example.

Kuru. In the mid 1950s, when the remote parts of Papua New Guinea were first explored by Australians and Westerners, Kuru was first described in research[217]. Kuru was, at that time and at least since 1941, an endemic disease among some tribes of New Guinea aborigines, especially among the Fore linguistic group and neighboring tribes[218]. *Kuru* in the Fore language means “to shiver,” and along with other signs of cerebellar ataxia, shivering is a hallmark of the disease. The ritual consumption of dead relatives as a symbol of respect and mourning is the attributed route of transmission. As a consequence, the incidence has steadily fallen after cessation of cannibalism in Papua New Guinea[210]. In a concise and extremely clairvoyant observation published in 1959, Bill Hadlow noted the epidemiological, clinical, and neuropathological similarities between Kuru and scrapie[219]. These were followed up by Carleton Gajdusek who, in 1966, succeeded in transmitting Kuru to three chimpanzees[220]. Soon thereafter, serial passage of Kuru and of several other prion diseases was demonstrated in

chimpanzees and other primates[221-222]. Investigators have since transmitted human prion disease to various species, including laboratory rodents.

Genetic CJD and Gerstmann-Sträussler-Scheinker syndrome. Several mutations in the prion protein gene (*PRNP*) have been found in families with hereditary or genetic CJD (gCJD). gCJD occurs with point mutations mostly affecting the region between the second and the third helix of the carboxy-terminus. However, insertions in the octarepeat region (OR) in the amino-terminus, and even one instance of a premature termination codon at position 145, have also been associated with human prion disease. The inheritance was, in all cases, autosomal dominant, often with very high penetrance. The clinicopathological disease phenotype varies depending on the actual mutation, as well as on polymorphisms at codon 129, and most likely on a plethora of yet unidentified modifiers and cofactors[223].

The first descriptions of Gerstmann-Sträussler-Scheinker syndrome (GSS) originate from 1928 and 1936 in an Austrian family[224-225]. In the following years, analogous disorders have been described, but its classification as a TSE lagged until 1981, when Masters and colleagues reported that inoculation of brain tissue from three patients with GSS resulted in spongiform encephalopathy in nonhuman primates[226]. The authors also defined clinical hallmarks of GSS (earlier age at onset, longer disease duration, and prominent cerebellar ataxia) differentiating the disease from CJD. Nowadays, GSS is considered an autosomal dominantly-inherited TSE caused by mutations in the prion protein open reading frame, manifesting typically with progressive cerebellar ataxia or spastic paraparesis and cognitive decline. In addition to the regions affected in gCJD, mutations altering the sequence of the central domain can cause GSS. Its distinctive neuropathological feature is the presence of widespread, large and multicentric amyloid plaques[227].

GSS is generally transmissible[226, 228-229]; therefore, its classification as a TSE is widely accepted. However, the overall experimental transmissibility of GSS to nonhuman primates and rodents is low. Only for the most common GSS-associated mutations (P102L), and only in approximately one third of the cases, were brain homogenates derived from patients reproducibly capable of inducing disease upon transmission[230]. The less frequent mutations causing GSS often failed to

induce disease after experimental transmission to nonhuman primates and rodents, and in many cases transmissibility was never assessed[230-231].

Fatal Familial Insomnia (FFI) is the descriptive name given to a disease identified in 1986. Five members of an Italian family presented with insomnia and dysautonomia[232]. In 1992, the disease-causing mutation in the prion protein gene (D178N) was identified, thereby allowing the classification of FFI as a genetically determined prion disease[233]. The final proof that FFI is a TSE was achieved when FFI was successfully transmitted to mice[234]. FFI typically affects the thalamus, and accordingly, the core clinical features are disruption of the normal sleep-wake cycle, sympathetic overactivity, endocrine abnormalities, and impaired attention[227]. In addition to the pathogenic point mutation D178N, the methionine-valine polymorphism at codon 129 of the *PRNP* gene controls the disease phenotype. Whereas D178N-129MM (homozygosity for methionine at codon 129) was associated with FFI, heterozygosity at codon 129 (D178N-129MV) segregated with the familial CJD subtype[235]. However, Zarranz et al. reported more recently that this genotype-phenotype association is not absolute. In one study, several patients have been identified with a CJD phenotype and a D178N-129MM genotype. The authors concluded that rather than being separate disease entities, prion disease phenotypes such as FFI and CJD represent two extreme manifestations of a continuous disease spectrum[236]. In addition to the familial form of fatal insomnia, a sporadic form of the disease, termed sporadic fatal insomnia, was described, which is not associated with mutations in the *PRNP* gene[237-238].

6.1.2 Risk factors determining prion susceptibility

The pivotal factors determining susceptibility to prion disease of the exposed population remain largely unknown. Presence of the cellular prion protein is certainly essential, since the absence of PrP^C prevents disease in mice inoculated peripherally or intracerebrally with prions[33, 35], yet PrP^C expression alone is not sufficient to sustain prion replication[239-240]. Intensive research has been carried out to identify further risk factors, the major one being the Met/Val polymorphism at codon 129 of the *PRNP* gene[241]. Almost all vCJD patients to date have been found to be

homozygous for Met at this codon[6, 242-243] and heterozygosity at codon 219 ($219^{Glu/Lys}$) is associated with decreased risk of developing sCJD[244].

Much less is known about the non-genetic risk factors. Analyses of epidemiological data of different prion diseases, including scrapie, BSE, and vCJD suggested that the risk for TSEs may be age-dependent[245-247], but no further non-genetic risk factors are known. It has been known for a long time that injections of the immunomodulatory glucocorticosteroid prednisone prolonged incubation time after intraperitoneal, but not intracerebral, injection of scrapie-infected brain homogenate[248], suggesting that the lymphoid system acts as a "Trojan horse" instead of a defense mechanism during scrapie pathogenesis. Indeed, prion replication occurs in lymphoid tissues long before neuroinvasion and subsequent detection in the central nervous system (CNS)[249].

6.1.3 Immune system in prion diseases

Within secondary lymphoid organs, follicular dendritic cells (FDCs) play a key role in peripheral prion replication and disease pathogenesis. FDCs located within germinal centers express high levels of PrP^{C} and accumulate PrP^{Sc} (Ref [250]). Maturation and maintenance of FDCs depend on tumor necrosis factor alpha (TNF-α) and lymphotoxins (LT-α and LT-β). Mice lacking TNF-α, complement components and their receptors, LT-α, LT-β, or LT-β receptor are partially resistant to peripheral prion infection[251-252]. Mice treated with an inhibitor of LT-β-receptor signaling (LT-βR-Ig) displayed a reversible dedifferentiation of FDCs. This leads to a decreased susceptibility to orally or intraperitoneally administered prions[253-255]. Accordingly, in inflammatory conditions, extravasating immune cells enable prion replication at the sites of chronic inflammation[256-257] and may even lead to prion excretion[258]. Newborn mice whose immune system has not fully matured were shown to display a strongly reduced susceptibility to extracerebrally administered prions[259]. The increase in susceptibility with age correlated with the immunocytochemical detection of PrP^{C} on maturing FDCs[260].

Mature FDCs are unlikely to transport prions to peripheral nerve terminals. However, the relative distance between FDCs and peripheral nerves[261], and PrP^C expression in the peripheral nervous system[262] determine prion neuroinvasion efficiency and onset of terminal disease. Also, sympathectomy delays or prevents scrapie following intraperitoneal prion inoculation[263]. The precise mechanisms of prion transport from prion replicating germinal centers to peripheral nerves remain elusive. While germinal center B-cells do not appreciably contribute to intrasplenic prion trafficking[264-265], the identity of the crucial actuators of trafficking, be they hematopoietic or stromal cells, or even subcellular particles, remains to be determined. The presence of antigen presenting cells (APCs) was described to be a prerequisite for lympho- and neuroinvasion after peripheral prion infection[266-270], although others have questioned their importance[271].

It was reported that repeated administration of CpG-containing oligodeoxynucleotides (CpG-ODN) decreases the susceptibility to prions[272]. Since CpG-ODN activate the Toll-like receptor 9 (TLR9), these surprising findings were interpreted as evidence that activation of the innate immune system may be protective against prions. However, subsequently it was found that repeated injections of CpG-ODN dramatically compromise morphology and functionality of murine lymphoid organs[273]. Due to the mechanisms discussed above, the immunosuppressive properties of CpG-ODN are much more likely to account for the reported antiprion effects than any conjectured immune activation[274].

6.2 Scientific aims

Since the immune system has an essential role in peripheral prion pathogenesis, I hypothesized that stimulation of the immune system might increase susceptibility to peripherally administered prions[274].

To test this, I first aimed at establishing an experimental protocol that leads to broad stimulation of both innate and adaptive components of the immune system for a protracted period of time.

Subsequently, using the established protocol, I aimed at answering the question of whether susceptibility is increased in immunized compared to control wt mice following peripheral and/or central administration of prions.

6.3 Mice, material and methods

6.3.1 Mice and scrapie inoculation

Female wt (C57BL/6) mice were obtained from Harlan, NL and maintained under specific pathogen-free (SPF) conditions. Housing and experimental protocols were in accordance with the Swiss Animal Protection Law and mice were held in compliance with the regulations of the Veterinäramt, Kanton Zürich. Mice were infected intraperitoneally (i.p.) with 100 µl brain homogenate derived from terminally scrapie sick CD-1 mice, homogenized in PBS/0.32M sucrose, or intracerebrally (i.c.) with 30 µl brain homogenate. Different doses of prions derived from a RML6 infected terminally sick wt mouse were injected intraperitoneally (i.p.) or intracerebrally (i.c.) (i.p. doses: 0.33 ng, 10 ng, 300 ng; i.c. doses: 10 pg, 300 pg, 9 ng brain homogenate). Mice were euthanized at 0, 70 and 400 dpi or when terminally scrapie sick.

6.3.2 Repetitive immunization

Repetitive immunization was performed in female wt (C57BL/6) mice by repeated injections of CpG-ODN and BSA/alum. BSA was diluted in 200 µl of freshly prepared $Al(OH)_3$ to a final concentration of 50 µg BSA per injection per mouse as described[265]. Intraperitoneal injections of either 30 µg CpG-ODN (Coley pharma, ODN 1826) or BSA/alum were performed as indicated in **Fig.52**, starting 6 weeks prior to prion inoculation.

6.3.3 Western blot analysis and NaPTA precipitation

Tissue homogenates (brain; spleen) were adjusted to 8 mg/ml protein, and treated with proteinase K (20-50 µg/ml, 30 min, 37°C). 50 µg of total protein was loaded onto a NuPAGE® Novex 12% Bis-Tris Gel (Invitrogen) and separated. Proteins were then transferred to nitrocellulose membrane (see below). For detection of PrP^{Sc} in spleen homogenates NaPTA (sodium phosphotungstic acid) precipitation was performed. 10% spleen homogenates were

prepared in PBS on ice. Cellular debris was removed by centrifugation at 500 g for 1-2 min. The resulting supernatant was adjusted to 500 µl with PBS, and mixed 1:1 with 4% Sarkosyl in PBS. Samples were incubated for 15 min at 37°C under constant agitation. Benzonase and $MgCl_2$ were added to a final concentration of 50 U/ml and 1 mM respectively, and incubated for 30 min at 37°C under continuous agitation. Further, samples were digested with 30 µg/ml proteinase K (PK) for 60 min at 37°C with agitation and pre-warmed NaPTA stock solution (pH 7.4) was added to a final concentration of 0.3% and the sample was incubated at 37°C for 30 min with shaking, followed by centrifugation at 37°C for 30 min at 14.000 g in an Eppendorf microcentrifuge. The pellet was resuspended in 30 µl 0.1% Sarkosyl in PBS and the sample was heated at 95°C for 5 min in SDS-containing loading buffer before loading onto NuPAGE® Novex 12% Bis-Tris Gel (Invitrogen). All gels were transferred to nitrocellulose (Schleicher & Schuell) using XCell II Blot Module (Invitrogen). Membranes were blocked with TBST containing 5% non-fat milk, decorated with monoclonal antibody POM1[144, 275] followed by incubation with the secondary anti-mouse IgG_1 (Zymed) and visualized by enhanced chemiluminescence (ECL, Socochim, Pierce).

6.3.4 Histology, immunohistochemistry, and histoblot

Paraffin sections (2 µm) and frozen sections (5 or 10 µm) of various organs were stained with hematoxylin-eosin. Antibodies raised against the following antigens were used for immunohistochemistry: FDC-M1 (Mfge8) for mature FDCs (clone 4C11; 1:50; Becton Dickinson), B220/CD45R for B-cells (Pharmingen; 1:400), CD35 for CR1 (clone 8C12, Pharmingen, San Diego, CA; 1:100), CD3 for T-cells (clone SP7, NeoMarkers; 1:300), F4/80 for macrophages (Serotec; 1:50), PNA for germinal center B-cells (Vector L-1070; 1:100), MOMA-1 for metallophilic marginal zone macrophages (BMA, Augst, Swizerland; 1:50), GFAP for astrocytes (DAKO, Carpinteris, CA; 1:300), and Iba-1 for microglia (WAKO; 1:2500).

PrP stains were performed on formalin-fixed brain tissues treated with concentrated formic acid to inactivate prions and postfixed again in formalin. Subsequently, tissues were embedded in

paraffin. After deparaffination, sections (2 μm) were incubated for 6 min in 98% formic acid and washed in distilled water for 30 min. Sections were heated to 100°C in a steamer in citrate buffer (pH 6.0) for 3 min, and allowed to cool down to room temperature. Sections were incubated in Ventana buffer and stains were performed on a NEXES immunohistochemistry robot (Ventana instruments, Switzerland) using an IVIEW DAB Detection Kit (Ventana). After incubation with protease 1 (Ventana) for 16 min, sections were incubated with anti-PrP SAF-84 (SPI bio; 1:200) for 32 min. Sections were counterstained with hematoxylin. Histoblot analysis was performed as described[276]. Image acquisition was performed on an Axiophot-microscope (Zeiss) equipped with a JVC digital camera (KY-F70; 3CCD).

6.3.5 *In situ* hybridization

Digoxigenin (DIG)-labeled *Mfge8* riboprobe was obtained by transcription of pBluescript II KS+ (Stratagene) containing the open reading frame of *Mfge8* and using a DIG RNA labeling kit (Roche). ISH was performed on spleen cryosections. Sections were fixed in 4% paraformaldehyde PBS, followed by acetylation. After prehybridization, 200 ng/ml of DIG-labeled RNA probe was added to the hybridization buffer and incubated at 72°C overnight. DIG-labeled probes were detected by anti-DIG–alkaline phosphatase Fab-fragments (Roche). Cell nuclei were stained with DAPI (4',6-Diamidine-2'-phenylindole dihydrochloride; Roche). For more information see also chapter **5.3.10**.

6.3.6 RNA isolation from spleen and real-time PCR analysis

RNA isolation buffer (RLT; Qiagen) was added to flash frozen spleens prior to homogenization (Medic tools). RNA was purified using RNeasy (Qiagen) as described by the manufacturer. Synthesis of cDNA was performed with QuantiTect, Reverse Transcription kit (Qiagen). Samples were analyzed by real-time PCR using QuantiFast SYBR Green PCR kit (Qiagen) and 7900HT (Fast Real-Time PCR systems; Applied Biosystems). The following primer

combinations were used [forward primer (FW), reverse primer (RV)]: Mfge8 FW: 5'-ATA TGG GTT TCA TGG GCT TG-3'; Mfge8 RV: 5'-GAG GCT GTA AGC CAC CTT GA-3'; GAPDH FW: 5'-CCA CCC CAG CAA GGA GAC-3'; GAPDH RV: 5'- GAA ATT GTG AGG GAG ATG CT-3'

6.3.7 PrP^C sandwich ELISA

96-well plates were coated with 20 ng of purified POM1 antibody overnight at 4°C. Plates were washed with PBS containing 0.1% (vol/vol) Tween 20 (PBST), and blocked with 5% Top-Block (Fluka) in TBST for 2 h at room temperature (RT). After washing, plates were incubated with 50 µl of spleen homogenates containing 500 µg/ml total protein in sample buffer (1% Top block in PBST). The total protein concentrations of the spleen homogenates were determined using a standard colorimetric assay based on bicinchoninic acid (BCA, Pierce). Each sample was analyzed in triplicates. For the standard curve, serially diluted recombinant mouse PrP23-230 in PBST containing 1% Top Block was used. After 1 h at RT plates were washed extensively and then probed with biotinylated POM2[144, 275] at a concentration of 200 ng/ml in PBST containing 1% Top Block, for 1 h at room temperature. After washing, plates were incubated with horseradish peroxidase conjugated Avidin (1:1000 dilution, BD-Pharmingen) for 1 h at RT. Plates were developed with Stabilized Chromogen SB02 (Biosource). The chromogenic reaction was stopped by adding the same volume of 0.5 M H_2SO_4. Optical density was measured at 405 nm. The PrP^C concentration in each sample was calculated according to a standard curve derived from the values of recombinant PrP.

6.3.8 Fluorochrome labeling

1 mg of Cy5 NHS ester (Amersham Biosciences; Cat. No. PA15101) was dissolved in 1 ml (conc. 1 mg/ml) water-free DMSO. 1 ml of the POM2 antibody[144, 275] (conc. 2 mg/ml) and of 0.5 M borate buffer (pH 8.0) leading to an antibody concentration of 1.81 mg/ml. 2 mg POM2 (1.1 ml) were used for the labelling reaction (Dye/antibody ratio = 2.5/1). 2 mg POM2 were mixed

with 24.80 ml of Cy5 dye (31.25 nmol). The Cy5 dye was added to the antibody while vortexing and further on incubated under permanent agitation for 1 h at RT (light protected). The unincorporated Cy5 dye was removed in a size-exclusion column and the labeled antibody was dialyzed against 2 l of PBS over night.

6.3.9 Flow cytometric analysis

Splenic cells or blood cells were isolated and incubated with primary antibodies: POM2-Cy5 (1:250), FITC- or PE-labeled anti-CD11b antibody, FITC- or PE-labeled anti-CD11c antibody, PE-labeled anti-CD19 antibody, FITC-labeled anti-B220 antibody, PE-labeled anti-Ly6G antibody, PE-labeled anti-CD8, PE-labeled anti-CD3 antibody (all 1:100, Pharmingen), PerCP-labeled anti-CD4 (1:750), or FITC-labeled anti-CD21 and PE-labeled anti-CD23 (1:100 and 1:250, respectively). Erythrocyte lysis was performed using BD FACS^{TM} Lysing Solution. Cells were washed with PBS containing 2% FCS and live gated blood cells were further analyzed with a flow cytometer (DAKO or BD Biosciences) and FlowJow software program.

6.4 Results

6.4.1 Stimulation of the immune system by repetitive immunization

Starting 6 weeks prior to prion inoculation, wt mice (C57BL/6) were immunized and repeatedly boosted with generic antigens unrelated to prions, with the goal of achieving sustained activation of immune cells and activation-related morphological changes within lymphoreticular organs. A mixture of CpG-ODN, bovine serum albumin (BSA) and alum was repeatedly injected intraperitoneally during a period of two weeks (**Fig. 52**). For the following two weeks, treatment was suspended in order to prevent damage to secondary lymphoid organs, as observed following long-term administration of CpG-ODN (data not shown). Mice were then injected every other week for 20 weeks with BSA/alum.

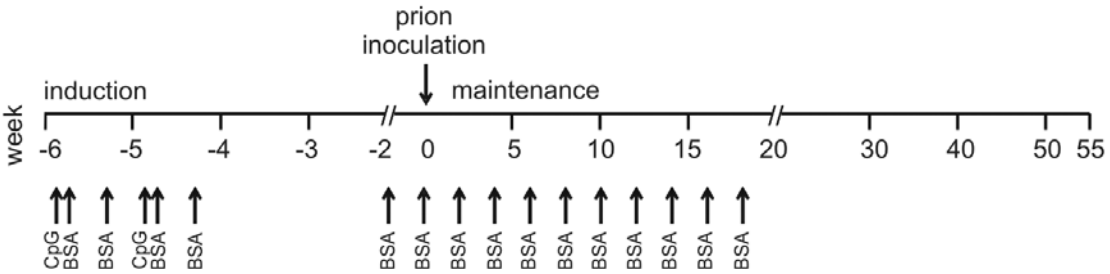

Figure 52: Treatment scheme for immunization. Arrows denote the time points of injections of CpG oligodeoxynucleotides and bovine serum albumin (BSA). Treatment included an induction (-6 to -4 weeks) and a maintenance phase (-2 to +18 weeks).

At the time point of prion inoculation, selected animals were sacrificed to evaluate organs and blood for histological, cytological, and biochemical evidence of immune stimulation or inflammation. Compared to age and gender-matched, non-immunized wt controls, immunized animals displayed typical features of immune stimulation. Spleens of immunized mice were significantly heavier, yet the concentration of splenic PrP^C (weight/weight) remained unchanged (**Fig. 53a**), indicating that the total amount of splenic PrP^C was increased. In peripheral blood, chronic immunization resulted in significantly elevated cell counts of erythrocytes, neutrophils, and monocytes. Lymphocyte counts were marginally increased but did not reach statistical significance (**Fig. 53b**). I investigated serum levels of various cytokines. IL-6 was elevated in immunized mice, whereas IL-12 (p70) was reduced and IL-1α was unaltered.

IFN-γ was also increased though not significantly (**Fig. 53c**), TNF-α was below detection limit in all animals analyzed (data not shown).

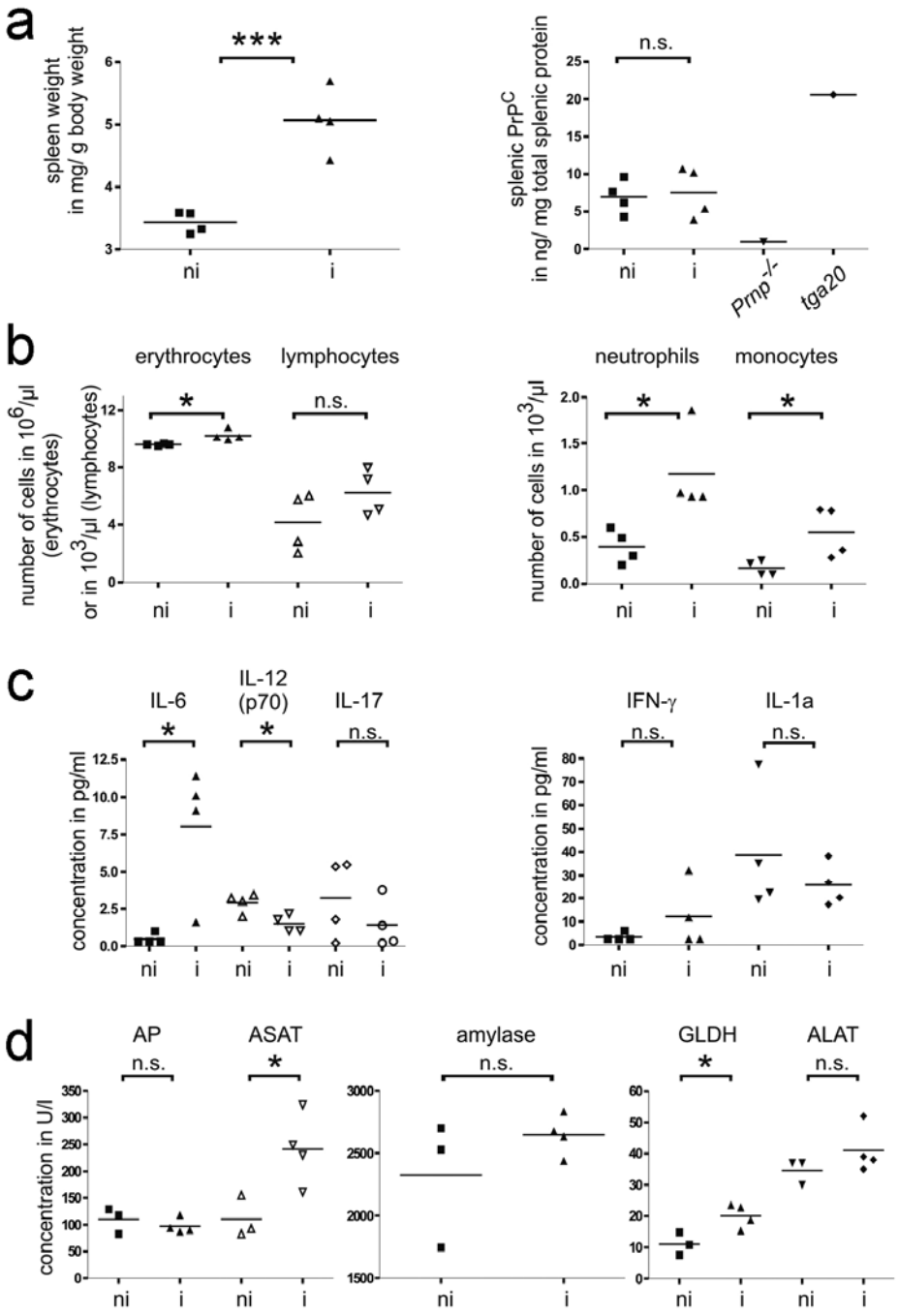

Figure 53: Repetitive immunization of wt mice. (a-d) Selected immunized (i) and non- immunized mice (ni) sacrificed at the time point of prion inoculation. **(a)** Relative spleen weight and splenic PrP^C levels as determined by ELISA. *Prnp*$^{-/-}$ spleen served as negative, *tga20* spleen as positive control. Hematological cell counts **(b)**, serum levels of selected cytokines **(c)**, and blood chemistry **(d)** (AP: alkaline phosphatase; ASAT: aspartate amino transferase; GLDH: glutamate dehydrogenase; ALAT: alanine amino transferase) showed mild polyglobulia, leukocytosis, and mild liver damage in immunized mice. Unpaired t-tests: (*) $p < 0.05$; (***) $p = 0.001$; (n.s.) not significantly different.

Splenic white pulp follicles appeared more densely packed upon immunization (3.78 ± 0.31 and 7.89 ± 2.71 follicles/mm^2 in histological sections of non-immunized mice and immunized mice, respectively; p=0.029). Immunized mice showed a significant increase in density and size of PNA$^+$ germinal centers and Mfge8$^+$ follicular dendritic cell networks in spleens. In addition, I observed a loosening of MOMA-1$^+$ metallophilic macrophage festoons in the marginal zone following immunization as described previously[273] (**Fig. 54**). Marginal zones were also broader in B220 and CD21/35 immunostains. Accordingly, flow cytometry of splenocytes showed a higher percentage of CD21/35$^+$CD23$^-$ marginal zone B-cells in immunized mice than in control mice (**Fig.55**).

Mfge8 transcription is not only confined to germinal centers, but also occurs in cells located in the marginal zone which were suggested to represent FDC precursors [277]. However, *in situ* hybridization did not identify any differences in *Mfge8*$^+$ cells residing within the marginal zones of immunized and control mice (**Fig. 56**). Instead, immunization increased the prevalence of splenic GR1/Ly6g$^+$ granulocytes, as verified by immunohistochemistry and flow cytometry (**Fig. 54-55**), and increased the number of CD68$^+$ macrophages in splenic white pulp follicles (**Fig. 54**). In contrast, the number of splenic CD11b$^+$ and CD11c$^+$ cells was unaffected (**Fig. 55**). Although total splenic PrP^C protein concentration was unaltered, flow cytometry revealed a slight, yet significant increase in PrP^C surface expression by splenic B220$^+$ and CD4$^+$ cells (**Fig. 55**).

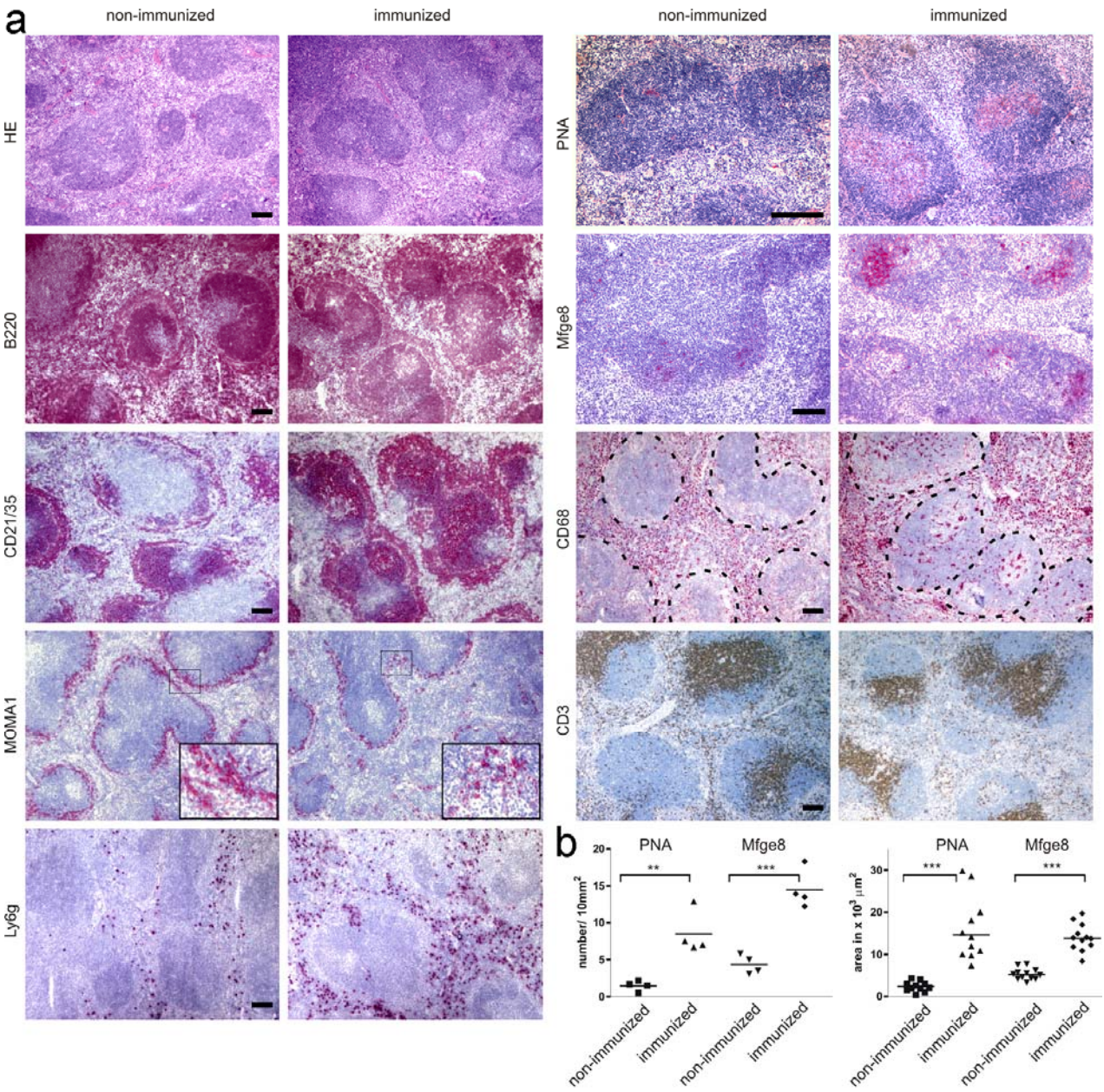

Figure 54: Splenic histology of immunized mice. (a) Spleens of non-immunized and immunized mice were analyzed at the time point of inoculation by histology with hematoxylin-eosin (HE) and immunohistochemistry for B-cells (B220), complement receptors (CD21/35), metallophilic marginal zone macrophages (MOMA-1), granulocytes (Ly6g), germinal center B-cells (PNA), FDCs (Mfge8), macrophages (CD68), and T-cells (CD3). The overall splenic microarchitecture was preserved. Immunized mice showed broader marginal zones, some loosening of splenic MOMA-1$^+$ metallophilic marginal zone macrophage festoons and a reduction of the density of MOMA-1$^+$ cells compared to non-immunized animals. Following immunization, granulocytes (Ly6g) in the red pulp and macrophages (CD68) in the white pulp (indicated by dashed lines) were increased. **(b)** Densities and size of PNA$^+$ germinal center B-cells and FDC networks (Mfge8) were also increased in immunized mice. Scale bars: 100 µm. Statistics were performed using unpaired t-test, two-tailed.

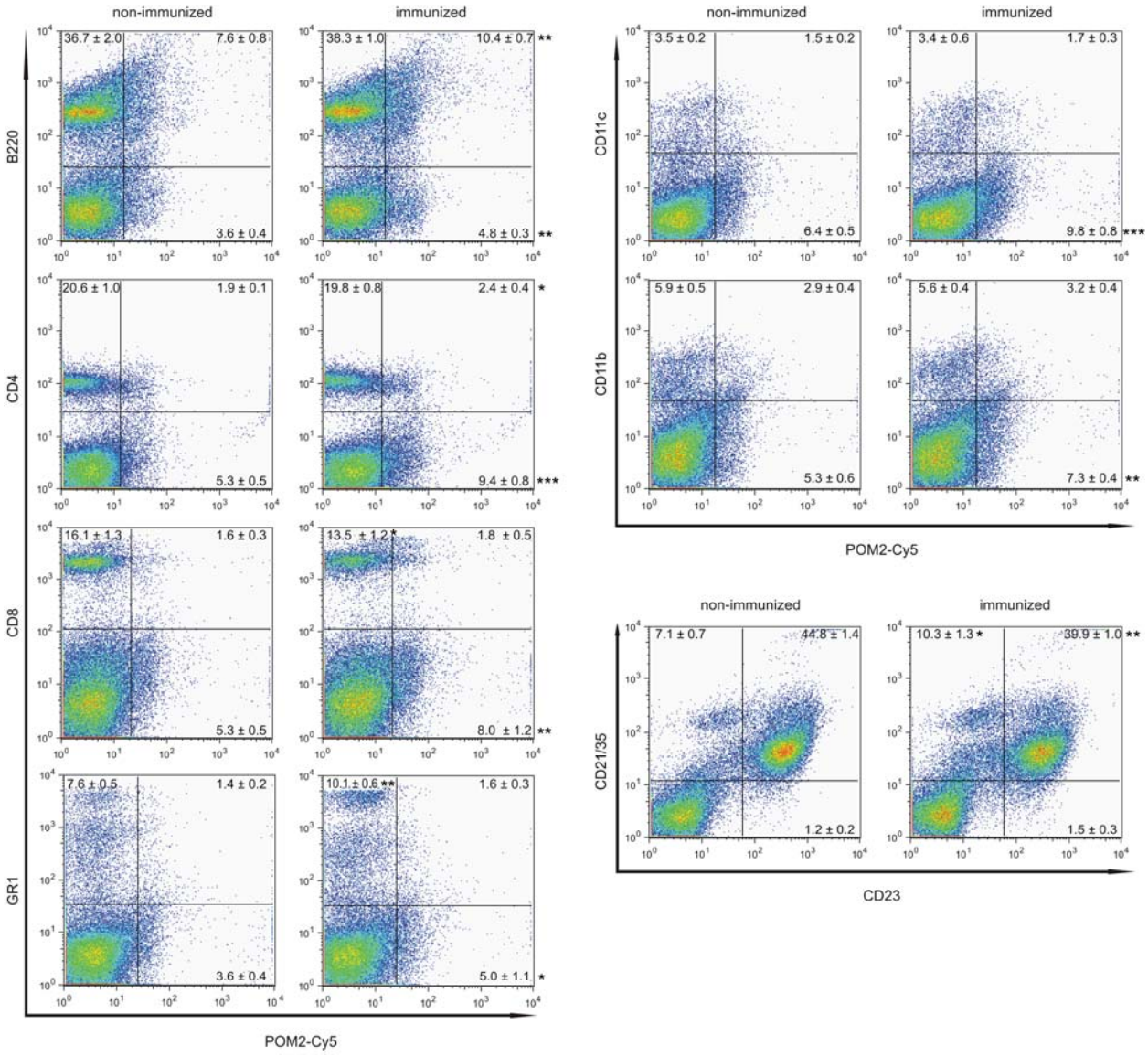

Figure 55: Splenic cell populations in immunized mice. Splenic cells were isolated and co-stained for PrP^C and B220, CD4, CD8, GR1, CD11c, or CD11b; alternatively co-staining for CD21/35 and CD23 was performed. Results from representative samples are shown. Four mice per group were analyzed. Numbers in the diagram indicate average percentages of cells ± standard deviation. Statistical analysis was performed using unpaired t-test, two-tailed. Significantly different percentages are labeled in the right lower scattergram with (*) $p < 0.05$; (**) $p < 0.01$; or (***) $p < 0.001$.

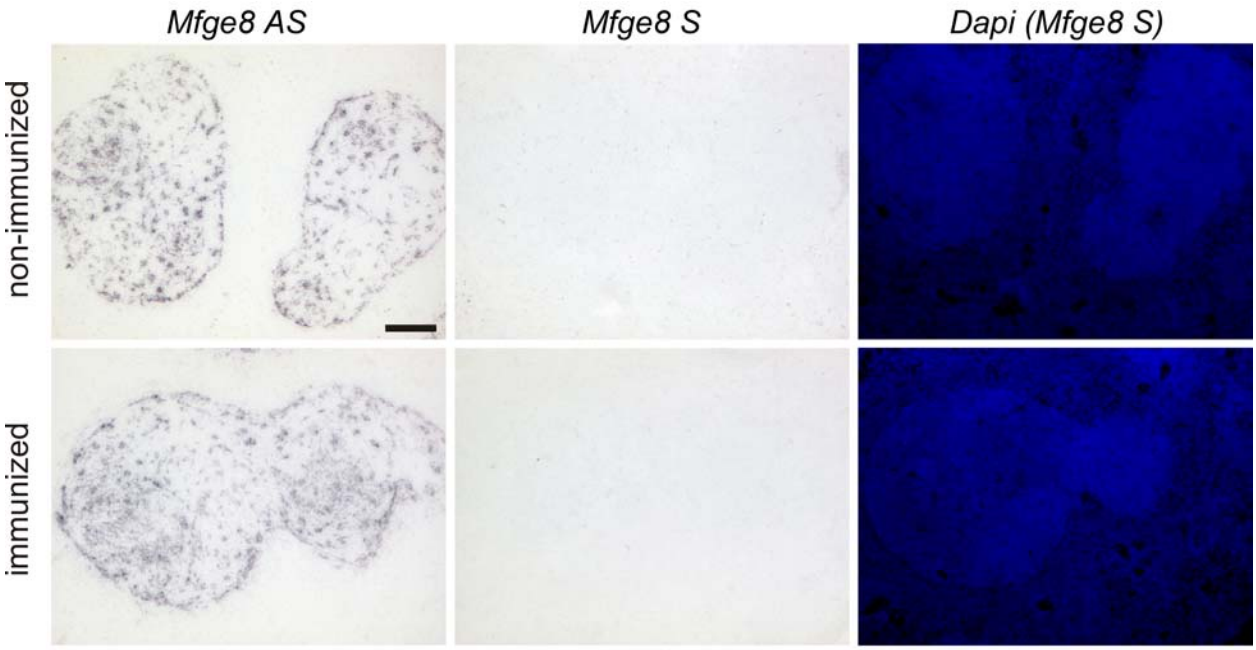

Figure 56: *In situ* hybridization for *Mfge8* mRNA. Spleens of non-immunized and immunized mice were analyzed at the time point of inoculation by *in situ* hybridization for *Mfge8* mRNA. Consecutive sections were hybridized with *Mfge8* antisense (AS) and control sense probe (S) as well as DAPI stains. Scale bar = 100 μm.

Histological analysis of mesenteric lymph nodes (MLNs) showed a trend towards increased numbers of lymphoid follicles (non-immunized mice: 6 ± 2.31; immunized mice: 11.75 ± 1.44 follicles/ lymph node section, p=0.11; **Fig. 57a**). Furthermore, histology showed that immunized mice had a normal architecture of lung, heart, kidney, and pancreas, yet developed lobular hepatitis with loss of hepatocytes and multifocal infiltrates of lymphocytes, macrophages, eosinophils, and neutrophils (**Fig. 57b** and data not shown). Hepatocellular damage was confirmed by elevation of the liver enzymes glutamate dehydrogenase (GLDH) and aspartate amino transferase (ASAT; **Fig. 53d**). Hepatitis might be explained by the hepatotoxic effects of IL-6, which was increased in serum of immunized mice as previously reported[278].

Serum amylase and alkaline phosphatase (AP) levels were normal (**Fig. 53d**), suggesting that there was no damage to the exocrine pancreas and the bile ducts. Finally, immunization induced a mild peritonitis with macrophages and lymphocytes in the peritoneum (**Fig. 57c**).

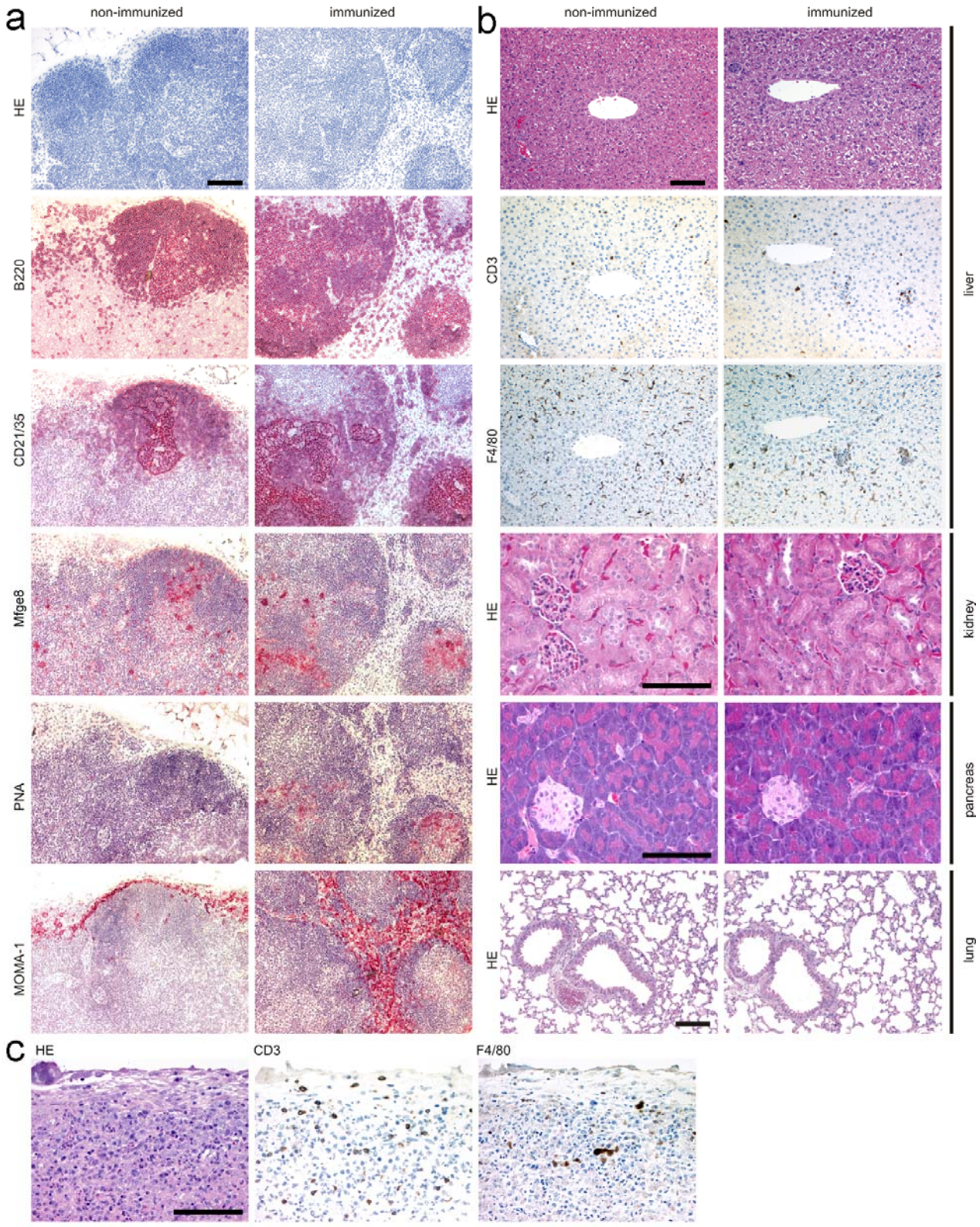

Figure 57: Various organs at the time point of inoculation. (a) Stains and immunohistochemistry on mesenteric lymph nodes (MLNs): HE, B-cells (B220), germinal center B cells and FDCs (CD21/35), FDCs (Mfge8), germinal centers (PNA) and metallophilic marginal zone macrophages (MOMA-1). **(b)** Lung, kidney, pancreas show normal architecture. Lobular hepatitis in immunized mice: loss of hepatocytes, and infiltrates of T cells (CD3), macrophages (F4/80), eosinophils, and neutrophils. **(c)** Peritonitis in immunized mice: T-cells (CD3), and macrophages (F4/80) infiltrating peritoneum. Scale bars = 100 μm.

6.4.2 Increased prion susceptibility in immunized mice

Groups of mice (4 ≤ n ≤ 16) were inoculated intraperitoneally (i.p.) or intracerebrally (i.c.) with low, medium or high doses of prion infectivity. Upon i.p. inoculation with 10 ng of RML6 brain homogenate, 8 of 16 immunized mice (50%) succumbed to scrapie at 223 ± 8.2 days post inoculation (dpi). When exposed to the same dose of prions, non-immunized animals (n=16) remained scrapie-free for >500 dpi (**Fig. 58**).

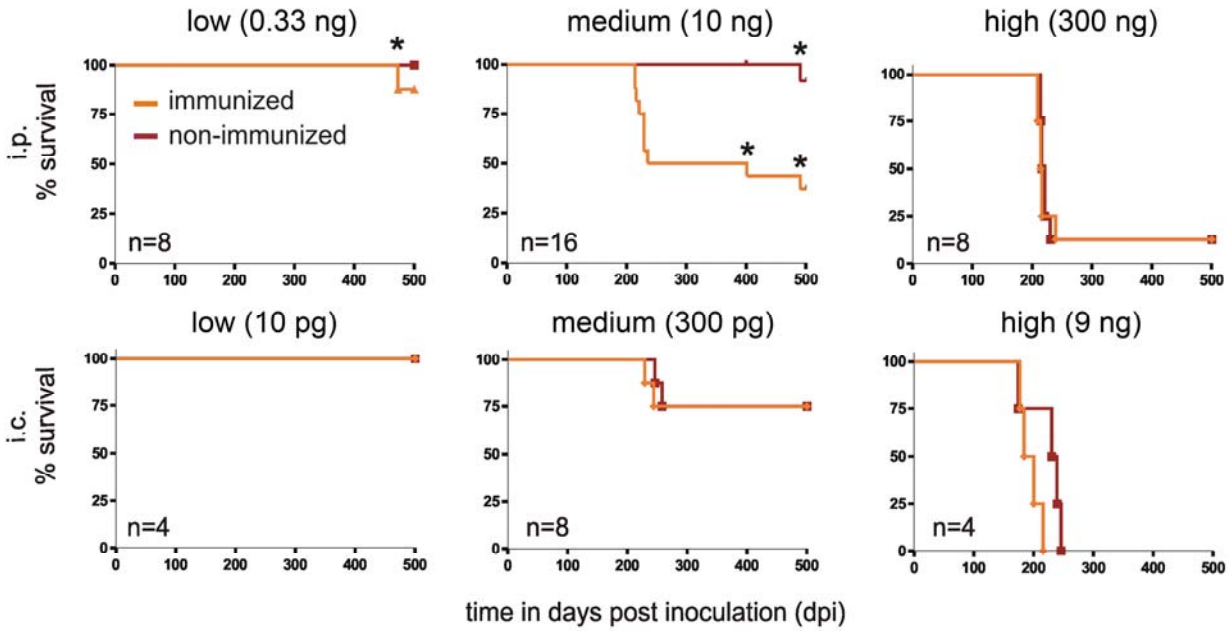

Figure 58: Survival of immunized (i) and non-immunized (ni) mice inoculated intraperitoneally (i.p.) or intracerebrally (i.c.) with prions. While all mice inoculated i.p. or i.c. with a low dose of prions (0.33 ng i.p. or 10 pg i.c. RML6 brain homogenate; left panel) survived until 500 dpi, all mice inoculated i.c. with a high dose of prions (9 ng; right lower panel) died of scrapie. Seven of 8 mice (87.5%) inoculated i.p. with a high dose of prions (300 ng) succumbed to scrapie independently of immunization (right upper panel). In the medium dose group (10 ng i.p. or 300 pg i.c.; medium panels) there was no difference in survival rates in i.c. inoculated mice (75% in both groups). While non-immunized mice inoculated i.p. with a medium dose of prions remained healthy, 50% of the immunized mice developed scrapie. Intercurrent deaths (not scrapie-associated) occurred > 400 dpi; time points are marked with a star above the curve. All brains of mice dying without clinical signs of scrapie were tested by Western blot and did not contain PrP^{Sc} (data not shown).

This difference in survival was highly significant (p=0.0024, Fisher's exact test) and could have two non-exclusive explanations: 1) immunization may increase the accumulation, spread,

and/or propagation of prions, or 2) immunization may promote the progression of subclinical infection to clinically overt disease. To study the latter possibility, I investigated non-immunized mice that had received the same dose of peripherally administered prions (10 ng) for subclinical signs of prion infection at 400 dpi. Non-immunized mice did not display PrP^{Sc} in brains and spleens, nor did they show any histological signs of prion disease such as astrogliosis and microglial activation (**Figs. 58-60**). In addition, I observed no difference in the time intervening between onset of clinical signs and development of terminal scrapie (data not shown). Therefore, repeated immunization of wt mice increased the susceptibility to prion diseases by modulating prion accumulation, spread, and/or propagation rather than by simply affecting the onset of clinical signs.

While inducing scrapie in immunized mice, the dose of prion inoculum utilized in the previous experimental series was insufficient to establish infection in non-immunized mice. I next tested the effect of administering a dose that would induce a 100% attack rate in non-immunized mice. I inoculated immunized and non-immunized mice i.p. with a 30-fold higher dose of prions (300 ng RML6 brain homogenate). No difference in the percentage of mice succumbing to disease was observed: 7 of 8 mice in both groups (87.5%; Fisher's exact test p=1.0) developed terminal scrapie. This indicates that immunization selectively lowers the size of the minimal infectious dose, while it does not change the course of the disease when larger doses are administered. Accordingly, the incubation times in non-immunized (219 ± 5.7 dpi; n=8) and in immunized mice (217 ± 10.3 dpi; n=8) inoculated with the highest dose were similar to those in immunized mice that had received the medium dose (223 ± 8.2 dpi, n=16; ANOVA p=0.3). Therefore, stimulation of the immune system by repeated immunization does not accelerate the general progression of the disease, but rather renders mice susceptible to amounts of peripherally administered prions that would be innocuous to non-immunized wt mice.

I suspected that alterations in lymphoid organs mediate the observed differences in susceptibility. As these events are not thought to be relevant to CNS prion pathogenesis, I expected that the difference in susceptibility would be abolished in immunized versus non-immunized mice inoculated i.c. with prions. The injection of 300 pg RML6 brain homogenate

caused disease in 2 of 8 mice (25%) in both groups. Survival curves did not significantly differ (logrank test, *p*=1). A 30-fold higher prion dose (9 ng RML6 brain homogenate) inoculated i.c. elicited an attack rate of 4 of 4 (100%) in both groups. Although immunization of wt mice strongly increased prion susceptibility to i.p. administered prions, prion susceptibility remained unchanged after i.c. inoculation. This emphasizes the role of peripheral immune system components in determining prion susceptibility. Despite the absence of differential susceptibility, there were slight differences in the incubation times at high and medium dose of prion challenge. However, in both instances these differences were not statistically significant (high dose: 9 ng i.c.; non-immunized: 222 ± 32.8 dpi; immunized: 194 ± 17.4 dpi, unpaired t-test *p*=0.18; medium dose: 300 pg i.c.; non-immunized: 246/258 dpi; immunized: 229/244 dpi).

I then inoculated immunized and naïve mice i.p. with 0.33 ng RML6 homogenate, or i.c. with 10 pg RML6 homogenate. None of these mice (immunized or naive) developed scrapie or neurological signs up to 500 dpi. These data and the absence of astrogliosis and microglia activation in brains of the non-immunized mice (10 ng i.p. at 400 dpi) described above argues against any neurotoxic effects of BSA/alum/CpG-ODN.

6.4.3 PrP^{Sc} distribution patterns and histopathological features in terminally scrapie-sick mice

Brains of all mice developing clinical signs of scrapie were investigated for histological features of prion disease, including astrogliosis, spongiosis, PrP deposition and microglial activation (**Fig. 59**). There were no differences in these histological hallmarks of scrapie. In contrast, those non-immunized mice (n=4) inoculated i.p. with prions (10 ng RML6 brain homogenate) that remained healthy lacked any histological features of prion disease at 400 dpi. Although the SAF84 antibody is commonly used to detect PrP aggregates, it is not specific for PrP^{Sc}. Therefore, in addition I investigated brains by histoblot (**Fig. 59**) and immunoblot (**Fig. 60**). Both techniques demonstrated the presence of PrP^{Sc} in all clinically scrapie-sick mice.

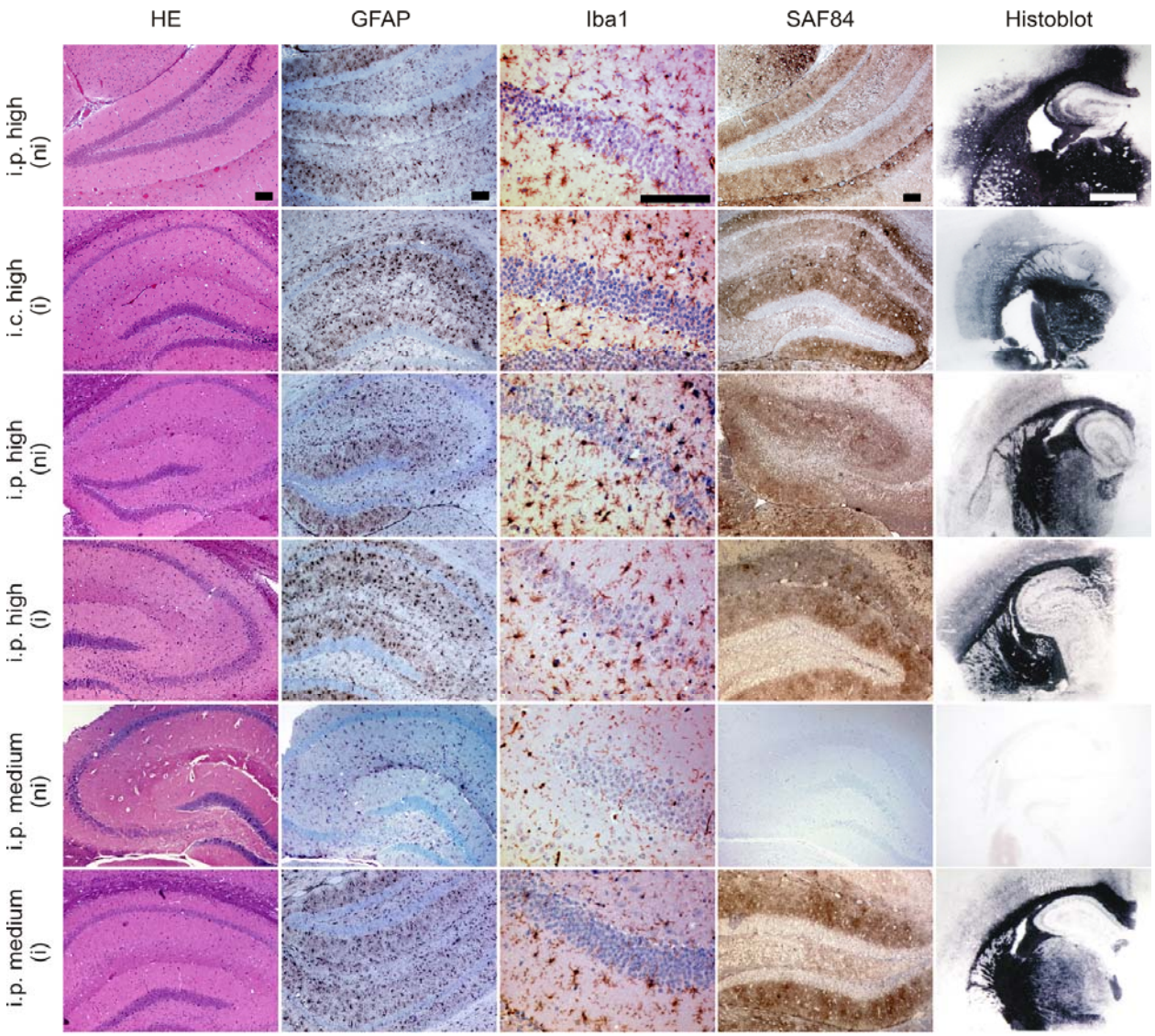

Figure 59: Brain pathology of terminally sick or asymptomatic mice. Immunized (i) and non-immunized mice (ni) inoculated intracerebrally (i.c.) or intraperitoneally (i.p.) with medium or high dose of prions were analyzed by histology. HE stains and immunohistochemistry were performed as indicated: astrocytes (GFAP), microglia (Iba1), PrP deposits (SAF84), showing astrogliosis, microglia activation, and prion protein deposition in terminally sick mice from each of the experimental groups. Histoblot analyses detected PrP^{Sc} in the brains of all terminally sick mice with similar distribution patterns. Non-immunized mice inoculated i.p. with a medium dose of prions remained healthy up to 500 dpi, and displayed much less $GFAP^{+}$ astrocytes and $Iba1^{+}$ microglia cells, and lacked both PrP deposits (SAF84) and PrP^{Sc} (histoblot) at 400 dpi. Scale bars: histoblot = 1 mm; histology = 100 μm.

Similarly, spleens of terminally sick mice were investigated histologically and biochemically by histoblot and immunoblot. There was no difference in splenic histology of immunized mice compared to control (**Fig. 61a**), and PrP^{Sc} deposition pattern (**Fig. 61b**). Furthermore, I could

not detect an overt difference in the PrP^{Sc} deposition as determined by immunoblot (**Fig. 61c**). As in brains, PrP^{Sc} was not detectable in spleens of healthy non-immunized mice at 400 dpi (n=4) that had received 10 ng RML6 brain homogenate i.p. (**Fig. 61b-c**).

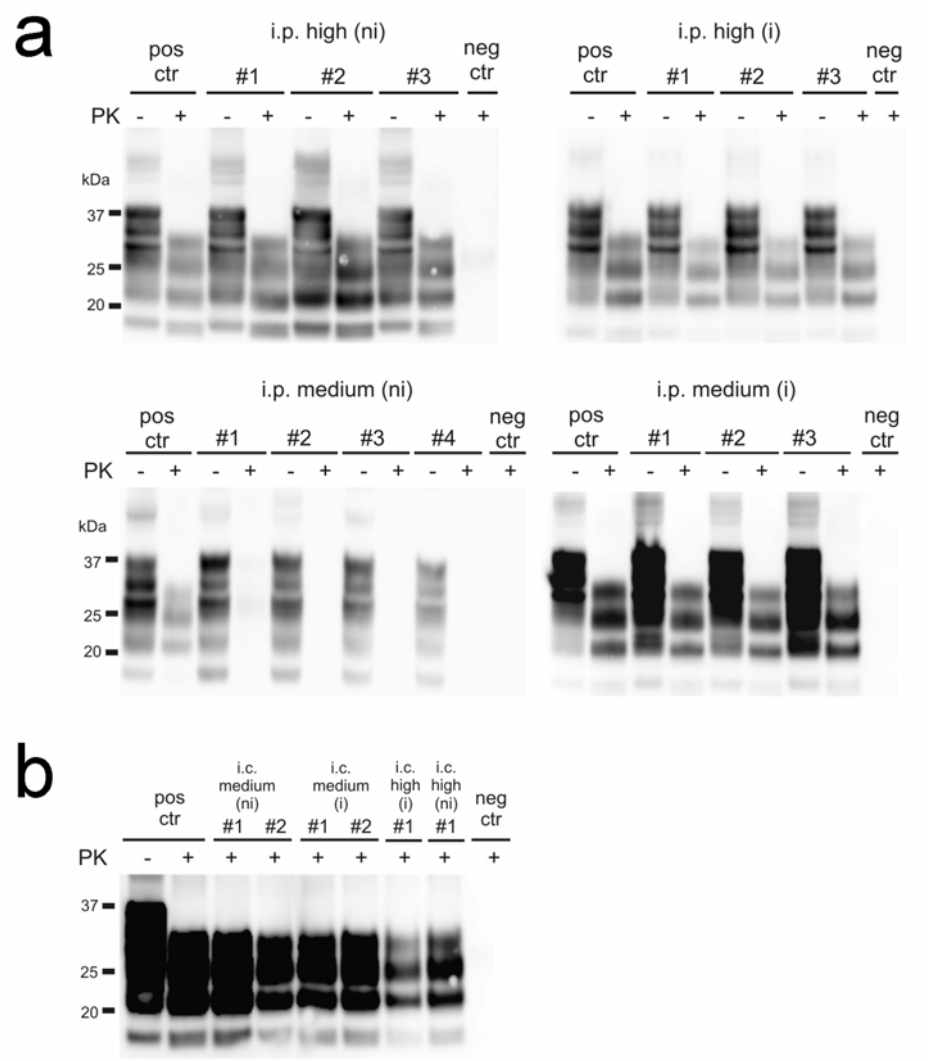

Figure 60: PrP^{Sc} in brains of terminally sick or asymptomatic mice. Immunized (i) and non-immunized mice (ni) inoculated **(a)** intraperitoneally (i.p.) or **(b)** intracerebrally (i.c.) with medium or high doses of prions were analyzed by Western blots for the presence of PrP^{Sc}. Brain homogenates were analyzed with (+) and without (-) previous proteinase K (PK) treatment as indicated. Homogenate derived from a terminally scrapie-sick mouse served as positive control (pos ctr), and healthy wt mouse tissue as negative control (neg ctr), respectively. Molecular weights are indicated on the left side of the blots. All terminally sick mice showed considerable amounts of PrP^{Sc} in the brain. In contrast, non-immunized mice inoculated i.p. with a medium dose of prions [i.p. medium (ni)] lacked PrP^{Sc}.

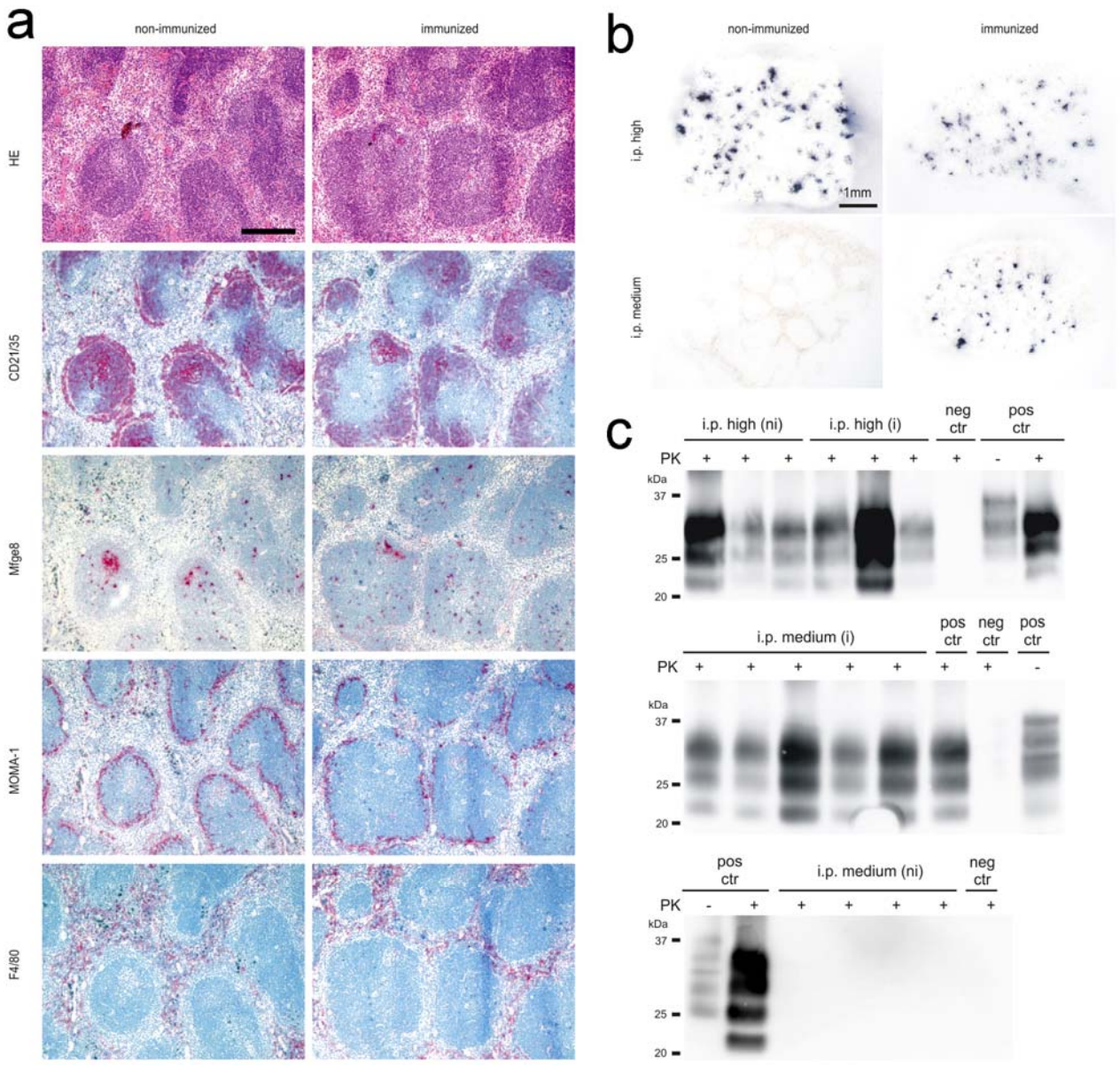

Figure 61: Histology, histoblots, and Western blots of spleens from terminally sick or asymptomatic mice. (a) Spleens of immunized (i) and non-immunized mice (ni) inoculated intraperitoneally (i.p.) with medium or high dose of prions were analyzed by histology. Histological and immunohistochemical stains were performed as indicated. MOMA-1^{+} cells were reduced in immunized mice. All terminally sick mice of the various experimental groups carried PrP^{Sc} in their spleens as shown by histoblot **(b)** and confirmed by Western Blot **(c)**. Asymptomatic, non-immunized mice inoculated i.p. with a medium dose of prions [i.p. medium (ni)] were killed at 400 dpi. No PrP^{Sc} was detectable by histoblot analysis **(b)** and Western blot analysis **(c)**. Controls and abbreviations are as in **Fig. 60**. Scale bars: histoblot = 1 mm; histology = 200 μm.

6.4.4 No difference in splenic PrP^{Sc} deposition at 70 dpi

At 70 dpi there was no difference in PrP^{Sc} load in spleens of immunized mice vs. non-immunized controls. PrP^{Sc} was detectable after sodium phosphotungstic acid (NaPTA) precipitation in spleens of 1 of 4 immunized mice and of 1 of 4 non-immunized mice (**Fig. 62a**). The early presence of PrP^{Sc} in spleens (at 70 dpi) did not correlate with the observed difference in prion susceptibility. PrP^{Sc} was below the limit of detection of the NaPTA immunoblot technique in mesenteric lymph nodes of non-immunized and immunized mice at 70 dpi (**Fig. 62a**). Since it was previously reported that immune stimulation might increase expression levels of PrP^{C} on blood cells[279], I further analyzed PrP expression and cellular blood composition by flow cytometry analysis. There was no significant increase of PrP on $CD19^{+}$ B-cells, $CD3^{+}$ T-cells, or $CD11b^{+}/CD11c^{+}$ monocytes in immunized vs. non-immunized mice. However, the overall PrP expression on all live-gated blood cells was slightly increased in immunized vs. non-immunized mice, but this trend was not significant (immunized: 30.4 ± 2.81% of PrP positive white blood cells; non-immunized: 25.3 ± 1.57%; unpaired t-test p=0.12, values in mean ± standard error of the mean; **Fig. 62b** and data not shown).

I did observe a significant increase in PrP signal on live-gated blood cells in prion infected mice (immunized and non-immunized: 27.9 ± 1.6% of PrP positive white blood cells) compared to non-inoculated, naive mice (16.6 ± 1.8%; unpaired t-test $p<0.002$; **Fig. 62b** and data not shown). This rise in PrP signal can either be attributed to increased protein expression, decreased turn-over, or possibly accumulation of PrP^{Sc} on blood cells. As previously shown by hematology, there was no significant difference in the percentage of blood lymphocytes. However, there was a trend towards an increase of $CD19^{+}$ B-cells in immunized, vs. non-immunized mice (**Fig. 62b**).

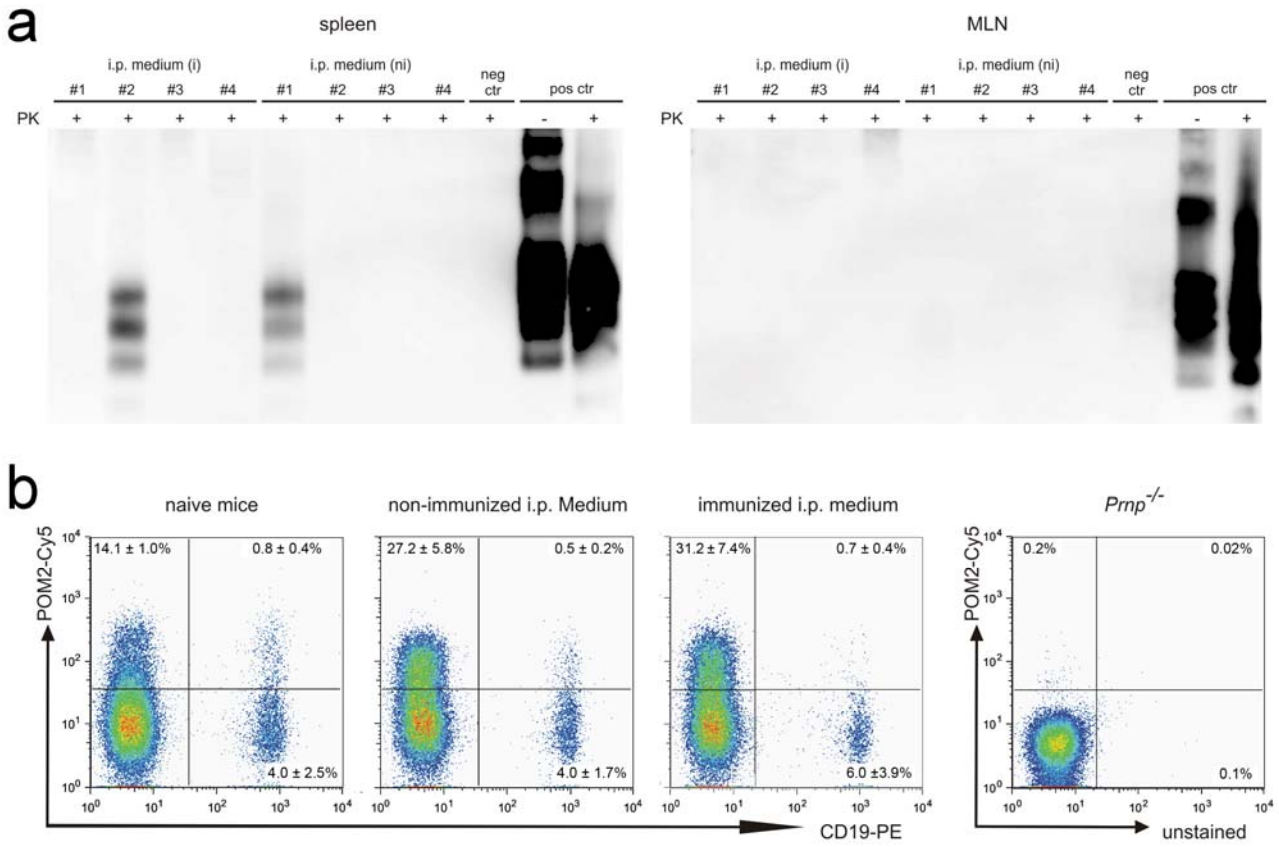

Figure 62: PrP in spleens, mesenteric lymph nodes (MLNs), and on blood cells of inoculated mice at 70 dpi. Mice were inoculated i.p. with a medium dose of prions and analyzed at 70 dpi. **(a)** NaPTA-enhanced Western blots of spleen and MLN homogenates. I detected PrP^{Sc} in spleens of 1 of 4 mice in both, the immunized (i) and non-immunized (ni) group. Controls and abbreviations are as in **Fig. 60**. No PrP^{Sc} deposition was detectable in MLNs of the same mice by NaPTA-enhanced Western blotting. **(b)** Flow cytometry analysis of white blood cells from immunized and non-immunized mice inoculated i.p. with prions, as well as noninoculated, non-immunized "naive" mice. Co-staining for PrP (Cy5-labeled POM2 antibody) and CD19 (PE-labeled anti-CD19 antibody) in representative samples. Four mice per group were analyzed. Numbers in the diagram indicate averages (as percentages) ± standard deviation. Blood from a PrP deficient mouse (*Prnp*$^{-/-}$) served as negative control.

6.5 Discussion

6.5.1 Immunization with CpG and BSA/alum enhances prion susceptibility

The outcome of encounters between a pathogen and its host is determined by two sets of parameters: the intrinsic virulence of the pathogen and the susceptibility of the host. Susceptibility is a measure of the likelihood to contract disease after exposure to a defined inoculum of a given pathogen. In addition to host-intrinsic modifiers, susceptibility to most pathogens is profoundly influenced by exogenous cofactors. Whereas immunodeficiencies greatly increase susceptibility to most conventional pathogens, theoretical considerations prompted me to investigate whether susceptibility to prions may be enhanced by stimulation of the immune system. Indeed, I have identified controlled, repetitive immunization as an important host factor that dramatically increases the susceptibility to peripherally administered prions. Following injection of a low dose of prions, 50% of the immunized mice developed scrapie while all non-immunized mice remained scrapie-free for > 500 dpi.

In most instances, the likelihood of survival after exposure to infectious agents or poisons is normally distributed, and therefore cumulative dose-survival curves display sigmoidal responses with subthreshold doses failing to elicit disease and high doses plateauing towards maximal effects. As a consequence, variations in host susceptibility are typically visible only within a limited range of doses. Here, I tested three different doses of prions in immunized and non-immunized mice. The lowest dose led to 100% survival, whereas the highest dose led to 12.5% (i.p.) and 0% (i.c.) survival, in both groups. The medium dose of intraperitoneally administered prions was associated with an attack rate of 50% in immunized mice only, which nominally corresponds to one LD50 unit (dose causing death in 50% of the exposed hosts) and to the turning point of the postulated sigmoid response curve. Therefore, in this paradigm, the medium dose allowed for optimal sensitivity in the identification of immunization as a factor altering prion susceptibility.

6.5.2 Impact of other immue activating conditions on prion diseases

Treatment with complete Freund's adjuvant (CFA) was reported to prolong survival of prion-inoculated mice, irrespective of whether the challenge was i.c. or i.p.[280]. These results implied that CFA treatment might have a therapeutic effect in experimental scrapie, possibly by reducing the rate of PrP^{Sc} accumulation in the brain. In my experiments I did not detect any influence on susceptibility to i.c. administered prions, and a sensitizing effect after peripheral prion administration. Possible explanations for this discrepancy are (1) the different agents and protocols (site of injection, frequency) used for immunization and (2) the different titers of prion inocula applied.

Another study reported that transient systemic inflammation induced by i.p. administration of LPS acutely exacerbates cognitive and motor symptoms after inoculation with the mouse-adapted ovine prion strain Me7 and accelerates disease progression[281]. Accordingly, I found that immunized mice inoculated i.c. with prions became terminally sick slightly earlier than controls. Although I investigated the influence of other immunizing agents on another prion strain, my finding might well be explained by an acceleration of disease progression, as suggested[281]. In contrast, I focused on differences in disease susceptibility rather than disease onset and progression.

Another study investigated the impact on experimental autoimmune encephalomyelitis (EAE) on prion susceptibility and incubation time. Increased prion susceptibility was observed after low dose i.c. inoculation[282], whereas I could not observe any change in prion susceptibility after low dose i.c. inoculation. This may point to additional EAE-related effects on prion transport, e.g. disturbance of the blood-brain barrier.

It was previously reported that susceptibility of mice to BSE and RML5 prions is not affected by the activation of dendritic cells[271]. Also, it was found that chronic lymphofollicular inflammation of kidney, pancreas, and liver did not overtly alter susceptibility[256]. However, in all of these studies the scrapie attack rates were 100% in both the experimental and the control groups of mice, suggesting that the size of the prion inocula have precluded the sensitive detection of susceptibility shifts. This interpretation is congruent with my finding of indistinguishable attack

rates in non-immunized and immunized mice peripherally exposed to a relatively large inoculum (300 ng of brain homogenate).

It had been previously reported that repeated injection of CpG-ODN protects mice from prion infections[272], suggesting beneficial effects of immune hyperactivity on prion susceptibility, but this treatment was subsequently found to disturb microarchitecture and functionality of lymphoid organs[273]. Therefore, the interpretation of the current findings crucially relies on the integrity of the immune system. Indeed, histology, hematology, and serum chemistry failed to identify immuno-suppressive consequences of the herein described treatment. My data add weight to the conjecture that immunization increases susceptibility to prions and that the previously described protective effects were caused by immuno-disruption rather than by stimulation of the immune system.

6.5.3 How might immunization enhance prion susceptibility?

The increased susceptibility of immunized mice was restricted to peripheral prion exposure and was not observed after i.c. prion inoculation. Evidently, immune modulation affects the speed and/or the extent of prion replication outside but not within the CNS. This suggests that CNS cells are constitutively competent for prion replication, whereas peripheral sites (which may comprise not only lymphoid compartments but also e.g. peripheral nerves) appear to be susceptible to immunological modifiers.

The precise mechanisms by which repetitive immunization increases prion susceptibility remain unknown. Any of the steps involved in peripheral prion spread, including transfer of prions to lymphoid tissues, prion accumulation and propagation within lymphoid tissues, and prion transfer from lymphoid tissues to structures of the nervous system, might be affected by immunization.

The kinetics of PrP^{Sc} accumulation in lymphatic organs might arguably play an important role in susceptibility to peripheral prion administration. While all terminally sick mice carried PrP^{Sc} in the spleen, PrP^{Sc} was undetectable in spleens of all mice that remained healthy. At early time

points (70 dpi), before neuroinvasion had taken place[35], there was no difference in splenic PrP^{Sc} load. Hence, chronic inflammation determines the susceptibility towards prions by a mechanism that is independent of the early splenic PrP^{Sc} accumulation. Also, the absence of PrP^{Sc} from MLNs at 70 dpi suggests that at least in early stages of disease, and under the conditions studied here, MLNs do not play an essential role in prion pathogenesis.

The absence of PrP^{Sc} from spleens at ≥400 dpi despite its presence at earlier stages suggests the existence of a splenic prion clearance mechanism. Maybe repetitive immunization of the immune system facilitates neuroinvasion by reducing splenic prion clearance. The reduced numbers of MOMA-1^+ marginal zone macrophages in immunized mice could contribute to an inhibited prion clearance. MOMA-1^+ cells play an important role in capturing blood borne antigens[283]. Involvement of splenic macrophages in prion clearance in the early phase of infection has been reported, and it was even proposed that marginal zone macrophages are critically involved in this process [284]. This suggests that a decreased prion uptake by MOMA-1^+ cells might lead to a more efficient prion translocation into germinal centers in immunized mice in my study. In this context, it has previously been suggested that CpG-ODN treatment inhibits prion clearance by microglial cells in vitro[279].

I have found an increase in marginal zone B-cells in immunized mice. It is conceivable that alterations in the number of marginal zone B-cells in combination with a decreased number of MOMA-1^+ cells might enhance prion uptake into the germinal centers, thereby influencing prion susceptibility. APCs were proposed to either support prion clearance or to accomplish prion transport[266-271]. Immunohistochemical as well as flow cytometry analysis of blood and spleen from immunized mice did not reveal a significant change of $CD11c^+$ or $CD11b^+$ APCs. Therefore, it is very unlikely that quantitative changes in APCs would contribute to the observed increase in prion susceptibility.

FDCs play an important role in prion replication and are known to co-localize with PrP^{Sc}. In my study, there was an increase in size and density of FDC networks following immunization. This might well explain the increased susceptibility in immunized mice. Alternatively, chronic stimulation of the immune system may alter the transfer of prions from lymphoid organs to the

nervous system. This transfer has previously been shown to be rate-limiting in prion pathogenesis, involving FDCs within germinal centers and tyrosine hydroxylase (TH) positive sympathetic nerve endings. Since immune activation can alter splenic innervation[285], I wondered whether the distance between FDCs and terminal nerve endings was changed, contributing to the increased prion susceptibility of immunized mice. However, staining for tyrosine hydroxylase failed to show altered distances between nerve endings and follicles (data not shown).

Altered PrP^C levels in secondary lymphoid organs can potentially impact prion susceptibility or prion incubation time. Immunization in this study did not alter the overall splenic PrP^C levels as determined by ELISA. Interestingly, by flow cytometry, a slight increase in PrP^C cell surface expression was detected on splenic B- and $CD4^+$ T-cells in immunized mice. I cannot exclude that this slightly increased PrP^C expression on either of the two cell types contributes to increased susceptibility. However, previous studies have shown that PrP^C neither on B- nor on T-cells alone suffices for efficient prion replication[239, 286]. Therefore, I presume that PrP^C levels on B- and T-cells are not the susceptibility determining factors in my study.

CpG-ODN and LPS treatment can increase the cell surface level of PrP^C on macrophages, and it has been suggested that macrophages can replicate prions transiently after stimulation with LPS or CpG-ODN[279]. The conditions used here for immunization did not significantly increase PrP levels on white blood cells or splenic $CD11c^+$ or $CD11b^+$ cells. Therefore, it is unlikely that PrP levels on white blood cells or antigen presenting cells within the spleen determined prion susceptibility in my study.

I have found an increased density of splenic granulocytes following immunization. This might have an impact on prion susceptibility. Since the role of granulocytes in prion pathogenesis is unknown, no definite conclusions can be drawn. Similarly, the impact of $CD68^+$ cells appearing in the white pulp follicles of immunized mice and its effect on peripheral prion replication remain unknown. Alum, which was used as an immunization adjuvant in my study, was recently shown to induce influx of monocytic dendritic cells into the peritoneum. This Nalp3-dependent influx[287] may conceivably represent a mechanism for efficient transfer of prions to secondary lymphoid

organs. It will be interesting to test whether interference with this pathway modulates prion susceptibility.

In summary, I conclude that either (1) increased density and size of FDC networks in splenic germinal centers, (2) decreased clearance of prions by changing the cellular compartment of the marginal zone (e.g. marginal zone macrophages, marginal zone B-cells), or (3) both, are most likely responsible for increased prion susceptibility upon immunization.

6.5.4 Does chronic immune stimulation correlate with CJD risk?

In the light of the above results, it will be of interest to determine whether stimulation of the immune system may contribute to the individual susceptibility of humans towards prions. States of chronically stimulated immune system are common in humans, and can occur e.g. in chronic infectious diseases, autoimmune disorders, and allergies. Exposure to BSE prions is the assumed cause of vCJD, yet it is not known which factors determined that some unfortunate individuals among the European population developed vCJD while most others remained healthy. Epidemiological retrospective and prospective studies may help to clarify whether particular immune stimuli correlate with the likelihood to contract vCJD or other acquired prion diseases.

7 REFERENCES

1. Nishida, N.*, et al.* A mouse prion protein transgene rescues mice deficient for the prion protein gene from purkinje cell degeneration and demyelination. *Lab Invest* 79, 689-697 (1999).

2. Baumann, F.*, et al.* Lethal recessive myelin toxicity of prion protein lacking its central domain. *Embo J* 26, 538-547 (2007).

3. Thomas J. Kindt, B.A.O., Richard A. Goldsby. *Kuby Immunology* (W. H. Freeman and Company, New York, 2007).

4. Aguzzi, A. & Weissmann, C. Prion research: the next frontiers. *Nature* 389, 795-798 (1997).

5. Prusiner, S.B. Novel proteinaceous infectious particles cause scrapie. *Science* 216, 136-144 (1982).

6. Aguzzi, A., Baumann, F. & Bremer, J. The prion's elusive reason for being. *Annu Rev Neurosci* 31, 439-477 (2008).

7. Aguzzi, A. & Polymenidou, M. Mammalian prion biology: one century of evolving concepts. *Cell* 116, 313-327 (2004).

8. Deleault, N.R., Harris, B.T., Rees, J.R. & Supattapone, S. Formation of native prions from minimal components in vitro. *Proc Natl Acad Sci U S A* 104, 9741-9746 (2007).

9. Trepel. *Neuroanatomie* (Elsevier GmbH, Urban & Fischer Verlag, Munich, 2008).

10. Popko, B. Myelin maintenance: axonal support required. *Nat Neurosci* 13, 275-277 (2010).

11. Nave, K.A. & Trapp, B.D. Axon-glial signaling and the glial support of axon function. *Annu Rev Neurosci* 31, 535-561 (2008).

12. Nave, K.A. Myelination and the trophic support of long axons. *Nat Rev Neurosci* 11, 275-283 (2010).

13. Woodhoo, A.*, et al.* Notch controls embryonic Schwann cell differentiation, postnatal myelination and adult plasticity. *Nat Neurosci* 12, 839-847 (2009).

14. Jessen, K.R. & Mirsky, R. The origin and development of glial cells in peripheral nerves. *Nat Rev Neurosci* 6, 671-682 (2005).

15. Taveggia, C.*, et al.* Neuregulin-1 type III determines the ensheathment fate of axons. *Neuron* 47, 681-694 (2005).

16. Michailov, G.V.*, et al.* Axonal neuregulin-1 regulates myelin sheath thickness. *Science* 304, 700-703 (2004).

17. Black, J.A., Foster, R.E. & Waxman, S.G. Rat optic nerve: freeze-fracture studies during development of myelinated axons. *Brain Res* 250, 1-20 (1982).

18. Zhou, L. & Griffin, J.W. Demyelinating neuropathies. *Curr Opin Neurol* 16, 307-313 (2003).

19. Marrosu, M.G.*, et al.* Charcot-Marie-Tooth disease type 2 associated with mutation of the myelin protein zero gene. *Neurology* 50, 1397-1401 (1998).

20. Laura, M.*, et al.* Rapid progression of late onset axonal Charcot-Marie-Tooth disease associated with a novel MPZ mutation in the extracellular domain. *J Neurol Neurosurg Psychiatry* 78, 1263-1266 (2007).

21. Scherer, S.S. & Wrabetz, L. Molecular mechanisms of inherited demyelinating neuropathies. *Glia* 56, 1578-1589 (2008).

22. Lappe-Siefke, C.*, et al.* Disruption of Cnp1 uncouples oligodendroglial functions in axonal support and myelination. *Nat Genet* 33, 366-374 (2003).

23. Edgar, J.M.*, et al.* Early ultrastructural defects of axons and axon-glia junctions in mice lacking expression of Cnp1. *Glia* 57, 1815-1824 (2009).

24. Edgar, J.M.*, et al.* Oligodendroglial modulation of fast axonal transport in a mouse model of hereditary spastic paraplegia. *J Cell Biol* 166, 121-131 (2004).

25. Yin, X.*, et al.* Myelin-associated glycoprotein is a myelin signal that modulates the caliber of myelinated axons. *J Neurosci* 18, 1953-1962 (1998).

26. Nguyen, T.*, et al.* Axonal protective effects of the myelin-associated glycoprotein. *J Neurosci* 29, 630-637 (2009).

27. Kassmann, C.M.*, et al.* Axonal loss and neuroinflammation caused by peroxisome-deficient oligodendrocytes. *Nat Genet* 39, 969-976 (2007).

28. Heuß, D. Diagnostik bei Polyneuropathien. in *DGN guideline* (2008). www.dgn.org

29. Shy, M., Kamholz, J, Li, J. Mutations in Schwann cell genes causing inherited neuropathies. in *The biology of Schwann cells* (ed. P. Armati) (Cambridge University Press, Cambridge, 2007).

30. Stahl, N., Borchelt, D.R., Hsiao, K. & Prusiner, S.B. Scrapie prion protein contains a phosphatidylinositol glycolipid. *Cell* 51, 229-240 (1987).

31. Hornemann, S.*, et al.* Recombinant full-length murine prion protein, mPrP(23-231): purification and spectroscopic characterization. *FEBS Lett* 413, 277-281 (1997).

32. Riek, R.*, et al.* NMR structure of the mouse prion protein domain PrP(121-231). *Nature* 382, 180-182 (1996).

33. Büeler, H.R.*, et al.* Normal development and behaviour of mice lacking the neuronal cell-surface PrP protein. *Nature* 356, 577-582 (1992).

34. Manson, J.C., Clarke, A.R., McBride, P.A., McConnell, I. & Hope, J. PrP gene dosage determines the timing but not the final intensity or distribution of lesions in scrapie pathology. *Neurodegeneration* 3, 331-340 (1994).

35. Büeler, H.R.*, et al.* Mice devoid of PrP are resistant to scrapie. *Cell* 73, 1339-1347 (1993).

36. Moore, R.C.*, et al.* Ataxia in prion protein (PrP)-deficient mice is associated with upregulation of the novel PrP-like protein doppel *J Mol Biol* 292, 797-817 (1999).

37. Rossi, D.*, et al.* Onset of ataxia and Purkinje cell loss in PrP null mice inversely correlated with Dpl level in brain. *EMBO J* 20, 694-702 (2001).

38. Sakaguchi, S.*, et al.* Loss of cerebellar Purkinje Cells in aged mice homozygous for a disrupted PrP gene. *Nature* 380, 528-531 (1996).

39. Weissmann, C. & Aguzzi, A. Perspectives: neurobiology. PrP's double causes trouble. *Science* 286, 914-915 (1999).

40. Roucou, X. & LeBlanc, A.C. Cellular prion protein neuroprotective function: implications in prion diseases. *J Mol Med* 83, 3-11 (2005).

41. Kuwahara, C.*, et al.* Prions prevent neuronal cell-line death. *Nature* 400, 225-226 (1999).

42. Bounhar, Y., Zhang, Y., Goodyer, C.G. & LeBlanc, A. Prion protein protects human neurons against Bax-mediated apoptosis. *J Biol Chem* 276, 39145-39149 (2001).

43. Ma, J., Wollmann, R. & Lindquist, S. Neurotoxicity and Neurodegeneration When PrP Accumulates in the Cytosol. *Science* 298:, 1781-1785 (2002).

44. Roucou, X., Guo, Q., Zhang, Y., Goodyer, C.G. & LeBlanc, A.C. Cytosolic prion protein is not toxic and protects against Bax-mediated cell death in human primary neurons. *J Biol Chem* (2003).

45. Roucou, X.*, et al.* Cellular prion protein inhibits proapoptotic Bax conformational change in human neurons and in breast carcinoma MCF-7 cells. *Cell Death Differ* 12, 783-795 (2005).

46. Diarra-Mehrpour, M.*, et al.* Prion protein prevents human breast carcinoma cell line from tumor necrosis factor alpha-induced cell death. *Cancer Res* 64, 719-727 (2004).

47. Shyu, W.C.*, et al.* Overexpression of PrPC by adenovirus-mediated gene targeting reduces ischemic injury in a stroke rat model. *J Neurosci* 25, 8967-8977 (2005).

48. Weise, J.*, et al.* Upregulation of cellular prion protein (PrPc) after focal cerebral ischemia and influence of lesion severity. *Neurosci Lett* 372, 146-150 (2004).

49. McLennan, N.F.*, et al.* Prion protein accumulation and neuroprotection in hypoxic brain damage. *Am J Pathol* 165, 227-235 (2004).

50. Weise, J.*, et al.* Deletion of cellular prion protein results in reduced Akt activation, enhanced postischemic caspase-3 activation, and exacerbation of ischemic brain injury. *Stroke* 37, 1296-1300 (2006).

51. Spudich, A.*, et al.* Aggravation of ischemic brain injury by prion protein deficiency: Role of ERK-1/-2 and STAT-1. *Neurobiol Dis* 20, 442-449 (2005).

52. Mitteregger, G.*, et al.* The role of the octarepeat region in neuroprotective function of the cellular prion protein. *Brain Pathol* 17, 174-183 (2007).

53. Milhavet, O. & Lehmann, S. Oxidative stress and the prion protein in transmissible spongiform encephalopathies. *Brain Res Brain Res Rev* 38, 328-339 (2002).

54. Brown, D.R., Schmidt, B. & Kretzschmar, H.A. Effects of oxidative stress on prion protein expression in PC12 cells. *Int J Dev Neurosci* 15, 961-972 (1997).

55. White, A.R.*, et al.* Prion protein-deficient neurons reveal lower glutathione reductase activity and increased susceptibility to hydrogen peroxide toxicity. *Am J Pathol* 155, 1723-1730 (1999).

56. Brown, D.R., Nicholas, R.S. & Canevari, L. Lack of prion protein expression results in a neuronal phenotype sensitive to stress. *J Neurosci Res* 67, 211-224 (2002).

57. Brown, D.R., Schulz-Schaeffer, W.J., Schmidt, B. & Kretzschmar, H.A. Prion protein-deficient cells show altered response to oxidative stress due to decreased SOD-1 activity. *Exp Neurol* 146, 104-112 (1997).

58. Klamt, F.*, et al.* Imbalance of antioxidant defense in mice lacking cellular prion protein. *Free Radic Biol Med* 30, 1137-1144 (2001).

59. Wong, B.S.*, et al.* Increased levels of oxidative stress markers detected in the brains of mice devoid of prion protein. *J Neurochem* 76, 565-572. (2001).

60. Brown, D.R.*, et al.* Normal prion protein has an activity like that of superoxide dismutase [published erratum appears in Biochem J 2000 Feb 1;345 Pt 3:767]. *Biochem J* 344 Pt 1, 1-5 (1999).

61. Jones, S.*, et al.* Recombinant prion protein does not possess superoxide dismutase activity. *Biochem J* (2005).

62. Hutter, G., Heppner, F.L. & Aguzzi, A. No Superoxide Dismutase Activity of Cellular Prion Protein in vivo. *Biol Chem* 384, 1279-1285 (2003).

63. Waggoner, D.J.*, et al.* Brain Copper Content and Cuproenzyme Activity Do Not Vary with Prion Protein Expression Level. *J Biol Chem* 275, 7455-7458 (2000).

64. Choi, S.I.*, et al.* Mitochondrial dysfunction induced by oxidative stress in the brains of hamsters infected with the 263 K scrapie agent [In Process Citation]. *Acta Neuropathol (Berl)* 96, 279-286 (1998).

65. Lee, D.W.*, et al.* Alteration of free radical metabolism in the brain of mice infected with scrapie agent. *Free Radic Res* 30, 499-507 (1999).

66. Miele, G., Jeffrey, M., Turnbull, D., Manson, J. & Clinton, M. Ablation of cellular prion protein expression affects mitochondrial numbers and morphology. *Biochem Biophys Res Commun* 291, 372-377 (2002).

67. Fournier, J.G., Escaig Haye, F., Billette de Villemeur, T. & Robain, O. Ultrastructural localization of cellular prion protein (PrPc) in synaptic boutons of normal hamster hippocampus. *C R Acad Sci III* 318, 339-344 (1995).

68. Moya, K.L.*, et al.* Immunolocalization of the cellular prion protein in normal brain. *Microsc Res Tech* 50, 58-65. (2000).

69. Sales, N.*, et al.* Cellular prion protein localization in rodent and primate brain. *Eur J Neurosci* 10, 2464-2471 (1998).

70. Tateishi, J., Kitamoto, T., Kretzschmar, H. & Mehraein, P. Immunhistological evaluation of Creutzfeldt-Jakob disease with reference to the type PrPres deposition. *Clin Neuropathol* 15, 358-360 (1996).

71. Laine, J., Marc, M.E., Sy, M.S. & Axelrad, H. Cellular and subcellular morphological localization of normal prion protein in rodent cerebellum. *Eur J Neurosci* 14, 47-56 (2001).

72. Mironov, A., Jr.*, et al.* Cytosolic prion protein in neurons. *J Neurosci* 23, 7183-7193 (2003).

73. Grigoriev, V.*, et al.* Submicroscopic immunodetection of PrP in the brain of a patient with a new-variant of Creutzfeldt-Jakob disease. *Neurosci Lett* 264, 57-60 (1999).

74. Jeffrey, M.*, et al.* Synapse loss associated with abnormal PrP precedes neuronal degeneration in the scrapie-infected murine hippocampus. *Neuropathol Appl Neurobiol* 26, 41-54 (2000).

75. Kitamoto, T.*, et al.* Abnormal isoform of prion proteins accumulates in the synaptic structures of the central nervous system in patients with Creutzfeldt-Jakob disease. *Am J Pathol* 140, 1285-1294 (1992).

76. Matsuda, H.*, et al.* A chicken monoclonal antibody with specificity for the N-terminal of human prion protein. *FEMS Immunol Med Microbiol* 23, 189-194 (1999).

77. Roikhel, V.M., Mats, V.N., Fokina, G.I., Ravkina, L.I. & Pogodina, V.V. Reaction of mouse CNS cells to the scrapie agent in early stages of experimental infection. *Acta Virol* 27, 400-406 (1983).

78. Ferrer, I., Rivera, R., Blanco, R. & Marti, E. Expression of proteins linked to exocytosis and neurotransmission in patients with Creutzfeldt-Jakob disease [In Process Citation]. *Neurobiol Dis* 6, 92-100 (1999).

79. Clinton, J., Forsyth, C., Royston, M.C. & Roberts, G.W. Synaptic degeneration is the primary neuropathological feature in prion disease: a preliminary study. *Neuroreport* 4, 65-68 (1993).

80. Barrow, P.A., Holmgren, C.D., Tapper, A.J. & Jefferys, J.G. Intrinsic physiological and morphological properties of principal cells of the hippocampus and neocortex in hamsters infected with scrapie. *Neurobiol Dis* 6, 406-423 (1999).

81. Johnston, A.R., Fraser, J.R., Jeffrey, M. & MacLeod, N. Synaptic plasticity in the CA1 area of the hippocampus of scrapie- infected mice. *Neurobiol Dis* 5, 188-195 (1998).

82. Bouzamondo-Bernstein, E.*, et al.* The neurodegeneration sequence in prion diseases: evidence from functional, morphological and ultrastructural studies of the GABAergic system. *J Neuropathol Exp Neurol* 63, 882-899 (2004).

83. Carleton, A., Tremblay, P., Vincent, J.D. & Lledo, P.M. Dose-dependent, prion protein (PrP)-mediated facilitation of excitatory synaptic transmission in the mouse hippocampus. *Pflugers Arch* 442, 223-229 (2001).

84. Colling, S.B., Collinge, J. & Jefferys, J.G.R. Hippocampal Slices From Prion Protein Null Mice - Disrupted Ca2+-Activated K+ Currents. *Neuroscience Letters* 209, 49-52 (1996).

85. Collinge, J.*, et al.* Prion protein is necessary for normal synaptic function. *Nature* 370, 295-297 (1994).

86. Mallucci, G.R.*, et al.* Post-natal knockout of prion protein alters hippocampal CA1 properties, but does not result in neurodegeneration. *Embo J* 21, 202-210 (2002).

87. Herms, J.W., Tings, T., Dunker, S. & Kretzschmar, H.A. Prion protein affects Ca2+-activated K+ currents in cerebellar purkinje cells. *Neurobiol Dis* 8, 324-330 (2001).

88. Lledo, P.M., Tremblay, P., Dearmond, S.J., Prusiner, S.B. & Nicoll, R.A. Mice Deficient For Prion Protein Exhibit Normal Neuronal Excitability and Synaptic Transmission in the Hippocampus. *Proceedings of the National Academy of Sciences of the United States of America* 93, 2403-2407 (1996).

89. Maglio, L.E., Perez, M.F., Martins, V.R., Brentani, R.R. & Ramirez, O.A. Hippocampal synaptic plasticity in mice devoid of cellular prion protein. *Brain Res Mol Brain Res* 131, 58-64 (2004).

90. Maglio, L.E., Martins, V.R., Izquierdo, I. & Ramirez, O.A. Role of cellular prion protein on LTP expression in aged mice. *Brain Res* 1097, 11-18 (2006).

91. Curtis, J., Errington, M., Bliss, T., Voss, K. & MacLeod, N. Age-dependent loss of PTP and LTP in the hippocampus of PrP-null mice. *Neurobiol Dis* 13, 55-62 (2003).

92. Tobler, I.*, et al.* Altered circadian activity rhythms and sleep in mice devoid of prion protein. *Nature* 380, 639-642 (1996).

93. Criado, J.R.*, et al.* Mice devoid of prion protein have cognitive deficits that are rescued by reconstitution of PrP in neurons. *Neurobiol Dis* 19, 255-265 (2005).

94. Gohel, C.*, et al.* Ultrastructural localization of cellular prion protein (PrPc) at the neuromuscular junction. *J Neurosci Res* 55, 261-267 (1999).

95. Re, L.*, et al.* Prion protein potentiates acetylcholine release at the neuromuscular junction. *Pharmacol Res* 53, 62-68 (2006).

96. Kanaani, J., Prusiner, S.B., Diacovo, J., Baekkeskov, S. & Legname, G. Recombinant prion protein induces rapid polarization and development of synapses in embryonic rat hippocampal neurons in vitro. *J Neurochem* 95, 1373-1386 (2005).

97. Chen, S., Mange, A., Dong, L., Lehmann, S. & Schachner, M. Prion protein as trans-interacting partner for neurons is involved in neurite outgrowth and neuronal survival. *Mol Cell Neurosci* 22, 227-233 (2003).

98. Lopes, M.H.*, et al.* Interaction of cellular prion and stress-inducible protein 1 promotes neuritogenesis and neuroprotection by distinct signaling pathways. *J Neurosci* 25, 11330-11339 (2005).

99. Santuccione, A., Sytnyk, V., Leshchyns'ka, I. & Schachner, M. Prion protein recruits its neuronal receptor NCAM to lipid rafts to activate p59fyn and to enhance neurite outgrowth. *J Cell Biol* 169, 341-354 (2005).

100. Steele, A.D., Emsley, J.G., Ozdinler, P.H., Lindquist, S. & Macklis, J.D. Prion protein (PrPc) positively regulates neural precursor proliferation during developmental and adult mammalian neurogenesis. *Proc Natl Acad Sci U S A* 103, 3416-3421 (2006).

101. Itoh, Y.*, et al.* A variant of Gerstmann-Straussler-Scheinker disease carrying codon 105 mutation with codon 129 polymorphism of the prion protein gene: a clinicopathological study. *J Neurol Sci* 127, 77-86 (1994).

102. Walis, A., Liberski, P.P. & Brown, P. Ultrastructural alterations in the optic nerve in transmissible spongiform encephalopathies or prion diseases--a review. *Folia Neuropathol* 42 Suppl B, 153-160 (2004).

103. Walis, A.*, et al.* Ultrastructural changes in the optic nerves of rodents with experimental Creutzfeldt-Jakob Disease (CJD), Gerstmann-Straussler-Scheinker disease (GSS) or scrapie. *J Comp Pathol* 129, 213-225 (2003).

104. Radovanovic, I.*, et al.* Truncated Prion Protein and Doppel Are Myelinotoxic in the Absence of Oligodendrocytic PrPC. *J. Neurosci.* 25, 4879-4888 (2005).

105. Li, A.*, et al.* Neonatal lethality in transgenic mice expressing prion protein with a deletion of residues 105-125. *EMBO J* 26, 548-558 (2007).

106. Shmerling, D.*, et al.* Expression of amino-terminally truncated PrP in the mouse leading to ataxia and specific cerebellar lesions. *Cell* 93, 203-214 (1998).

107. Mouillet-Richard, S.*, et al.* Signal transduction through prion protein. *Science* 289, 1925-1928. (2000).

108. Schneider, B.*, et al.* NADPH oxidase and extracellular regulated kinases 1/2 are targets of prion protein signaling in neuronal and nonneuronal cells. *Proc Natl Acad Sci U S A* 100, 13326-13331 (2003).

109. Mouillet-Richard, S.*, et al.* Modulation of serotonergic receptor signaling and cross-talk by prion protein. *J Biol Chem* 280, 4592-4601 (2005).

110. Toni, M.*, et al.* Cellular prion protein and caveolin-1 interaction in a neuronal cell line precedes fyn/erk 1/2 signal transduction. *J Biomed Biotechnol* 2006, 69469 (2006).

111. Chiarini, L.B.*, et al.* Cellular prion protein transduces neuroprotective signals. *Embo J* 21, 3317-3326 (2002).

112. Zanata, S.M.*, et al.* Stress-inducible protein 1 is a cell surface ligand for cellular prion that triggers neuroprotection. *Embo J* 21, 3307-3316 (2002).

113. Prado, M.A.*, et al.* PrPc on the road: trafficking of the cellular prion protein. *J Neurochem* 88, 769-781 (2004).

114. York, R.D.*, et al.* Role of phosphoinositide 3-kinase and endocytosis in nerve growth factor-induced extracellular signal-regulated kinase activation via Ras and Rap1. *Mol Cell Biol* 20, 8069-8083 (2000).

115. Zhang, Y., Moheban, D.B., Conway, B.R., Bhattacharyya, A. & Segal, R.A. Cell surface Trk receptors mediate NGF-induced survival while internalized receptors regulate NGF-induced differentiation. *J Neurosci* 20, 5671-5678 (2000).

116. Kaneko, K.*, et al.* COOH-terminal sequence of the cellular prion protein directs subcellular trafficking and controls conversion into the scrapie isoform. *Proc Natl Acad Sci U S A* 94, 2333-2338 (1997).

117. Marella, M., Lehmann, S., Grassi, J. & Chabry, J. Filipin Prevents Pathological Prion Protein Accumulation by Reducing Endocytosis and Inducing Cellular PrP Release. *J Biol Chem* 277, 25457-25464 (2002).

118. Peters, P.J.*, et al.* Trafficking of prion proteins through a caveolae-mediated endosomal pathway. *J Cell Biol* 162, 703-717 (2003).

119. Vey, M.*, et al.* Subcellular colocalization of the cellular and scrapie prion proteins in caveolae-like membranous domains. *Proc Natl Acad Sci U S A* 93, 14945-14949 (1996).

120. Shyng, S.L., Heuser, J.E. & Harris, D.A. A glycolipid-anchored prion protein is endocytosed via clathrin-coated pits. *J Cell Biol* 125, 1239-1250 (1994).

121. Taylor, D.R., Watt, N.T., Perera, W.S. & Hooper, N.M. Assigning functions to distinct regions of the N-terminus of the prion protein that are involved in its copper-stimulated, clathrin-dependent endocytosis. *J Cell Sci* 118, 5141-5153 (2005).

122. Di Guglielmo, G.M., Le Roy, C., Goodfellow, A.F. & Wrana, J.L. Distinct endocytic pathways regulate TGF-beta receptor signalling and turnover. *Nat Cell Biol* 5, 410-421 (2003).

123. Kirkham, M. & Parton, R.G. Clathrin-independent endocytosis: new insights into caveolae and non-caveolar lipid raft carriers. *Biochim Biophys Acta* 1746, 349-363 (2005).

124. Parton, R.G. & Richards, A.A. Lipid rafts and caveolae as portals for endocytosis: new insights and common mechanisms. *Traffic* 4, 724-738 (2003).

125. Sunyach, C.*, et al.* The mechanism of internalization of glycosylphosphatidylinositol-anchored prion protein. *Embo J* 22, 3591-3601 (2003).

126. Taylor, D.R. & Hooper, N.M. The low-density lipoprotein receptor-related protein 1 (LRP1) mediates the endocytosis of the cellular prion protein. *Biochem J* 402, 17-23 (2007).

127. Cheng, F., Lindqvist, J., Haigh, C.L., Brown, D.R. & Mani, K. Copper-dependent co-internalization of the prion protein and glypican-1. *J Neurochem* 98, 1445-1457 (2006).

128. Keshet, G.I., Ovadia, H., Taraboulos, A. & Gabizon, R. Scrapie-infected mice and PrP knockout mice share abnormal localization and activity of neuronal nitric oxide synthase. *J Neurochem* 72, 1224-1231 (1999).

129. Graner, E.*, et al.* Cellular prion protein binds laminin and mediates neuritogenesis. *Brain Res Mol Brain Res* 76, 85-92 (2000).

130. Graner, E.*, et al.* Laminin-induced PC-12 cell differentiation is inhibited following laser inactivation of cellular prion protein. *FEBS Lett* 482, 257-260. (2000).

131. Gauczynski, S.*, et al.* The 37-kDa/67-kDa laminin receptor acts as the cell-surface receptor for the cellular prion protein. *Embo J* 20, 5863-5875 (2001).

132. Rieger, R., Edenhofer, F., Lasmezas, C.I. & Weiss, S. The human 37-kDa laminin receptor precursor interacts with the prion protein in eukaryotic cells *Nat Med* 3, 1383-1388 (1997).

133. Schmitt-Ulms, G.*, et al.* Binding of neural cell adhesion molecules (N-CAMs) to the cellular prion protein. *J Mol Biol* 314, 1209-1225 (2001).

134. Colognato, H. & Yurchenco, P.D. Form and function: the laminin family of heterotrimers. *Dev Dyn* 218, 213-234 (2000).

135. Maness, P.F. & Schachner, M. Neural recognition molecules of the immunoglobulin superfamily: signaling transducers of axon guidance and neuronal migration. *Nat Neurosci* 10, 19-26 (2007).

136. Manson, J.C.*, et al.* 129/Ola mice carrying a null mutation in PrP that abolishes mRNA production are developmentally normal. *Mol Neurobiol* 8, 121-127 (1994).

137. Heikenwalder, M.*, et al.* Lymphotoxin-dependent prion replication in inflammatory stromal cells of granulomas. *Immunity* 29, 998-1008 (2008).

138. Chesebro, B.*, et al.* Anchorless prion protein results in infectious amyloid disease without clinical scrapie. *Science* 308, 1435-1439 (2005).

139. Fischer, M.*, et al.* Prion protein (PrP) with amino-proximal deletions restoring susceptibility of PrP knockout mice to scrapie. *EMBO J* 15, 1255-1264 (1996).

140. Genoud, N.*, et al.* Disruption of Doppel prevents neurodegeneration in mice with extensive Prnp deletions. *Proc Natl Acad Sci U S A* 101, 4198-4203 (2004).

141. Behrens, A.*, et al.* Absence of the prion protein homologue Doppel causes male sterility. *EMBO J* 21, 3652-3658 (2002).

142. Mombaerts, P.*, et al.* RAG-1-deficient mice have no mature B and T lymphocytes. *Cell* 68, 869-877 (1992).

143. Zielasek, J., Martini, R. & Toyka, K.V. Functional abnormalities in P0-deficient mice resemble human hereditary neuropathies linked to P0 gene mutations. *Muscle Nerve* 19, 946-952 (1996).

144. Polymenidou, M.*, et al.* The POM monoclonals: a comprehensive set of antibodies to non-overlapping prion protein epitopes. *PLoS ONE* 3, e3872 (2008).

145. Bermingham, J.R., Jr.*, et al.* The claw paw mutation reveals a role for Lgi4 in peripheral nerve development. *Nat Neurosci* 9, 76-84 (2006).

146. Ogata, T.*, et al.* Opposing extracellular signal-regulated kinase and Akt pathways control Schwann cell myelination. *J Neurosci* 24, 6724-6732 (2004).

147. Prinz, M.*, et al.* Intrinsic resistance of oligodendrocytes to prion infection. *J Neurosci* 24, 5974-5981 (2004).

148. Watt, N.T. & Hooper, N.M. Reactive oxygen species (ROS)-mediated beta-cleavage of the prion protein in the mechanism of the cellular response to oxidative stress. *Biochem Soc Trans* 33, 1123-1125 (2005).

149. Mange, A.*, et al.* Alpha- and beta- cleavages of the amino-terminus of the cellular prion protein. *Biol Cell* 96, 125-132 (2004).

150. Meotti, F.C.*, et al.* Involvement of cellular prion protein in the nociceptive response in mice. *Brain Res* 1151, 84-90 (2007).

151. Nico, P.B.*, et al.* Altered behavioural response to acute stress in mice lacking cellular prion protein. *Behav Brain Res* 162, 173-181 (2005).

152. Nazor, K.E., Seward, T. & Telling, G.C. Motor behavioral and neuropathological deficits in mice deficient for normal prion protein expression. *Biochim Biophys Acta* 1772, 645-653 (2007).

153. Lobao-Soares, B.*, et al.* Cellular prion protein regulates the motor behaviour performance and anxiety-induced responses in genetically modified mice. *Behav Brain Res* 183, 87-94 (2007).

154. Leo, S., Straetemans, R., D'Hooge, R. & Meert, T. Differences in nociceptive behavioral performance between C57BL/6J, 129S6/SvEv, B6 129 F1 and NMRI mice. *Behav Brain Res* 190, 233-242 (2008).

155. Brooks, S.P., Pask, T., Jones, L. & Dunnett, S.B. Behavioural profiles of inbred mouse strains used as transgenic backgrounds. I: motor tests. *Genes Brain Behav* 3, 206-215 (2004).

156. Brooks, S.P., Pask, T., Jones, L. & Dunnett, S.B. Behavioural profiles of inbred mouse strains used as transgenic backgrounds. II: cognitive tests. *Genes Brain Behav* 4, 307-317 (2005).

157. Liu, T.*, et al.* Intercellular transfer of the cellular prion protein. *J Biol Chem* 277, 47671-47678 (2002).

158. Griffiths, I.*, et al.* Axonal swellings and degeneration in mice lacking the major proteolipid of myelin. *Science* 280, 1610-1613 (1998).

159. Edgar, J.M.*, et al.* Age-related axonal and myelin changes in the rumpshaker mutation of the Plp gene. *Acta Neuropathol* 107, 331-335 (2004).

160. Gatzinsky, K.P., Holtmann, B., Daraie, B., Berthold, C.H. & Sendtner, M. Early onset of degenerative changes at nodes of Ranvier in alpha-motor axons of Cntf null (-/-) mutant mice. *Glia* 42, 340-349 (2003).

161. Britsch, S. The neuregulin-I/ErbB signaling system in development and disease. *Adv Anat Embryol Cell Biol* 190, 1-65 (2007).

162. Parkin, E.T.*, et al.* Cellular prion protein regulates beta-secretase cleavage of the Alzheimer's amyloid precursor protein. *Proc Natl Acad Sci U S A* 104, 11062-11067 (2007).

163. Hu, X.*, et al.* Bace1 modulates myelination in the central and peripheral nervous system. *Nat Neurosci* 9, 1520-1525 (2006).

164. Willem, M.*, et al.* Control of peripheral nerve myelination by the beta-secretase BACE1. *Science* 314, 664-666 (2006).

165. Rutishauser, D.*, et al.* The comprehensive native interactome of a fully functional tagged prion protein. *PLoS ONE* 4, e4446 (2009).

166. Keshet, G.I., Bar-Peled, O., Yaffe, D., Nudel, U. & Gabizon, R. The cellular prion protein colocalizes with the dystroglycan complex in the brain. *J Neurochem* 75, 1889-1897. (2000).

167. Hundt, C.*, et al.* Identification of interaction domains of the prion protein with its 37-kDa/67-kDa laminin receptor. *Embo J* 20, 5876-5886 (2001).

168. Feltri, M.L. & Wrabetz, L. Laminins and their receptors in Schwann cells and hereditary neuropathies. *J Peripher Nerv Syst* 10, 128-143 (2005).

169. Nodari, A.*, et al.* Alpha6beta4 integrin and dystroglycan cooperate to stabilize the myelin sheath. *J Neurosci* 28, 6714-6719 (2008).

170. McMahon, H.E.*, et al.* Cleavage of the Amino Terminus of the Prion Protein by Reactive Oxygen Species. *J Biol Chem* 276, 2286-2291. (2001).

171. Sunyach, C., Cisse, M.A., da Costa, C.A., Vincent, B. & Checler, F. The C-terminal products of cellular prion protein processing, C1 and C2, exert distinct influence on p53-dependent staurosporine-induced caspase-3 activation. *J Biol Chem* 282, 1956-1963 (2007).

172. Walmsley, A.R., Watt, N.T., Taylor, D.R., Perera, W.S. & Hooper, N.M. alpha-cleavage of the prion protein occurs in a late compartment of the secretory pathway and is independent of lipid rafts. *Mol Cell Neurosci* 40, 242-248 (2009).

173. Fournier, J.G. Cellular prion protein electron microscopy: attempts/limits and clues to a synaptic trait. Implications in neurodegeneration process. *Cell Tissue Res* 332, 1-11 (2008).

174. Fields, R.D. & Burnstock, G. Purinergic signalling in neuron-glia interactions. *Nat Rev Neurosci* 7, 423-436 (2006).

175. Petrakis, S. & Sklaviadis, T. Identification of proteins with high affinity for refolded and native PrPC. *Proteomics* 6, 6476-6484 (2006).

176. Gould, R.M., Byrd, A.L. & Barbarese, E. The number of Schmidt-Lanterman incisures is more than doubled in shiverer PNS myelin sheaths. *J Neurocytol* 24, 85-98 (1995).

177. Hoshi, T.*, et al.* Nodal protrusions, increased Schmidt-Lanterman incisures, and paranodal disorganization are characteristic features of sulfatide-deficient peripheral nerves. *Glia* 55, 584-594 (2007).

178. Sharghi-Namini, S.*, et al.* The structural and functional integrity of peripheral nerves depends on the glial-derived signal desert hedgehog. *J Neurosci* 26, 6364-6376 (2006).

179. Rios, J.C.*, et al.* Paranodal interactions regulate expression of sodium channel subtypes and provide a diffusion barrier for the node of Ranvier. *J Neurosci* 23, 7001-7011 (2003).

180. Isaacs, J.D., Jackson, G.S. & Altmann, D.M. The role of the cellular prion protein in the immune system. *Clin Exp Immunol* 146, 1-8 (2006).

181. Ip, C.W.*, et al.* Immune cells contribute to myelin degeneration and axonopathic changes in mice overexpressing proteolipid protein in oligodendrocytes. *J Neurosci* 26, 8206-8216 (2006).

182. Le Pichon, C.E.*, et al.* Olfactory behavior and physiology are disrupted in prion protein knockout mice. *Nat Neurosci* 12, 60-69 (2009).

183. Franklin, R.J. & Barnett, S.C. Olfactory ensheathing cells and CNS regeneration: the sweet smell of success? *Neuron* 28, 15-18 (2000).

184. Niewiadomska, M.*, et al.* Impairment of the peripheral nervous system in Creutzfeldt-Jakob disease. *Arch Neurol* 59, 1430-1436 (2002).

185. Neufeld, M.Y., Josiphov, J. & Korczyn, A.D. Demyelinating peripheral neuropathy in Creutzfeldt-Jakob disease. *Muscle Nerve* 15, 1234-1239 (1992).

186. Koop, O.*, et al.* Absence of mutations in the prion-protein gene in a large cohort of HMSN patients. *Neuromuscul Disord* 15, 549-551 (2005).

187. Richt, J.A.*, et al.* Production of cattle lacking prion protein. *Nat Biotechnol* 25, 132-138 (2007).

188. Yu, G.*, et al.* Functional disruption of the prion protein gene in cloned goats. *J Gen Virol* 87, 1019-1027 (2006).

189. Zhu, C.*, et al.* Production of Prnp -/- goats by gene targeting in adult fibroblasts. *Transgenic Res* 18, 163-171 (2009).

190. Yu, G.*, et al.* Generation of goats lacking prion protein. *Mol Reprod Dev* 76, 3 (2009).

191. Kuhlenbaumer, G.*, et al.* Mutations in SEPT9 cause hereditary neuralgic amyotrophy. *Nat Genet* 37, 1044-1046 (2005).

192. Buser, A.M., Erne, B., Werner, H.B., Nave, K.A. & Schaeren-Wiemers, N. The septin cytoskeleton in myelinating glia. *Mol Cell Neurosci* 40, 156-166 (2009).

193. Nagata, K., Asano, T., Nozawa, Y. & Inagaki, M. Biochemical and cell biological analyses of a mammalian septin complex, Sept7/9b/11. *J Biol Chem* 279, 55895-55904 (2004).

194. Hashimoto, M.*, et al.* Neuroprotective effect of sonic hedgehog up-regulated in Schwann cells following sciatic nerve injury. *J Neurochem* 107, 918-927 (2008).

195. Werner, H.B.*, et al.* Proteolipid protein is required for transport of sirtuin 2 into CNS myelin. *J Neurosci* 27, 7717-7730 (2007).

196. Collinge, J. Molecular neurology of prion disease. *J Neurol Neurosurg Psychiatry* 76, 906-919 (2005).

197. Kovacs, G.G. & Budka, H. Prion diseases: from protein to cell pathology. *Am J Pathol* 172, 555-565 (2008).

198. Frigg, R., Klein, M.A., Hegyi, I., Zinkernagel, R.M. & Aguzzi, A. Scrapie pathogenesis in subclinically infected B-cell-deficient mice. *J Virol* 73, 9584-9588 (1999).

199. Aguzzi, A. & Haass, C. Games played by rogue proteins in prion disorders and Alzheimer's disease. *Science* 302, 814-818 (2003).

200. Aguzzi, A., Montrasio, F. & Kaeser, P.S. Prions: health scare and biological challenge. *Nat Rev Mol Cell Biol* 2, 118-126. (2001).

201. Cuille, J. & Chelle, P.L. Experimental transmission of trembling to the goat. *C R Seances Acad Sci* 208, 1058-1160 (1939).

202. Creutzfeldt, H.G. Über eine eigenartige herdförmige Erkrankung des Zentralnervensystems. *Z. ges. Neurol. Psychiatr.* 57, 1-19 (1920).

203. Jakob, A. Über eigenartige Erkrankungen des Zentralnervensystems mit bemerkenswertem anatomischem Befunde. (Spastische Pseudosklerose-Encephalomyelopathie mit disseminierten Degenerationsherden). *Z. ges. Neurol. Psychiatr.* 64, 147-228 (1921).

204. Aguzzi, A. & Glatzel, M. Prion infections, blood and transfusions. *Nat Clin Pract Neurol* 2, 321-329 (2006).

205. Wells, G.A.*, et al.* A novel progressive spongiform encephalopathy in cattle. *Vet Rec* 121, 419-420 (1987).

206. Aguzzi, A. Between cows and monkeys. *Nature* 381, 734 (1996).

207. Aguzzi, A. & Weissmann, C. Spongiform encephalopathies: a suspicious signature. *Nature* 383, 666-667 (1996).

208. Bruce, M.E.*, et al.* Transmissions to mice indicate that 'new variant' CJD is caused by the BSE agent *Nature* 389, 498-501 (1997).

209. Hill, A.F.*, et al.* The same prion strain causes vCJD and BSE. *Nature* 389, 448-450 (1997).

210. Collinge, J.*, et al.* Kuru in the 21st century--an acquired human prion disease with very long incubation periods. *Lancet* 367, 2068-2074 (2006).

211. Andrews, N.J.*, et al.* Deaths from variant Creutzfeldt-Jakob disease in the UK. *Lancet* 361, 751-752 (2003).

212. Duffy, P.*, et al.* Possible person-to-person transmission of Creutzfeldt-Jakob disease. *N Engl J Med* 290, 692-693 (1974).

213. Will, R.G. Acquired prion disease: iatrogenic CJD, variant CJD, kuru. *Br Med Bull* 66, 255-265 (2003).

214. Llewelyn, C.A.*, et al.* Possible transmission of variant Creutzfeldt-Jakob disease by blood transfusion. *Lancet* 363, 417-421 (2004).

215. Peden, A.H., Head, M.W., Ritchie, D.L., Bell, J.E. & Ironside, J.W. Preclinical vCJD after blood transfusion in a PRNP codon 129 heterozygous patient. *Lancet* 364, 527-529 (2004).

216. Wroe, S.J.*, et al.* Clinical presentation and pre-mortem diagnosis of variant Creutzfeldt-Jakob disease associated with blood transfusion: a case report. *Lancet* 368, 2061-2067 (2006).

217. Gajdusek, D.C. & Zigas, V. Degenerative disease of the central nervous system in New Guinea - the endemic occurrence of 'kuru' in the native population. *N Engl J Med* 257, 974-978 (1957).

218. Gajdusek, D.C. & Reid, L.H. Studies on kuru. IV. The kuru pattern in Moke, a representative Fore village. *Am J Trop Med Hyg* 10, 628-638 (1961).

219. Hadlow, W.J. Scrapie and kuru. *Lancet* 2, 289-290 (1959).

220. Gajdusek, D.C., Gibbs, C.J. & Alpers, M. Experimental transmission of a Kuru-like syndrome to chimpanzees. *Nature* 209, 794-796 (1966).

221. Gajdusek, D.C., Gibbs, C.J., Jr. & Alpers, M. Transmission and passage of experimenal "kuru" to chimpanzees. *Science (AAAS)* 155, 212-214 (1967).

222. Gajdusek, D.C., Gibbs, C.J., Jr., Asher, D.M. & David, E. Transmission of experimental kuru to the spider monkey (Ateles geoffreyi). *Science (AAAS)* 162, 693-694 (1968).

223. Kovacs, G.G.*, et al.* Mutations of the prion protein gene phenotypic spectrum. *J Neurol* 249, 1567-1582 (2002).

224. Gerstmann, J., Sträussler, E. & Scheinker, I. Über eine eigenartige hereditär-familiäre Erkrankung des Zentralnervensystems. Zugleich ein Beitrag zur Frage des vorzeitigen lokalen Alterns. *Z. Neurol* 154, 736-762 (1936).

225. Gerstmann. über ein noch nicht beschriebenes Reflexphänomen bei einer Erkrankung des zerebellären Systems. *Wien. Medizin Wochenschr* 78, 906–908 (1928).

226. Masters, C.L., Gajdusek, D.C. & Gibbs, C.J. Creutzfeldt-Jakob disease virus isolations from the Gerstmann-Straussler syndrome with an analysis of the various forms of amyloid plaque deposition in the virus-induced spongiform encephalopathies. *Brain* 104, 559-588 (1981).

227. Collins, S., McLean, C.A. & Masters, C.L. Gerstmann-Straussler-Scheinker syndrome,fatal familial insomnia, and kuru: a review of these less common human transmissible spongiform encephalopathies. *J Clin Neurosci* 8, 387-397 (2001).

228. Hsiao, K.*, et al.* Linkage of a prion protein missense variant to Gerstmann-Sträussler syndrome. *Nature* 338, 342-345 (1989).

229. Tateishi, J., Kitamoto, T., Hashiguchi, H. & Shii, H. Gerstmann-Straussler-Scheinker disease: immunohistological and experimental studies. *Ann Neurol* 24, 35-40 (1988).

230. Tateishi, J., Kitamoto, T., Hoque, M.Z. & Furukawa, H. Experimental Transmission of Creutzfeldt-Jakob Disease and Related Diseases to Rodents. *Neurology* 46, 532-537 (1996).

231. Brown, P.*, et al.* Human spongiform encephalopathy: the National Institutes of Health series of 300 cases of experimentally transmitted disease. *Ann Neurol* 35, 513-529 (1994).

232. Lugaresi, E.*, et al.* Fatal familial insomnia and dysautonomia with selective degeneration of thalamic nuclei. *N Engl J Med* 315, 997-1003 (1986).

233. Medori, R.*, et al.* Fatal familial insomnia, a prion disease with a mutation at codon 178 of the prion protein gene *N Engl J Med* 326, 444-449 (1992).

234. Tateishi, J.*, et al.* First experimental transmission of fatal familiar insomnia. *Nature* 376, 434-435 (1995).

235. Goldfarb, L.G.*, et al.* Creutzfeldt-Jakob disease cosegregates with the codon 178Asn PRNP mutation in families of European origin. *Ann Neurol* 31, 274-281 (1992).

236. Zarranz, J.J.*, et al.* Phenotypic variability in familial prion diseases due to the D178N mutation. *J Neurol Neurosurg Psychiatry* 76, 1491-1496 (2005).

237. Mastrianni, J.A.*, et al.* Prion protein conformation in a patient with sporadic fatal insomnia *N Engl J Med* 340, 1630-1638 (1999).

238. Parchi, P.*, et al.* A subtype of sporadic prion disease mimicking fatal familial insomnia. *Neurology* 52, 1757-1763 (1999).

239. Raeber, A.J.*, et al.* Ectopic expression of prion protein (PrP) in T lymphocytes or hepatocytes of PrP knockout mice is insufficient to sustain prion replication. *Proc Natl Acad Sci U S A* 96, 3987-3992 (1999).

240. Raeber, A.J.*, et al.* PrP-dependent association of prions with splenic but not circulating lymphocytes of scrapie-infected mice. *EMBO J* 18, 2702-2706 (1999).

241. Collinge, J., Beck, J., Campbell, T., Estibeiro, K. & Will, R.G. Prion Protein Gene Analysis in New Variant Cases of Creutzfeldt-Jakob Disease. *Lancet* 348, 56 (1996).

242. Zeidler, M.*, et al.* New variant Creutzfeldt-Jakob disease: neurological features and diagnostic tests. *Lancet* 350, 903-907 (1997).

243. Hill, A.F.*, et al.* Investigation of variant Creutzfeldt-Jakob disease and other human prion diseases with tonsil biopsy samples. *Lancet* 353, 183-189 (1999).

244. Shibuya, S., Higuchi, J., Shin, R.W., Tateishi, J. & Kitamoto, T. Codon 219 Lys allele of PRNP is not found in sporadic Creutzfeldt-Jakob disease. *Ann Neurol* 43, 826-828 (1998).

245. Matthews, L., Coen, P.G., Foster, J.D., Hunter, N. & Woolhouse, M.E. Population dynamics of a scrapie outbreak. *Arch Virol* 146, 1173-1186 (2001).

246. Ferguson, N.M., Donnelly, C.A., Woolhouse, M.E. & Anderson, R.M. The epidemiology of BSE in cattle herds in Great Britain. II. Model construction and analysis of transmission dynamics. *Philos Trans R Soc Lond B Biol Sci* 352, 803-838 (1997).

247. Boelle, P.Y., Cesbron, J.Y. & Valleron, A.J. Epidemiological evidence of higher susceptibility to vCJD in the young. *BMC Infect Dis* 4, 26 (2004).

248. Outram, G.W., Dickinson, A.G. & Fraser, H. Reduced susceptibility to scrapie in mice after steroid administration. *Nature* 249, 855-856 (1974).

249. Aguzzi, A. Prions and the immune system: a journey through gut, spleen, and nerves. *Adv Immunol* 81, 123-171 (2003).

250. Kitamoto, T., Muramoto, T., Mohri, S., Doh ura, K. & Tateishi, J. Abnormal isoform of prion protein accumulates in follicular dendritic cells in mice with Creutzfeldt-Jakob disease. *J Virol* 65, 6292-6295 (1991).

251. Mabbott, N.A.*, et al.* Tumor necrosis factor alpha-deficient, but not interleukin-6-deficient, mice resist peripheral infection with scrapie. *J Virol* 74, 3338-3344 (2000).

252. Prinz, M.*, et al.* Lymph nodal prion replication and neuroinvasion in mice devoid of follicular dendritic cells. *Proc Natl Acad Sci U S A* 99, 919-924 (2002).

253. Montrasio, F.*, et al.* Impaired prion replication in spleens of mice lacking functional follicular dendritic cells. *Science* 288, 1257-1259 (2000).

254. Mabbott, N.A., Mackay, F., Minns, F. & Bruce, M.E. Temporary inactivation of follicular dendritic cells delays neuroinvasion of scrapie. *Nat Med* 6, 719-720 (2000).

255. Mabbott, N.A., Young, J., McConnell, I. & Bruce, M.E. Follicular dendritic cell dedifferentiation by treatment with an inhibitor of the lymphotoxin pathway dramatically reduces scrapie susceptibility. *Journal of Virology* 77, 6845-6854 (2003).

256. Heikenwalder, M.*, et al.* Chronic lymphocytic inflammation specifies the organ tropism of prions. *Science* 307, 1107-1110 (2005).

257. Ligios, C.*, et al.* PrPSc in mammary glands of sheep affected by scrapie and mastitis. *Nat Med* 11, 1137-1138 (2005).

258. Seeger, H.*, et al.* Coincident scrapie infection and nephritis lead to urinary prion excretion. *Science* 310, 324-326 (2005).

259. Outram, G.W., Dickinson, A.G. & Fraser, H. Developmental maturation of susceptibility to scrapie in mice. *Nature* 241, 536-537 (1973).

260. Ierna, M., Farquhar, C.F., Outram, G.W. & Bruce, M.E. Resistance of neonatal mice to scrapie is associated with inefficient infection of the immature spleen. *J Virol* 80, 474-482 (2006).

261. Prinz, M.*, et al.* Positioning of follicular dendritic cells within the spleen controls prion neuroinvasion. *Nature* 425, 957-962 (2003).

262. Glatzel, M. & Aguzzi, A. PrP(C) expression in the peripheral nervous system is a determinant of prion neuroinvasion. *J Gen Virol* 81, 2813-2821 (2000).

263. Glatzel, M., Heppner, F.L., Albers, K.M. & Aguzzi, A. Sympathetic innervation of lymphoreticular organs is rate limiting for prion neuroinvasion. *Neuron* 31, 25-34. (2001).

264. Raymond, C.R. & Mabbott, N.A. Assessing the involvement of migratory dendritic cells in the transfer of the scrapie agent from the immune to peripheral nervous systems. *J Neuroimmunol* (2007).

265. Heikenwalder, M., Federau C., von Boehmer, L., Schwarz, P., Wagner, M., Zeller, N., Haybaeck, J., Prinz, M., Becher, B. and Aguzzi A. Germinal center B cells are dispensable in prion transport and neuroinvasion. *J Neuroimmunol* (2007).

266. Cordier-Dirikoc, S. & Chabry, J. Temporary depletion of CD11c+ dendritic cells delays lymphoinvasion after intraperitonal scrapie infection. *J Virol* 82, 8933-8936 (2008).

267. Levavasseur, E.*, et al.* Experimental scrapie in 'plt' mice: an assessment of the role of dendritic-cell migration in the pathogenesis of prion diseases. *J Gen Virol* 88, 2353-2360 (2007).

268. Mohan, J., Bruce, M.E. & Mabbott, N.A. Neuroinvasion by scrapie following inoculation via the skin is independent of migratory Langerhans cells. *J Virol* 79, 1888-1897 (2005).

269. Raymond, C.R., Aucouturier, P. & Mabbott, N.A. In vivo depletion of CD11c+ cells impairs scrapie agent neuroinvasion from the intestine. *J Immunol* 179, 7758-7766 (2007).

270. Aucouturier, P.*, et al.* Infected splenic dendritic cells are sufficient for prion transmission to the CNS in mouse scrapie. *J Clin Invest* 108, 703-708 (2001).

271. Dore, G., Leclerc, C. & Lazarini, F. Treatment by CpG or Flt3-ligand does not affect mouse susceptibility to BSE prions. *J Neuroimmunol* 197, 74-80 (2008).

272. Sethi, S., Lipford, G., Wagner, H. & Kretzschmar, H. Postexposure prophylaxis against prion disease with a stimulator of innate immunity. *Lancet* 360, 229-230. (2002).

273. Heikenwalder, M.*, et al.* Lymphoid follicle destruction and immunosuppression after repeated CpG oligodeoxynucleotide administration. *Nat Med* 10, 187-192 (2004).

274. Aguzzi, A. & Sigurdson, C.J. Antiprion immunotherapy: to suppress or to stimulate? *Nat Rev Immunol.* 4, 725-736 (2004).

275. Polymenidou, M.*, et al.* Coexistence of multiple PrPSc types in individuals with Creutzfeldt-Jakob disease. *Lancet Neurol* 4, 805-814 (2005).

276. Taraboulos, A.*, et al.* Regional mapping of prion proteins in brain. *Proc Natl Acad Sci U S A* 89, 7620-7624 (1992).

277. Kranich, J.*, et al.* Follicular dendritic cells control engulfment of apoptotic bodies by secreting Mfge8. *J Exp Med* 205, 1293-1302 (2008).

278. Naugler, W.E.*, et al.* Gender disparity in liver cancer due to sex differences in MyD88-dependent IL-6 production. *Science* 317, 121-124 (2007).

279. Gilch, S.*, et al.* CpG and LPS can interfere negatively with prion clearance in macrophage and microglial cells. *Febs J* 274, 5834-5844 (2007).

280. Tal, Y.*, et al.* Complete Freund's adjuvant immunization prolongs survival in experimental prion disease in mice. *J Neurosci Res* 71, 286-290 (2003).

281. Cunningham, C.*, et al.* Systemic Inflammation Induces Acute Behavioral and Cognitive Changes and Accelerates Neurodegenerative Disease. *Biol Psychiatry* (2008).

282. Friedman-Levi, Y.*, et al.* Fatal neurological disease in scrapie-infected mice induced for experimental autoimmune encephalomyelitis. *J Virol* 81, 9942-9949 (2007).

283. Oehen, S.*, et al.* Marginal zone macrophages and immune responses against viruses. *J Immunol* 169, 1453-1458 (2002).

284. Beringue, V.*, et al.* Role of spleen macrophages in the clearance of scrapie agent early in pathogenesis. *J Pathol* 190, 495-502 (2000).

285. Yang, H., Wang, L., Huang, C.S. & Ju, G. Plasticity of GAP-43 innervation of the spleen during immune response in the mouse. Evidence for axonal sprouting and redistribution of the nerve fibers. *Neuroimmunomodulation* 5, 53-60 (1998).

286. Raeber, A.J.*, et al.* Studies on prion replication in spleen. *Developmental Immunology* 8, 291-304 (2001).

287. Kool, M.*, et al.* Cutting Edge: Alum Adjuvant Stimulates Inflammatory Dendritic Cells through Activation of the NALP3 Inflammasome. *J Immunol* 181, 3755-3759 (2008).

Supplementary Table 1. Primers used for genome-wide STR analysis

marker	sequence primer forward	sequence primer reverse	marker	sequence primer forward	sequence primer reverse
D10Mit103.1	TATGCCGACAATATTTCATTGC	GCCTCTGCATACATACCAATACC	D14Mit126.1	CCTGTCCCACAACACCTTTT	TATACATATGGGTAGCACTGAGTGG
D10Mit14.1	AGAGGGGACAAGGAGAGACC	AAGGTTTGGGTTCAGTTCCC	D14Mit127.1	AAACTTTACCTACCAGTGTCAAGTTAG	GTGTTGAACAACTCTATGTCTGTCTG
D10Mit20.1	CACCCTCACACAGATATGCG	GCATTGGGAAGTCCATGAGT	D14Mit170.1	TGTGTATGATTGTGTGGGGG	AGAAAGCAAACTTGCAAATATTCA
D10Mit207.1	TTTAAGCAAAACACCCATACACA	TCTGAGGGTACCTGTAGTCATGC	D14Mit174.1	ACTGCAGAGTCCACACAAGTG	TCTGAGCCACTATGCCTGG
D10Mit213.1	CTCCTCCTACTGATTGTCCCC	GGGACAAACTTTTAAAAATTGCA	D14Mit263.1	TGAGCACAGAGCCTATGTGG	ACAGAGAAATACCATGAAAACACC
D10Mit230.1	AGATAGCCTAGGGGGTGCAT	ATCAGTTTCCAATCGCTGCT	D14Mit40.2	TCCCGGGGATCAGTAAAATAT	CAAGGTGGCCTCTGACTTTC
D10Mit233.1	GTGCTTTATATTGGAGATCATCACA	GTCCCGAATTTCACATACATAGC	D14Mit44.1	AGTCACACCTGTAGAGTAAGCACA	GCTACTGCCTCGGTTTGTG
D10Mit31.1	CATAAGGAGCACAGGCATGA	CCCTCTACGTGCATGCTGTA	D14Mit48.1	TTTCTAGCCCTGACCCCC	TCTGTTCACTCTGTGTAATTCTCC
D10Mit38.1	CGATGAGCCCTAACACCAAT	CCTGTTACAAACTAAACCAAACCC	D14Mit5.1	CACATGAACAGAGGGGCAG	GTCATGAAGTGCCCACCTTT
D10Mit86.1	TTTGCCTGTAACAAGCCAGA	TTGAGGCTATCAGTTTAAAATCCC	D14Mit60.1	AGGCTGCCCATAAAAGGG	GTTTGTGCTAATGTTCTCATCTGG
D10Mit95.1	CCAGCCTAGAAAACCAAGCA	ACAGTGCTTCCGGAAAAATG	D15Mit107.1	CAACACTTATACACTTGTGTCAGGG	TCATGGTTGGAACAGCAGAC
D11Mit143.1	TTTATATTTTCAGGCTGTTCAGAGG	AACCTCTTTGCACACAAGAACA	D15Mit159.1	CACAGGCATACATAGAAATGTGC	CAACTTGTCAGGGTCTACTGAGG
D11Mit186.1	AAAACACATTTACATGCATGGTG	TGTGTGCACTTAAGCCCTGA	D15Mit242.1	GGTATACACACACACAATTTCAAGG	GAAAATAGTACCACAGAAGTTTGGG
D11Mit189.1	ACCATGTAATCCGATGCCAT	AGATGAATGTAATTGACCTACTTCCA	D15Mit252.1	CTTCAAACATGTTATCATTGTCACA	CTTCTGTATTCACAGGTGCTCG
D11Mit2.1	TCCCAGAGGTCTCCAAGACA	CCACAGTGTGTGATGTCTTC	D15Mit262.1	TTTATTAAAGCCAAACAGAGATTGC	AACATTGTATTTGGGTCATTGTG
D11Mit285.1	CATGAATCCATCACCAGCAG	TTTTTCAGTCATGCAGGCAG	D15Mit67.1	AGCTTCAACAGTGAAACATAGCC	CTGCTGTGTGCACTTATGCA
D11Mit326.1	CTATGGCAGGCACATGACTG	TTAAAAGTGGTTTCAGGTGTGTATG	D15Mit70.1	CATTGAGGGTTTGTAGGTTGG	ACCCCTGCAAGTTGTCTTTG
D11Mit333.1	CATGTGGTTATTTTCTAGCCCC	AGGCATCAATAACTATTTTTCAGTG	D15Mit80.1	TGAAGTCATCTTTCAATTTTCTCC	CGAAGATGCCTGCCAAATAT
D11Mit4.1	CAGTGGGTCATCAGTACAGCA	AAGCCAGCCCAGTCTTCATA	D16Mit101.2	TTATGAAATGTTTTATCTTTTGGGG	CTCCAGATGTAGAAATTAAAATCTTGG
D11Mit54.1	AGGCTGGTGGCTAGTGTCC	AAGTCTTGCGCTGCATCTTT	D16Mit131.1	TGGTGGTGGTGTTGATGGTA	AAGACCATTTCTAATAAACAACACCC
D11Mit71.1	GCCATACCTGGTAGCGTGTT	AATTTTCAGATGTAGCCATAAGCC	D16Mit153.1	CCTTCCAGGACCACAAAGAA	GAAAGAACTAGGAATGGAGAAAAGG
D11Mit86.1	TTGACATTGTGACAAAGACTTTCA	AAGGCATCATGAGGTTTTTAGTG	D16Mit189.1	ACAGTGTTTGTTTGTTTGTTTGTG	CAGTACAGGAAGTCTTTGCATCC
D12Mit11.1	TATTAAAAGGCAATGGGAGGG	TTGACTTCAGAGTGATTTCCAGG	D16Mit52.1	ACACATGTGCAAGCCTAACC	TTATCCCTGGAATCTGGGG
D12Mit143.1	CCCTATGCATGTACATTGTGAA	CGTGGGCATTTATCTTTCCT	D16Mit60.1	AAATGGTCAGCCCTGAAGC	TGCCTCACCCTTTGAAGTGT
D12Mit158.1	CATTGGGCAATGGAATTTG	ATGAGAGAAAACCAGAAACAAAGG	D16Mit86.2	TAATGTGGCAAGCAACCAAA	GCATGTTTCCATGTGTCTGG
D12Mit182.1	GTACATACAATACATCACACAAACGG	GGCAAGAAAACAGACCAATAGG	D17Mit1.1	TGCTTGAAATCCTGGGTTCA	TGCAAAAATGTATGTGCCTG
D12Mit285.2	GCCTCTTTCTAAATTTTTATGTTGTT	GTCTGTCTGTCTGTCTTTTTCACA	D17Mit143.2	GCTTTCTTGAAGACGTGGGA	CACAGGATGCTTGTAAGCACA
D12Mit59.1	AGTGAAATTCAGAGCACAAAAGC	ACCCTATATCTCCATGGTACGTG	D17Mit180.1	AGACACTGTCTAAAAACACAAGATGG	TTGTGTTCATATGCATGTGTGC
D12Mit7.1	CCGGGGATCTAAAACTACAT	TCTAATCTCAGCCCAATGGT	D17Mit20.1	AGAACAGGACACCGGACATC	TCATAAGTAGGCACACCAATGC
D12Mit91.1	GATTCAAGACAAGACTCCTGCA	CGCCCCCTCATGTTTTATC	D17Mit245.1	TGTGCTCTGGCTAGGGAGTT	CACATTCATATGTACACACACATGC
D13Mit151.1	ACAAATTAAAGACAAAATGTCTGCA	TGTGCACACCAGCATACAAA	D17Mit39.1	CCTCTGAGGAGTAACCAAGCC	CACAGAGTTCTACCTCCAACCC
D13Mit19.1	GGTGAGTTGTGTAATGATGGACA	AGCAACAGGGCTACTAAACACA	D17Mit51.1	TCTGCCCTGTAACAGGAGCT	CTTCTGGAATCAGAGGATCCC
D13Mit213.1	GCCTGAAACTCTACATAAAATACATCC	AGTTTCATTGCTTTAGTTACATTTTCA	D17Mit81.1	CAATCTATCTCATATGCATCTCTGTG	GTCTGGTGCACCTGTCCTC
D13Mit275.1	TTAGCAAGGGAACAGAGAGAGG	CAATCAAGGTATCCCTGTCTCC	D18Mit12.1	TTGTCAGTTTCTTGTGAGGGG	TGTTTAATAAGCCTTTTCCTGAGG
D13Mit56.1	CCTGTAACTCCAGATCCTGAGG	CAGTTGACCGAAATAGTCATTCC	D18Mit177.1	CTGTAGTTTATCAGTTCACCCTGTG	TGTGCTGTTAAACAAATATCTCTGG
D13Mit78.1	ACAGCACGGGTTTATCATCC	TATGCCTGCCAGGCTTCTAT	D18Mit186.1	AAGTGTTGGGCAAAGGCTAA	CTTTAGTATAGTGTGCATGAGTGTGA
D13Mit88.1	ACTGATGGCTCATGAGACCC	AAAATTAATAGGAACTGCAAGGG	D18Mit194.1	CCACCACATAAGGGAGGAAA	GTTTGTTGTTGTTCTATTTTCAAACA

marker	sequence primer forward	sequence primer reverse
D18Mit208.1	GACACATTTATGAGTCAGTCAGCC	TGTGAACCCAGGTCATGTGT
D18Mit48.1	TTGCACTCACAGGGCACAT	TCAGAGTTTCCAGAAGACACCA
D18Mit64.1	TCAGATTCACTGCTAAGTCTTTTC	AGCAAGAAAAGCAGGTGAGG
D18Mit222.1	AATCCAAGATTGACATGTGGC	CTTAGATGCCCTGTCTTAAAAAAA
D19Mit103.1	CCCATGTCCTTTGTTTCCC	GAAGCGCTATCACTGGATCC
D19Mit26.1	TTGTTACACAGCAAAATCCTGC	TTGAGGAGTAAGGCAAAAAAGG
D19Mit28.1	TCTTCATGCCCAAAAGAGCT	GCATCCTGAATCTCCTGCC
D19Mit33.1	CCTTTTCAAGAGCATCCTTAAA	GGTGGGACTTGAGAGATGCA
D19Mit6.1	ATTAGTAAACTGACTCCCATGCG	CTCATGAGTCCCCTGGGTTA
D19Mit68.1	CCAATACAAATCAGACTCAATAGTCG	AGGGTCTCCCCATCTTCCTA
D19Mit88.1	AACAGTGCAACTTTGGAGGC	TCATTGGAACTGTCTTAACAGTGC
D19Mit90.1	GTGGGAATCAATTTTAGTATGAACA	GGATGCTTGATATCATGTACATACA
D1Mit132.1	TATTGTTTATGGAAATTGGACCC	CATCTCTGAAGGAAAAAGTGCA
D1Mit159.1	TCTGGGGCCACTATGAGATC	TCACAATCAGAAAATATTATGAGACTC
D1Mit169.1	CGCTGACTGCTACTTTATTATATTCC	TCTGATTTACTGTCAATCAAGAGACC
D1Mit17.1	GTGTCTGCCTTTGCACCTTT	CTGCTGTCTTTCCATCCACA
D1Mit206.1	TGAGGCACCTTTGTATTCAGC	CCAGATGTCTTTGAACATTCTCC
D1Mit21.2	CGCTGGACAATCTTATAATTGCA	TCGAATCCCAACAACCACAT
D1Mit215.1	GGAGCAGAGTGTGAGAAGGG	CCAGTGTGAGCCCATTCC
D1Mit292.1	GAACTGGAGGTTTGCTACTGC	GGACATTGTTATCTCAGTTTTCTTC
D1Mit308.1	GAGGCTATGAGTCAAATGGACC	TTTATGAGGTGCTGAGATGCA
D1Mit411.1	GGAAACTGGAAAAGGGGGTA	TAGCATTGCTCTTTGGTTTCTG
D1Mit430.1	TATTAATGTTGAAGCCAGAAGCC	CTTTAATCATCTCTGTGGCAAGG
D1Mit495.1	CCACCTTGCTCCAAAAGAAA	TCTGAGAGGCTGCCACAATA
D1Mit60.1	GGTTTCTGCACTCAGATTTGC	TGCTCTCCTTTCTTCAAAGAAG
D2Mit1.1	CTTTTTCGTATGTGGTGGGG	AACATTGGGCCTCTATGCAC
D2Mit61.1	AAAGTCAACTGCTTTCAGTTACCC	CACAGAAGTGCCCTTGCATA
D2Mit327.1	TAGGGGATCTGATGCCTCTG	GCCCATTGAGCACTTTTGAT
D2Mit100.1	GTGTTCCTAAGGTTGTATTTTGGC	GAAATTTGACAATTGCTAGGTGC
D2Mit308	CAATCCACTTAGGAGAAATGTCG	TTTTCCTGCTTTTAAATTGATTCA
D2Mit395.1	AGGTCAGCCTGGACTATATGG	AGCATCCATGGGATAATGGT
D2Mit405	TGATTATATCTTGGAATACACGTGTG	CTGTGTAGCAAAACAGTTTATGGC
D2Mit396	GGTAATTATCTGGCTACTCCAATAGG	CCTCAGTTGTTAGGAAATTTTGTG
D2Mit493	GTCTCTACCTGAGTTTCCATCACA	TCCCGAGTTGTCCCTCTATG
D2Mit107	GGGAGTGAAGCCAGCATAAG	AACTGACTGAGTTTCAAAGTGCC
D2Mit279	GGGAAAAGAAACTCCGCTTT	CTGAGTTTACTGCTTAACACAACATA
D2Mit70	ATTGAAGCATGGTTAAGATTAGGC	TGTTTTAAACAACGCCAAAGG
D2Mit208	CAAAAAGCCACAGCCACC	GTTTATAATCAAGAGGCTATCTTGGG
D2Mit411.1	ACACTCACAACTACGAGATAAAGCC	AGGTCATTAGGGCTGTCTTCC

marker	sequence primer forward	sequence primer reverse
D2Mit209	ATGAGACAAATTACATACATGCACA	TGGATGTGTGTCAGTGCAGA
D2Mit21	GGCTTAGGCCCAAATTTTCT	TGGAAAGCTCATCTCTTCCT
D2Mit513	TTTTGTCGCACCATGTAGATG	GATTGCATTCCTGGGGTG
D2Mit404.1	GATGGTGATGATGATGATGATG	GACGCGCACAGGAAATAGAT
D2Mit285.1	TCAATCCCTGTCTGTGGTAGG	TATGACACTTACAAGGTTTTTGGTG
D2Mit113.1	CTCACGTGAGGGTCATGAGA	CTTCTCTACCTTCCTCAGAAGCC
D2Mit148.1	GTTCTCTGATCTACGGGCATG	TTCACTTCTACAAGTTCTACAAGTTCC
D3Mit147.1	TCTGCCTCTGTTAGATAGATATCCG	TTGTTCATCTATCCTCTGAAGTTCC
D3Mit200.1	CAACTTCAGTTTCTCATTTGAATTG	GCAAATGGAAGAGGTTTCTCC
D3Mit203.1	CTGAATCCTTATGTCCACTGAGG	GGGCACCTGCATTCATGT
D3Mit256.1	TACATTGCTTTTTGCTTTGAGTG	GTCGAATGTTATCAGAATTTGCA
D3Mit311.1	CGCCTGGTGGTAGTGGTG	CAGTGACTTAAGTACCCTTGACTCC
D3Mit320.1	AATGAAATCTCACGAGAGGCA	AAGCCAGGAGCAGAGTCAAG
D3Mit352.1	CGCAAAAGGCAGAGGTAAGT	TGCTTGCCTCTCTCCACC
D3Mit51.1	GGCACTGATAGCAGGCCTAG	TCTCTTCTGGTATTTCCTTCCG248
D3Mit57.1	TCCAGTTACTTGGTGAACTCCA	ATATGTGTACATGTTCATGGTGTG
D4Mit17.1	TGGCCAACCTCTGTGCTTCC	ACAGTTGTCCTCTGACATCC
D4Mit170.1	TTCCATCGAGTGACTTGATCC	CAGAGTGGCTGTCATCTGGA
D4Mit18.1	AATTAGCCCGGAGCTTGATT	GCTTCCATACATTTGCTTTTCC
D4Mit196.1	TTGACTGGTCTTATATATCTCTATCCC	TATATTAAATGCTAACTGCTAAGCACA
D4Mit203.1	GAATTCTTCCTGGGCCTTTC	CAAGAGCCCAGGTGTGGTAT
D4Mit251.1	AAAAATCGTTCTTTGACTTCTACATG	TTTAAAAGGGTTTCTTTATCCTGTG
D4Mit256.1	CTGGAGAGTTAGAATGGGGTACC	CAACAGAGGCGCTTCCTAAC
D4Mit268.1	TAATCTGATCCAAACACTAAATCAGA	GCAGCCTTATGGAAACTTTCA
D4Mit308.1	TATGGATCCACTCTCCAGAAA	CAAAGTCTCCTCCAAGGCTG
D4Mit348.1	ACCAAACTTGAGTTCTATGTAAGAACA	TGCTTACATATCAAAACAATACAGACA
D5Mit10.1	CGAGAAGTTGGAAAGACCCA	GGCACCCATGCCTCTATG
D5Mit146.1	TTAAATCTGAAGGTGTGGCTATAGC	GAGATTGCAAGTAAAGTGAGAGAGG
D5Mit158.1	AAAGACGCTGAGGAGTCACTG	CAGGAGACCTTGTAATAAAGGAAA
D5Mit201.1	GAGGACTCCTTCGATTTCCC	TTCCTAAGCAGGAACTGACCA
D5Mit309.1	TAGAGCCTATTTCAAACCCCC	GTTGCATCCATAGCAAGCAA
D5Mit352.1	CCCAGAGCCCACATCAAG	TAGGTGGGTGTGTCTCTCCC
D5Mit425.1	TCGCCTTTCTTTCCCTCC	AAAATTACATTTGCATCTGGGG
D5Mit95.1	TGTTCTTGTCCATGTCTGATCC	AACCAAAGCATGAAACAGCC
D5Mit98.1	TCCTTCATTTTATCTTCTGCCC	TGAATTCACTCTCGCACCTG
D6Mit100.1	CTTGAGTAGGTCTCAGTGCGG	CACATGCACACACAGAAGCA
D6Mit116.1	ACATTTCTTTGTGAGGTTCCTTG	CAGGTTTTTTGAAAGACACTCTTG
D6Mit123.1	GGAAGGAGCAGGTCCAATAC	CTCCCAACCACCAAGACCTA
D6Mit138.1	GCTCTTATTAATGAAGAAGAAGGAGG	CAAAGAAAGCATTTCAAGACTGC

marker	sequence primer forward	sequence primer reverse
D2Mit422	TGAGTGCAAAGTGCCTCAAC	AAGTTGTCAAAGTGTTAGACAAGGG
D6Mit14.1	ATGCAGAAACATGAGTGGGG	CACAAGGCCTGATGACCTCT
D6Mit209.1	CTCCCCCTCTGTGTGATTGT	TTATTACACCAGACCCATGTGG
D6Mit284.1	GGCTGCTGAGAAACAACCTC	TGAGTATTGAGCCAAATCCTCC
D6Mit36.1	ACCATCTGCATGGACTCACA	GTTGAAGAGGACGACCAAGTG
D6Mit374.1	TTCTGGCTCTTAACAGTCTGTCC	TACATATGCCAATGATATTCTCCC
D6Mit86.1	GACCAAACCAGAAGCCCCT	GGAATGTAGCCCTAAGTTGGA
D7Mit101.1	TACAGTGTGAACATGTAGGGGTG	TCCCAACATGGATGTGCTAA
D7Mit109.1	TCAACACCAGGAAGTCTCTTCA	CCTCCATCTCCCATCCAATA
D7Mit21.1	GGGTTGAACCTTACAGGGGT	ATCAAACCAGCCCAAGTGAC
D7Mit223.1	ATGCACATGAGTGTGTGTATGC	TCCTGTGTCTGACGCTCATC
D7Mit228.1	ATTCTTGGCCTTTTCTTGTAACA	AAACCTCCACACTGACTTCCA
D7Mit248.1	AATCAGGCAACTCAGGCACT	TCCTTAGGTCTCCAGTGAAAGC
D7Mit259.1	CCCCTCCTCCTGACCTCTT	GTCTCCATGGGAACCACACT
D7Mit294.1	TAGTGGGAAAGAGAGAAACAATCC	TAATGTTTAATCTTGTCGTCTTAGTGG
D7Mit323.1	TTTCACCTTCTAATCCTACTTCCTG	TGTCCAGAACAGGAAATAGAGTACC
D7Mit350.1	TCTGCATCTCACTGTCCCAG	ATCTACAAATGAGTTTCTAAGGACTGC
D7Mit83.1	GGGAGTTGTCATGGGCAG	TAACCAAAAACCTATGCTATCAGA
D7Mit98.1	CGCCATAGAACAGATTTGATACC	ATGGGTCTCAGATATCCCACC
D8Mit112.1	ATATCAGGCATGCATTATGATCC	TCTCTCTAGTGGGATTATCAACACA
D8Mit124.1	CAACTGTGTATCATAAACTGGGAA	GAAGAATCACTCAGCAGTGTATGG
D8Mit155.1	TTGGACAGGGAAAATTCTGC	TGAGGACTTGCTTTAAGAGTACTCC
D8Mit178.1	AAAATCAACTGTTTACATTTGAGCC	AGAGCACGCAGTGTGTATGC
D8Mit211.1	CAGAACACTGTCCTGAAAAGTCC	TACCCACAAACCTGTATTTAAATTAA
D8Mit289.1	AAAAAGAAAAGAAGGCTTAGTAATGTG	CTTGCTATTCATTGCAAAATTCC
D8Mit292.1	AGTCAAGGCATTTAAAATTAACTGG	CTGGGTTTGCTAGTGAAAGATG
D8Mit339.2	ACCTATGGTACACACACATCGC	CAAACATTTTTAGGCATTTAGATCC
D8Mit45.1	GAACAGGACCAATAAAATGAAAGC	CTACCTTACCAAACTTCCCGG
D8Mit46.2	GCCTGGGCTACATGAGACTC	GGGAATTCCAATACACTAAAGGG
D8Mit47.1	AAGATGTGCTTACTCTGACTTCCC	GGATCTATCCACATGTGGTGC
D8Mit49.1	TCTGTGCATGGCTGTGTATG	TGGTGTGCTGCTGATGCT
D8Mit63.1	TCTGGAACACAGTCCAATTCC	ATATGTGTGAGGGTTTTACCGG
D8Mit92.1	CTCAGGCTATCTTGGACATGC	TGGCTCACATCTGTGCTTTC
D9Mit129.1	TTGTCTTTTAACCTCCTGGAGC	TCCCATCTTTCTCCTTGTGG
D9Mit151.1	TGGTCAAGGTGTGGTATCGA	AAAACTCAGCATCCAATGGG
D9Mit2.1	GTGGTCTGCCCTCTTCACAT	CAAAGCCAGTCCAACTCCAA
D9Mit201.1	CCTGCAAGCCAACTACATGA	GCAAAAATGAAGTTCAAAAGGG
D9Mit250.1	CCCAAAAACCTATTTGCAGTG	GTGACATGATTCCTTCAGTCTTACC
D9Mit285.1	CAAATACATTGCTGATTATATCAGAGA	GGACTCTAGATCTCATCAGGGA

marker	sequence primer forward	sequence primer reverse
D9Mit336.1	AAGTGGTTCACAGAAATGTATACAGG	TTTTCTTTCTGTGGTAAAGGGG
D9Mit347.1	CCTCCACATGTGCACTGCT	CTGTCCATCTATCATCTATCTGTCTG
D9Mit355.1	CTCATTCACTTCCTGGTCCTG	GAAGGAAAGCCCACACTTTG
D9Mit90.1	AGGAGTCTCCCTGTACCTACACC	AAGTAGAGGGGAGGAATGAACC
D9Mit97.1	TCTCACTACTGCCTGCCAGA	TAGATTTCTCAGGCAAGGAAGC
DXMit121.1	GGACCCCAGTTCTTTCTTACATA	GTAAAACTGGGGGAATGGCTTAG
DXMit132.1	GTTAGGATTGCTGGTTGCGT	TCAACTCAACTGCAACATACCC
DXMit172.1	TACCACAGTTTGAATAAAGATGTGTG	GAAGAAACCATGACTCCTCTTTG
DXMit216.1	ATTTGGAACAGCAGCGTTG	TGTTTACACAATCTATCCAGTTACAGC
DXMit223.1	TTGGTTTGGGGTTTTTTTTG	ATTCCTGATAATGTCTTCTGGACA
DXMit64.1	AATATGTAAGGACAGCCTTCTCAG	AGAGGAGAGACAGGTCCAGGA
DXMit81.1	GAGGAGCATCAACCTTCTCG	GAGGTGGGGAGAAACAGAGG

9 CURRICULUM VITAE AND PUBLICATIONS

Surname: BREMER

Given names: Juliane Elisabeth Irmgard

Date of birth: February, 13th 1980

Place of birth: Berlin, Germany

Nationality: German

School education

06/1998	General qualification for university entrance/ baccalaureate at the Paul Natorp grammar school in Berlin, Germany

University Education

09/1998 - 03/1999	Biochemistry at the Free University of Berlin (FU Berlin), Germany, one semester
04/1999 - 12/2005	Medical studies at the Free University of Berlin (FU Berlin), Germany
12/2005	Final medical exam, license to practice medicine in Germany
Since 02/2006	MD-PhD student at the University of Zurich, faculty of science

Clinical electives (4 weeks each)

08/2003 - 10/2003	Department of Gynaecology and Obstetrics at the Komfo-Anoyke-Teaching-Hospital in Kumasi, Ghana
03/2003 - 04/2003	Institute of Clinical Pharmacology and Toxicology at the Charité - Campus Benjamin Franklin (CBF), Berlin, Germany
09/2002 - 10/2002	Paediatrics in an outpatient office (Praxis) in Berlin, Germany
08/2001 – 09/2001	Department of Internal Medicine (Gastroenterology) at the Hospital of Stralsund, Germany

Clinical internships (as a final year medical student)

06/2005 - 09/2005	Department of Internal Medicine at the University Hospital of Zurich, Switzerland (16 weeks)
02/2005 - 06/2005	Department of Neurology and Clinical Neurophysiology at the Charité - CBF, Berlin, Germany (16 weeks)

12/2004 - 02/2005	Clinic for Accident and Rehabilitation surgery at the Unfallkrankenhaus Berlin, Germany (8 weeks)
10/2004 - 12/2004	Department of Surgery at the St. Thomas' Hospital in London, UK (8 weeks)

Medical thesis

07/2002 - 11/2008	Doctoral thesis in Medicine "Expression and functionality of transcription factors regulating endothelin-converting-enzyme-1 in brain tumours"; Academic title "Dr. med." obtained at the Charité Berlin in 01/2009

Advanced medical training

02/2006 – 12/2009	Resident physician at the Institute of Neuropathology, University Hospital Zurich, Switzerland
since 01/2010	Resident physician in the Department of Neurology, University Hospital Zurich, Switzerland

Grants

2003	Travel grant for the clinical elective at the Department of Gynaecology and Obstetrics (Komfo-Anoyke-Teaching-Hospital, Kumasi, Ghana) by the Allianz Private Krankenversicherungs-AG, Germany
2008	Research grant by the medical faculty of the University of Zurich (100.000 CHF for 2 years)

Awards and prizes

06/2004	First prize in the Benjamin-Franklin-Contest
09/2009	Theodor Schwann Award 2009 for the work "Axonal prion protein is required for peripheral myelin maintenance" at the annual meeting of the German society of neuropathology in Düsseldorf, Germany

Teaching experience

Summer 2009/ 2010	Lecturer in the course "Diseases of the nervous system", BIO404, University of Zurich
04/2003 - 03/2005	Tutor at the Institute of Hygiene at the Charité - CBF, Berlin, Germany
10/2001 - 08/2002	Tutor at the Institute of Clinical Chemistry and Pathobiochemistry at the Charité - CBF, Berlin, Germany

Oral presentations at international meetings

09/2009 "Axonal prion protein is required for peripheral myelin maintenance" at the annual meeting of the German society of neuropathology in Dusseldorf, Germany

07/2009 "Axonal prion protein is required for peripheral myelin maintenance" at the third international Charcot-Marie-Tooth Consortium Meeting in Antwerp, Belgium

Publications – original articles

1. Funke-Kaiser H, Thomas A, ***Bremer J***, Kovacevic SD, Scheuch K, Bolbrinker J, Theis S, Lemmer J, Zimmermann A, Zollmann FS, Herrmann SM, Paul M, Orzechowski HD (2003): Regulation of the major isoform of human endothelin-converting enzyme-1 by a strong housekeeping promoter modulated by polymorphic microsatellites. *J Hypertens.* 21 (11): 2111-24.

2. Heikenwalder M, Kurrer MO, Margalith I, Kranich J, Zeller N, Haybaeck J, Polymenidou M, Matter M, ***Bremer J***, Jackson W, Lindquist S, Sigurdson CJ, Aguzzi A (2008): Lymphotoxin-dependent prion replication in inflammatory stromal cells of granulomas. *Immunity* 29 (6): 998-1008.

3. Haybaeck J, Zeller N, Wolf MJ, Weber A, Wagner U, Kurrer MO, ***Bremer J,*** Iezzi G, Graf R, Clavien PA, Thimme R, Blum H, Nedospasov SA, Zatloukal K, Ramzan M, Ciesek S, Pietschmann T, Marche PN, Karin M, Kopf M, Browning JL, Aguzzi A, Heikenwalder M (2009): A lymphotoxin-driven pathway to hepatocellular carcinoma. *Cancer Cell.* 16 (4): 295-308.

4. Baumann F, Pahnke J, Radovanovic I, Rülicke T, ***Bremer J***, Tolnay M, Aguzzi A (2009): Functionally relevant domains of the prion protein identified in vivo. *PLoS One.* 4 (9): e6707.

5. ***Bremer J***, Heikenwalder M, Haybaeck J, Tiberi C, Krautler NJ, Kurrer MO, Aguzzi A (2009): Repetitive immunization enhances the susceptibility of mice to peripherally administered prions. *PLoS One.* 4 (9): e7160.

6. Recher M, Sahrbacher U, ***Bremer J***, Arndt B, Steiner U, Fontana A (2010): Treatment of inclusion body myositis: is low-dose intravenous immunoglobulin the solution? *Rheumatol Int.* [Epub ahead of print]

7. Wegener S, ***Bremer J***, Komminoth P, Jung HH, Weller M (2010): Paraneoplastic Necrotizing Myopathy with a Mild Inflammatory Component: A Case Report and Review of the Literature. *Case Rep Oncol.* 3 (1): 88-92.

8. ***Bremer J***, Baumann F, Tiberi C, Wessig C, Fischer H, Schwarz P, Steele AD, Toyka KV, Nave KA, Weis J, Aguzzi A (2010): Axonal prion protein is required for peripheral myelin maintenance. *Nature Neurosci*. 13 (3): 310-318.

9. ***Bremer J***, O'Connor T, Tiberi C, Rehrauer H, Weis J, Aguzzi A (2010): Ablation of Dicer from murine Schwann cells increases their proliferation while blocking myelination. *PLoS One.* 5 (8): e12450.

Publications – review

Aguzzi A, Baumann F, ***Bremer J*** (2008): The prion's elusive reason for being. *Annu Rev Neurosci.* 31: 439-77. Review.

Publications – book chapters

1. ***Bremer J***, Wiendl H (2007) Neurology. In: Das Zweite - kompakt, Neurologie, Psychiatrie, Psychosomatik. Editors: Schaps, Kessler, Fetzner; Springer-Verlag GmbH & Co. KG Berlin, Heidelberg

2. ***Bremer J***, Neitzel H (2008) Human genetics. In: Das Zweite - kompakt, Grundlagen. Editors: Schaps, Kessler, Fetzner; Springer-Verlag GmbH & Co. KG Berlin, Heidelberg

3. Aguzzi A, ***Bremer J*** (2008) Prion diseases. In: Harrison's Principles of Internal Medicine, 17th edition in German. Editors: Dietel, Suttorp, Zeitz; ABW Wissenschaftsverlag GmbH, Berlin

4. Jung HH, ***Bremer J***, Weller M (2010) Gene therapy for myositis. In: Gene Therapy for Autoimmune and Inflammatory Diseases. Editors: Chernajovsky, Robbins; Birkhäuser Verlag GmbH, Basel

10 ACKNOWLEDGEMENTS

First of all I would like to thank Adriano Aguzzi for all his generosity and support during the four years of my thesis, for his valuable suggestions on projects, for the opportunity to work in such a well-equipped institute, for hour-long paper-writing sessions, and for the laboratory meetings that allowed for intensive scientific discussion.

I would like to thank all my co-workers inside the lab for the exellent collaborations and scientific discussions, especially Mathias Heikenwälder and Frank Baumann. Special thanks goes also to Cinzia Tiberi, Mirzet Delic, Petra Schwarz, Tracy Lynn O'Connor, Monika Wolf, Nicolas Zeller, Heike Fischer, Anna Maria Calella, Johannes Haybäck, Donal McHugh - without their help, the work would have been much less efficient and certainly also less fun.

For introducing me into the field of neuropathology and myopathology and for fruitful discussions at the microscope, I would like to thank Michel Mittelbronn, Hildegard Dohmen-Scheufler, Hans-Hilmar Goebel, David Capper, Ekkehard Hewer, Michael Kurrer, Patrick Harter, Umberto De Girolami, Stefan Prokop, Heike Fischer, Dino Saban, Doren Lemm, and Manuela Neumann.

Furthermore, I would like to thank Adriano Aguzzi and the heads of the receiving institutes for the possibility to visit several laboratories in Europe for learning special techniques and/or for collaborations, including Dies Meijer in Rotterdam, Klaus Armin Nave in Göttingen, Joachim Weis in Aachen, Casten Wessig and Klaus Toyka in Würzburg. In Göttingen, I would like to thank also Hauke Werner, Wiebke Möbius, Ursula Fünfschilling, Schanila Nawaz, Olaf Jahn, Marina Ueker, Michael Sereda, and in Aachen Hannelore Mader for their support.

For providing mice, I would like to thank Giovanna Mallucci, Dies Meijer, Jean Manson, John Collinge, Susan Lindquist and Walker Jackson. I thank Thomas Rülicke for performing pronuclear injections of the PLP-PrP construct. Furthermore, I thank Wendy B. Macklin for providing the PLP-promoter cassette, Paul Saftig and A. Rittger for providing nerves of BACE1$^{-/-}$ mice, and for antibodies J.A. Girault (anti-paranodine/Caspr) and M.T. Dours-Zimmermann (anti-versican antibody).

For discussions and suggestions during my PhD thesis, I would like to thank the members of my PhD committee, Ueli Suter and Martin Schwab.

I would like to thank Hans Welzl and Inger Drescher for introducing me into and helping me with the behavioral tests. Furthermore, I would like to thank Andrea Patrignani, Hubert Rehrauer, Sabina Wirth-Hafen, Stefan Zoller from the Functional genomics center Zürich for their support.

Furthermore, I would like to thank Cristobal Tostado, Rita Moos, Birgit Riepl, Norbert Wey, Monika Bieri, Silvia Behnke, André Fitsche, Maggy Arras, Kai Scheufler, Sei-ichi Yusa, Bruno Guhl, Hans-Peter Gautschi, Mareike Schroff Wagner, Dimitri Goriounov, Li-chun Infanger, Giuseppe Manco, Veronika Kana, Mario Novulone, Dorothea Rutishauser, Peter Nilsson, Christina Sigurdson, Christine Sturzenegger, Jacqueline Wiedler, Victor Escalante, Alexandre Ruffieux, Urs Egli, Sarah Amzallag, Winfried Förderer, Andrea Schifferli, Marianne König, Andrea Läuchli, Mehrangiz Häring-Hodaey, Angelika Ruf, Margrit Suter, Andrea Wyss, Manuela Petras, Brigitte Piccapietra, Boris Ballmer, Laura Varrica, Stephan Wäckerlin, Timo Böge, Nike Kräutler, Thorsten Läufer, André Wethmar, Jan Kranich, Gitta Seleznik, Paolo Dametto, José Barros de Oliveira-Martins, Jeppe Pedersen, Claire Bridel, Christian Julius for help, suggestions, and discussion.

I would like to thank the University of Zürich for funding parts of this thesis by a career development award (Forschungskredit).

Finally I wish to express my deepest gratitude to my parents Margot and Karsten Bremer, without their constant and unconditioned support and without their genes, this work would not have been possible.